2014

The Regulation of Skeletal Muscle Mass and Mitochondrial Biogenesis by gp130/STAT3 Signaling during Cancer Cachexia

Melissa Puppa
University of South Carolina - Columbia

THE REGULATION OF SKELETAL MUSCLE MASS AND MITOCHONDRIAL BIOGENESIS BY GP130/STAT3 SIGNALING DURING CANCER CACHEXIA

by

Melissa Puppa

Bachelor of Science
Roanoke College, 2008

Submitted in Partial Fulfillment of the Requirements

For the Degree of Doctor of Philosophy in

Exercise Science

Norman J. Arnold School of Public Health

University of South Carolina

2013

Accepted by:

James Carson, Major Professor

Angela Murphy, Committee Member

Greg Hand, Committee Member

Raja Fayad, Committee Member

Lacy Ford, Vice Provost and Dean of Graduate Studies

DEDICATION

This dissertation is dedicated in loving memory of Robin Cameron.

ACKNOWLEDGEMENTS

I need to first thank my husband Benjamin without whom I may not have finished this degree. I would like to extend a special thank you to my parents Robert and Elaine for their inspiration and always knowing what to say, even if I didn't want to hear it. I would like to thank Dr. James Carson whose patience and guidance have helped me achieve more than I could have imagined. I would like to thank my dissertation committee members Dr. Greg Hand, Dr. Angela Murphy, and Dr. Raja Fayad who have given their time and expertise to better my work. I thank them for their contribution and their good-natured support. I would like to thank the members both past and present of the IMB lab who have assisted me throughout my time: James White, Shu Sato, Kandy Velazquez, Aditi Narsale, Song Gao, Justin Hardee, Kimbell Hetzler, Sonia Thomas, Johannes Aartun, Josh Mangum, and Dennis Fix and any not specifically mentioned here. I would like to thank my coaches and family at CFR and CCF for their unfailing love and support.

Funding for this dissertation was primarily provided by Dr. James Carson and the IMB Laboratory: NIH Grant 1 R01 CA121249-01.

ABSTRACT

Cachexia affects nearly 70% of all cancer patients depending on the cancer, and decreases cancer survival. Cachexia is associated with muscle mass loss that is accompanied by a loss in muscle oxidative capacity, a decrease in protein synthesis and an increase in protein degradation. While progress has been made in understanding some of the mechanisms underlying the cachectic condition, there are currently no approved pharmaceutical interventions to slow or stop cachexia progression. The purpose this study was to determine the role of skeletal muscle gp130 and STAT3 signaling in the regulation of cachexia induced muscle atrophy and mitochondrial loss. Specific aim 1 examined the regulation of cachexia-induced mitochondrial loss by IL-6 trans signaling, systemic STAT3 signaling and muscle specific gp130 signaling. Inhibition of systemic inflammatory signaling attenuated muscle and body weight loss; while, muscle gp130 inhibition did not. Inhibition of inflammatory signaling at all levels attenuated skeletal muscle mitochondrial loss and while systemic STAT3 and muscle gp130 inhibition relieved cachexia-suppression of mitochondrial fusion, only inhibition of trans IL-6 signaling blocked cachexia-induction of mitochondrial fission protein. Specific aim 2 examined the regulation of muscle protein turnover by skeletal muscle gp130/STAT3 during cancer cachexia. Inhibition of muscle gp130 attenuated muscle loss during LLC-induced cachexia. This was associated with suppression of protein degradation pathways without relieving the inhibition of muscle protein synthesis. The third specific aim was to

determine if acute contraction could activate mitochondrial biogenesis in severely cachectic muscle. Contraction alone was unable to up regulate muscle mTOR signaling and mitochondrial proteins in cachectic muscle; however, STAT/NFκB inhibition relieved cachexia-suppression of contraction-induced mTOR signaling and up-regulated markers of mitochondrial biogenesis. In summary, inflammatory signaling through STAT3 and muscle gp130 regulate the suppression mitochondrial content and the induction of muscle protein degradation; however, it does not mediate the cachexia suppression of muscle protein synthesis. These findings provide insight of potential targets for pharmacological therapies for the treatment of cancer cachexia. Additionally, combination therapies involving inflammation inhibition with exercise may be most beneficial for the treatment of cancer cachexia.

TABLE OF CONTENTS

LIST OF TABLES

LIST OF FIGURES

LIST OF ABBREVIATIONS

AH-130 ..... Yoshida ascites hepatoma AH 130

AKT ..... Protein Kinase B

AMP ..... Adenosine monophosphate

AMPK ..... AMP-activated protein kinase

Apc ..... Adenomatous polyposis coli

ATP ..... Adenosine triphosphate

BL-6 ..... C57BL/6

BW ..... Body Weight

C/EBPβ ..... CCAAT/enhancer binding protein beta

C-26 ..... C-26 colon adenocarcinoma

CNTF ..... Ciliary Neurotrophic Factor

Con ..... Control

COPD ..... Chronic obstructive pulmonary disease

Cre ..... Cre recombinase

DNA ..... Deoxyribonucleic acid

DRP-1 ..... Dynamin-related protein 1

EDL ..... extensor digitorum longus

ELISA ..... Enzyme-linked immunosorbent assay

ERK ..... Extracellular signal-regulated kinase

FIS1 ..... Mitochondrial fission protein 1

FNIII ..... Fibronectin type III

FOXO ..... forkhead transcription factor

GAPDH ..... Glyceraldehyde 3-phosphate dehydrogenase

Gas ..... Gastrocnemius

GLUT4 ..... Glucose transporter 4

gp130 ..... Glycoprotein 130 receptor

HFD ..... High Fat Diet

HIV-AIDS ..... Human immunodeficiency virus- acquired immune deficiency syndrome

Hz ..... Hertz

IL-1 ..... Interleukin 1

IL-11 ..... Interleukin 11

IL-6 ..... Interleukin 6

IL-6KO ..... Interleukin-6 Knockout

IL-6R ..... Interleukin-6 receptor

IMF ..... Intermyofibrilar

INFγ ..... Interferon gamma

IOD ..... Integrated optical density

JAK ..... Janus Kinase

kDa ..... Kilodalton

LIF ..... Leukemia Inhibitory Factor

LLC ..... Lewis Lung Carcinoma

LoFS ..... Low Frequency Electrical Stimulation

MAC 16 ..... murine adenocarcinoma 16

MAPK..... Mitogen-activated protein kinase

MFN1 ..... mitofusin 1

MFN2 ..... mitofusin 2

Min ..... $Apc^{Min/+}$

mRNA.....messenger RNA

ms ..... Millisecond

mtDNA .....Mitochondrial DNA

mTOR .....mammalian target of rapamycin

MuRF-1 .....Muscle RING-finger protein-1

NFκB .....Nuclear Factor-kappaB

NRF1 ..... Nuclear respiratory factor 1

NRF2 ..... Nuclear respiratory factor 2

NUGEMPs..... Nuclear genes encoding mitochondrial proteins

OPA1 .....Optic Atrophy 1

OSM .....Oncostatin M

PBS..... Phosphate buffered saline

PDTC.....Pyrrolidine dithiocarbamate

PGC-1..... peroxisome proliferator-activated receptor coactivator-1

PI3K..... Phosphoinositide 3-kinase

Pla.....plantaris

PPAR ..... peroxisome proliferator-activated receptors

PROb-BDIX..... Berlin–Druckrey IX Rats

PVDF ..... Polyvinylidene fluoride

Quad ..... Quadriceps

RNA..... Ribonucleic acid

SDH ..... Succinate Dehydrogenase

SDS..... Sodium dodecyl sulfate

sgp130Fc..... soluble glycoprotein 130 fusion protein

sIL-6R..... soluble IL-6 receptor

skm-gp130 ..... skeletal muscle specific glycoprotein 130r knockout

Sol..... Soleus

SS ..... Subsarcolemmal

STAT3 ..... Signal Transducer and Activator of Transcription 3

Stim ..... Stimmulated

TA..... Tibialis Anterior

TBST ..... Tris Buffered Saline and Tween

TFAM ..... Mitochondrial transcription factor A

TNFα ..... Tumor Necrosis Factor alpha

V ..... Volts

CHAPTER 1

INTRODUCTION

Cancer cachexia accounts for approximately 20% of all cancer related deaths and about 40% of deaths related to colon cancer (Bruera, 1997; Tisdale, 2002). Cachexia is defined as the unintentional loss of body weight with an underlying disease present (Evans et al., 2008; Fearon et al., 2011; Muscaritoli et al., 2010). While cachexia consists of the loss of both skeletal muscle and adipose tissue, maintenance of skeletal muscle mass has proven to be of importance. A potential mediator of skeletal muscle mass during cachexia is the inflammatory cytokine interleukin 6 (IL-6). Inflammation is a prominent feature during the promotion and progression of colon cancer cachexia, and high IL-6 levels are correlated with cachexia in late stage cancer patients (Iwase et al., 2004). Over-expression of IL-6 in tumor bearing mice can decrease skeletal muscle mass in a dose dependent manner (White et al., 2012a). Inhibition of IL-6 signaling via an IL-6 receptor antibody or by knocking out IL-6 attenuates skeletal muscle wasting in the $Apc^{Min/+}$ (Min) mouse model of cachexia; however it is unclear whether these actions are from the systemic inhibition of IL-6 signaling or whether they are dependent on the local inhibition of IL-6 signaling in the muscle itself (Baltgalvis et al., 2008b; White et al., 2011b).

IL-6 is a pleotropic cytokine secreted from many different tissues including skeletal muscle. IL-6 has both pro-inflammatory and anti-inflammatory properties as well as the ability to activate target genes for cell proliferation, differentiation, and apoptosis (Heinrich et al., 2003). During cachexia, IL-6 may act on the tumors, stimulating growth and differentiation, or IL-6 may act directly on peripheral tissues, such as skeletal muscle, that are atrophying. The initiation and progression of cachexia in the Min mouse is directly related to tumor burden and circulating IL-6 levels (Baltgalvis et al., 2008b;

White et al., 2011b). IL-6 signals through glycoprotein 130 (gp130/CD130) to activate downstream signaling. This occurs by binding with either the soluble IL-6 receptor (trans signaling) or the membrane IL-6 receptor (classical signaling) and forming a complex with gp130 to activate downstream signaling including the JAK/STAT, RAS/ERK, and MAPK pathways during classical signaling (Ernst and Jenkins, 2004). Trans signaling can activate downstream signaling in tissues that do not express the IL-6 receptor, or express IL-6 receptor in very low levels such as the kidney (Nechemia-Arbely et al., 2008). Trans signaling can also enhance the actions of IL-6 on tissues that express the IL-6 receptor. The role of trans IL-6 signaling during the progression of cachexia is unknown. Additionally the role of the skeletal muscle specific IL-6 signaling through gp130 is unknown. Bonetto et. al. showed that muscle STAT3 signaling, a downstream mediator of inflammatory and IL-6-gp130 signaling, is necessary for inflammation and cancer-induced muscle wasting in some tumor bearing mice (Bonetto et al., 2012; Bonetto et al., 2011). STAT3 inhibition can attenuate muscle loss through suppression of muscle atrophy signaling, suggesting that the JAK/STAT pathway is an important downstream mediator of IL-6-gp130 signaling in skeletal muscle during cachexia. The role of classical and trans IL-6 signaling and whether IL-6 is acting through local or systemic STAT3 activation during cancer cachexia remains uninvestigated.

Mitochondrial biogenesis and function, is associated with a muscle's metabolic capacity and substrate utilization flexibility (Chomentowski et al.). Muscle mitochondrial function is related to muscle apoptosis, autophagy, and protein turnover thus mediating skeletal muscle mass (Romanello and Sandri, 2010). We have shown that IL-6 is sufficient to induce atrophy in C2C12 myotubes by decreasing protein synthesis,

increasing degradation, and altering mitochondrial dynamics and content (White et al., 2012c). Mitochondria are dysregulated in the skeletal muscle of rodents with cancer cachexia (White et al., 2011a; White et al., 2012c). Many studies have shown that the dysregulation of muscle mitochondrial signaling, including decreased mitochondrial biogenesis, altered dynamics, and decreased function, can lead to muscle loss (Romanello et al., 2010). These results have been extended to the cachexia field by our experiments in the $Apc^{Min/+}$ mouse which show a loss of mitochondrial content with the progression of cachexia and IL-6 overexpression (White et al., 2011a; White et al., 2012c). We have shown that systemic inhibition of IL-6 signaling after the initiation of cachexia can attenuate mitochondrial dysfunction in the $Apc^{Min/+}$ mouse (White et al., 2012c), however it is unknown whether these actions were due to suppression of classical or trans IL-6 signaling and whether systemic or muscle specific signaling IL-6 signaling was responsible. Exercise training, which is known to increase mitochondrial plasticity, can prevent mitochondrial dysfunction even in the presence of elevated circulating IL-6 (Puppa et al., 2011d). While IL-6 signaling appears to be a regulator of mitochondrial function during cachexia, it is unclear whether these actions involve direct signaling in the muscle through the muscle gp130 or if IL-6 action on alternative tissues leads to dysregulation of skeletal muscle mitochondria.

Inhibition of either STAT3 or IL-6 attenuates muscle loss with cancer (Baltgalvis et al., 2008b; Bonetto et al., 2012; Bonetto et al., 2011; White et al., 2011b; White et al., 2012c). While there is evidence showing that IL-6 inhibition preserves skeletal muscle quality related to mitochondrial biogenesis and function, and suppresses skeletal muscle protein degradation, it is unclear if these actions are from local inhibition at the level of

the skeletal muscle or if systemic inhibition of IL-6 signaling is important for the protection of muscle quality during cachexia. STAT3 inhibition preserves skeletal muscle mass during cancer cachexia, however, STAT3 regulation of muscle protein synthesis and mitochondrial plasticity during cancer cachexia remains to be established. The overall goal of this proposal is to determine the regulation of skeletal muscle mass and mitochondrial biogenesis by gp130/STAT3 signaling and muscle contraction during cancer cachexia. Our *central hypothesis* is that IL-6 signaling through gp130 and STAT3 will mediate muscle mass and suppression of mitochondrial biogenesis/function during cachexia, and inhibition of inflammatory signaling will increase mitochondrial plasticity and enhanced cachectic muscle's response to contraction.

Specific Aim #1 will determine if attenuation of systemic trans IL-6 signaling, STAT3 or local IL-6 signaling through gp130 can prevent mitochondrial loss and altered mitochondrial dynamics during cancer cachexia.

Specific Aim #2 will determine if IL-6 signaling through muscle gp130 receptor/ STAT3 regulates the disruption of muscle mass in the cachectic muscle.

Specific Aim #3 will determine if the transcription and translation of proteins regulating mitochondrial biogenesis are altered with acute contraction during cachexia.

Working Model: Initially the proposal will examine if the inhibition of IL-6 trans signaling, global STAT/NFκB signaling, or muscle gp130 signaling can prevent decreases in skeletal muscle mitochondrial biogenesis and dynamics after the initiation of cancer cachexia in tumor bearing mice (AIM 1). Next the proposal will examine if gp130 receptor signaling, global STAT/NFκB signaling, or global IL-6 signaling can prevent the decreased cachexia induced muscle mass loss in the Lewis lung carcinoma (LLC) implantable tumor model of cachexia (AIM 2). The $Apc^{Min/+}$ and LLC models differ in rate of cachexia progression, and overall tumor burden relative to body size, but IL-6/STAT3 has a documented role for muscle wasting in both models. Next the proposal will proceed to examine the contraction mediated regulation of mitochondrial biogenesis in response to acute contractions (AIM 3). Understanding the role of the gp130 receptor and STAT3 signaling regulation of muscle mass will provide a guide for developing specific pharmaceutical and therapeutic targets for the prevention and treatment of cachexia.

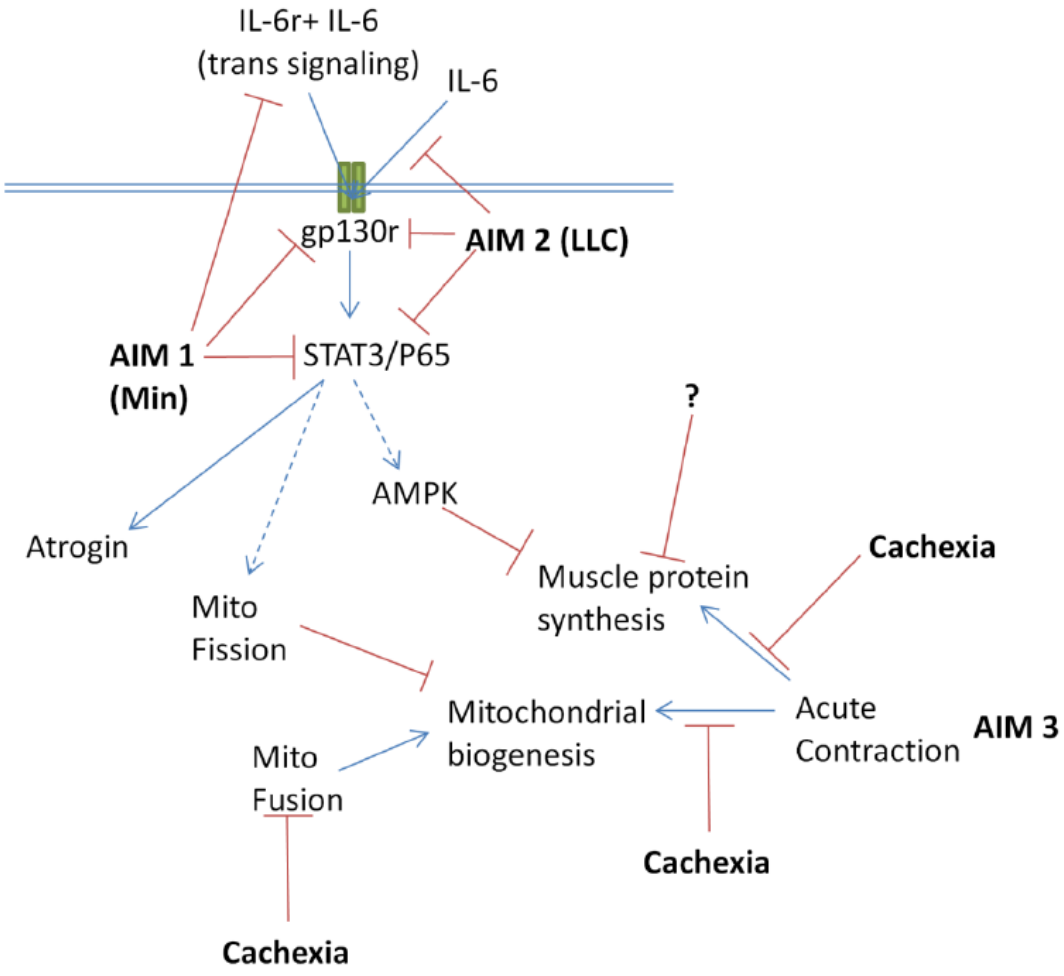

Figure 1.1 Working Model

CHAPTER 2

LITERATURE REVIEW

2.1 Cachexia

Cachexia is a severe condition associated with many chronic diseases that leads to body weight loss comprised of skeletal muscle mass and adipose tissue loss. From the greek root “kakos” meaning bad and “hexis” meaning condition, cachexia leads to increased mortality and morbidity. Cachexia is defined as the unintentional loss of 5% of body weight including muscle and fat mass given an underlying disease. The progression of the disease is classified based on the amount of body weight that has been lost, and body weight loss is positively correlated with mortality (Evans et al., 2008). Many diseases are associated with cachexia including HIV-AIDS, renal failure, diabetes, chronic heart failure, and many cancers (Deans and Wigmore, 2005). Cachexia accounts for approximately 20% of cancer deaths and approximately 40% of colon cancer related deaths (Tan and Fearon, 2008; Tisdale, 2003). Although it is a growing field of research the molecular mechanisms causing the loss of skeletal muscle with cachexia are poorly understood.

The cachectic condition is associated with altered metabolism, chronic inflammation, impaired immune function, and overall weakness, ultimately leading to increased morbidity and mortality (Tisdale, 2009). Although some patients experience anorexia associated with the cachexia, studies have shown nutritional interventions to be ineffective in preventing further weight loss (Grosvenor et al., 1989). Approximately 50% of patients with advanced cancer experience anorexia (Walsh et al., 2000). Several factors may contribute to the decreased appetite in some cachexia patients. Decreases in taste, early satiety, increased brain tryptophan, and increased cytokine production may all lead to anorexia associated cachexia (Tisdale, 2001).

Not all forms of cancer lead to cachexia; however, patients who develop cachexia are more susceptible to a decreased response to chemotherapy, prolonged recovery time, increased risk of infection, and decreased survival after chemotherapy (Esper and Harb, 2005; Evans et al., 2008; Tisdale, 2009; von Haehling et al., 2009). The loss of muscle mass including the diaphragm leads to impaired muscle function, and work capacity ultimately leading to reduced mobility, respiratory function, and a quality of life (O'Gorman et al., 1998; Persson and Glimelius, 2002; Saini et al., 2006; Scott et al., 2003). Therapies and treatments for cancer cachexia are limited due to the lack of knowledge of the causes. While there are currently no approved therapies or treatments for cachexia, the use of animal models has provided valuable insight into the mechanisms of muscle wasting and the development of potential therapeutic targets.

2.2 Models of Cachexia

There are many models of cancer cachexia currently being utilized to understand the condition. Both genetic and tumor implantation models are being used to explore the mechanisms behind skeletal muscle and fat mass atrophy with cancer. As well, cell culture models have also been utilized to further understand the direct impact of specific factors including several different cytokines on muscle mass regulation. While human studies have been conducted, it is difficult to control for tumor burden and rate of cachexia development so many investigators use rodent models of cachexia to minimize confounders while trying to understand the mechanisms of the condition.

Apc$^{Min/+}$

The $Apc^{Min/+}$ (Min) mouse is a widely used model of colon cancer cachexia that is bred on the C57BL/6 background. The Min mouse has a naturally occurring nonsense mutation at codon 850 in the *Adenomatous polyposis coli (Apc)* gene predisposing the animals to multiple intestinal adenomas (Moser et al., 1990). Cachexia is initiated around 16 weeks of age, and the average lifespan of these mice is approximately 20 to 26 weeks (Puppa et al., 2011c). The initiation and progression of cachexia in this mouse is directly related to the intestinal tumor burden and circulating IL-6 levels (Baltgalvis et al., 2009a; Baltgalvis et al., 2008b; Baltgalvis et al., 2010; White et al., 2012a; White et al., 2011a; White et al., 2012c). While many models of cancer cachexia involve rapid development of large tumors, the Min mouse more closely mimics the human condition with a slower development of cachexia and a smaller tumor burden than some of the tumor implantation models.

The Min mouse develops an IL-6 dependent cachexia as demonstrated by Baltgalvis et al, who crossed the Min mouse with the IL-6 knockout mouse (IL-6 KO). The Min IL-6 KO mouse did not develop cachexia; however, when IL-6 was over-expressed in these mice they quickly developed cachexia (Baltgalvis et al., 2008b). The Min mouse has been shown to have a decrease in body weight that corresponds both to tumor burden and to circulating IL-6 levels (Puppa et al., 2011c). Although nobody has identified the exact source of the IL-6, data suggest that the tumor may be secreting large amounts of IL-6. The Min mouse has also been shown to respond to an IL-6 receptor antibody therapy which when given after the initiation of cachexia, after 5% body weight loss, was able to attenuate further muscle and body weight loss without rescuing the decrease in muscle protein synthesis rate (White et al., 2011b). Other work has shown

that exercise training can impair the development of polyps in the intestines and exercise can attenuate muscle loss in the Min mouse in spite of high circulating IL-6 levels (Puppa et al., 2011d). While data show that IL-6 mediates muscle loss in the Min mouse the direct effects of IL-6 signaling on skeletal muscle in the Min mouse remain to be established.

C-26 adenocarcinoma

Another commonly used model is the C-26 adenocarcinoma model of cancer cachexia. In this model C-26 cells are implanted subcutaneously in Balb/c mice. Tumors develop within 14 days and the mice become cachectic very rapidly. While the Min model develops many small intestinal polyps over the course of the first 12 weeks, the C-26 model develops one large tumor that can encompass more than 15% of the animal's total body weight. The C-26 model of cachexia is associated with increases in circulating IL-6 and insulin resistance (Aulino et al., 2010). Inhibition of IL-6 signaling can attenuate wasting and reduce tumor burden in this model of cachexia as seen with the administration of an IL-6 receptor antibody and inhibition of STAT3 signaling in skeletal muscle (Bonetto et al., 2012; Bonetto et al., 2011; Soda et al., 1995; Strassmann et al., 1993; Strassmann et al., 1992; Strassmann and Kambayashi, 1995). Several studies have shown that exercise can slow tumor growth in this model of cancer cachexia and attenuate wasting (al-Majid and McCarthy, 2001). Studies have also shown that pharmaceutical agents to treat insulin resistance associated with muscle wasting, including metformin and rosaglidazone, can attenuate muscle loss and improve overall health of the animals (Asp et al., 2010). While this model is used often and provides many of the hallmarks of the human condition it is a rapid model taking 15-30 days to

develop a 10% loss in body weight and 24% loss in muscle mass (Aulino et al., 2010; Bonetto et al., 2012; Bonetto et al., 2011). The accelerated model taken in combination with the large tumor burden makes this model less like the human condition; but still a valid model to study the mechanisms of cancer cachexia.

Lewis Lung Carcinoma

Another commonly used model is the Lewis Lung Carcinoma (LLC) model of cancer cachexia. Similar to the C-26 model, tumor cells are implanted subcutaneously and allowed to develop into a tumor. These tumors are generally fast growing and can secrete IL-6 and/or TNFα (Wang et al., 2012). Inhibition of TNFα receptor-1 is effective in attenuating muscle wasting in this model (Carbo et al., 2002; Llovera et al., 1998); however, when LLC cells over-expressing IL-6 are transplanted into the C57BL/6 mouse it induces body weight loss without producing detectable levels of TNFα in the plasma (Ohe et al., 1993). Additionally STAT3 has been shown to be elevated in the skeletal muscle of mice implanted with LLC tumor cells (Bonetto et al., 2012). Because the Lewis Lung Carcinoma develops on a C57BL/6 background it makes it a widely used model of cachexia, as many transgenic mice are available on the C57BL/6 background. Inhibition of potential cachectic mediators such as myostatin (Busquets et al., 2012; Murphy et al., 2011), FOXO (Reed et al.), and C/EBPβ (Zhang et al., 2011) have been shown to attenuate muscle mass loss through suppression of protein catabolism pathways demonstrating the complexity of the cachectic condition. In the LLC mouse model of cachexia ATP generation is suppressed and mitochondrial uncoupling is increased (Tzika et al., 2013). However, increasing mitochondrial biogenesis through PGC-1α alone does not prevent the development of cancer cachexia (Wang et al., 2012). Interestingly, PGC-

1α4 transgenic mice have attenuated LLC-induced muscle mass loss that is associated with increases in IGF-1 mRNA and decreases in protein degradation markers (Ruas et al., 2012). These data suggest a potential role for mitochondrial dysregulation in the progression of LLC-induced cachexia. The LLC model of cachexia has been shown to be a reliable model for identifying potential mechanisms in the progression of cancer cachexia.

Mac 16

The murine adenocarcinoma 16 (Mac 16) has been used as a dependable model of cancer cachexia without inducing anorexia (Monitto et al., 2001). The Mac16 tumor model of cachexia uses NMRI nude Balb/c mice as a host (Bing et al., 2000; Bing et al., 2001). Over the course of a month, mice develop a 20-30% loss in body weight after tumor implantation. Associated with the decreased muscle mass and body weight is a decrease in blood glucose levels that is unrelated to food consumption (Bing et al., 2001). While many models of cachexia have been shown to be dependent on cytokine production, the Mac16 model appears to be dependent on a 24kDa glycopeptide and other lipolitic and proteolytic factors (Beck et al., 1990; Lorite et al., 1997; Monitto et al., 2001; Mulligan et al., 1992). Circulating levels of IL-6 are not detectable in this model of cachexia and anti-TNFα antibody therapy was ineffective in preventing the muscle mass loss (Mulligan et al., 1992), suggesting other proteolytic factors are driving disease progression in this model of cachexia.

AH-130

The Yoshida AH-130 cell line has been used to induce cancer cachexia in rats. The AH-130 cell line is derived from hepatoma cells. Cachexia develops very rapidly in this model inducing body weight and muscle mass loss after only seven days of tumor implantation (Costelli et al., 1993; Costelli et al., 2006; Figueras et al., 2005; Tessitore et al., 1987). As well as showing rapid weight loss this model has been widely used to establish altered protein turnover in skeletal muscle with increases in protein degradation without alterations in protein synthesis (Tessitore et al., 1987). Inhibition of the cytokine TNFα, which is constantly secreted by the tumor (Catalano et al., 2003), improves muscle mass through decreases in protein degradation, but does not offer complete protection from cachexia, once again suggesting other mechanisms are involved (Costelli et al., 1993; Costelli et al., 2006).

PROb-BDIX

The PROb BDIX model of cancer cachexia is a rat model that uses cancer cells derived from pancreatic cancer. As well as an increased inflammatory profile the PROb BDIX model develops anorexia (Dumas et al., 2010; Julienne et al., 2012). Because of the development of anorexia associated with the cachexia, this model is widely used to study nutritional interventions. Fish oil can delay the occurrence of anorexia/cachexia in this model but does not completely prevent the muscle mass loss (Dumas et al., 2010). Recently, this model has been used to show a decrease in mitochondrial capacity in skeletal muscle that is not associated with a decrease in the efficiency of the mitochondria to produce energy. As with many of the other models of cachexia, muscle proteolysis appears to be driven by increases in the muscle ubiquitin E3-ligases, MURF-1 and Atrogin (Julienne et al., 2012). While this model is not widely utilized, it develops a rapid

cachexia that is not dependant on the anorexia. More work is required for characterizing this model to use in cachexia research.

Table 2.1. Characterization of rodent models of cancer cachexia. Muscle loss is represented by the % loss in gastrocnemius muscle weight compared to control animals at the same time point.

Model	Background	Tumor origin	Muscle Loss	Cytokines	Time to develop cachexia
$Apc^{Min/+}$	C57BL/6	Intestine/colon	~32-43%(White et al., 2011b)	IL-6	16-20 weeks
C26	Balb/c	Colon	~25-30%(Bonetto et al., 2011)	IL-6	14-21days
LLC	C57BL/6	Lung	~25-36%(Das et al., 2011; Penna et al.)	IL-6, TNFα	13-30days
MAC16	NMRI	Colon	~14-20%(Bing et al., 2000)	-	12-30days
AH-130	Wistar rats	Liver	~37-40%(Tessitore et al., 1987)	TNFα	7-14days
PROb	BDIX rats	Colon	~14-22%(Julienne et al., 2012)	TNFα	35 days

2.3 Inflammation

Chronic inflammation is a problem commonly associated with many disease states. Acute exposure to inflammatory mediators is thought to be beneficial as it aids in the recovery from tissue injury; however long term exposure to inflammation is seen as detrimental to the host and can lead to metabolic dysregulation and protein degradation. Inflammation during cachexia is regulated by pro and anti-inflammatory cytokines. Interleukin-6 (IL-6), IL-1β, Interferon gamma (INFγ), and tumor necrosis factor alpha (TNFα) are the most commonly studied cytokines related to cachexia and muscle wasting (Agustsson et al., 2007; Batista et al., 2012; Grossberg et al., 2010; Kalra and Tigas, 2002; Saini et al., 2006; Tisdale, 2005). Exposure to high levels of either IL-6 or TNFα

has been shown to induce skeletal muscle atrophy in vitro and in vivo without an underlying disease state (De Larichaudy et al., 2012; Dehoux et al., 2007; Frost et al., 1997; Haddad et al., 2005). Both IL-6 and TNFα contribute to muscle mass loss by inducing the ubiquitin proteasome pathway through increases in the muscle specific E3-ligases, atrogin/MAFbx and MuRF-1 (De Larichaudy et al., 2012; Dehoux et al., 2007; Haddad et al., 2005).

Inflammation is increased in the cachectic state and is associated with increased mortality (Deans and Wigmore, 2005). When inflammation is reduced through the use of anti-inflammatory agents improvements in body weight and lean tissue mass have been seen (Solheim et al., 2013). The two predominant inflammatory pathways associated with cancer cachexia are the JAK/STAT pathway activated through the IL-6/gp130 receptor complex, and TNFα acting through the TRAF/TRADD and NFκB pathway. Plasma concentrations of interleukin-6 are correlated with the progression of cachexia in late-stage cancer patients (Iwase et al., 2004) and anti-cytokine therapies have proven to be moderately effective in rodent models of cancer cachexia (Deans and Wigmore, 2005; Jones et al., 2011; Strassmann and Kambayashi, 1995).

Glycoprotein 130 receptor

The glycoprotein 130 (gp130) receptor is the IL-6 signal transducer and is a transmembrane receptor for the IL-6 family of cytokines. Found on chromosome 5q11, gp130 is ubiquitously expressed in tissues throughout the body and systemic deletion of the receptor is embryonic lethal (Rodriguez et al., 1995; Saito et al., 1992; Yoshida et al., 1996). Several different cytokines signal through the gp130 receptor forming either a

heterodimer or homodimer with the cytokine, its receptor and gp130. Some of these cytokines include interleukin-11 (IL-11), ciliary neurotrophic factor (CNTF), leukemia inhibitory factor (LIF), oncostatin M (OSM), and interleukin-6 (Heinrich et al., 2003; Kishimoto et al., 1995). Upon dimerization, gp130 leads to the downstream activation of the JAK/STAT pathway.

The gp130 receptor is composed of an Ig-like binding domain and five fibronectin type III (FNIII) repeats on the extracellular portion of the receptor. The first two FNIII repeats form the cytokine binding module. The transmembrane domain is followed by the box1 and box2 regions and the leucine motif where Jak/STAT3 activation occurs on tyrosine residues (Heinrich et al., 2003). Mutations in the intracellular region of the gp130 receptor leads to inactivation of the Jak/STAT pathway and IL-6 receptor signaling (Haan et al., 2002; Stahl et al., 1994).

Gp130 is a potential therapeutic target for diseases involving chronic inflammation such as insulin resistance and obesity (Febbraio, 2007). Early increases of gp130 have been observed in the skeletal muscle of diabetic mice (Toledo-Corral and Banner). Activation of the gp130 receptor through binding of CNTF or IL-6 has been shown to activate AMP-activated protein kinase (AMPK), a regulator of metabolism, and enhance glucose uptake and fatty acid oxidation (Kelly et al., 2004; Watt et al., 2006). Watt et al showed that gp130 in the presence of IL-6R is sufficient for AMPK activation and is not dependent on STAT3 activation. Additionally, gp130 is necessary for the CNTFR and IL-6R activation of AMPK (Watt et al., 2006). These data suggests that gp130 may be a key regulator of ATP turnover and AMPK activity; however, the specific role of skeletal muscle gp130 in the regulation of cancer cachexia is unknown.

Interleukin 6

Interleukin 6 (IL-6) is a pleiotropic cytokine expressed throughout the body. IL-6 is a 26 kDa protein mainly secreted from T cells and macrophages to produce an immune response; however, other tissues can also secrete the cytokine. Although very controversial in its role, IL-6 can operate as both a pro-inflammatory cytokine and an anti inflammatory cytokine. IL-6 acts through binding the IL-6 receptor which binds the gp130 receptor forming a homodimer complex that activates downstream signaling (Schwantner et al., 2004). Several intracellular signaling pathways can be activated by the IL-6-gp130 interaction including JAK/STAT, RAS/ERK, and PI3K/Akt (Ernst and Jenkins, 2004; Heinrich et al., 1998). IL-6 binds the IL-6r either in its soluble form or it binds membrane bound IL-6r. The IL-6 receptor and the gp130 are both type 1 membrane proteins meaning that they have one transmembrane domain and an extracellular N-terminus. The IL-6 receptor then binds with the gp130 on the membrane causing gp130-homodimerization. Once the homodimer is formed it autophosphorylates tyrosine residues of the gp130 allowing for STAT3 to bind, phosphorylate, and dimerize leading to nuclear translocation and up regulation of STAT3 activated genes.

IL-6 also acts as a myokine that is it is secreted from skeletal muscle to work in an autocrine/paracrine fashion signaling skeletal muscle responses. As well as being secreted from skeletal muscle IL-6 is secreted from adipose tissue and as part of the innate immune response. IL-6 is elevated in skeletal muscle during contraction and may activate usage of extracellular substrates for fuel during contraction (Febbraio and Pedersen, 2005; Petersen and Pedersen, 2005); however, chronic exposure to IL-6 can

lead to skeletal muscle atrophy through induction of protein degradation and alterations in mitochondrial dynamics (Haddad et al., 2005; White et al., 2012c).

IL-6 is elevated in many different cachectic conditions including obesity, arthritis, HIV/AIDS, COPD, and cancer; however; a complete knockout of IL-6 may also be detrimental as shown by the fact that IL-6 knockout mice develop mature onset insulin resistance and obesity (Wallenius et al., 2002). The initiation and progression of some cachexia models is directly related to tumor burden and circulating IL-6 levels (Baltgalvis et al., 2008b; White et al., 2011b). Our lab has shown that IL-6 is directly related to cachexia severity in the Min mouse (Baltgalvis et al., 2008b; Puppa et al., 2011c) and inhibition of IL-6 through use of an IL-6 receptor antibody or IL6KO mice attenuates/prevents the development of cachexia (Baltgalvis et al., 2008b; White et al., 2011b). During cachexia, IL-6 may act on the tumors, stimulating growth and differentiation, or IL-6 may act directly on peripheral tissues, such as skeletal muscle, that are atrophying. Skeletal muscle is one target of IL-6 that may be contributing to the overall decline in health with the progression of cachexia and muscle loss. IL-6 is known to decrease muscle protein synthesis and increase degradation leading to a loss in skeletal muscle. Recent studies have demonstrated that inhibition of downstream signaling, STAT3, or of the IL-6 receptor attenuated muscle mass loss in animal models of cachexia (Bonetto et al., 2012; Bonetto et al., 2011). Over expression of IL-6 and IL-6 family members can induce cachexia in animal models and can induce atrophy in C2C12 myotubes, but exercise in the presence of increase IL-6 is able to attenuate the cachectic condition (Baltgalvis et al., 2008b; Bonetto et al., 2012; Bonetto et al., 2011; Puppa et al.,

2011d). These data indicate a need for further investigation on the mechanisms of IL-6 action during cancer cachexia.

Classical vs. Trans IL-6 signaling

Unlike the gp130 that is ubiquitously expressed the IL-6 receptor is limited in its expression (Jones et al., 2001). IL-6 can act on tissues in two ways. Classical signaling of IL-6 occurs when IL-6 binds the membrane bound IL-6Rα, this causes dimerization of the gp130 receptor allowing for the activation of downstream targets. The second way that IL-6 can act on tissues is through trans signaling. In trans signaling circulating IL-6 binds to the soluble IL-6 receptor. Soluble IL-6r is formed through one of two mechanisms. The ectodomain of the IL-6 receptor can be cleaved from T cells by ADAM17 resulting in the shedding of soluble IL-6r or it can be produced through translation of alternatively spliced IL-6r mRNA (Briso et al., 2008; Rose-John, 2012). Once IL-6 is bound to the soluble IL-6r it can bind to gp130 on any tissue type and activate IL-6 target genes in tissues that would normally be unresponsive to IL-6.

The roles for classical and trans signaling are still relatively unexplored; however, there is some evidence showing a potential for targeting trans signaling to alleviate symptoms of arthritis and cancer. Furthermore, IL-6 trans signaling has been implicated in a more pro-inflammatory response to stimuli, whereas, classical signaling is thought to have more anti-inflammatory properties (Rose-John, 2012). Dr. Rose-John has successfully developed a fusion protein to inhibit IL-6 trans signaling both in vitro and in vivo (Atreya et al., 2000; Barkhausen et al.; Jones et al., 2011; Lo et al., 2011; Nechemia-Arbely et al., 2008; Nowell et al., 2003; Rose-John, 2012; Waetzig and Rose-John, 2012).

Inhibition of the soluble IL-6r and IL-6 trans signaling in experimental models of arthritis and colitis lead to improvements in disease outcomes (Atreya et al., 2000; Klover et al., 2003; Nowell et al., 2003). We have shown that inhibition of both classical and trans IL-6 signaling together prevents the loss of muscle mass in the Min mouse partially through improvements in muscle mitochondrial content and dynamics and attenuation of protein degradation without alterations in protein synthesis (White et al., 2012c). The role of IL-6 trans signaling in the regulation of skeletal muscle mass and mitochondrial biogenesis during cachexia requires further investigation.

2.4 Skeletal Muscle Mitochondria

The mitochondria are vital to the proper function of skeletal muscle. Many people consider the mitochondria to be the powerhouse of the cell, being in charge of ATP generation; however this is not its only function. The mitochondria also regulate signaling related to apoptosis, autophagy, and protein turnover (Romanello and Sandri, 2010). Despite the textbook images of mitochondria looking like a nice rounded almost kidney bean shape, the mitochondria actually form a complex network weaving throughout the muscle and is constantly undergoing dynamic changes. Skeletal muscle mitochondria are divided into two distinct populations each having specific functions. The subsarcolemma fraction (SS), located directly under the plasma membrane, accounts for approximately 20% of the muscle's mitochondria (Hoppeler, 1986). SS mitochondria are mainly responsible for providing energy for transport of substrates and signaling that occurs at the plasma membrane. The intermyofibrillar fraction (IMF) of mitochondria is located between the myofibrils, closer to the contractile elements. The main function of the IMF fraction is providing ATP for muscle contraction. Skeletal muscle has a high

energy demand so without either of these two populations of mitochondria the muscle is unable to properly function.

Mitochondria are highly plastic and adapt readily to changes in the surrounding environment. Up regulation of mitochondria is required for muscle to adapt to additional energy demands that are placed on the muscle such as that from exercise. Mitochondrial biogenesis occurs through several signaling pathways. Mitochondrial biogenesis occurs when stress, from exercise for example, is placed on the muscle. This stress activated the energy sensor AMPK to signal for decreases in energy consuming processes such as protein synthesis and increases in processes to produce energy including mitochondrial biogenesis. AMPK up regulates the peroxisome-proliferator gamma-activated receptor coactivator (PGC)-1α (Jager et al., 2007; Zong et al., 2002), a well accepted control protein for mitochondrial biogenesis. PGC-1α has been shown to up regulate nuclear encoded mitochondrial proteins (NUGEMPs) through translocation to the nucleus and association with transcription factors (Wu et al., 1999). Not only does PGC-1α help to up regulate mitochondrial protein transcription, it can act in a positive feedback to up regulate itself. Recent literature has shown that mTOR is important in the regulation of PGC-1α and can operate with PGC-1α to activate the transcription of many oxidative genes (Cunningham et al., 2007). When the mTOR complex is inhibited there is a severe decrease in muscle oxidative capacity and function (Schieke et al., 2006) suggesting that mTOR is an important mediator for the maintenance of mitochondria.

As well as playing a role in protein synthesis the mitochondria play a vital role in protein degradation, apoptosis, and autophagy. One way in which the mitochondria can work to regulate protein degradation is through regulation of FOXO3. Mitochondrial

fission can induce phosphorylation and activation of AMPK which regulates FOXO3 and atrogenes independently of activation of Akt. When FOXO is blocked even in the presence of mitochondrial fission, muscle atrophy is prevented (Romanello et al.). When FOXO3 is blocked in healthy skeletal muscle hypertrophy and growth of the muscle occur (Reed et al.).

Mitochondrial Dynamics

As mentioned previously, mitochondria are quite dynamic, constantly undergoing morphological changes to adapt to the cellular conditions. The processes regulating these mitochondrial dynamics are called mitochondrial fission and fusion (Yaffe, 1999). Mitochondrial fission is the process of a mitochondrion separating into two, similar to cellular division, whereas mitochondrial fusion is the process of two mitochondria coming together to form one larger mitochondrion. Fission is regulated through the expression of dynamin related protein-1 (DRP1) and Fis1. DRP1 locates on the outer mitochondrial membrane where it is thought to associate with Fis1 to signal for fission of the mitochondria (Benard and Karbowski, 2009; Romanello and Sandri). The exact mechanisms of mitochondrial fission are unclear; however the inhibition of Fis1 can reduce autophagy in skeletal muscle (Romanello et al.). Fission may be important for the maintenance of healthy mitochondrial function by targeting dysfunctional mitochondria for autophagy/degradation. Fusion of the mitochondria is regulated by mitochondrial fusion proteins, mitofusin 1 and 2 (Mfn1/Mfn2), and optic atrophy protein 1 (OPA1). Mfn1/2 localize on the outer mitochondrial membrane and act to tether the two fusing mitochondria together (Koshiba et al., 2004) whereas OPA1 is found on the inner mitochondrial membrane and may act as an anchor during the fusion process and may

assist in the fusion of the inner mitochondrial membranes (Benard and Karbowski, 2009). Mitochondrial fusion has been shown to help regulate mitochondrial DNA stability. MFN2 is decreased in skeletal muscle of obese individuals and may have a role in the regulation of skeletal muscle metabolism (Mingrone et al., 2005). Inhibition of mitochondrial fusion in mice leads to decreases in mitochondrial DNA and ultimately muscle atrophy (Chen et al., 2010). While tightly regulated by many genes MFN2 has been shown to be regulated by both PGC-1α and PGC-1β (Liesa et al., 2008; Soriano et al., 2006). The expression of mitochondrial fission and fusion proteins are tightly correlated with mitochondrial enzyme activity and levels of PGC-1α (Garnier et al., 2005). Disruption of mitochondrial dynamic can lead to many diseases such as insulin resistance and mitochondrial myopathies (Liesa et al., 2009).

2.5 Cachexia and Mitochondrial Loss

Loss of muscle mass in cancer cachexia is in part due to loss and dysregulation of mitochondria, which is a prominent feature of many wasting conditions (Li et al., 2007; Romanello et al.; White et al.). Both oxidative and gylcolytic hindlimb muscles have reduced mitochondrial content, and oxidative protein expression in severe cachexia (White et al., 2011a; White et al., 2012c). The loss of muscle oxidative capacity in the later stages of cachexia also corresponds with severe insulin resistance as seen by the inability to clear glucose during a glucose tolerance test late in cachexia (Puppa et al., 2011c). The loss of mitochondria and increase in fission appear to be pivotal in the regulation of skeletal muscle mass with the progression of cachexia directly relating to disease state. Recently, cachexia was shown to decrease skeletal muscle oxidative capacity; however this decrease was not associated with alterations in mitochondrial ATP

production efficiency (Julienne et al., 2012). The overall ability of skeletal muscle to produce ATP is decreased in tumor bearing mice, which could be contributing the increased fatigue in the cachectic patient (Tzika et al., 2013). Interestingly, PGC-1α transgenic mice are not protected from muscle mass loss despite increased mitochondrial content (Wang et al., 2012); however, overexpression of PGC-1α4 can prevent cancer induced muscle mass loss and is shown to regulate skeletal muscle hypertrophy (Ruas et al., 2012). The regulation of muscle hypertrophy by the mitochondria is relatively unexplored and required further investigation.

Inhibition of systemic and skeletal muscle inflammatory signaling may be one approach to decreasing muscle wasting. Inhibition of systemic IL-6 signaling after the initiation of cachexia can increase mitochondrial biogenesis, decrease mitochondrial fission, and increase mitochondrial fusion (White et al., 2012c). Additionally inhibition of other inflammatory signaling including NFκB and MAPK can restore muscle mass, increase muscle force, and improve mitochondrial complex activity in cachectic rodents (Fermoselle et al., 2013). Inhibition of IL-6, NFκB, and MAPK in these experiments leads to decreased tumor burden making it difficult to understand if the effects on muscle mitochondria are directly related to the tumor burden. Other therapeutic interventions such as the administration of nutraceuticals, anti-oxidants, or exercise are shown to have beneficial effects on muscle wasting (Fermoselle et al., 2013; Siddiqui et al., 2009). Anti-oxidant therapy can increase mitochondrial function without altering the tumor burden; however, there was no improvement in muscle mass suggesting that improvements in mitochondrial capacity alone are not sufficient to prevent muscle wasting (Fermoselle et al., 2013).

2.6 Skeletal Muscle Protein turnover

Skeletal muscle comprises about 40% total body weight in humans and is vital for all movement (Zhang et al., 2007) and loss of skeletal muscle mass can lead to decreased quality of life. Not only is skeletal muscle vital to moving the body, but it is also the main amino acid reservoir of the body for other tissues. Skeletal muscle mass is maintained by a balance of protein synthesis and protein degradation. Alterations in the balance will result in muscle growth (increased synthesis or decreased degradation) or muscle mass loss (decreased synthesis or increased degradation). Skeletal muscle loss is a potent factor in the progression of the cachexia and therapies to attenuate muscle loss are being investigated.

Protein synthesis

Skeletal muscle protein synthesis is regulated by several factors. Nutrient status, hormones, use, and inflammatory signaling can all impact the rates of protein synthesis. The common regulatory point of the different pathways that controls protein synthesis is the mammalian target of rapamyocin (mTOR). Increases in nutrient availability will lead to the up-regulation of protein synthesis through increases in insulin signaling through the IGF-1/PI3K/AKT pathway. Nutrient availability can further increase protein synthesis by relieving the AMPK inhibition of mTOR. This occurs by preventing AMPK from phosphorylating TSC2, an inhibitor of mTOR activity (Bolster et al., 2002). The exact mechanism of hormones on the regulation of protein synthesis is not fully understood; however, androgen depletion induces suppressed protein synthesis associated with increased expression of REDD1, an inhibitor of mTOR, and decreased IGF-1 (White et

al., 2013a). Contraction is another stimulus that can regulate skeletal muscle protein synthesis. Contraction is thought to act through both the IGF-1/AKT pathway to up-regulate mTOR as well as through MAPK/ERK signaling cascade. Once mTOR is activated it phosphorylates p70S6 kinase, leading to increase S6 ribosomal protein, and 4EPB1 which relieves the repression of eIF-4E and increases translation initiation (Glass, 2005).

Cancer cachexia is associated with decreased skeletal muscle protein synthesis and anabolic resistance (Tisdale, 2009). During cancer cachexia an increase in AMPK activity as well as a suppression of IGF-1 is observed and contributes to the suppressed protein synthesis (White et al., 2011b; White et al., 2013b). While IL-6 can directly decrease protein synthesis in C2C12 myotubes, the inhibition of IL-6 after the initiation of cachexia has no effects on skeletal muscle protein synthesis (White et al., 2011b). Additionally, IL-6 in the presence of insulin is able to increase markers of protein synthesis in C2C12 myotubes, but this anabolic plasticity is lost in cachectic mice. Inhibition of AMPK through the administration of Compound C can also relieve IL-6 inhibition of protein synthesis marker in cell culture (White et al., 2013b). Interestingly exercise, even under conditions of inflammation, can increase markers of protein synthesis in skeletal muscle of Min mice, while treadmill exercise displayed no improvements in protein synthesis were seen in a mouse model of chronic kidney disease, however the duration of this exercise was significantly less than in the Min model (Wang et al., 2009; White et al., 2011b). Overloading the plantaris muscle during chronic kidney failure-induced cachexia does result in improvements in muscle protein synthesis (Wang

et al., 2009). These data suggest exercise may be able to override the cachexia-suppression of muscle protein synthesis despite increased systemic inflammation.

Protein Degradation

While the multiple pathways that regulate protein synthesis seem to converge at mTOR, signals regulating protein degradation appear to converge at FOXO. FOXO activation allows proteins to be targeted for degradation by the ubiquitin proteasome pathway and evidence shows that FOXO is important for degradation through autophagy. Phosphorylation of FOXO causes FOXO to be sequestered in the cytosol making it inactive. Upon dephosphorylation FOXO enters the nucleus to up-regulate transcription of several E3 ligases including MURF and Atrogin-1 (Ramaswamy et al., 2002). The E3 ligases then tag the proteins for degradation by placing a ubiquitin tag on the protein. Once tagged the protein is degraded by the proteasome.

The role of protein degradation during cancer cachexia has been well established. Both ATP dependant and independent degradation is increased during cancer cachexia (White et al., 2011b). Inflammatory signaling appears to be a potent mediator of cachexia-induced muscle proteolysis. Administration of IL-6 to C2C12 myotubes increases atrogin-1 protein expression (White et al., 2013b). Inhibition of systemic IL-6 signaling can attenuate ATP dependant protein degradation in cachectic mice (White et al., 2011b). Skeletal muscle inhibition of STAT3 and FOXO3 have both been shown to decrease muscle degradation pathways and improve overall skeletal muscle mass (Bonetto et al., 2012; Bonetto et al., 2011; Reed et al., 2012). While inhibition of muscle protein degradation can attenuate skeletal muscle mass during the cachectic condition, the

long term ramifications of suppressed protein degradation are unknown. Inhibition of protein degradation alone may lead to muscle dysfunction through the accumulation of damaged proteins; however, this remains to be investigated.

2.7 A Role for Exercise with Cachexia

In healthy individuals, mitochondrial protein content of PGC-1α, citrate synthase, and mitochondrial creatine kinase are directly correlated with mitochondrial fusion, and fusion and are associated with increased exercise capacity (Garnier et al., 2005). Exercise training can successfully attenuate the cachectic condition when started prior to the onset of cachexia, even in the presence of high circulating cytokines (Puppa et al., 2011a). One possible mechanism for the protective effects of exercise is the increase in mitochondrial capacity. Exercise training has a large impact on mitochondrial capacity in skeletal muscle. One of the main changes in skeletal muscle with exercise training is the increase in mitochondrial capacity and content (Holloszy and Coyle, 1984). Repeated bouts of exercise show progressive and sustained increases in several mitochondrial proteins such as PGC-1α, mitochondrial transcription factor A (Tfam), and nuclear respiratory factors (NRF) (Baar et al., 2002; Gordon et al., 2001; Hood et al., 2006) which allow for mitochondrial biogenesis and increased mitochondrial function. As well as increasing mitochondrial biogenesis exercise training can increase expression of mitochondrial fusion proteins and decrease mitochondrial fission proteins (White et al., 2012c). Such changes may increase mTOR and reduce the chronic activation of AMPK and FOXO seen in cachexia thus suppressing protein degradation and inducing synthesis.

It is widely accepted that cancer cachexia affects glycolytic muscle prior to affecting the more oxidative muscles. By increasing the mitochondrial capacity of skeletal muscle, making it more oxidative, the muscle may be protected. Exercise may be one potential therapeutic approach to combat this issue. The affects of exercise after the onset of cachexia and muscle loss are unknown. Exercise induces expression of fission related proteins immediately post; however, there is up regulation of mitochondrial fusion proteins and biogenesis after exercise. Although the cachectic muscle already has increases in fission and decreased mitochondrial content, exercise may be able to reverse this condition and return the muscle to a state in which fully functional mitochondria are present. Several studies have shown that SS mitochondrial are more susceptible to change than the IMF mitochondria (Menshikova et al., 2006). Research still needs to be done to determine if the loss of mitochondria in cancer cachexia is specific to the SS population or if it extends to the IMF population. It is reasonable to assume that IMF mitochondria are decreased with severe cachexia considering the fact that the SS population only accounts for approximately 20% of muscle mitochondria and a decrease in IMF mitochondria would correlate with the decrease in muscle mass and force production. Once the muscle mass has been lost and the muscle is in a catabolic state it may not be able to be returned to the pre catabolic state, however exercise may be able to prevent further loss of muscle mass. More research needs to be done to examine the effects of exercise on muscle after the initiation of cachexia and if exercise after onset of cachexia is able to restore normal mitochondrial dynamics and function. Research investigating the effects of resistance exercise on cachectic patients' ability to hypertrophy muscle is lacking and is an area for further investigation.

Few studies have looked at the effect of an acute bout of exercise on the regulation of mitochondrial fission and fusion. What research has been conducted demonstrates that mitochondria fission is increased after an acute bout of exercise while mitochondrial fusion is suppressed (Bo et al.; Cartoni et al., 2005; Ding et al.). Although there is little research available about the changes in mitochondrial dynamics with an acute bout of exercise, a wide body of literature shows that exercise, even an acute bout, up-regulates mitochondrial biogenesis, partially through the activation of AMPK. After an acute bout of exercise PGC-1α is rapidly up-regulated leading to a subsequent increase in mitochondrial associated gene transcription and mitochondrial biogenesis (Baar et al., 2002; Pilegaard et al., 2003). Up-regulation of these genes persists for up to 4 hours before returning to baseline levels (Pilegaard et al., 2000). Since the effects are short lived it shows the importance of regular physical activity to increase mitochondrial capacity. As well as increases in mitochondrial capacity, insulin sensitivity is increased immediately following an acute bout of exercise, in part due to the up-regulation of genes regulating glycolysis and fatty acid oxidation and overall improvements of metabolic flexibility.

Exercise is well known to help improve insulin sensitivity, and is commonly used to treat insulin resistance in various disease states including diabetes (Hawley, 2004), cachexia, and obesity (Bradley et al., 2008; Duncan et al., 2003). In healthy rodents, exercise improves both glucose tolerance (James et al., 1983) and insulin sensitivity (James et al., 1984). The exact mechanism is still unclear, however potential mechanisms by which exercise can improve insulin resistance are to reduce inflammation (Kondo et al., 2006; Mattusch et al., 2000), improve muscle respiratory capacity (Holloszy, 1967;

Mole et al., 1971; Oscai and Holloszy, 1971) and improve insulin signaling (Houmard et al., 1999). Both acute bouts of exercise and exercise training can have positive effects on insulin sensitivity. After an acute bout of exercise insulin sensitivity is increased for at least 16 hours and the effects can last up to 48 hours. These improvements in insulin sensitivity most likely stem from increases in skeletal muscle glucose transporter type 4, GLUT4, protein content and increased translocation of GLUT 4 to the plasma membrane. GLUT4 is a glucose transporter protein that is spread throughout the cytoplasm in the rested state. After ingestion of glucose or after exercise, GLUT4 moves from the cytosol and associates with the plasma membrane to take up glucose into the cell to be used as energy. GLUT4 can be stimulated both by insulin and by contraction. In the insulin resistant individual GLUT4 expression is not decreased in the skeletal muscle, but insulin stimulated signaling is suppressed (Handberg et al., 1990; Kahn, 1992) . The acute effects of exercise on glucose uptake occur in an insulin independent manner and rely mainly on the contraction stimulated increase in GLUT4 translocation (Brozinick et al., 1992; King et al., 1993). As mentioned previously these effects are short lived and if another bout of exercise or muscle contraction is not conducted the cells will return to the pre exercise state.

Improvements in lipid metabolism are important for the maintenance of insulin sensitivity. When there is an accumulation of lipid in the body it can inhibit insulin signal transduction. Exercise up regulates lipid oxidation and improves mitochondrial capacity to perform beta oxidation. While mitochondrial capacity is decreased in cancer cachexia (White et al., 2011a) exercise training is able to up regulate mitochondrial capacity even in conditions when cancer and inflammation are present (Puppa et al., 2011a). Skeletal

muscle mitochondrial function plays a pivotal role in muscle glucose uptake, and impairments in the oxidative capacity have been associated with insulin resistance (Lanza and Nair, 2009; Morino et al., 2006). Altered mitochondria content is also related to a diminished ability of muscle to efficiently oxidize fatty acids, leading to decreased muscle metabolic flexibility (Chomentowski et al.). The loss of muscle oxidative capacity in cancer cachexia corresponds with severe insulin resistance as seen by the inability to clear glucose during a glucose tolerance test late in cachexia (Puppa et al., 2011c). Training maintains the increased levels of mitochondria and improves metabolic flexibility. As metabolic flexibility is improved, insulin sensitivity is also improved.

Exercise training can result in long term improvements on insulin sensitivity. Insulin acts through the PI3K signaling pathway to up regulate protein synthesis and muscle glucose uptake. PI3K has been shown to be decreased in insulin resistant individuals (Goodyear et al., 1995) and is one reason for the decrease in insulin stimulated translocation of GLUT4 with insulin resistance. Exercise increases PI3K signaling potentially through increases in the insulin receptor substrate; however the evidence is variable as reviewed by Hawley et al (Hawley and Lessard, 2008). PI3K activates downstream signaling to enhance glucose uptake and improve insulin sensitivity. As well as increasing the ability of insulin to activate its signaling cascade directly exercise training causes an increase in the activation of AMPK. As mentioned earlier AMPK is an energy sensor for the cell and can regulate lipid metabolism, protein synthesis, mitochondrial biogenesis and glucose uptake, which are all dysregulated in cancer. Exercise training increases protein levels of AMPK, but despite the increase in AMPK exercise training induced an increase in muscle protein synthesis even in the

cachectic condition. The increased muscle protein synthesis rates are due to activation of the IGF-1 Akt/mTOR pathway that is suppressed in cancer cachexia (White et al., 2011b). Exercise is also able to attenuate the chronic activation of AMPK that is seen with severe muscle wasting (Puppa et al., 2011a; White et al., 2011b). The improvements in the regulation of AMPK activity may be due to the improvements in glucose uptake which could alleviate the energy stress that is placed on the muscle due to the cancer and metabolic inflexibility.

Exercise and IL-6

Exercise benefits have been well documented in patients with many chronic diseases, and exercise is widely recommended for obese and insulin resistant patients. Exercise has the potential to challenge systemic disorders and local intracellular signaling that regulates muscle homeostasis. The potential beneficial effects of exercise are dependent on many variables, including exercise type (i.e., endurance or resistance), and whether the muscle responses are induced by a single acute bout of exercise, or an adaptation occurring because of repeated exercise bouts. We have published that treadmill exercise trained cachectic mice over-expressing IL-6 are not susceptible to body weight and muscle mass loss despite elevated muscle inflammatory signaling (Puppa et al., 2011d). IL-6 is known to be a key player in the adaptations to skeletal muscle contraction. Skeletal muscle is known to be an endocrine organ that can secrete IL-6 after contraction and plays a role in muscle metabolism. IL-6KO mice have been used to study the necessity of IL-6 for exercise and load induced adaptations, and IL-6KO mice have been shown to have altered adaptations. IL-6KO mice that have undergone synergistic ablation have been shown to have decreased myonuclei number and decreased satellite

cell activation (Serrano et al., 2008) and have been shown to have an increase in extracellular matrix remodeling and non contractile tissue (White et al., 2009) after overload. It has also been reported that IL-6KO mice have a decreased endurance capacity, an increased fat mass, and decreased oxygen consumption during exercise by 8 months of age (Faldt et al., 2004). Related to muscle protein and mitochondrial responses to exercise, Kelly et al. demonstrated that activation of AMPK is suppressed in IL-6KO mice and there was lower activation of AMPK after exercise compared with the wild type controls (Kelly et al., 2004). After a bout of exercise, high fat diet (HFD) fed IL-6KO mice showed decreased glucose uptake in the EDL and these mice with access to wheels still developed a decreased systemic insulin sensitivity (Benrick et al., 2012). Since AMPK is a key player in mitochondrial biogenesis and regulating protein synthesis these data suggest that there will be alterations in these parameters; however, this remains to be examined. While these studies have shown that a systemic IL-6 knockout has alterations in skeletal muscle adaptations some of which could be induced by the lack of IL-6 on other tissues such as the liver and adipose tissue where IL-6 is known to play a vital role, the direct role of IL-6 signaling on skeletal muscle remains to be examined in healthy or diseased models.

2.8 Conclusion

Taken together the current body of literature displays many gaps in understanding the regulation of muscle mass during cancer cachexia and the direct role of IL-6 family signaling on muscle protein turnover and mitochondrial biogenesis and function in skeletal muscle. While we understand that mitochondrial biogenesis and content are suppressed during cachexia, we do not know what is causing the loss. It could be that

decreases in substrate availability lead to degradation of dysfunctional mitochondria in an attempt to preserve the tissue, or inflammation could be directly targeting the mitochondria leading to dysfunction and loss. A wide body of literature shows up regulation of mitochondrial content with exercise and contraction. Exercise, which induces an acute inflammatory response, prior to the development of severe cachexia is able to attenuate the condition and is associated with improved skeletal muscle homeostasis. The current proposal aims to understand the role of inflammation in dysregulation of the mitochondria during cachexia and if an acute bout of contraction can induce mitochondrial changes in severely cachectic animals.

CHAPTER 3

THE ROLE OF SYSTEMIC AND MUSCLE IL-6 SIGNALING ON MITOCHONDRIAL LOSS DURING THE PROGRESSION OF CANCER CACHEXIA IN THE *APC*$^{MIN/+}$ MOUSE[1]

[1] Melissa Puppa, Aditi Narsale, Stefan Rose-John, Angela Murphy, Greg Hand, Raja Fayad, and James Carson. To be submitted.

3.1 Abstract

The interleukin-6 (IL-6) family of cytokines and their associated signaling is implicated in cachexia development and progression. IL-6 activates gp130/STAT by signaling through either classical or trans IL-6 signaling. The *Apc*$^{Min/+}$ (Min) mouse develops an IL-6 dependent cachexia. We have previously demonstrated that systemic inhibition IL-6 signaling after the initiation of cachexia attenuates progression of cachexia and improves signaling regulating mitochondrial dysfunction. We have also demonstrated that inhibition of muscle gp130 in LLC implanted mice attenuates cachexia. Therefore, the purpose of this study was to examine the role of IL-6 trans signaling and local gp130 signaling on skeletal muscle mitochondrial regulation during cachexia. To inhibit trans signaling Min mice were administered sgp130Fc (150ug, 1/wk) for two weeks after the initiation of cachexia, and skeletal muscle knockout of gp130 (skm-gp130) in the Min mouse was used to examine the muscle gp130. Administration sgp130Fc attenuated body weight and muscle mass loss in Min mice, while skm-gp130 did not attenuate muscle mass loss. STAT3 and AMPK which were elevated with cachexia were suppressed with sgp130Fc and in skm-gp130 Min mice. Loss of mitochondrial oxidative capacity was attenuated with sgp130Fc and skm-gp130. While mitochondrial fission was inhibited by sgp130Fc, skm-gp130 attenuated cachexia-induced MFN loss. These data point to differential roles of IL-6 trans signaling and muscle gp130 signaling for the regulation of skeletal muscle mitochondrial loss during cancer cachexia in the Apc$^{Min/+}$ mouse. Further work is necessary to delineate the contribution of IL-6 trans signaling on other tissues to the pathogenesis of cachexia.

Key Words: Muscle, Trans IL-6, Cancer Cachexia, Apc$^{Min/+}$

3.2 Introduction

Chronic inflammation is a hallmark of cachexia. IL-6 is elevated in many different cachectic conditions including obesity, arthritis, HIV/AIDS, COPD, and cancer; however; a complete knockout of IL-6 may also be detrimental as shown by the fact that global IL-6 knockout mice develop mature onset insulin resistance and obesity (Wallenius et al., 2002). The initiation and progression of cachexia in the $Apc^{Min/+}$ (Min) mouse is directly related to tumor burden and circulating IL-6 levels (Baltgalvis et al., 2008b; White et al., 2011b). Our lab has shown that IL-6 is directly related to cachexia severity in the Min mouse (Baltgalvis et al., 2008b; Puppa et al., 2011c) and inhibition of IL-6 through use of an IL-6 receptor antibody or IL6KO mice attenuates/prevents the development of cachexia (Baltgalvis et al., 2008b; White et al., 2011b). During cachexia, IL-6 may act on the tumors, stimulating growth and differentiation, or IL-6 may act directly on peripheral tissues, such as skeletal muscle, that are atrophying. Skeletal muscle is one target of IL-6 that may be contributing to the overall decline in health with the progression of cachexia and muscle loss. Recent studies have demonstrated that inhibition of STAT3 or of the IL-6 receptor attenuated muscle mass loss in animal models of cachexia (Bonetto et al., 2012; Bonetto et al., 2011). Over expression of IL-6 and IL-6 family members can induce cachexia in animal models, but exercise in the presence of increase IL-6 is able to attenuate the cachectic condition (Baltgalvis et al., 2008b; Bonetto et al., 2012; Bonetto et al., 2011) leaving the direct role of IL-6 on skeletal muscle function during cachexia unexplored.

Unlike the gp130 that is ubiquitously expressed the IL-6 receptor is limited (Jones et al., 2001). IL-6 can act on tissues in two ways. Classical signaling of IL-6 occurs when

IL-6 binds the membrane bound receptor, this causes dimerization of the gp130 receptor allowing for the activation of downstream targets. In trans signaling the soluble IL-6 receptor can bind to gp130 on any tissue type and activate IL-6 target genes since gp130 is ubiquitously expressed. The roles for classical and trans signaling are still relatively unexplored; however, there is evidence showing a potential for targeting trans signaling to alleviate symptoms in arthritis and cancer. Furthermore, IL-6 trans signaling has been implicated in a more pro-inflammatory response to stimuli, whereas, classical signaling is thought to have more anti-inflammatory properties (Rose-John, 2012). Dr. Rose-John has successfully developed a fusion protein to inhibit IL-6 trans signaling both in vitro and in vivo (Atreya et al., 2000; Barkhausen et al.; Jones et al., 2011; Lo et al., 2011; Nechemia-Arbely et al., 2008; Nowell et al., 2003; Rose-John, 2012; Waetzig and Rose-John, 2012).

We have demonstrated that inhibition of classical and trans IL-6 signaling together prevents the loss of muscle mass in the Min mouse partially through improvements in muscle mitochondrial content and dynamics and decreases in protein degradation without improvements in muscle protein synthesis (White et al., 2011b; White et al., 2012c). The role of IL-6 trans signaling in the regulation of skeletal muscle mass and during cachexia requires further investigation. Inhibition of skeletal muscle gp130 in the LLC tumor implanted mice and in C2C12 myotubes treated with LLC conditioned medium attenuated muscle atrophy without improvements in protein synthesis (Puppa et al., 2013b). It is unknown how skeletal muscle gp130 signaling regulates muscle loss in an IL-6 dependent model of cachexia. Skeletal muscle inhibition of STAT3 can prevent cancer-induced muscle wasting through inhibition of muscle E3 ligases, however the effects of STAT3 inhibition on mitochondrial dysregulation and the

regulation of protein synthesis are unknown. There is a lack of understanding how IL-6 through gp130/STAT3 signaling regulates skeletal muscle mitochondria. Therefore, the purpose of this study was to examine the role of IL-6 trans signaling and muscle gp130 signaling on skeletal muscle mitochondrial regulation during cachexia. We hypothesized that inhibition of either skeletal muscle gp130 or IL-6 trans signaling will attenuate cachexia suppression of mitochondrial loss during cachexia through improvements in altered mitochondrial dynamics.

3.3 Methods

Animals. Male mice on a C57BL/6 background were bred with the gp130 fl/fl mice provided by Dr. Colin Stewart's lab in collaboration with Dr. Hennighausen (NCI) (Zhao et al., 2004). Gp130 fl/fl female mice were bred with male $Apc^{Min/+}$ mice from our colony at the University of South Carolina. The resulting male gp130 fl/fl $Apc^{Min/+}$ mice were bred with female cre-expressing mice driven by myosin light chain from Dr. Steven Burden (NYU) (Bothe et al., 2000). The resulting fl/fl cre/cre (skm-gp130) and fl/fl cre/cre $Apc^{Min/+}$ (skm-gp130 Min) mice have a skeletal muscle deletion of the gp130 protein. Offspring were genotyped for $Apc^{Min/+}$ as previously described (Mehl et al., 2005), cre recombinase (forward 5' AAG CCC TGA CCC TTT AGA TTC CAT TT 3', reverse 5' AAA ACG CCT GGC GAT CCC TGA AC 3', wild type 5' GCG GGC TTC TTC ACG TCT TTC TTT 3'), floxed gp130 (forward 5' ACG TCA CAG AGC TGA GTG ATG CAC 3', reverse 5' GGC TTT TCC TCT GGT TCT TG 3'), by taking tail snips at the time of weaning. All mice were group housed and provided standard rodent chow (Harlan Teklad Rodent Diet, #8604) and water *ad libitum*. The room was maintained on a 12:12 light:dark cycle with the light period starting at 0700. All animal experimentation was approved by the University of South Carolina's Institutional Animal Care and Use Committee.

IL-6 trans signaling inhibition: A subset of animals was aged to 16 weeks when Min mice had initiated body weight loss. Mice were treated by weekly IP injections with a soluble gp130 fusion protein, sgp130Fc, (150ug/mouse, a generous gift from Dr. Rose-John). sgp130Fc has previously been shown to inhibit IL-6 trans signaling (Nowell et al., 2003; Rose-John, 2003)

Western Blot analysis: Western blot analysis was performed as previously described (Puppa et al., 2011d). Briefly, frozen gastrocnemius muscle was homogenized in Mueller buffer and protein concentration was determined by the Bradford method (Bradford, 1976). Muscle homogenates (20-40 µg protein) were fractionated on SDS-polyacrylamide gels (6% to 12%). The gels were transferred to PVDF membrane and stained with ponceau to ensure equal loading. Membranes were blocked in 5% Tris-buffered saline with 0.1% Tween 20 (TBST) milk for 1 h at room temperature. Primary antibodies for p-AMPK, total AMPK, p-S6RP, total S6RP, p-STAT3, total STAT3, atrogin-1, cytochrome C (cell signaling, PGC-1α (Santa Cruz), FIS (Sigma), and Mfn1(Novus Biologicals) were incubated at dilutions of 1:1000 to 1:4000 overnight at 4°C in 1% TBST milk. Secondary anti-rabbit or anti-mouse IgG-conjugated secondary antibodies were incubated with the membranes at 1:2000 to 1:5000 dilutions for 1 h in 1% TBST milk. Enhanced chemiluminescence (Bio Express) was used to visualize the antibody-antigen interactions and developed by autoradiography. Digitally scanned blots were analyzed by measuring the integrated optical density (IOD) of each band using digital imaging software (ImageJ).

mtDNA: Mitochondrial capacity was performed as previously described (White et al., 2012b). DNA was isolated using DNAzol® Reagent (Invitrogen). Briefly, muscle (20 to 30 mg) was homogenized in 1 ml DNAzol, pelleted with 100% ethanol, and re-suspended in 8 mM NaOH. Quantitative real-time PCR analysis was carried out in 25 µl reactions consisting of 2x SYBR green PCR buffer (AmpliTaq Gold DNA Polymerase, Buffer, dNTP mix, AmpErase UNG, MgCl2) (Applied Biosystems), 0.150 µg DNA, DI water,

and 60 nM of each primer. PCR was run with the DNA sample with Cytochrome B Forward, 5′ - ATT CCT TCA TGT CGG ACG AG −3′; Cytochrome B Reverse, 5′ - ACT GAG AAG CCC CCT CAA AT - 3′, Gapdh Forward, 5′ - TTG GGT TGT ACA TCC AAG CA - 3′; Gapdh Reverse, 5′ - CAA GAA ACA GGG GAG CTG AG - 3′. Samples were analyzed on an ABI 7300 Sequence Detection System. Reactions were incubated for 2 minutes at 50°C and 10 minutes at 95°C, followed by 40 cycles consisting of a 15-s denaturing step at 95°C and 1-minute annealing/extending step at 60°C. Data were analyzed by ABI software (Applied Biosystems) using the cycle threshold (CT). The ratio between mtDNA and nuclear DNA genes was normalized to wild-type mice and used as an index of mitochondrial content.

Succinate dehydrogenase staining (SDH): SDH staining was conducted as previously described (Nachlas et al., 1957). Briefly, 10 µm thick sections from the mid-belly of the tibialis anterior muscle were cut at −20°C on a cryostat and slides were stored at −80°C until staining was performed. The sections air dried for 10 minutes then incubated in a solution of 0.2 M phosphate buffer (pH 7.4), 0.1 M MgCl2, 0.2 M succinic acid and 2.4 mM nitroblue tetrazolium (NBT, Sigma) at 37°C for 45 minutes. The sections were washed three minutes in water and then dehydrated in 50% ethanol. Stained slides were mounted with Permount (Calbiochem). Digital photographs were taken from each section at 25X magnification and fibers were quantified with imaging software (Image J, NIH). Fibers were considered SDH positive if they were 2 standard deviations above background. SDH-positive fibers were counted in each section in a blinded fashion.

RNA Isolation/PCR: RNA isolation, cDNA synthesis and real-time PCR were performed as previously described (White et al., 2013b) , using reagents from Applied Biosystems.

Gp130 (forward 5' CAG CGT ACA CTG ATG AAG GTG GGA AA 3', reverse 5' GCT GAC TGC AGT TCT GCT TGA 3') , IGF-1(White et al., 2013a), REDD1 (White et al., 2013a), IL-6 (Washington et al., 2011), and GAPDH primers were purchased from IDT (Coralville, Iowa, USA). Data were analyzed by ABI software using the cycle threshold (CT).

Plasma IL-6: Blood was collected at sacrifice via a retro-orbital sinus puncture and centrifuged at 10,000×*g* for 10 min. Plasma was collected and stored at −80°C until analysis. Using commercial ELISA kits for IL-6 (Invitrogen) according to the manufacturer's instructions, circulating levels of fasting IL-6 were measured.

Tumor Count: Intestinal polyp number and distribution was determined as previously described (REF). Intestinal sections from mice were fixed with 4% PFA, stained briefly in 0.1% methylene blue, and then placed under a dissecting microscope. The polyp number was counted by using tweezers to pick through the intestinal villi and identify polyps. Polyp sizes were categorized based on size (<1, 1-2, >2mm).

Statistics: A one-was ANOVA was used to determine the effect cachexia on soluble IL-6R levels. A two-way ANOVA was used to determine the effect of treatment (IL-6 trans inhibition and skeletal muscle gp130 deletion) X genotype. A one-way ANOVA was used to determine the effects of IL-6 trans inhibition and skm-gp130 loss on body weight and muscle mass loss in min mice. Post-hoc analyses were performed with Student-Newman-Keuls method. Pre-planned t-test was used to look at the effect of the $Apc^{Min/+}$ genotype within the control group and is indicated by a single asterisk. Significance was set at $p<0.05$.

3.4 Results

IL-6 trans signaling and muscle gp130 regulation of body weight during cachexia

The $Apc^{Min/+}$ (Min) mouse is an IL-6 dependent model of cancer cachexia. IL-6 can act through membrane bound IL-6 receptor as well as the soluble IL-6 receptor, sIL-6R. Plasma levels of sIL-6R were elevated in Min mice prior to body weight loss (Fig 3.1A). In mice demonstrating severe cachexia, greater than 10% body weight loss, sIL-6R was elevated further (Fig 3.1A). We sought to determine if inhibition of trans IL-6 signaling or muscle specific gp130 loss (skm-gp130) could attenuate cachexia. Min mice demonstrated a loss of body weight (Table 3.1). Inhibition of IL-6 trans signaling through the administration of a soluble gp130 fusion protein (sgp130Fc) after the initiation of cachexia attenuated further body weight loss whereas the loss of muscle gp130 (skm-gp130) did not protect from body weight loss (Fig 3.1B). The attenuation of body weight loss was associated with improved muscle mass and fat mass in Min mice that was not seen with skm-gp130 loss (Fig 3.1C/Table3.1). While Min mice demonstrated elevated IL-6 levels, inhibition of IL-6 trans signaling trended to decrease plasma IL-6 levels, $p=0.12$, and skm-gp130 loss had no effect on plasma IL-6 levels (Table 3.1). Neither trans IL-6 inhibition or skm-gp130 inhibition had an effect on cachexia induced spleenomegaly or on total tumor number. These data suggest that inhibition of IL-6 trans signaling may attenuate the cachectic condition independently of muscle gp130 signaling.

IL-6 trans signaling and muscle gp130 regulation of muscle mass during cachexia

To determine how inhibition of IL-6 trans signaling may be acting to attenuate muscle mass loss we measured regulators of cancer-induced muscle mass loss (Fig 3.-2).

Cachexia induced a 6 fold increase in skeletal muscle STAT3 phosphorylation which was blocked by both sgp130Fc administration and in skm-gp130 mice (Fig 3.2A). Additionally, the 2 fold induction of AMPK phosphorylation induced by cancer-cachexia was attenuated by sgp130Fc and skm-gp130 (Fig 3.2A). Cachexia suppressed mTOR signaling through ribosomal protein S6 by 57% (Fig 3.2B). The suppression of skeletal muscle mTOR signaling was unaltered by sgp130Fc or skm-gp130. Cachexia induced the E3 ligase, atrogin, expression. This induction was attenuated by both trans signaling inhibition and muscle gp130 inhibition (Fig 3.2B). These data demonstrate that IL-6 signaling during caner cachexia act through the muscle gp130 receptor to activate protein degradation pathways, but signaling through IL-6 trans pathways or muscle gp130 is not responsible for the suppression of muscle protein synthesis.

IL-6 trans signaling and muscle gp130 regulation of mitochondrial biogenesis during cachexia

Because muscle mitochondrial content has been shown to be decreased with cachexia and inhibition of systemic IL-6 signaling can attenuate mitochondrial dysfunction, we sought to determine whether inhibition of trans IL-6 signaling or muscle gp130 loss would prevent the cachexia-induced loss of mitochondrial biogenesis and dynamics. Cachexia suppressed PGC-1α and cytochrome c protein content (Fig 3.3A). Inhibition of skm-gp130 or IL-6 trans signaling attenuated the cachexia-suppression of PGC-1α protein (Fig 3.3A); however the cachexia suppression of PGC-1α mRNA was unaltered by either sgp130Fc or skm-gp130 (Fig 3.3B). There was a main effect of sgp130Fc to increase cytochrome c protein content regardless of cachexia; however, skm-gp130 was unable to prevent the cachexia suppression of cytochrome c protein (Fig

3.3A). There was no effect of cachexia on TFAM mRNA levels; however, sgp130Fc increased TFAM mRNA regardless of cancer (Fig 3.3B).

We next examined the effects of skm-gp130 and trans IL-6 inhibition on mitochondrial dynamics. Cachexia suppressed protein and mRNA levels of mitochondrial fusion marker MFN1 (Fig 3.3C/D). Inhibition of trans IL-6 signaling increased MFN protein levels in wild type mice; however, it was unable to attenuate the cachexia suppression of MFN1 protein (Fig 3.3C), and there was no effect of sgp130Fc on MFN1 mRNA levels (Fig 3.3D). Skm-gp130 was able to attenuate the cachexia suppression of MFN1 protein (Fig 3.3C) and there was a main effect of skm-gp130 to increase MFN1 mRNA levels despite cachexia (Fig 3.3D). Mitochondrial fission protein FIS was increased by cachexia (Fig 3.3C). Interestingly, skm-gp130 increased FIS1 protein regardless of cachexia. Pre-planned t-test revealed that sgp130Fc attenuated the cachexia induction of FIS protein. Additionally, the cachexia induction of FIS mRNA levels was attenuated by both skm-gp130 and sgp130Fc (Fig 3.3D). These data demonstrate that IL-6 signaling through gp130 and trans signaling may differentially regulate mitochondrial dynamics.

IL-6 trans signaling and muscle gp130 regulation of mitochondrial content during cachexia

We have previously described a loss of skeletal muscle mitochondrial content during the progression of cachexia in Min mice (White et al., 2011a). Suppression of mitochondrial content, measured by mitochondrial DNA and SDH staining, was evident in Min mice (Fig 3.4). There was a trend, $p=0.09$, for skm-gp130 mice to have elevated

mitochondrial DNA content regardless of cachexia (Fig 3.4A). Coinciding with this finding muscle oxidative capacity measure by SDH staining was increased with skm-gp130 loss regardless of cachexia (Fig 3.4B). The cachexia suppression of SDH dark stained fibers was attenuated by sgp130Fc administration (Fig 3.4B). These data demonstrate that IL-6 signaling through muscle gp130 may be responsible for the suppression of muscle oxidative capacity with cachexia.

3.5 Discussion

Cancer cachexia, associated with muscle mass loss, directly impacts patient survival and quality of life (Evans et al., 2008; Fearon et al., 2011; Muscaritoli et al., 2010). While the mechanisms underlying the condition are complex and can differ based on the type and severity of cancer. The progression of cachexia is directly associated with increased morbidity and mortality and account for 20% of all cancer deaths (Bruera, 1997; Tisdale, 2002). Muscle oxidative capacity has been associated with susceptibility to muscle wasting (Tisdale, 2009), and muscle mitochondria loss has been well documented in many cachectic conditions (Li et al., 2007; Romanello et al.; White et al., 2011a). Inflammation has been indicated as a potential regulator of muscle mitochondrial loss during cachexia (White et al., 2012b). However, the role of systemic inflammation and muscle specific signaling on mitochondrial loss during cachexia remains to be investigated. To our knowledge this is the first study to examine the effects of trans IL-6 signaling and signaling through the muscle gp130 receptor on the regulation of mitochondrial loss during cachexia. Interestingly, we show differential regulation of mitochondrial dynamic by IL-6 trans signaling and skm-gp130 signaling; however, inhibition of either was able to prevent the loss of mitochondria with cachexia. Further work is necessary to determine if mitochondria remain functional when these signaling pathways are inhibited.

We have previously shown that inhibition of systemic IL-6 signaling through the administration of an IL-6r antibody attenuated the loss of body weight and muscle mass after the initiation of cachexia, and this was associated with suppression of muscle STAT3, increased muscle mitochondrial content, and suppression of muscle protein

degradation pathways (White et al., 2013b; White et al., 2012b). Others have demonstrated that inhibition of muscle STAT3 can attenuate muscle protein degradation pathways (Bonetto et al., 2012; Bonetto et al., 2011); however, STAT3 regulation of muscle mitochondria was not examined. STAT3 not only has well defined transcriptional functions, but can also translocate to the mitochondria where it increases oxidative phosphorylation (Qiu et al., 2011). We demonstrate that suppression of muscle STAT3 phosphorylation through inhibition of muscle IL-6 signaling increased muscle oxidative capacity. Further work is needed to the role of STAT3 on the regulation of muscle mitochondrial content and the regulation of mitochondrial associated STAT3 during cancer cachexia.

We demonstrate that increased mitochondrial content was not sufficient to attenuate muscle mass loss during IL-6 dependent cachexia. While inhibition of trans IL-6 signaling was sufficient to attenuate muscle loss and prevent mitochondrial loss, muscle specific inhibition of gp130 signaling was not sufficient to prevent wasting despite increased mitochondrial content. These findings are similar to those of Wang et al. who demonstrated that increased mitochondrial content through over-expression of PGC-1α was not sufficient to prevent cancer-induced muscle loss (Wang et al., 2012). Presumably the increase in mitochondrial content would be functional as it has been shown that the decrease in mitochondrial oxidative capacity with cachexia is not associated with decreases in the ability of the remaining mitochondria to produce ATP (Julienne et al., 2012). Further work is necessary to determine if the increased mitochondrial content is functional or if there is a buildup of dysfunctional mitochondria.

Recent literature has shown that mTOR is important in the regulation of PGC-1α and can operate with PGC-1α to activate the transcription of many oxidative genes (Cunningham et al., 2007). When the mTOR complex is inhibited there is a severe decrease in muscle oxidative capacity and function (Schieke et al., 2006) suggesting that mTOR is an important mediator for the maintenance of mitochondria. We show that oxidative capacity and PGC-1α were increased with inhibition of IL-6 trans signaling and muscle gp130; however, muscle signaling related to mTOR remained suppressed. These data suggest that the increase in oxidative capacity may not be sufficient to relieve the cachexia suppression of mTOR signaling. Further work is necessary to determine the mechanism behind mTOR suppression with cancer cachexia.

Interestingly gp130 may be a negative regulator of mitochondrial as we have demonstrated that gp130 is more highly expressed in glycolytic fibers (Puppa et al., 2013b) and inhibition of muscle gp130 signaling increased mitochondrial oxidative capacity. The increase in oxidative capacity skm-gp130 mice was also associated with an increase in FIS protein expression and inhibition of mitochondrial fusion was attenuated in skm-gp130 mice. Inhibition of trans IL-6 signaling was unable to prevent the suppression of mitochondrial fusion, but attenuated the increase in fission. Mitochondrial remodeling and increased mitochondrial fission has been associated with muscle atrophy following fasting or denervation, and contributes to activation of protein degradation (Romanello et al., 2010; Romanello and Sandri, 2010). The overall increase in mitochondrial remodeling seen in skm-gp130 mice may lead to increased autophagy which can act independently of atrogin to suppress muscle mass, while trans IL-6 may be suppressing atrophy through inhibition of fission. There may be higher mitochondrial

turnover in skm-gp130 mice. Further work is necessary to determine gp130 regulation of mitochondria and autophagy pathways during cachexia.

In summary we demonstrate that inhibition of trans IL-6 signaling is sufficient to attenuate muscle mass loss however it may be through more systemic effects as muscle gp130 inhibition is not sufficient to attenuate cachexia-induced muscle mass loss. Inhibition of both muscle gp130 and trans IL-6 signaling were sufficient to attenuate the loss of mitochondria associated with cancer cachexia. Trans IL-6 and muscle gp130 differentially regulated muscle mitochondrial dynamics. Further work is necessary to understand the differential regulation of mitochondrial dynamics by systemic and local IL-6 signaling. While inhibition of IL-6 signaling at the muscle was sufficient to prevent mitochondrial loss systemic IL-6 inhibition appears to be more beneficial for the treatment of cachexia.

Acknowledgements

The authors thank Ms. Tia Davis and Dr. Marj Peña for technical assistance with the animal breeding. The skeletal muscle-specific cre-expressing mice were a gift from Dr. Steven Burden. The gp130 fl/fl mice were a gift from Dr. Colin Stuart & Dr. Hennighausen, NCI. The research described in this report was supported by research grant R01 CA121249 to JAC from the National Cancer Institute.

Table 3.1. The effect of trans IL-6 and muscle gp130 inhibition on cachexia development. Body weight was measured throughout the duration of the study and at sacrifice (SAC). Tibia length, spleen, epididymal (Epi) fat, intestines and plasma were collected at the time of sacrifice. All values are mean ±sem. Two-way ANOVA was used to determine the effects of genotype x treatment (trans IL-6 inhibition, sgp130Fc, and muscle gp130 loss, skm-gp130). # Main effect of Min, ^ compared to control group within genotype, $p<0.05$.

BL-6	**control**	**sgp130Fc**	**skm-gp130**
N	**9**	**4**	**5**
Peak BW (g)	27.3 ± 0.5	27.5 ± 0.6	27.8 ± 1.2
SAC BW (g)	27.3 ± 0.5	27.2 ± 0.8	27.8 ± 1.2
Tibia Length (mm)	17.1 ± 0.0	17.1 ± 0.1	17.1 ± 0.1
Spleen (mg)	89 ± 8	84 ± 2	98 ± 13
Epi Fat (mg)	465 ± 49	365 ± 35	399 ± 33
Min			
N	**11**	**6**	**6**
Peak BW (g)	24.2 ± 0.4$^{\#}$	24.1 ± 0.5$^{\#}$	23.2 ± 2.2$^{\#}$
SAC BW (g)	19.7 ± 0.6$^{\#}$	22.8 ± 0.8$^{\#\wedge}$	20.3 ± 1.0$^{\#}$
Tibia Length (mm)	16.7 ± 0.1$^{\#}$	16.6 ± 0.1$^{\#}$	16.5 ± 0.1$^{\#}$
Spleen (mg)	452 ± 48$^{\#}$	453 ± 60$^{\#}$	507 ± 43$^{\#}$
Epi Fat (mg)	5 ± 5$^{\#}$	121 ± 48$^{\#\wedge}$	4 ± 3$^{\#}$
Tumor Number	80 ± 13	49 ± 11	87 ± 8
IL-6 (pg/ml)	106 ± 62	10 ± 4	74 ± 22

3.6 Figure Legends

Figure 3.1. The effect of trans IL-6 and muscle gp130 inhibition on the development of cachexia. A) Circulating plasma soluble IL-6 receptor, sIL-6R, was measured in control BL-6 mice, weight stable Min mice, WS, and in severely cachectic min mice, >10%BW loss. B) The percentage of body weight loss from peak body weight in Min mice treated with sgp130Fc or lacking muscle gp130 (skm-gp130). C) Gastrocnemius was measured at the time of sacrifice in BL-6 and Min mice with sgp130Fc or skm-gp130. All values are Mean ± SEM. One-way ANOVA was used to analyze changes in sIL-6R and the percent body weight loss. * significantly different from BL-6, ∞ significantly different from WS Two-way ANOVA was used to determine the effects of genotype x treatment on gastrocnemius mass. # Main effect of Min, † significantly different from all other comparisons. $p<0.05$.

Figure 3.2. The effect of trans IL-6 and muscle gp130 inhibition on the signaling regulating skeletal muscle mass during cachexia. A) Western blot analysis of the ratio of phosphorylation to total STAT3 and AMPK were measured in the gastrocnemius muscle of BL-6 and Min mice lacking gp130 (skm-gp130) or treated with sgp130Fc for two weeks (Fc). B) Western blot analysis of atrogin and the ratio of phosphorylation to total S6 were measured in the gastrocnemius. All values are Mean ± SEM. Two-way ANOVA was used to determine the effects of genotype x treatment. # Main effect of Min, † significantly different from all other comparisons. $p<0.05$.

Figure 3.3. The effect of trans IL-6 and muscle gp130 inhibition on mitochondrial biogenesis and dynamics during cancer cachexia. A) Western blot analysis of the ratio

of PGC-1α and cytochrome c (Cyto C) were measured in the gastrocnemius muscle of BL-6 and Min mice lacking gp130 (skm-gp130) or treated with sgp130Fc for two weeks (Fc). B) Skeletal muscle mRNA levels of PGC-1α and TFAM were measured in gastrocnemius of mice using real time PCR. C) Protein expression and D) mRNA levels of markers of mitochondrial fusion (MFN1) and fission (FIS). All values are Mean ± SEM. Two-way ANOVA was used to determine the effects of genotype x treatment. # Main effect of Min, & Main effect of sgp130Fc, @ Main effect of skm-gp130, † significantly different from all other comparisons. * significant compared with BL-6 control based on pre-planned t-test. $p<0.05$.

Figure 3.4. The effect of trans IL-6 and muscle gp130 inhibition on mitochondrial content during cancer cachexia. Mitochondrial content was measured as A) the ratio of mitochondrial DNA:nuclear DNA and B) the percentage of fibers stained after succinate dehydrogenase staining. All values are Mean ± SEM. Two-way ANOVA was used to determine the effects of genotype x treatment @ Main effect of skm-gp130 * significant compared with BL-6 control based on pre-planned t-test. $p<0.05$.

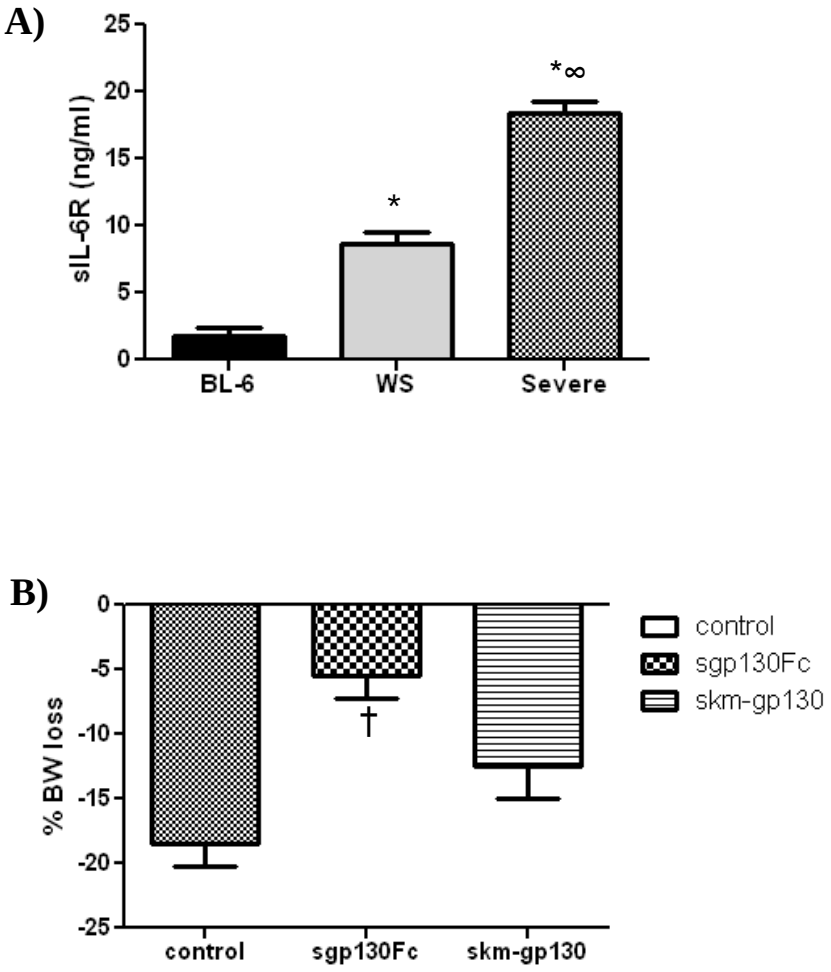
A)
sIL-6R (ng/ml)
25
20
15
10
5
0
*
*∞
BL-6
WS
Severe
B)
% BW loss
0
-5
-10
-15
-20
-25
†
control
sgp130Fc
skm-gp130
control
sgp130Fc
skm-gp130

Figure 3.1.

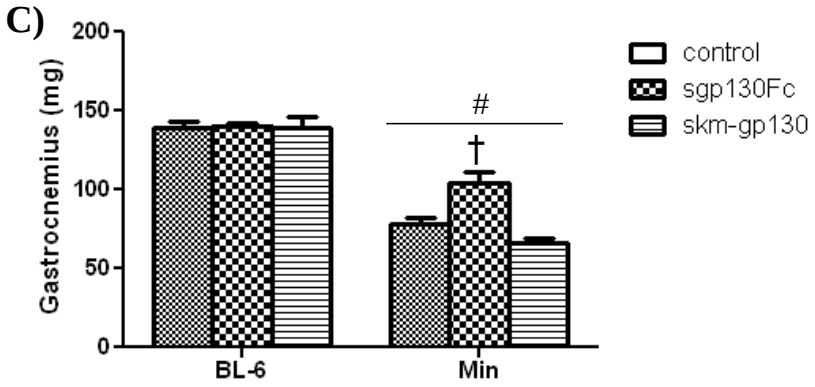

Figure 3.1. The effect of trans IL-6 and muscle gp130 inhibition on the development of cachexia. A) Circulating plasma soluble IL-6 receptor, sIL-6R, was measured in control BL-6 mice, weight stable Min mice, WS, and in severely cachectic min mice, >10%BW loss. B) The percentage of body weight loss from peak body weight in Min mice treated with sgp130Fc or lacking muscle gp130 (skm-gp130). C) Gastrocnemius was measured at the time of sacrifice in BL-6 and Min mice with sgp130Fc or skm-gp130. All values are Mean ± SEM. One-way ANOVA was used to analyze changes in sIL-6R and the percent body weight loss. * significantly different from BL-6, ∞ significantly different from WS Two-way ANOVA was used to determine the effects of genotype x treatment on gastrocnemius mass. # Main effect of Min, † significantly different from all other comparisons.. $p<0.05$.

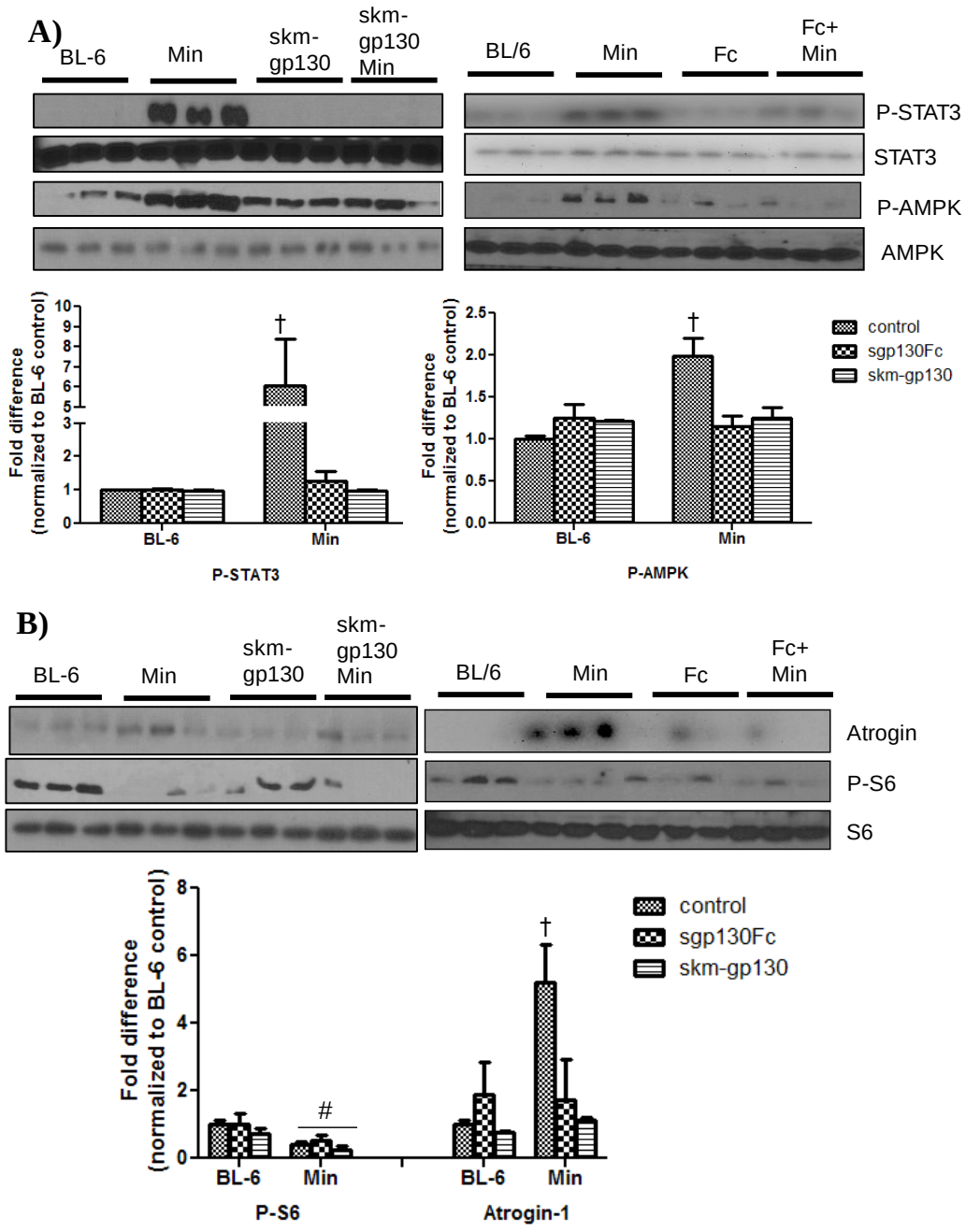

Figure 3.2. The effect of trans IL-6 and muscle gp130 inhibition on the signaling regulating skeletal muscle mass during cachexia. A) Western blot analysis of the ratio of phosphorylation to total STAT3 and AMPK were measured in the gastrocnemius muscle of BL-6 and Min mice lacking gp130 (skm-gp130) or treated with sgp130Fc for two weeks (Fc). B) Western blot analysis of atrogin and the ratio of phosphorylation to total S6 were measured in the gastrocnemius. All values are Mean ± SEM. Two-way ANOVA was used to determine the effects of genotype x treatment. # Main effect of Min, † significantly different from all other comparisons. $p<0.05$.

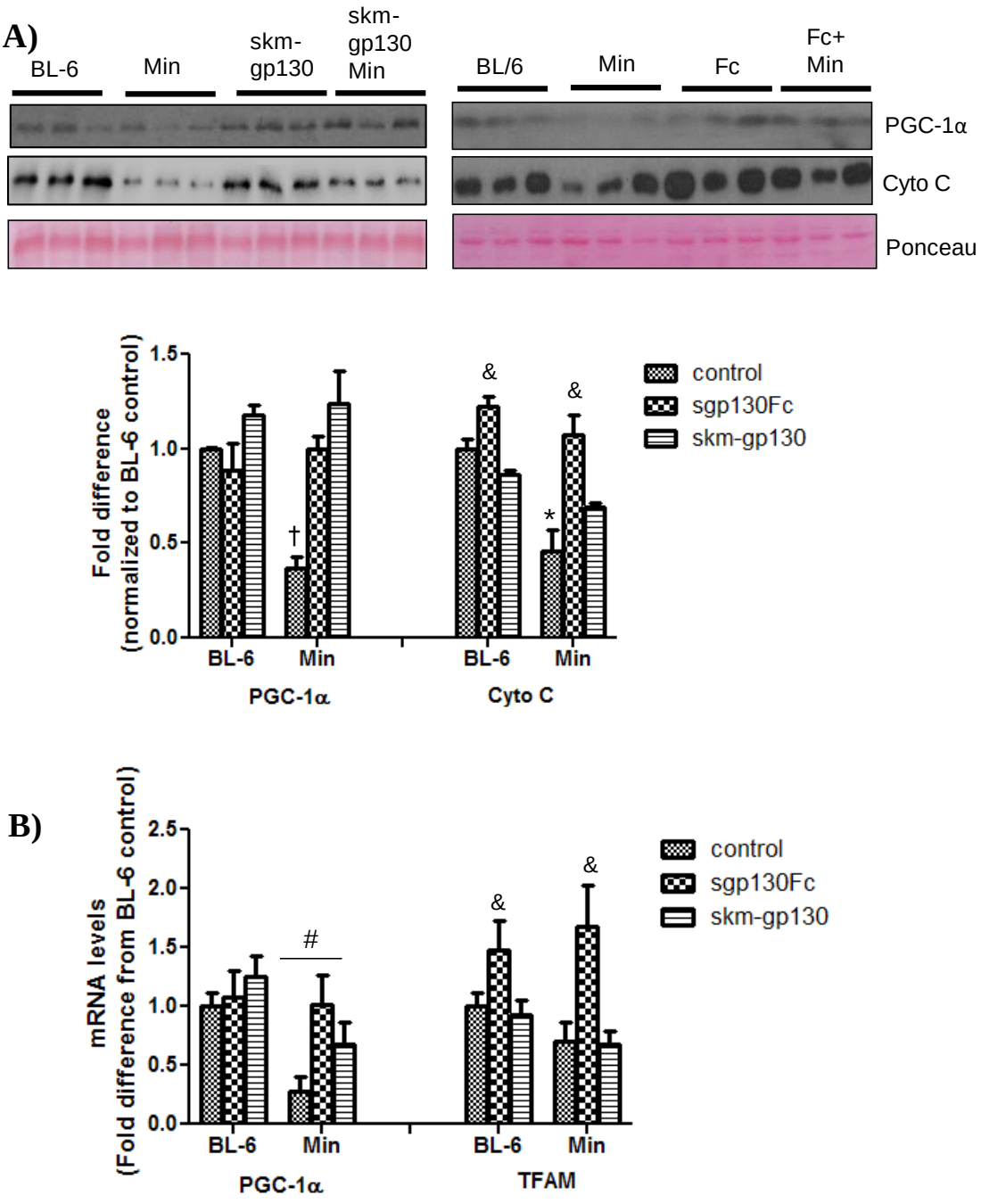
A)
BL-6
Min
skm-gp130
skm-gp130 Min
BL/6
Min
Fc
Fc+ Min
PGC-1α
Cyto C
Ponceau
Fold difference (normalized to BL-6 control)
1.5
1.0
0.5
0.0
†
&
&
*
BL-6
Min
BL-6
Min
PGC-1α
Cyto C
control
sgp130Fc
skm-gp130
B)
mRNA levels (Fold difference from BL-6 control)
2.5
2.0
1.5
1.0
0.5
0.0
#
&
&
BL-6
Min
BL-6
Min
PGC-1α
TFAM
control
sgp130Fc
skm-gp130

Figure 3.3.

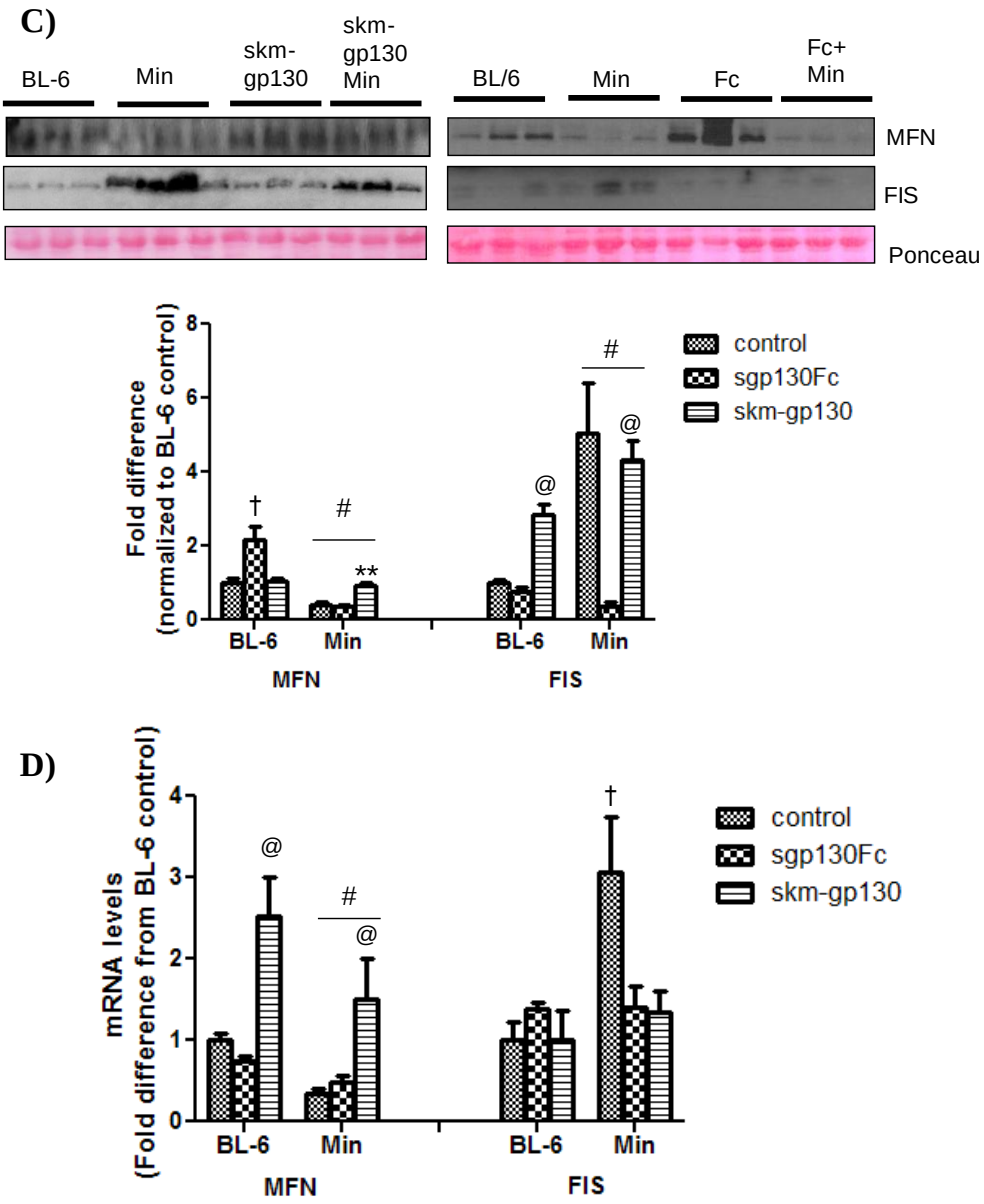

Figure 3.3. The effect of trans IL-6 and muscle gp130 inhibition on mitochondrial biogenesis and dynamics during cancer cachexia. A) Western blot analysis of the ratio of PGC-1α and cytochrome c (Cyto C) were measured in the gastrocnemius muscle of BL-6 and Min mice lacking gp130 (skm-gp130) or treated with sgp130Fc for two weeks (Fc). B) Skeletal muscle mRNA levels of PGC-1α and TFAM were measured in gastrocnemius of mice using real time PCR. C) Protein expression and D) mRNA levels of markers of mitochondrial fusion (MFN1) and fission (FIS). All values are Mean ± SEM. Two-way ANOVA was used to determine the effects of genotype x treatment. # Main effect of Min, & Main effect of sgp130Fc, @ Main effect of skm-gp130, ** significant compared with min control, † significantly different from all other comparisons. * significant compared with BL-6 control based on pre-planned t-test. $p<0.05$.

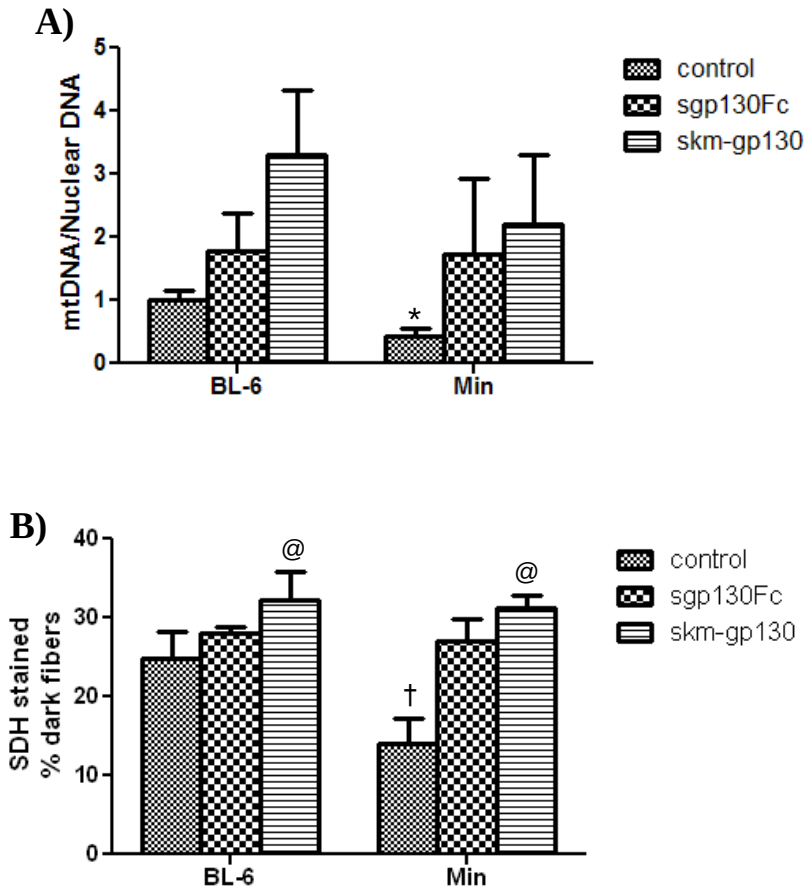

Figure 3.4. The effect of trans IL-6 and muscle gp130 inhibition on mitochondrial content during cancer cachexia. Mitochondrial content was measured as A) the ratio of mitochondrial DNA:nuclear DNA and B) the percentage of fibers stained after succinate dehydrogenase staining. All values are Mean ± SEM. Two-way ANOVA was used to determine the effects of genotype x treatment @Main effect of skm-gp130 *significant compared with BL-6 control based on pre-planned t-test. $p<0.05$.

CHAPTER 4

THE ROLE OF PYRROLIDINE DITHIOCARBAMATE ON THE REGULATION OF SKELETAL MUSCLE MASS DURING CANCER-INDUCED CACHEXIA[2]

[2] Melissa Puppa, Aditi Narsale, Angela Murphy, Greg Hand, Raja Fayad, and James Carson. To be submitted

4.1 Abstract

Cancer cachexia is associated with significant loss of muscle mass. Increases in inflammation play a key role in the dysregulation of skeletal muscle proteostasis. During cachexia there is a significant loss in skeletal muscle protein synthesis and an increase in muscle protein degradation. While much attention has been paid to combating cachexia-induced increases in protein degradation, researching is lacking in treatments for the inflammation-suppression of muscle protein synthesis during cachexia. Therefore the purpose of this study was to determine if the anti-inflammatory compound, pyrrolidine dithiocarbamate (PDTC), could alter cachexia induced dysregulation of skeletal muscle proteostasis. $Apc^{Min/+}$ mice were administered PDTC daily for two weeks after the initiation of cachexia. PDTC attenuated cachexia-induced body weight and muscle mass loss. Two weeks of PDTC administration suppressed cachexia-induced inflammatory signaling related to STAT3 and AMPK phosphorylation. Inhibition of inflammatory signaling was associated with a suppression of muscle Atrogin-1 protein expression. The cachexia suppression of mTOR target, S6, was blocked by PDTC and this corresponded with an increase in skeletal muscle protein synthesis. PDTC blocked the cachexia-induced decrease in skeletal muscle mitochondrial content and suppression of mitochondrial fusion protein MFN1; however PDTC and cachexia both resulted in increases in mitochondrial FIS expression. These data demonstrate that administration of PDTC after the induction of cachexia can improve skeletal muscle proteostasis and mitochondrial capacity. Further work is required to understand the long term effects of PDTC administration in cachectic muscle.

Keywords: cachexia, protein synthesis, mitochondria, skeletal muscle, inflammation

4.2 Introduction

Cachexia, a condition associated with muscle mass and adipose tissue loss, accounts for 40% of colon cancer related deaths (Fox et al., 2009; Tisdale, 2002). Although there are several clinical features present that may aid in diagnosing the cachectic patient including inflammation, insulin resistance, anorexia, altered metabolism, and muscle proteolysis, ~80% of patients with gastrointestinal cancers have already experienced significant weight loss at the time of diagnosis (Bruera, 1997). Cachexia significantly impairs patient quality of life and patients who develop cachexia are more susceptible to a decreased response to chemotherapy, prolonged recovery time, increased risk of infection, and decreased survival after chemotherapy (Esper and Harb, 2005; Evans et al., 2008; Tisdale, 2009; von Haehling et al., 2009). There are currently no approved pharmaceutical therapies for the treatment of cancer cachexia; however, several likely therapies including anti-cytokine therapies and appetite stimulants are in development (Ando et al., 2013; Murphy and Lynch, 2009).

The $Apc^{Min/+}$ (Min) mouse is an IL-6 dependent model of cancer cachexia that displays many of the hallmarks of cachexia such as increased inflammation and alterations in skeletal muscle proteostasis. The Min mouse has a naturally occurring mutation the *Adenomatous polyposis coli (Apc)* gene predisposing the animals to multiple intestinal neoplasias (Moser et al., 1990). Similar to the human condition the Min mouse has a slow progression of body weight and muscle mass loss that is accompanied by inflammation, fatigue, increases in muscle protein breakdown, and suppression of muscle protein synthesis (Gallagher et al., 2012; White et al., 2011b; White et al., 2013b). Anti-IL-6 therapy after the initiation of cachexia is able to attenuate further muscle mass loss

through suppression of protein degradation and mitochondrial fission and, improvements in mitochondrial fusion and oxidative capacity; however, there was not release of the suppression of muscle protein synthesis with anti-IL-6 therapy (White et al., 2011b; White et al., 2012b). Other models have also demonstrated that inhibition of inflammatory signaling through gp130 and STAT3 can attenuate muscle mass loss through suppression of protein degradation without alterations in the suppression of protein synthesis (Bonetto et al., 2012; Bonetto et al., 2011; Puppa et al., 2013b).

The small thiol compound, pyrrolidine dithiocarbamate (PDTC) has been shown to have both anti-inflammatory and antioxidant properties (Chabicovsky et al., 2010; He et al., 2006; Shi et al., 2000). PDTC can inhibit activation of the IL-6 target, STAT3, and its association with transcriptional co-activators FOXO and C/EBPβ (He et al., 2006). Additionally PDTC has been shown to suppress inflammatory processes through NFκB inhibition (Cuzzocrea et al., 2002; La Rosa et al., 2004; Schreck et al., 1992); however this has not been seen in all studies (Huang et al., 2008). It has recently been shown that PDTC can up regulate ribosomal protein genes that are down-regulated by IL-6, and PDTC can increase the protein biosynthetic capacity of HepG2 cells in a rapamycin-independent manner (Song et al., 2011).

PDTC has been shown to attenuate muscle mass loss in several different models of cancer cachexia (Nai et al., 2007; Puppa et al., 2013b); however the role of PDTC on the regulation of muscle mass during cachexia is unknown. Therefore the purpose of this study was to determine if pyrrolidine dithiocarbamate (PDTC) could alter cachexia induced dysregulation of skeletal muscle proteostasis. We hypothesized that PDTC administration after the initiation of cachexia would rescue muscle mass through both

inhibition of protein degradation pathways and increases in muscle protein synthesis. To test this hypothesis, *Apc*$^{Min/+}$ mice were monitored until they had initiated body weight loss. PDTC or PBS was administered for two weeks and hindlimb muscle was harvested. The regulation of muscle protein synthesis and degradation was investigated.

4.3 Methods

Animals. *Apc*$^{Min/+}$ (Min) male mice, purchased from Jackson Laboratories, were crossed with C57BL/6 female mice at the Animal Resource Facilities at the University of South Carolina. Using a tail snip taken at the time of weaning, mice were genotyped for heterozygous expression of the *Apc* gene. Male mice were housed four to five per cage, with Min mice kept in separate cages from control C57BL/6 mice. All mice were group housed and provided standard rodent chow (Harlan Teklad Rodent Diet, #8604) and water *ad libitum*. The room was maintained on a 12:12 light:dark cycle with the light period starting at 0700. All animal experimentation was approved by the University of South Carolina's Institutional Animal Care and Use Committee.

Pyrrolidine dithiocarbamate (*PDTC):* Animals were aged to 16 weeks when Min mice had initiated body weight loss. Mice were randomly assigned to receive PBS or PDTC. Mice were treated by daily IP injections with 10mg/kg of PDTC in PBS (Nai et al., 2007). PDTC has been shown to decrease STAT3 activity through alterations in the stability of STAT3-Hsp90 complex (He et al., 2006). Mice were sacrificed after 2 weeks of treatment and tissues were harvested.

Western Blot analysis: Western blot analysis was performed as previously described (Puppa et al., 2011d). Briefly, frozen gastrocnemius muscle was homogenized in Mueller buffer and protein concentration was determined by the Bradford method (Bradford, 1976). Muscle homogenates (20-40 µg protein) were fractionated on SDS-polyacrylamide gels (6% to 12%). The gels were transferred to PVDF membrane and stained with ponceau to ensure equal loading. Membranes were blocked in 5% Tris-

buffered saline with 0.1% Tween 20 (TBST) milk for 1 h at room temperature. Primary antibodies for p-AMPK, total AMPK, , p-STAT3, total STAT, pP65, total P65, atrogin-1, and cytochrome C (cell signaling), anti-puromycin (Millipore), FIS (Sigma), and MFN1(Novus Biologicals) were incubated at dilutions of 1:2000 to 1:6,000 overnight at 4°C in 1% TBST milk. Secondary anti-rabbit or anti-mouse IgG-conjugated secondary antibodies were incubated with the membranes at 1:2,000 to 1:5,000 dilutions for 1 h in 1% TBST milk. Enhanced chemiluminescence (Bio Express) was used to visualize the antibody-antigen interactions and developed by autoradiography. Digitally scanned blots were analyzed by measuring the integrated optical density (IOD) of each band using digital imaging software (ImageJ).

mtDNA: Mitochondrial capacity was performed as previously described (White et al., 2012b). DNA was isolated using DNAzol® Reagent (Invitrogen). Briefly, muscle (20 to 30 mg) was homogenized in 1 ml DNAzol, pelleted with 100% ethanol, and re-suspended in 8 mM NaOH. Quantitative real-time PCR analysis was carried out in 25 µl reactions consisting of 2x SYBR green PCR buffer (AmpliTaq Gold DNA Polymerase, Buffer, dNTP mix, AmpErase UNG, MgCl2) (Applied Biosystems), 0.150 µg DNA, DI water, and 60 nM of each primer. PCR was run with the DNA sample with Cytochrome B Forward, 5′ - ATT CCT TCA TGT CGG ACG AG −3′; Cytochrome B Reverse, 5′ - ACT GAG AAG CCC CCT CAA AT - 3′, Gapdh Forward, 5′ - TTG GGT TGT ACA TCC AAG CA - 3′; Gapdh Reverse, 5′ - CAA GAA ACA GGG GAG CTG AG - 3′. Samples were analyzed on an ABI 7300 Sequence Detection System. Reactions were incubated for 2 minutes at 50°C and 10 minutes at 95°C, followed by 40 cycles consisting of a 15-s

denaturing step at 95°C and 1-minute annealing/extending step at 60°C. Data were analyzed by ABI software (Applied Biosystems) using the cycle threshold (CT). The ratio between mtDNA and nuclear DNA genes was normalized to wild-type mice and used as an index of mitochondrial content.

Succinate dehydrogenase staining (SDH): SDH staining was conducted as previously described (Nachlas et al., 1957). Briefly, 10 µm thick sections from the mid-belly of the tibialis anterior muscle were cut at −20°C on a cryostat and slides were stored at −80°C until staining was performed. The sections air dried for 10 minutes then incubated in a solution of 0.2 M phosphate buffer (pH 7.4), 0.1 M MgCl2, 0.2 M succinic acid and 2.4 mM nitroblue tetrazolium (NBT, Sigma) at 37°C for 45 minutes. The sections were washed three minutes in water and then dehydrated in 50% ethanol. Stained slides were mounted with Permount (Calbiochem). Digital photographs were taken from each section at 25X magnification and fibers were quantified with imaging software (Image J, NIH). Fibers were considered SDH positive if they were 2 standard deviations above background. A minimum of 120 fibers were counted from each animal. SDH-positive fibers were counted in each section in a blinded fashion.

RNA Isolation/PCR: RNA isolation, cDNA synthesis and real-time PCR were performed as previously described (White et al., 2013b) , using reagents from Applied Biosystems., and GAPDH primers were purchased from IDT (Coralville, Iowa, USA). Data were analyzed by ABI software using the cycle threshold (CT).

Plasma IL-6: Blood was collected at sacrifice via a retro-orbital sinus puncture and centrifuged at 10,000×*g* for 10 min. Plasma was collected and stored at −80°C until

analysis. Using commercial ELISA kits for IL-6 (Invitrogen) according to the manufacturer's instructions, circulating levels of fasting IL-6 were measured.

Tumor Count: Intestinal polyp number and distribution was determined as previously described (Puppa et al., 2011d). Intestinal sections from mice were fixed with 4% PFA, stained briefly in 0.1% methylene blue, and then placed under a dissecting microscope. The polyp number was counted by using tweezers to pick through the intestinal villi and identify polyps. Polyp sizes were categorized based on size (<1, 1-2, >2mm).

Statistics: A two-way ANOVA was used to determine the effect of PDTC administration x genotype. Pre-planned t-test was used to look at the effect of PDTC administration within the $Apc^{Min/+}$ genotype and is indicated by an asterisk. Post-hoc analyses were performed with Student-Newman-Keuls method. Significance was set at $p<0.05$.

4.4 Results

Body weight and muscle mass changes

STAT3 is a downstream target of IL-6 signaling. Pyrrolidine dithiocarbamate (PDTC) has been shown to inhibit STAT3 and NFκB signaling during cancer cachexia (Puppa et al., 2013b). Two weeks of PDTC administration increased body weight in both Min and BL-6 mice (Table 4. 1). While cachexia decreased body weight, PDTC administration after the initiation of cachexia attenuated body weight loss (Fig 4.1A). Similarly, muscle mass loss was decreased by 34% with cachexia. There was a main effect of PDTC to increase gastrocnemius muscle mass regardless of cachexia and Min mice treated with PDTC had a 17% increase in gastrocnemius mass (Fig 4.1B). Cachexia decreased epidydimal fat mass 75%. There was a main effect of PDTC to increase fat mass regardless of cachexia (Table 4.1).

Although there was an attenuation of body weight loss, PDTC did not affect overall tumor number in min mice. However, there was a decrease in percentage of large tumors >2mm with PDTC administration (Table 4.1). Cachexia was associated with an increase in plasma IL-6 and the decrease in large tumors with PDTC was not associated with a change in plasma IL-6. Cachexia induced spleenomegaly which was further accentuated by PDTC administration (Table 4.1). These data demonstrate that administration of PDTC can attenuate caner-induced body weight and muscle mass loss independent of reductions in plasma IL-6 levels.

Cachexia mediated muscle signaling

We next sought to determine if PDTC treatment could attenuate cachexia-induced inflammatory signaling in skeletal muscle. Cachexia increased the phosphorylation of STAT3 2.8 fold and P65 2.7 fold (Fig 4.2A). PDTC administration decreased the phosphorylation of STAT3 in both wild type and cachectic mice; however, there was a trend for PDTC to decrease P65 phosphorylation in Min mice, p=0.12 (Fig 4.2A). Additionally, AMPK phosphorylation was increased 11 fold in the cachectic mice. PDTC administration blocked cachexia-induced AMPK phosphorylation (Fig 4.2A). These data demonstrate that PDTC administration after the initiation of cachexia can block the cachexia-induction of skeletal muscle inflammatory signaling.

Cachexia is associated with alterations in skeletal muscle protein turnover, with increases in protein degradation and suppression of muscle protein synthesis. The expression of skeletal muscle E3 ligase, atrogin-1, was increased 73% with cachexia. There was a main effect of PDTC to decrease atrogin expression regardless of cachexia (Fig 4.3A). Cachexia suppressed mTOR target ribosomal protein S6. PDTC increased muscle S6 phosphorylation regardless of cachexia (Fig 4.3A). As is seen in the human condition, cachexia decreased muscle protein synthesis, which was measured by puromycin incorporation into the muscle, by 52%. PDTC blocked cachexia suppression of muscle protein synthesis in Min mice. Additionally PDTC increased muscle protein synthesis in wild type by 20% (Fig 4.3B). These data demonstrate that inhibition of STAT3/NFκB signaling may attenuate cachexia in part through a decrease in muscle protein degradation signaling and through increases in muscle protein synthesis.

Regulation of mitochondrial content

Cachexia is associated with increases in fatigue and decreased skeletal muscle mitochondrial content. Cachexia caused a 33% reduction in skeletal muscle oxidative capacity, measured by the percentage of succinate dehydrogenase positive fibers (Fig 4.4A). Inhibition of STAT3/NFκB signaling blocked the cachexia-suppression of muscle oxidative capacity. As we have previously published (White et al., 2011a), cachexia decreases skeletal muscle mitochondrial content (Fig 4.4B). There was a main effect of PDTC to increase mitochondrial content in the gastrocnemius muscle. The cachexia-suppression of mitochondrial content measured by the ratio of mitochondrial to nuclear DNA was blocked by PDTC administration (Fig 4.4B).

Mitochondria are regulated by the processes of mitochondrial fission and fusion termed mitochondrial dynamics. Cachexia decreased mitochondrial fusion protein MFN1 in Min mice (Fig 4.5A), as has been previously described (White et al., 2012c). There was a main effect of PDTC administration to increase MFN1, regardless of cachexia. Cachexia increased mitochondrial fission protein, FIS1; however, the cachexia-induced increase in FIS1 was unaltered by PDTC administration (Fig 4.5A). Coinciding with a decrease in mitochondrial content and increase fission, skeletal muscle Cytochrome C content was suppressed 31% with cachexia, and PDTC attenuated this suppression (Fig 4.5A). Skeletal muscle MFN1 mRNA levels were decreased 76% with cachexia, and PDTC attenuated this suppression (Fig 4.5B). Similar to the protein levels, both PDTC and cachexia increased FIS1 mRNA. These data demonstrate that systemic signaling through STAT/NFκB may regulate cachexia suppression of mitochondrial capacity and regulate mitochondrial fusion without suppressing mitochondrial fission.

4.5 Discussion

Chronic inflammation, a hallmark of cancer cachexia, is a potential therapeutic target to combat the condition. Although there are currently no approved treatments for cancer cachexia, two separate case studies in patients with cancer cachexia demonstrate improved symptoms with Tocilizumab, an IL-6r Ab, administration (Ando et al., 2013; Hirata et al., 2013). Inflammatory signaling through IL-6 and muscle gp130/STAT3 signaling are shown to regulate muscle protein degradation in tumor-bearing mice (Bonetto et al., 2012; Puppa et al., 2013b; White et al., 2011b; White et al., 2013b). However, significant gaps remain in our understanding of how cancer-induced systemic inflammation regulates the disruption of skeletal muscle protein turnover. We report that the small molecule pyrrolidine dithiocarbamate was able to suppress markers of muscle protein degradation, but also increased skeletal muscle protein synthesis and mitochondrial content without suppressing plasma IL-6 levels.

STAT3 and NFκB have well documented roles in the pathogenesis of skeletal muscle atrophy during cancer cachexia (Bonetto et al., 2012; Bonetto et al., 2011; Cai et al., 2004b; Guttridge et al., 2000); however, the focus of muscle loss with cachexia has been placed on the inhibiting the cachexia-induced muscle proteolysis. Long term inhibition of muscle proteolysis without release of protein synthesis inhibition may not be beneficial in the cachectic patient as it may lead to the accumulation of dysfunctional proteins increasing cellular stress. We demonstrate that PDTC can both inhibit protein degradation signaling and increase muscle protein synthesis without alterations in circulating IL-6 levels, suggesting that IL-6 may not be the main suppressor of protein synthesis during cancer cachexia. This is further supported by the fact that neither IL-6r

Ab administration nor muscle gp130 inhibition are able to alleviate the cachexia-suppression of muscle protein synthesis; but appear to regulate muscle catabolism (Bonetto et al., 2012; Puppa et al., 2013b; White et al., 2013b).

One potential mechanism through which PDTC may be attenuating skeletal muscle loss is through the suppression of inflammation induced protein degradation. Chronic IL-6 exposure is documented to induce skeletal muscle protein breakdown (Fujita et al., 1996; White et al., 2011b). IL-6 activates STAT3 which in turn leads to activation of several signaling pathways implicated in the regulation of cachexia-induced protein degradation including FOXO and C/EBPβ (Bonetto et al., 2012; Reed et al., 2012; Zhang et al., 2011). STAT3 can directly regulate IL-6 induced transcription of C/EBPβ (Niehof et al., 2001), and STAT3 can directly bind to the FOXO promoter as well as interact with cytoplasmic FOXO to regulate targeted transcription (Oh et al., 2012). PDTC decreased STAT3 activation which could be responsible for the overall suppression of muscle protein degradation signaling.

Few therapies have been shown to increase muscle protein synthesis in the cachectic patient. We demonstrate that PDTC can increase muscle protein synthesis in both healthy and cachectic mice. PDTC has been shown to increase protein biosynthetic capacity in HepG2 cells through a rapamycin independent mechanism (Song et al., 2011). PDTC may work through the rapamycin insensitive mTORC2 complex to up regulate muscle protein synthesis. mTOR2 requires ribosomes for signaling; however, little is known about the independent regulation of protein synthesis through mTORC2 (Zinzalla et al., 2011). Another mechanism by which PDTC could increase muscle protein synthesis is through decreased cachexia-induced AMPK phosphorylation. We have

recently demonstrated that inhibition of AMPK can attenuate IL-6 suppression of protein synthesis in C2C12 myotubes (White et al., 2013b). Additionally exercise training can suppress cachexia-induced AMPK activation and prevented decreases in protein synthesis (Puppa et al., 2011d; White et al., 2013b). PDTC inhibited cachexia-induced AMPK phosphorylation potentially relieving inhibition of protein synthesis.

As well as increasing muscle protein synthesis PDTC increased muscle mitochondrial content. Recent literature has shown that mTOR signaling is important in the regulation of many oxidative genes (Cunningham et al., 2007). When the mTOR complex is inhibited there is a decrease in muscle oxidative capacity and function (Schieke et al., 2006) suggesting that mTOR is an important mediator for the maintenance of mitochondria. As previously reported we demonstrate cachexia suppression of skeletal muscle mitochondria content (Bing et al., 2000; Fermoselle et al., 2013; Julienne et al., 2012; Tisdale, 2002; White et al., 2011a; White et al., 2012b). As well as playing a role in protein synthesis the mitochondria play a vital role in protein degradation, apoptosis, and autophagy. One way in which the mitochondria can work to regulate protein degradation is through regulation of FOXO. When FOXO is blocked even in the presence of mitochondrial fission, muscle atrophy is prevented (Romanello et al.). We demonstrate increased mitochondrial fission and fusion with PDTC. Cachexia induction of fission was unaltered by PDTC; however, cachexia suppression of fusion was attenuated with PDTC. Further work is needed to determine the regulation of FOXO by PDTC.

In conclusion we demonstrate that two weeks of PDTC treatment after the initiation of cachexia was able to prevent further body weight and muscle mass loss.

Cachexia induced activation of skeletal muscle STAT3 and AMPK were suppressed with PDTC. Interestingly, the suppression of muscle inflammatory signaling was independent of systemic IL-6. We report that PDTC could attenuate both activation of muscle protein degradation and suppression of muscle protein synthesis. Additionally, PDTC released cachexia suppression of muscle mitochondrial content that was associated with suppressed mitochondrial fusion, but not fission. Further work is needed to determine how PDTC attenuates the cachexia suppression of protein synthesis and mitochondrial content. These data suggest that PDTC may be of therapeutic value for the treatment of cachexia.

Table 4.1. The effect of pyrrolidine dithiocarbamate on cachexia development in *Apc*$^{Min/+}$ mice. Body weight (BW) was measured throughout the duration of the study. Tibia length, spleen, epididymal fat, intestines and plasma were collected at the time of sacrifice. All values are mean ±sem. Two-way ANOVA was used to determine the effects of genotype x treatment (PDTC). # Main effect of Min, & Main effect PDTC. * compared to control group within genotype, † significant from all other comparisons, $p<0.05$.

	BL-6		***Apc*$^{Min/+}$**	
	PBS	**PDTC**	**PBS**	**PDTC**
N	**5**	**5**	**5**	**6**
Peak BW (g)	25.7 ± 1.2	27.8 ± 1.1	24.0 ± 0.5	25.4 ± 0.4
16wk BW (g)	25.3 ± 1.1	27.2 ± 1.1	22.4 ± 0.3$^{\#}$	23.8 ± 0.5$^{\#}$
18wk BW (g)	25.7 ± 1.2	27.8 ± 1.1$^{\&}$	20.7 ± 0.5$^{\#}$	24.6 ± 0.2$^{\&\#}$
Tibia Length (mm)	16.7 ± 0.1	17.2 ± 0.1	16.6 ± 0.2	16.9 ± 0.1
Epididymal Fat	287 ± 41	429 ± 48$^{\&}$	41 ± 41$^{\#}$	135 ± 43$^{\#,\&}$
Spleen (mg)	106 ± 13	88 ± 8	424 ± 67†	661 ± 14†
Tumor Number	-	-	46 ± 11	56 ± 7
Tumors >2mm (%)	-	-	93 ± 5	69 ± 3*
IL-6 (pg/ml)	0.0 ± 0.0	0.0 ± 0.0	71 ± 24$^{\#}$	46 ± 8$^{\#}$

4.6 Figure Legends

Figure 4.1. The effect of pyrrolidine dithiocarbamate on the progression of cachexia in *Apc*$^{Min/+}$ mice. Mice were aged to 16 weeks when body weight loss was initiated and received two weeks of PDTC treatment. A) The percent body weight loss from the peak body weight to the time of sacrifice was calculated. B) Gastrocnemius muscle mass was measured at the time of sacrifice. T-test was used to analyze the effect of PDTC within the min, * Significant from Min control. Two-way ANOVA was used to analyze the effects of genotype and PDTC administration. & Main effect of PDTC, # Main effect of Min. Significance was set at $p<0.05$.

Figure 4.2. The effect of pyrrolidine dithiocarbamate on cachexia-induced muscle inflammatory signaling. Western blot analysis of cachexia induced muscle inflammatory signaling including P-STAT3 and P-AMPK was measure in the gastrocnemius of mice with and without PDTC administration for two weeks. Two-way ANOVA was used to analyze the effects of genotype and PDTC administration. & Main effect of PDTC, † Significantly different from all other comparisons. Significance was set at $p<0.05$.

Figure 4.3. The effect of pyrrolidine dithiocarbamate on the regulation of muscle protein turnover. A) Regulation of muscle protein turnover was measured using western blot analysis of Atrogin-1 as a marker of protein degradation and P-S6 as a marker of muscle mTOR signaling. B) Muscle protein synthesis was measured by the incorporation

of puromycin into skeletal muscle. Two-way ANOVA was used to analyze the effects of genotype and PDTC administration. & Main effect of PDTC, # Main effect of Min, † Significantly different from all other comparisons. Significance was set at $p<0.05$.

Figure 4.4. The effect of pyrrolidine dithiocarbamate on muscle mitochondrial content. A) Skeletal muscle mitochondrial oxidative capacity was measured by the percentage of dark succinate dehydrogenase (SDH) stained fibers. B) Mitochondrial content was measured as the ratio of mitochondrial Cytochrome B gene expression to nuclear GAPDH gene expression in gastrocnemius muscle. Pre-planned t-test was used to analyze the effect of PDTC within the min, * Significant from Min control. Two-way ANOVA was used to analyze the effects of genotype and PDTC administration. & Main effect of PDTC, # Main effect of Min. † Significantly different from all other comparisons. Significance was set at $p<0.05$.

Figure 4.5. The effect of pyrrolidine dithiocarbamate on the regulation of muscle mitochondria. A) Skeletal muscle protein content of mitochondrial fusion protein, MFN1, mitochondrial fission protein, FIS, and mitochondrial content marker cytochrome c was measured by Western blot analysis. B) Gastrocnemius muscle mRNA expression of mitochondrial dynamic regulators MFN1 and FIS, and mitochondrial biogenesis marker PGC-1α. Pre-planned t-test was used to analyze the effect of cachexia * Significant from BL-6 control. Two-way ANOVA was used to analyze the effects of

genotype and PDTC administration. & Main effect of PDTC, # Main effect of Min. † Significantly different from all other comparisons. Significance was set at $p<0.05$.

.

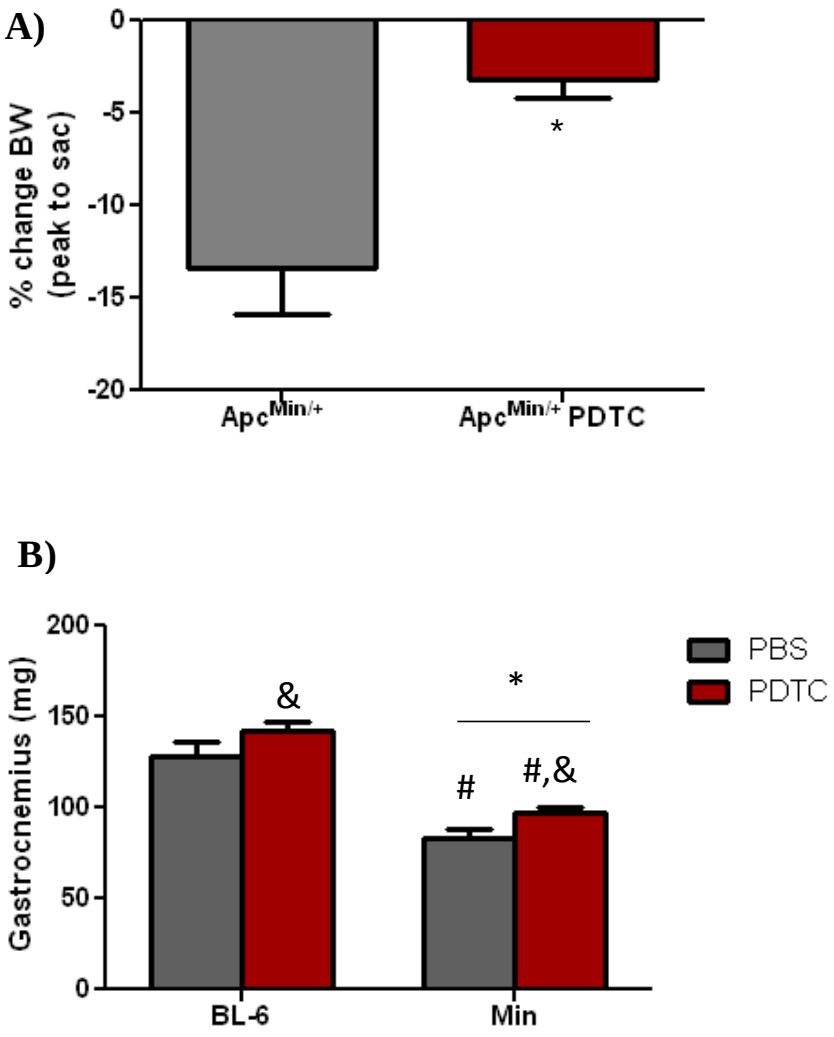

Figure 4.1. The effect of pyrrolidine dithiocarbamate on the progression of cachexia in *Apc*$^{Min/+}$ (Min) mice. Mice were aged to 16 weeks when body weight loss was initiated and received two weeks of PDTC treatment. A) The percent body weight loss from the peak body weight to the time of sacrifice was calculated. B) Gastrocnemius muscle mass was measured at the time of sacrifice. T-test was used to analyze the effect of PDTC within the min, * Significant from Min control. Two-way ANOVA was used to analyze the effects of genotype and PDTC administration. & Main effect of PDTC, # Main effect of Min. Significance was set at $p<0.05$.

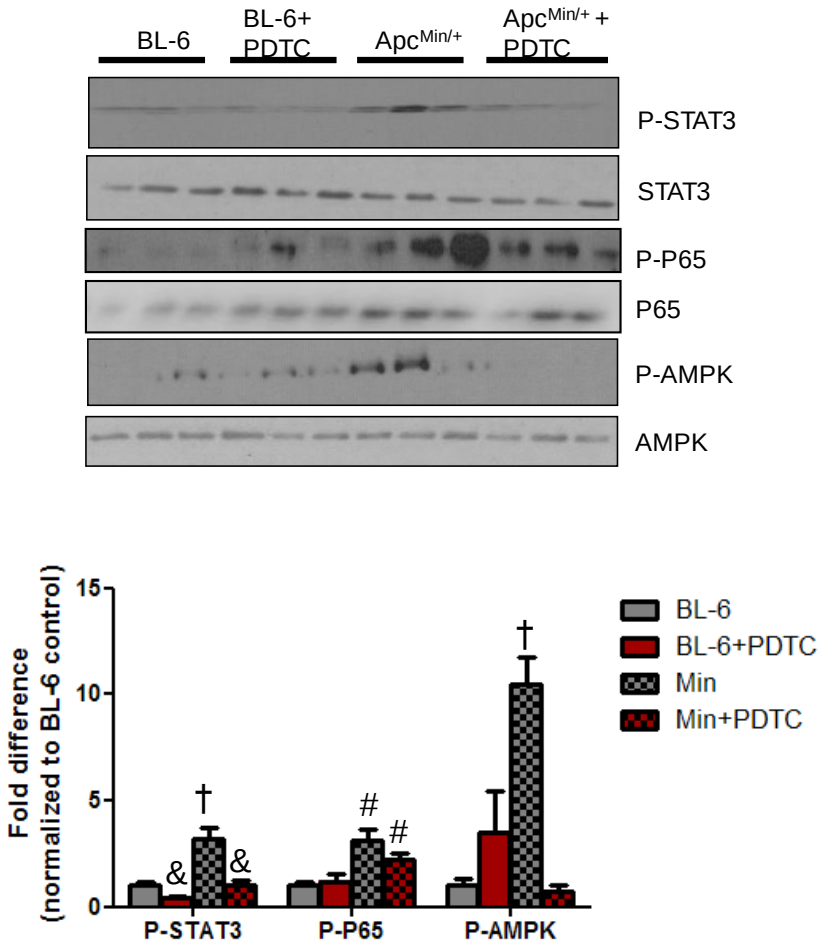

Figure 4.2. The effect of pyrrolidine dithiocarbamate on cachexia-induced muscle inflammatory signaling. Western blot analysis of cachexia induced muscle inflammatory signaling including P-STAT3 and P-AMPK was measure in the gastrocnemius of mice with and without PDTC administration for two weeks. Two-way ANOVA was used to analyze the effects of genotype and PDTC administration. & Main effect of PDTC, † Significantly different from all other comparisons. Significance was set at $p<0.05$.

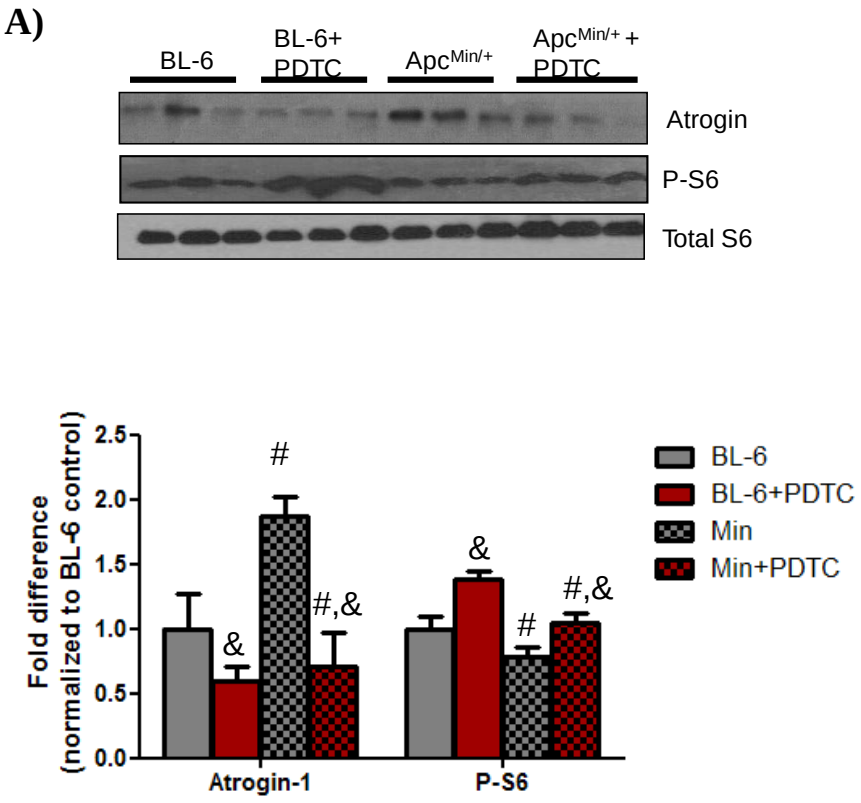
A)
BL-6
BL-6+ PDTC
ApcMin/+
ApcMin/+ + PDTC
Atrogin
P-S6
Total S6
Fold difference (normalized to BL-6 control)
2.5
2.0
1.5
1.0
0.5
0.0
#
&
#,&
&
#
#,&
Atrogin-1
P-S6
BL-6
BL-6+PDTC
Min
Min+PDTC

Figure 4.3

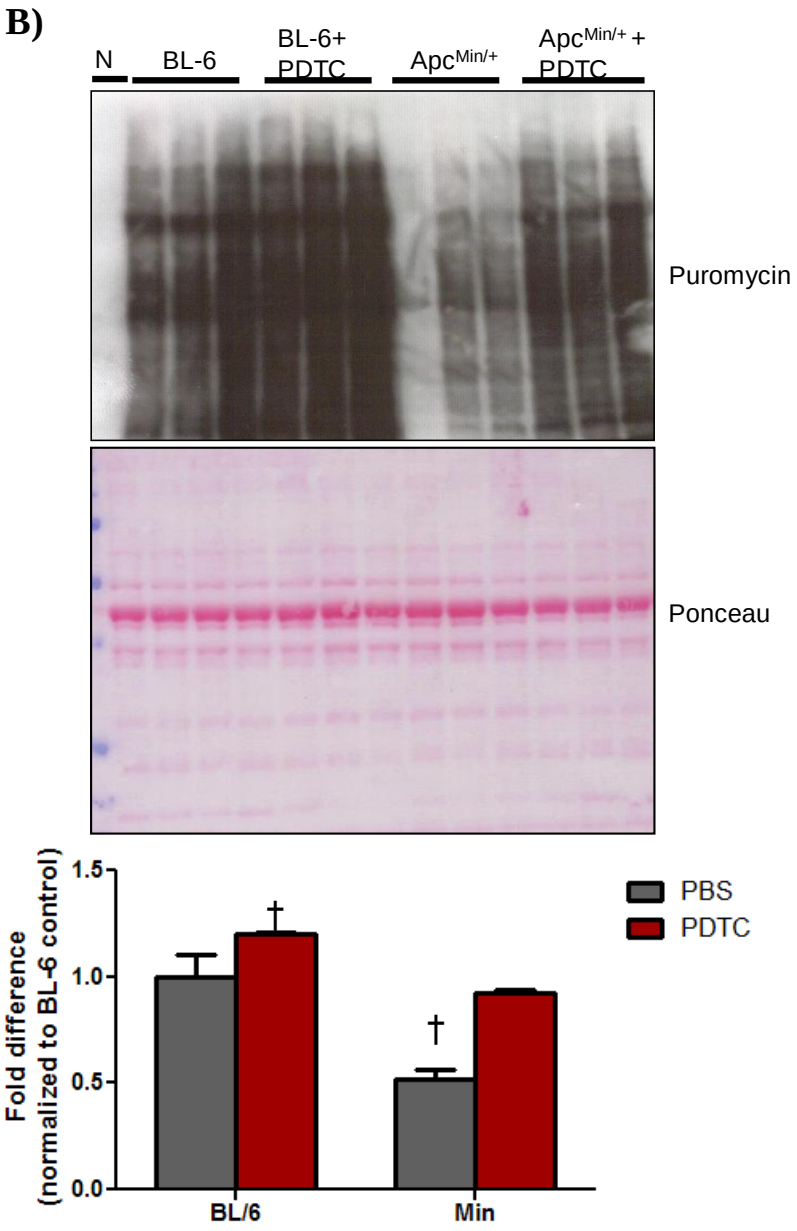

Figure 4.3. The effect of pyrrolidine dithiocarbamate on the regulation of muscle protein turnover. A) Regulation of muscle protein turnover was measured using western blot analysis of Atrogin-1 as a marker of protein degradation and P-S6 as a marker of muscle mTOR signaling. B) Muscle protein synthesis was measured by the incorporation of puromycin into skeletal muscle. Two-way ANOVA was used to analyze the effects of genotype and PDTC administration. & Main effect of PDTC, # Main effect of Min, † Significantly different from all other comparisons. Significance was set at $p<0.05$.

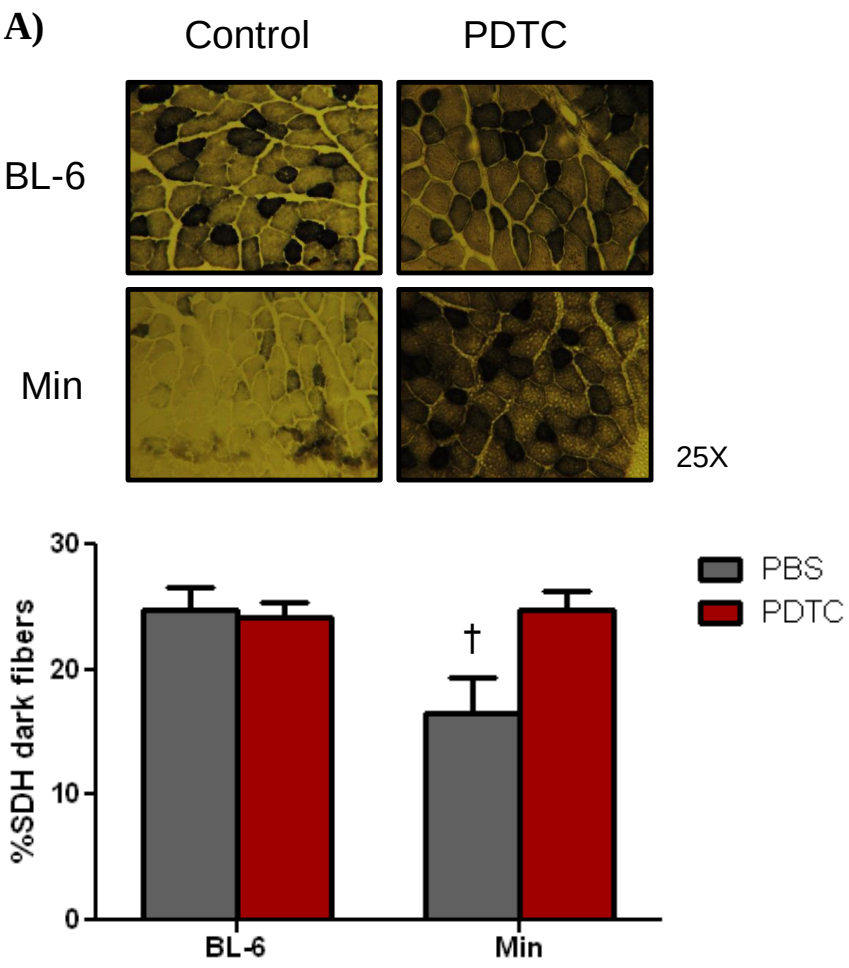
A)
Control
PDTC
BL-6
Min
25X
%SDH dark fibers
30
20
10
0
†
BL-6
Min
PBS
PDTC

Figure 4.4

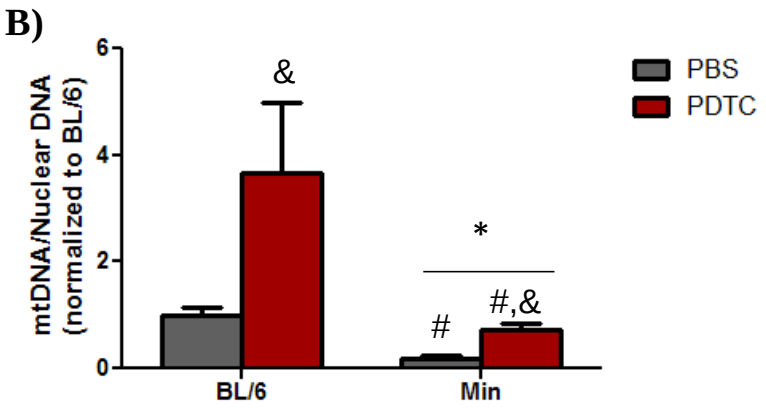

Figure 4.4. The effect of pyrrolidine dithiocarbamate on muscle mitochondrial content. A) Skeletal muscle mitochondrial oxidative capacity was measured by the percentage of dark succinate dehydrogenase (SDH) stained fibers. B) Mitochondrial content was measured as the ratio of mitochondrial Cytochrome B gene expression to nuclear GAPDH gene expression in gastrocnemius muscle. Pre-planned t-test was used to analyze the effect of PDTC within the min, * Significant from Min control. Two-way ANOVA was used to analyze the effects of genotype and PDTC administration. & Main effect of PDTC, # Main effect of Min. † Significantly different from all other comparisons. Significance was set at $p<0.05$.

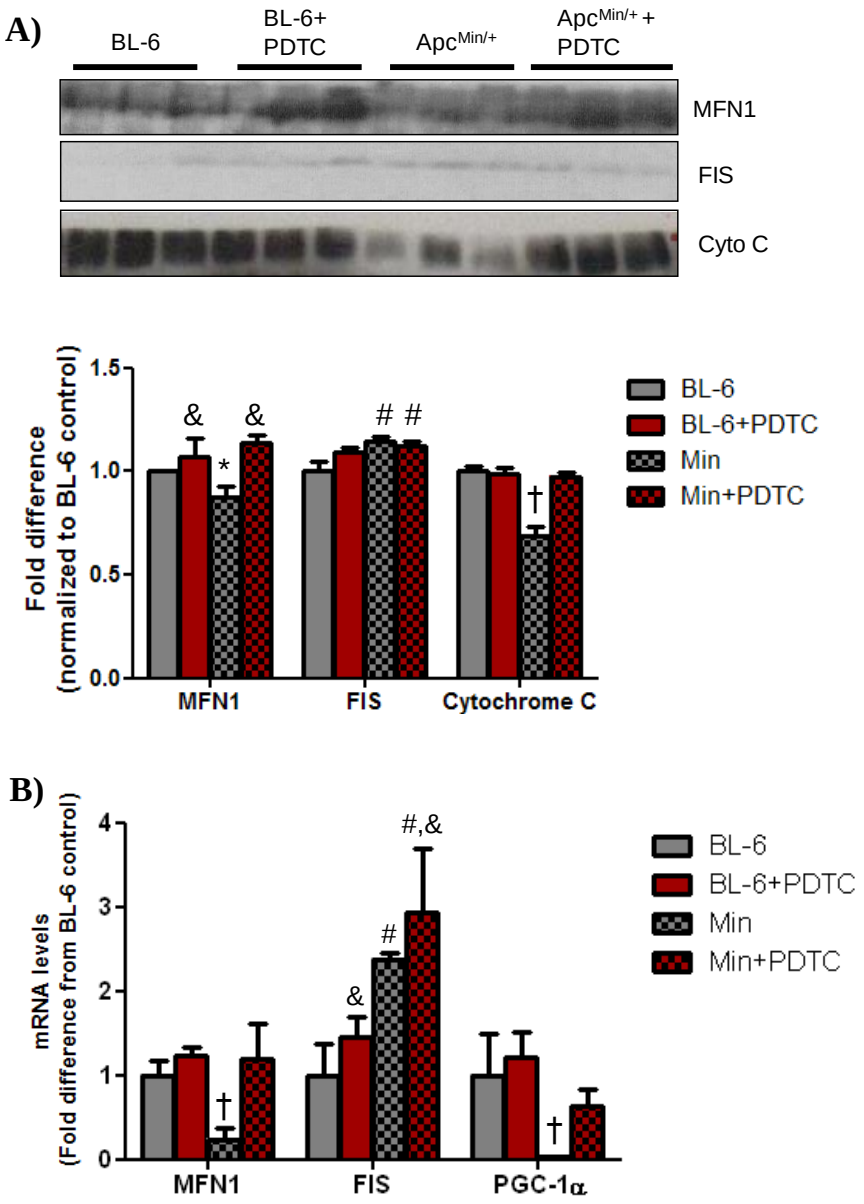

Figure 4.5. The effect of pyrrolidine dithiocarbamate on the regulation of muscle mitochondria. A) Skeletal muscle protein content of mitochondrial fusion protein, MFN1, mitochondrial fission protein, FIS, and mitochondrial content marker cytochorme c was measured by Western blot analysis. B) Gastrocnemius muscle mRNA expression of mitochondrial dynamic regulators MFN1 and FIS, and mitochondrial biogenesis marker PGC-1α. Pre-planned t-test was used to analyze the effect of cachexia * Significant from BL-6 control. Two-way ANOVA was used to analyze the effects of genotype and PDTC administration. & Main effect of PDTC, # Main effect of Min. † Significantly different from all other comparisons. Significance was set at $p<0.05$.

CHAPTER 5

SKELETAL MUSCLE GLYCOPROTEIN 130'S ROLE IN LEWIS LUNG CARCINOMA INDUCED CACHEXIA[3].

[3] Melissa Puppa, Song Gao, Aditi Narsale, and James Carson Accepted by FASEBJ. Reprinted here with permission of publisher.

5.1 Abstract

Chronic inflammation is associated with cancer cachexia-induced skeletal muscle mass loss. IL-6 cytokine family members are increased during cancer cachexia, and induce intracellular signaling through glycoprotein130 (gp130). While muscle STAT3 and circulating IL-6 are implicated in cancer-induced muscle wasting, there is limited understanding of muscle gp130's role in this process. Therefore, we investigated the role of skeletal muscle gp130 for cancer-induced alterations in the regulation of muscle protein turnover. Lewis lung carcinoma (LLC) cells were injected into 8-wk old mice with a skeletal muscle gp130 knockout, or wild-type mice. Skeletal muscle loss was attenuated by 16% in gp130 KO mice, which coincided with attenuated LLC-induced phosphorylation of muscle STAT3, p38, and FOXO3. The gp130 KO did not rescue mTOR inhibition or alter AMPK activation. The induction of atrogin expression and p38 phosphorylation in C2C12 myotubes administered LLC media was attenuated by gp130 inhibition, while mTOR inhibition was not rescued. STAT signaling inhibition in LLC treated myotubes did not attenuate the induction of p38 or AMPK phosphorylation. During LLC induced cachexia the skeletal muscle gp130 regulates muscle mass signaling through STAT3 and p38 for the activation of FOXO3 and atrogin, but does not directly regulate the suppression of mTOR.

KEYWORDS: cachexia, inflammation, skeletal muscle, gp130, Lewis Lung Carcinoma.

5.2 Introduction

Cachexia, the unintentional loss of body weight including muscle and fat mass, is associated with many cancer types (Evans et al., 2008; Fearon et al., 2011; Muscaritoli et al., 2010). Cachexia occurs in approximately 20% of all cancer patients and is responsible for 40% of colon cancer related deaths (Bruera, 1997; Tisdale, 2002). Chronic inflammation is associated with diseases that induce muscle wasting, including cancer (Tisdale, 2009). Several cytokines are up regulated with cachexia in both human cancer cachexia and animal models of cachexia such as the $Apc^{Min/+}$, the C26 adenocarcinoma, and the Lewis Lung carcinoma (LLC), including IL-6, TNFα, IL-1β, LIF, CNTF, IFN-γ, and IL-10 (Argiles et al., 2003; Bonetto et al., 2011; Fortunati et al., 2007; Tazaki et al., 2011). It is clear that cytokines play a vital role in the development of muscle atrophy with cachexia. The use of anti-cytokine therapies to combat muscle wasting during cancer induced cachexia has been widely used (Baltgalvis et al., 2008b; Matthys et al., 1991; White et al., 2011b). However, further research is required to understand if inflammatory cytokines exert direct or indirect effects on skeletal muscle to alter protein turnover and induce wasting.

Circulating levels of the IL-6 family cytokines are associated with cancer cachexia (Barton and Murphy, 2001; Bonetto et al., 2011; Kamoshida et al., 2006; Mori et al., 1991; Puppa et al., 2011b; Tisdale, 2009). IL-6 can signal via the classical pathway, through the membrane receptor, or trans pathway, utilizing soluble IL-6 receptor, to induce signaling; however gp130 is required for this signaling (Rose-John, 2012). IL-6 family cytokines signal through the gp130 by forming either a heterodimer or homodimer with the cytokine, its receptor and gp130. Gp130 dimerization leads to activation of

several intracellular signaling pathways including JAK/STAT, p38/MAPK, and PI3K/Akt (Ernst and Jenkins, 2004; Heinrich et al., 1998). In skeletal muscle these signaling pathways have been associated with the regulation of growth and atrophy (Bonetto et al., 2012; Schiaffino and Mammucari, 2011; Stitt et al., 2004). While studies have examined the role of STAT3 and IL-6 specifically, the role of gp130 in skeletal muscle wasting during cachexia has not been examined.

Skeletal muscle mass is regulated by a balance of protein synthesis and protein degradation, termed protein turnover. Altered protein turnover is an established regulatory point of both skeletal muscle mass loss and muscle growth. During cancer cachexia there is an increase in skeletal muscle protein degradation and suppression in muscle protein synthesis (MPS) (Tisdale, 2009). Muscle STAT3 signaling is sufficient to induce skeletal muscle atrophy both *in vitro* and *in vivo*, and STAT3 inhibition can attenuate cancer induced muscle atrophy (Bonetto et al., 2012; Bonetto et al., 2011). P38/MAPK and C/EBPβ also mediate cancer induced muscle atrophy through the inhibition of FOXO1/3 phosphorylation and activation of atrogin-1 (Zhang et al., 2011; Zhang and Li, 2012). While there is strong evidence that gp130 mediated signaling regulates cancer – induced protein degradation, its role in suppression of protein synthesis during cancer cachexia remains poorly defined.

Our lab and the work of others have defined important roles for IL – 6, muscle STAT3 and p38/MAPK signaling in cancer-induced muscle wasting (Bonetto et al., 2012; White et al., 2013b; Zhang et al., 2011), yet significant gaps remain in our understanding of the relationship of these signaling pathways to the IL-6 family of cytokines and their ability to regulate cachexia suppression of MPS. Gp130 is a common

regulatory point for the IL-6 family of cytokines, STAT3 and p38 signaling; however, STAT3 and p38 can be activated by other signaling cascades. Additionally, the gp130 regulates pathways other than STAT3 and p38/MAPK such as PI3K/Akt (Ernst and Jenkins, 2004). The purpose of this study was to examine the role of the skeletal muscle gp130 for the regulation of muscle protein turnover during LLC-induced cachexia. We hypothesize that skeletal muscle gp130 is necessary for muscle STAT3 mediated inhibition of mTOR signaling and FOXO3a activation during LLC-induced cachexia. We examined a muscle specific knockout of gp130 during LLC-induced cachexia. The role of systemic IL-6 and STAT signaling were investigated with administration of PDTC or IL-6r antibody to mice with LLC tumors.

5.3 Methods

Animals. Male mice on a C57BL/6 background were bred with the gp130 fl/fl mice provided by Dr. Colin Stewart's lab in collaboration with Dr. Hennighausen (NCI) (Zhao et al., 2004). Gp130 fl/fl male mice were bred with cre-expressing mice driven by myosin light chain (MLC) from Dr. Steven Burden (NYU) (Bothe et al., 2000). The resulting fl/fl cre/cre (skm-gp130) mice have a skeletal muscle deletion of the gp130 protein. Offspring were genotyped using tail snips for cre recombinase (forward 5' AAG CCC TGA CCC TTT AGA TTC CAT TT 3', reverse 5' AAA ACG CCT GGC GAT CCC TGA AC 3', wild type 5' GCGGGCTTCTTCACGTCTTTCTTT 3'), floxed gp130 (forward 5' ACG TCA CAG AGC TGA GTG ATG CAC 3', reverse 5' GGC TTT TCC TCT GGT TCT TG 3'). All animal experimentation was approved by the University of South Carolina's Institutional Animal Care and Use Committee.

IL-6 over-expression: A cohort of skm-gp130 and C57BL/6 mice were electroporated at 12wk of age with either an empty vector or an IL-6 plasmid (n=3-4/group) as previously described (Baltgalvis et al., 2008b). Muscle was taken at the time of sacrifice at 14 weeks of age

Lewis Lung Carcinoma implantation: C57BL/6 and skm-gp130 mice were injected with $1x10^6$ Lewis lung carcinoma cells (LLC) on the right flank subcutaneously at 8 weeks of age (Hariri et al., 2010). Body weights were measured weekly starting at 8 weeks of age. Tumors were allowed to grow for ~30 days and mice were sacrificed at 13 weeks of age.

IL-6/STAT3 inhibition in vivo: A separate cohort of C57BL/6 mice (n=17) were implanted with LLC tumor cells at 8 weeks of age. At 12 weeks of age animals were

randomized to receive IL-6 receptor antibody or PDTC for one week. No mice died during the one week of treatment; however, prior to randomization, 5 mice died or had to be euthanized due to excessive tumor burden or ulcerated tumors.

IL-6 receptor Antibody administration: After four weeks of tumor growth a subset of mice were treated with 100ug of IL-6 receptor (IL-6r) antibody (Chugai Pharmaceuticals) as previously described (White et al., 2012b) with modifications. Animals were treated with IP injections every three days for 1 week receiving IL -6r antibody once every three days.

Pyrrolidine dithiocarbamate (*PDTC):* After four weeks of tumor growth a subset of mice were treated by daily IP injections with 10mg/kg of PDTC in PBS (Nai et al., 2007) for 1 week.

Tissue sampling. At study end points mice were anesthetized with a ketamine/ xylazine/ acepromazine cocktail, and tissues were removed, weighed, and frozen at -80 °C until further analysis. Blood samples were collected in heparinized capillary tubes from the retro-orbital sinus.

C2C12 cells. C2C12 myoblasts (American Type Culture Collection, Manassas, VA) were cultured in Dulbecco's modified Eagle's medium (DMEM), supplemented with 10% FBS, 50U/ml penicillin and 50µg/ml streptomycin. Myoblast differentiation was induced as previously described (White et al., 2013b). Fully differentiated myotubes were treated with LLC conditioned media (LCM) for 4h or 72h replacing the media every 24h for control and treatment groups as previously described (Zhang et al., 2011). IL-6r Ab (Chugai Pharmaceuticals) and gp130 Ab (Santa Cruz, dialyzed in PBS at 4°C overnight)

were administered in the LCM for 72h at a 1: 1000 dilution. PDTC, 50μM (Sigma) and LLL12 (Bio-Vision), a STAT3 inhibitor (100nM) was administered in the LCM for the duration of the study (White et al., 2013b). To measure rate of protein synthesis, 1μM puromycin was added to culture medium 30min before protein collection (Goodman et al., 2011a). Cells were harvested as previously described (White et al., 2013b).

Myotube Diameter Measurement:

C2C12 myotubes diameter was quantified as previously published (White et al., 2013b). All measurements were conducted blindly.

Plasma IL-6: Plasma IL-6 was quantified as previously published (Puppa et al., 2011b). Briefly, blood samples centrifuged at 10,000×g for 10 min at 4°C. Plasma was collected and stored at −80°C until analysis. An ultra-sensitive mouse IL-6 ELISA (Invitrogen) was performed according to manufacturer's instructions.

RNA Isolation/PCR. RNA isolation, cDNA synthesis and real-time PCR were performed as previously described (White et al., 2013b) , using reagents from Applied Biosystems. Gp130 (forward 5' CAG CGT ACA CTG ATG AAG GTG GGA AA 3', reverse 5' GCT GAC TGC AGT TCT GCT TGA 3') , IGF-1(White et al., 2013a), REDD1 (White et al., 2013a), IL-6 (Washington et al., 2011), and GAPDH primers were purchased from IDT (Coralville, Iowa, USA). Data were analyzed by ABI software using the cycle threshold (CT).

Western Blot analysis: Western blot analysis was performed as previously described (Puppa et al., 2011d). Briefly, gastrocnemius muscle was homogenized and protein concentration was determined by the Bradford method (Bradford, 1976). Homogenates were fractionated on SDS-polyacrylamide gels and transferred to PVDF membrane. After blocking, antibodies for phosphorylated and total 4EBP1, AMPK, S6RP, STAT3, Akt, , ubiquitin, GAPDH (Cell signaling), p38 (Santa Cruz), FOXO3a, anti-puromycin (Millipore), and atrogin-1 (ECM Biosciences)were incubated at dilutions of 1:2000 to 1:6,000 overnight at 4°C in 1% TBST milk. Anti-rabbit or anti-mouse IgG-conjugated secondary antibodies (Cell signaling) were incubated with the membranes at 1:2,000 to 1:5,000 dilutions for 1 h in 1% TBST milk. Enhanced chemiluminescence was used to visualize the antibody-antigen interactions and developed by autoradiography. Blots were analyzed by measuring the integrated optical density (IOD) of each band using ImageJ software.

Statistical analysis. A two-way ANOVA was used to examine the effects of LLC and genotype. Post-hoc analyses were performed with Student-Newman-Keuls methods. Pre-planned t-tests were used examine the effect of gp130 loss in control mice to define the phenotype. One-way ANOVA was used to analyze all C2C12 experiments. Significance was set at $p<0.05$.

5.4 Results

Expression of gp130 in C57BL/6 mice

Gp130 mRNA expression was examined in adult C57BL/6 mice. Although gp130 is expressed in all cell types, muscle had significantly greater expression than the liver or kidney (Fig 5.1A). Skeletal muscle has the greatest expression level and heart expression was 67% lower than gastrocnemius skeletal muscle. Expression was greatest in the glycolytic TA muscle, and the lowest expression was found in the oxidative soleus muscle (Fig 5.1B). These data indicate that while gp130 is ubiquitously expressed, there is differential expression in tissues and amongst skeletal muscle phenotypes.

Characterization of skm-gp130 mice

The cre-loxP approach was used to generate a muscle specific knockout of the gp130 in C57BL/6 mice (Fig 5.1C & D) using MLC cre-expressing mice (Bothe et al., 2000), and gp130 fl/fl mice (Zhao et al., 2004). In skm-gp130 mice, the gp130 mRNA expression was significantly reduced in all hindlimb muscles examined and the heart, but not altered in the liver or kidney (Fig 5.1C). Heart CRE activity has been previously reported with this CRE mouse (Bothe et al., 2000). Since all cell types express gp130, cells in skeletal muscle other than myofibers will continue to express gp130. There was no effect of genotype on overall body size measured by tibia length (Table 5.1). There was a body weight increase in skm-gp130 mice (Table 5.1), which was associated with an increase in lean mass. This may be partially attributable to increased organ mass, for example skm-gp130 mice had significantly larger heart, and testes mass (Table 5.1). There was no effect of genotype on gastrocnemius muscle and epidydimal fat mass (Table 5.1).

Skeletal muscle gp130 loss attenuated Il-6 –induced STAT3 phosphorylation

IL-6 was systemically over expressed to examine gp130 function. Circulating IL-6 was not detectable in vector control mice, but was increased by over-expression in all genotypes (skm-gp130+/+ 86.2±12.1pg/mL; skm-gp130 +/- 70.2±14.2 pg/mL; skm-gp130 -/- 71.0±25.9 pg/mL). Skeletal muscle STAT3 phosphorylation (Y705) in mouse quadriceps increased 5 fold by IL-6 over-expression in wild-type mice. This induction was suppressed in skm-gp130 heterozygous mice and blocked in skm-gp130 homozygous mice (Fig 5.1D).

LLC induced body weight loss in skm-gp130 mice

We examined the role of the muscle gp130 in cancer-induced muscle loss using LLC implanted wild-type and skm-gp130 mice (Table 5.1, Fig 5.2). LLC-induced cachexia decreased muscle gp130 mRNA expression 50% (Fig 5.2A). We did not detect gp130 mRNA expression in control or LLC implanted skm-gp130 mice. Loss of muscle gp130 had no effect on tumor mass (Fig 5.2B). LLC decreased body weight 11% in wild-type mice, and this loss of body weight was not attenuated in skm-gp130 mice (Fig 5.2C). Cachexia-related lean body mass loss, measured by DEXA scanning, was attenuated in skm-gp130 mice when compared to wild-type-mice (Table 5.1). LLC induced a 20% reduction in gastrocnemius muscle mass, which was attenuated in skm-gp130 mice (Fig 5.2D). LLC implantation decreased epididymal fat mass 36% and induced spleenomegaly in wild-type mice. Muscle gp130 loss had no effect on LLC-induced epididymal fat mass loss or spleen size (Table 5.1). Plasma IL-6 was increased by LLC implantation and there was no effect of gp130 loss on circulating IL-6 levels (BL/6 0.0±0.0pg/ml; BL/6 LLC 38.7±13.9pg/ml; skm-gp130 0.0±0.0pg/ml; skm-gp130 LLC

16.7±8.1pg/ml). LLC had no effect on heart mass. However, skm-gp130 mice had heart enlargement that was not affected by the LLC tumor (Table 5.1). LLC implantation decreased bone mineral density in wild-type mice but not in skm-gp130 mice, suggesting a muscle bone interaction (Table 5.1).

LLC-induced muscle signaling pathways in skm-gp130 knockout mice

Signaling regulating muscle mass was examined in the gastrocnemius muscle of wild-type and skm-gp130 mice (Fig 5.3). LLC implantation increased muscle STAT3 phosphorylation and p65 phosphorylation, which were attenuated by skm-gp130 loss (Fig 5.3A). LLC-implantation induced muscle AMPK phosphorylation regardless of genotype, suggesting LLC-induced AMPK phosphorylation does not require muscle gp130. The phosphorylation of p38 was induced by LLC implantation in wild-type mice and skm-gp130 loss ablated this induction (Fig 5.3A). Basal STAT, AMPK, and p38 phosphorylation in muscle were not altered by gp130 loss, while Akt phosphorylation (Fig 5.3B). LLC induced Akt (T308) phosphorylation in wild-type mice, but phosphorylation of Akt (S473) was unaltered. The LLC induction of Akt (T308) was not affected by skm-gp130 loss.

The regulation of LLC-induced signaling mediating protein turnover through mTOR and FOXO3a was examined in the gastrocnemius (Fig 5.3C). In wild-type mice LLC suppressed the phosphorylation of mTOR substrates p-4EBP-1 and p-S6RP, and this suppression was not affected by skm-gp130 loss (Fig 5.3C). LLC implantation reduced FOXO3a phosphorylation, which was attenuated by skm-gp130 loss. LLC also induced atrogin-1 expression and the abundance of ubiquitinated proteins, which were attenuated by skm-gp130 loss (Fig 5.3C, 5.3D). We measured mRNA levels of IGF-1 and REDD1,

which are established regulators of muscle anabolic signaling through mTOR (Fig 5.3E). LLC cachexia decreased muscle IGF-1 mRNA expression and gp130 loss did not rescue this suppression. Basal REDD1 expression was suppressed in skm-gp130 mice. However, during LLC-induced cachexia REDD1 expression was induced regardless of genotype (Fig 5.3E). LLC-induced cachexia increased muscle IL-6 mRNA expression in both wild-type and skm-gp130 gastrocnemius muscle (Fig 5.3E).

The effect of LLC conditioned media on the regulation of C2C12 myotube growth

To examine the direct role of LLC secreted factors on the regulation of C2C12 myotube growth, myotubes were administered 15% or 25% LLC conditioned media (LCM). LCM decreased myosin heavy chain expression (Fig 5.4A), while only the higher dosage of LCM (25%) was sufficient ($p \leq 0.01$) to reduce myotube diameter (Control: 32.3 ± 0.7μM; 15% LCM 30.9±0.7μM; 25% LCM 29.0 ± 0.6μM). High dose LCM administration increased IL-6 mRNA levels, while 15% LCM had no effect on IL-6 mRNA levels (Control: 1.00 ± 0.10; 15% LCM 1.04±0.11; 25% LCM 1.52 ± 0.16 fold change from control). LCM induced p-STAT3 at 4h, which returned to baseline by 72h (Fig 5.4B). The phosphorylation of Akt (S473) was unaffected by LCM; however, LCM decreased mTOR phosphorylation and phosphorylation of substrates 4EBP1 and S6RP in a dose dependent manner (Fig 5.4C). AMPK was induced after 72h exposure to LCM (Fig 4C). LCM administration suppressed FOXO3a phosphorylation, while atrogin-1 protein expression was induced (Fig 5.4D).

IL-6 inhibition in LLC mediated C2C12 and in vivo atrophy

We have previously demonstrated that IL-6 can induce C2C12 myotube atrophy (White et al., 2013b), and we found circulating IL-6 to be significantly elevated ($p=0.03$)

with LLC-induced cachexia (C57BL/6 0.0±0.0pg/ml versus C57BL/6 LLC 38.07±13.9pg/ml). C2C12 myotubes were treated with either IL-6 or LCM and then administered IL-6 receptor antibody (IL-6r Ab). As previously reported p-STAT3 was induced by IL-6 administration (White et al., 2013b). IL-6r Ab blocked IL-6-induced STAT3 phosphorylation, but had no effect on LCM induced STAT3 phosphorylation (Fig 5A). LCM reduced the rate of protein synthesis in C2C12 myotubes 31%, and IL-6r Ab treatment was not sufficient to rescue this repression (Fig 5.5B). IL-6r Ab had no effect on LLC induced AMPK or Akt phosphorylation, or suppression of 4-EBP-1 (Fig 5.5C). LLC activation of protein degradation pathways, measured by FOXO3a phosphorylation and atrogin-1 expression were unaffected by IL-6r Ab administration (Fig 5.5C).

We examined the role of systemic IL-6 signaling during LLC induced cancer cachexia *in vivo*. Acute administration of IL-6r Ab to LLC implanted mice (Table 5.2) did not rescue the induction of p-STAT3, p-p38, or atrogin-1 (Fig 5.5D). Systemic IL-6 inhibition resulted in a reduction in mTOR substrate S6RP from the already suppressed levels of LLC implanted mice (Fig 5.5D). LLC decreased protein synthesis, and IL-6r Ab had no effect on this suppression (Fig 5.5E).

IL-6 signaling inhibition in LLC mediated C2C12 and in vivo atrophy

The effects of STAT3 inhibition on LLC induced myotube signaling was examined by Pyrrolidine dithiocarbamate (PDTC, a STAT3 and NFκB inhibitor), LLL12 (a STAT specific inhibitor) or gp130 antibody (gp130 Ab) administration. LLC induced STAT3 phosphorylation was blocked by PDTC, LLL12, and gp130 Ab (Fig 5.6A). Myotube diameter was decreased with LLC treatment (Fig 5.6B). Inhibition of gp130 attenuated LLC induced myotube atrophy, while IL-6 inhibition did not rescue myotube

diameter (Fig 5.6B). LLC suppressed protein synthesis was not rescued by PDTC, LLL12 and gp130 Ab administration (Fig 5.6C). Increased p65 phosphorylation was blocked by gp130 antibody administration and p38 phosphorylation attenuated. LCM-induced AMPK phosphorylation was not affected by gp130 Ab administration (Fig 5.6D). Inhibition of gp130 did not rescue inhibition of mTOR target, 4-EBP1 (Fig 5.6D), but did suppress the induction of atrogin-1 expression (Fig 5.6D). Specific STAT3 inhibition by LLL12 did not prevent LLC induced NFκB phosphorylation, p38 activation, or activation of AMPK (Fig 5.6E). LLL12 was unable to preserve mTOR signaling through 4EBP1; however, it suppressed LLC-induced atrogin-1 (Fig 5.6E). LCM activation of NFκB was blocked by PDTC (Fig 6F). PDTC had no effect on LLC induced AMPK activation, p38 phosphorylation, or 4-EBP1, but attenuated atrogin-1 expression (Fig 5.6F).

We examined acute administration of PDTC *in vivo* (Table 5.2) in cachectic mice bearing LLC tumors. PDTC reduced muscle STAT3 and p65 phosphorylation (Fig 5.6G). PDTC administration did not alter LLC induced AMPK or Akt phosphorylation. Interestingly, phosphorylation of p38 showed a trend ($p=0.07$) for increasing with PDTC treatment. Taken together these results demonstrate a role for gp130/STAT3 in LLC-induced cachexia for the regulation of muscle protein degradation; however the regulation of LLC-induced suppression of MPS requires further investigation.

5.5 Discussion

Chronic inflammation, a hallmark of cancer cachexia, is also a potential therapeutic target for the devastating condition. IL-6 and muscle JAK/STAT signaling can regulate muscle mass in tumor-bearing mice (Bonetto et al., 2012; White et al., 2011b; White et al., 2013b). Although no treatments for cancer cachexia currently are approved, 2 separate clinical case studies recently published demonstrate improved cancer patient cachexia symptoms with IL-6r Ab administration (Ando et al., 2013; Hirata et al., 2013). However, significant gaps remain in our understanding of how cancer-induced systemic inflammation regulates the disruption of skeletal muscle protein turnover. To this end our study provides novel information on the role of the skeletal muscle gp130 for the regulation of muscle protein turnover during LLC-induced cachexia. We report that skeletal muscle gp130 signaling is an important mediator of LLC-induced skeletal muscle mass loss, as skm-gp130 mice have attenuated skeletal muscle mass loss without altered tumor size or fat mass loss. We also report that loss of gp130 signaling attenuates the LLC- activation of both STAT3 and p38, while activating Akt phosphorylation. Although LLC-induced gp130 signaling is associated with activation of FOXO3 / Atrogin signaling, we also provide *in vivo* and cell culture data indicating that cancer-induced protein synthesis suppression is independent of these signaling pathways.

Several IL-6 family cytokines are elevated during cancer cachexia and have a potential regulatory role for LLC-induced muscle mass loss in the mouse (Kim et al., 2009; Matthys et al., 1991). Although the gp130 is ubiquitously expressed, our current study reports that gp130 mRNA expression is higher in skeletal muscle than the liver or

kidney. Interestingly, we also demonstrate differential expression of the gp130 mRNA in the oxidative and glycolytic muscle. Muscle gp130 mRNA expression also demonstrated plasticity, decreasing with the progression of cachexia. Contrasting with cancer, elevated skeletal muscle gp130 expression has been reported in diabetic mice (Toledo-Corral and Banner) , and the gp130 has been identified as a potential therapeutic target for obesity (Febbraio, 2007). Intracellular signaling initiated by gp130 can regulate growth, differentiation, and apoptosis (Ernst and Jenkins, 2004). Additionally, gp130 activation can phosphorylate AMPK, enhance glucose uptake and fatty acid oxidation independent of STAT3 (Kelly et al., 2004; Watt et al., 2006). This points to the potential for gp130 to have a dynamic role in the muscle response to the cancer environment. Further work is needed to determine if the gp130 alters muscle metabolic regulation during different stages of cachexia and muscle phenotype has a role in the response.

STAT3 has a role in the regulation of muscle protein degradation during wasting with cancer (Bonetto et al., 2012; Bonetto et al., 2011) and can regulates atrogin-1 expression in C-26 tumor bearing mice (Bonetto et al., 2012). However, the mechanism by which the cachectic environment and/or circulating IL-6 activate muscle STAT3 is not well understood. STAT3 can be activated by pro-inflammatory cytokines in the IL-6 family, but also can be activated by leptin (Baeza-Raja and Muñoz-Cánoves, 2004), IFN γ (Akimoto et al., 2005b) and epidermal growth factor signaling (Widegren et al., 1998).We have extended these findings to demonstrate a role for muscle gp130 signaling for the induction of FOXO3 activation and the atrogin-1 expression both *in vivo* and *in vitro*. LLC-induced muscle STAT3 phosphorylation was attenuated by muscle specific loss of gp130, and gp130 antibody administration blocked LLC media induced STAT3

phosphorylation in cultured myotubes. Our data suggest muscle STAT3 induction during LLC-induced cachexia may be at least in part independent of circulating IL-6. IL-6r antibody administration to LLC tumor bearing mice and LCM-treated myotubes was not sufficient to attenuate STAT3 phosphorylation, as in $Apc^{Min/+}$ mice (White et al., 2011b). While STAT3 has been closely linked with muscle mass loss through regulation of degradation pathways, there may be redundancy in the activation of protein degradation cachectic mediators such as myostatin (Murphy et al.), FOXO (Reed et al.), and C/EBPβ (Zhang et al., 2011). Interestingly, we have shown previously that chronically activated STAT3 does not lead to muscle mass loss in treadmill exercising mice (Puppa et al., 2011d), suggesting that STAT3 regulation of skeletal muscle mass can be circumvented by other signaling pathways.

p38, a member of mitogen-activated protein kinases, serves as a nexus for signal transduction and is involved in a large variety of cellular processes. In skeletal muscle, p38 can be activated by many stress signals including oxidative stress, inflammatory cytokines and exercise. Activation of this pathway can regulate many functions in muscle including myogenesis (Wu et al., 2000), exercise induced PGC-1α transcription (Akimoto et al., 2005b) and exercise induced glucose uptake (Widegren et al., 1998). However, chronic p38 activation in skeletal muscle has been implicated in pathologies, such as muscle wasting by activating the FOXO3/ atrogin-1 protein degradation pathway (Zhang et al., 2011; Zhang and Li, 2012). p38 MAPK signaling may participate in local activation of NFκB (Baeza-Raja and Muñoz-Cánoves, 2004), which is another upstream activator of atrogin-1/MAFbx expression and muscle wasting (Cai et al., 2004a). We report that LLC-induced muscle p38 phosphorylation is dependent on the presence of the

muscle gp130. Consistent with previous findings (Zhang et al., 2011), we see p38 activation in both *in vivo* LLC-induced cachexia and in LLC treated myotubes. Inhibition of gp130 caused the suppression of p38 while PDTC administration potentiated the p38 activation by LLC, which has previously been reported (Pfeilschifter et al.). Taken together, our results demonstrate that the gp130 is required for p38 activation in LLC induced cachexia, independent of STAT3. Further work is needed to integrate our understanding of gp130/p38/STAT3 cross-talk for the regulation of protein degradation in LLC induced cachexia.

There has been considerable progress in understanding muscle protein degradation regulation during cachexia, and as a result degradation processes are considered a control point of muscle mass loss with cachexia (Tisdale, 2009). However, muscle protein synthesis is suppressed with cancer cachexia in humans (Dworzak et al., 1998) and mice (White et al., 2011b), and this anabolic repression likely has physiological ramifications. mTOR functions as an integration point for hormone, nutrition, and contraction regulation of MPS, and subject to complex regulation (Frost and Lang; Goodman et al.). IGF-1 can activate PI3K/Akt signaling to induce mTOR activity and protein synthesis through TSC1/2 phosphorylation (Frost et al., 2009; Wu et al., 2000). Muscle IGF-1 expression is suppressed in several models of cachexia (Goodman et al.; Lantier et al.; White et al., 2011b), and the regulation of this suppressed expression is not well understood. We report that loss of muscle gp130 signaling, a reduction in STAT3 signaling, and inhibited p38 signaling are not sufficient to rescue suppressed muscle IGF-1 expression. Similarly, systemic IL-6 inhibition in $Apc^{Min/+}$ mice after the onset of cachexia was unable to completely rescue muscle IGF-1 expression

(White et al., 2011b). Despite suppressed IGF-1, Akt phosphorylation can increase during cachexia (White et al., 2011b), and cachexia-induced mTOR suppression is independent of Akt activation in the *Apc*$^{Min/+}$ mouse and the LLC implant model (White et al., 2011b). We demonstrate that gp130 / STAT3 signaling is not a direct regulator of cachexia-induced suppression of protein synthesis.

AMP-activated protein kinase (AMPK) is a cellular sensor of nutrient stress and can negatively regulate skeletal muscle mass (Goodman et al., 2011b). AMPK inhibits mTORC1 formation through phosphorylation of raptor and TSC1/2, resulting in suppressed protein synthesis. Additionally, AMPKα 1 & 2 knockouts produce skeletal muscle and cultured myotube hypertrophy (Lantier et al.). As it relates to the cachectic condition, AMPK can be activated by IL-6 in cultured myotubes and suppress protein synthesis (White et al., 2013b) and gp130 in the presence of IL-6r is sufficient for STAT3 independent AMPK activation (Watt et al., 2006). During LLC-induced cachexia muscle AMPK phosphorylation increased and LCM induced AMPK phosphorylation in C2C12 myotubes. However, inhibition of gp130, IL-6, or STAT3 signaling was not sufficient to attenuate LLC induction of AMPK. This suggests gp130/STAT3 independent mechanisms regulating AMPK during LLC-induced cancer cachexia. We have previously shown that treatment of C2C12 myotubes with compound C, an AMPK inhibitor, can alleviate IL-6 suppression of protein synthesis (White et al., 2013b). REDD1 is a potent suppressor of mTOR, which is increased in the cachectic condition (White et al., 2011b). REDD1 can suppress mTORC1 through the dissociation of TSC2/14-3-3 complex (Ho et al., 2005) and REDD1 can suppress mTOR independently of AMPK (Frost and Lang). The inhibition of skeletal muscle gp130 signaling did not

alter LLC-induced REDD1 expression. A better understanding of the mechanistic relationship between the regulation of protein degradation and synthesis in cachectic muscle is needed.

In summary this is the first study to examine the role of skeletal muscle gp130 regulation on protein turnover during cachexia. Inhibition of skeletal muscle gp130 attenuated LLC induced muscle atrophy. Additionally, activation of STAT3, p38, and NFκB were suppressed with skeletal muscle gp130 inhibition. The LLC-induced activation of FOXO3a protein degradation signaling was suppressed by gp130/STAT3 inhibition both *in vivo* and *in vitro*. Interestingly, inhibition of IL-6 was not sufficient to repress LLC-induced atrophy signaling. We report a gp130/STAT3 independent suppression of mTOR signaling. Further work is necessary to determine the LLC inhibition of protein synthesis during cachexia. Additionally, LLC tumor appears to not be an IL-6 dependent cachexia model, consequently further work is needed to establish the role of muscle gp130 on the regulation of cachexia that is more IL-6 dependent. Targeted gp130 therapies may be useful in combination with treatments that alleviate the suppression of mTOR signaling.

ACKNOWLEDGEMENTS

The authors thank Ms. Tia Davis and Dr. Marj Peña for technical assistance with the animal breeding. The skeletal muscle-specific cre-expressing mice were a gift from Dr. Steven Burden. The gp130 fl/fl mice were a gift from Dr. Colin Stuart & Dr. Hennighausen, NCI. The research described in this report was supported by research grant R01 CA121249 to JAC from the National Cancer Institute.

Table 5.1. Changes in body weight, fat mass, and muscle mass with LLC induced cachexia. At 8 weeks of age skm-gp130 mice were implanted with LLC cells ($1X10^6$). All muscle, epididymal (Epi) fat, and organs were excised and weighted at the time of sacrifice. Mice received a DEXA scan at the time of sacrifice. Bone mineral density (BMD) and tumor free lean mass were measured. All values are represented as Mean ± SEM. * different from control within genotype, † different from all other comparisons, $^{\#}$ main effect of skm-gp130, $^{\$}$ main effect of LLC $p<0.05$.

	BL/6		**skm-gp130**	
	Control (n=5)	LLC (n=6)	Control (n=5)	LLC (n=6)
Body Weight				
BW @ Sac (g)	25.2 ± 0.4	24.4 ± 1.1	27.2 ± 0.4$^{\#}$	27.5 ± 0.8$^{\#}$
BW-tumor (g)	25.2 ± 0.5	22.4 ± 0.5†	27.2 ± 0.4	24.7 ± 0.5*
Lean mass (g)	18.8 ± 0.3	17.3 ± 0.4†	20.2 ± 1.2$^{\#}$	19.3± 0.6$^{\#}$
Tibia Length (mm)	16.7 ± 0.1	16.8 ± 0.1	16.9 ± 0.1	16.8 ± 0.0
Epi Fat (mg)	376 ± 32	239 ± 55$^{\$}$	372 ± 25	258 ± 26$^{\$}$
Gastrocnemius (mg)	133.5 ± 2.4	106.8 ± 5.3†	125.8 ± 4.9	120.6 ± 5.6
Organs				
Heart (mg)	96.8 ± 0.9	99.2 ± 6.1.6	117.0 ± 4.6$^{\#}$	105.7 ± 2.6$^{\#}$
Testes (mg)	182 ± 3	178 ± 7	215 ± 6$^{\#}$	210 ± 5$^{\#}$
Spleen (mg)	87.6 ± 3.7	247.0 ± 58.4$^{\$}$	91.8 ± 1.8	244.0 ± 44.2$^{\$}$
BMD (g/cm^2)	0.0514 ± 0.001	0.0467 ± 0.001*	0.0482 ± 0.001	0.0493 ± 0.001

Table 5.2. Body weight, fat mass, and muscle mass in LLC induced cachexia with acute IL-6r-Ab or PDTC administration. At 8 weeks of age a separate group of mice were implanted with LLC cells ($1X10^6$). After 4 weeks of tumor growth mice were randomized and treated with PBS, IL-6r-Ab, or PDTC for one week. Body weights were measured. Muscles and fat were excised and weighed at the time of sacrifice. All values are represented as Mean ± SEM. One-way ANOVA was used to compare data across treatments. *Significant compared with control, †Significantly different from all other comparisons $p<0.05$.

	Control	**LLC**	**LLC + IL-6r Ab**	**LLC + PDTC**
	(n=5)	(n=4)	(n=4)	(n=4)
BW @ Sac (g)	27.3±1.2	23.4±2.4	26.2±0.9	24.4±1.3
BW - tumor (g)	27.3±1.2	20.1±1.4*	23.1±0.6*	22.1±0.8*
Tumor (g)	-	3.27±1.20	3.08±0.94	2.26±0.98
Epi Fat (mg)	429±48	111±16*	166±46*	165±47*
Gastrocnemius (mg)	141.6±7.2	92.5±6.8*	113.3±5.8*	99.3±5.3*
Spleen (mg)	104±22	397±59*	354±87*	277±70*
Tibia Length (mm)	16.9±0.2	16.5±0.1	16.6±0.1	16.5±0.1

5.6 Figure Legends

Figure 5.1. Mouse tissue expression of gp130. A) gp130 is differentially expressed in tissues. B) Differential expression of gp130 mRNA in the soleus (Sol), gastrocnemius (Gastroc), Tibialis anterior (TA) muscles of C57BL/6 mice. C) PCR analysis of gp130 mRNA (643bp product size) in the gastrocnemius (Gas), soleus (Sol),Tibialis anterior (TA) muscles, liver, kidney and heart of skm - gp130 +/+, skm-gp130$^{+/-}$ mice and skm-gp130$^{-/-}$ mice. D) STAT3 protein phosphorylation in heterozygous and homozygous skm- gp130 knockout after two weeks of IL-6 over-expression. All values are represented as Mean ± SEM. †Significantly different from all other comparisons. *Significantly different form genotype vector control, $p<0.05$.

Figure 5.2. The effect of skm-gp130 on development of cancer induced cachexia. At 8 weeks of age wild-type BL/6 mice and skm-gp130$^{-/-}$ (skm-gp130) mice were implanted with LLC tumor cells. Tumors were allowed to grow until 13 weeks of age. A) Skeletal muscle gp130 expression changes with LLC induced cachexia in wild-type and skm-gp130 mice in the gastrocnemius (ND:not detected). B) Tumor mass was measured at the time of sacrifice C) Percent change in body weight (BW) from genotype control and D) percent change in gastrocnemius muscle mass were calculated from weights collected at the time of sacrifice. All values are represented as Mean ± SEM .***significantly different from BL/6 $p<0.05$.

Figure 5.3. The effect of skm-gp130 on LLC induced signaling. A) Western blot analysis of p-STAT3, total STAT3, p-AMPK, total AMPK, p-p38, total p38 and p – NF - κB, total NF - κB protein expression. Ponceau stain was used to verify equal loading.

B.) Western blot analysis of p-Akt(T308), p-Akt(S473), and total Akt, Graphical analysis of western blots are expressed as a ratio of phosphorylated to total protein levels. C) Western blot analysis of mTOR signaling proteins p-4EBP1, total 4EPB1, p-S6, total S6, p-FOXO3, total FOXO3, and Atrogin. Ponceau stain was used to ensure equal loading. Graphical analysis of phospho- proteins is expressed as a ratio of phosphorylated to total protein levels. D) Levels of ubiquinated proteins were quantified by western blot analysis. Dashed line indicates different sections of same gel. E) Skeletal muscle mRNA expression of IGF-1, REDD1, and IL-6 was measured in the gastrocnemius. All values are represented as Mean ± SEM. Two-way ANOVA was used to analyze the effect of skm-gp130 and LLC. †significantly different from all other comparisons, **significantly different from BL/6 LLC, *significantly different BL/6 control $p<0.05$.

Figure 5.4. The effect of LLC conditioned media on Myosin Heavy Chain level, STAT3 signaling and protein turnover regulation in C2C12 myotubes. A) Myotube atrophy induced by 72h LCM was measured with protein levels of Myosin Heavy Chain. B) Inflammatory signaling, STAT3 induced by administration of LCM for 4 or 72h. C) Protein expression of p-AKT, total Akt, p-AMPK, total AMPK, p-mTOR, total mTOR, p-S6, total S6, p-4EBP1, and total 4EPB1 after 72h incubation with LCM was measured by western blots. Graphical analysis of mTOR signaling proteins are expressed as a ratio of phosphorylated to total protein levels. D) Protein expression of p-FOXO3, total FOXO3, Atrogin, and GAPDH was measured by western blots. Graphical analysis of AMPK and FOXO3 is expressed as a ratio of phosphorylated to total protein levels.. Values are the means ± SEM. Data were analyzed with one-way ANOVA. *:$p \leq 0.05$, **: $p \leq 0.01$, ***: $p \leq 0.005$, significant different from control group.

Figure 5.5. The effect of IL-6 inhibition on LLC induced signaling. A) p-STAT3 and total STAT3 protein expression was measured via western blot analysis in fully differentiated C2C12 cells treated with IL-6 (100ng/ml) or LCM (25%) with or without IL-6r Ab (1:1000) for 4h. B) Protein synthesis was measured by the incorporation of puromycin into proteins in C2C12 cells treated with LCM (25%) with or without IL-6r Ab (1:1000) for 72h. C) Protein expression of p-Akt, total Akt, p-AMPK, total AMPK, p-4EBP1, total 4EBP1, p-FOXO3, total FOXO3, Atrogin and GAPDH was measured by western blots in C2C12 cells treated with LCM (25%) with or without IL-6r Ab (1:1000) for 72h. Graphical analysis of Akt, AMPK, 4EBP1, and FOXO3 is expressed as a ratio of phosphorylated to total protein levels. D) IL-6r Ab was administered acutely *in vivo* in mice with LLC tumors for 1 week after tumor development. Western blot analysis of LLC associated signaling including STAT3, p38, Akt, S6RP, and atrogin-1 were measured. E) Protein synthesis was measured by incorporation of puromycin into the proteins 30 minutes after injection and measured by western blot. Dashed line indicates different sections of same gel. Values are the means ± SEM. Cell culture data were analyzed with one-way ANOVA and *in vivo* data analyzed with t-test. *:$p \leq 0.05$, **: $p \leq 0.01$, ***: $p \leq 0.005$, significant different from control group.

Figure 5.6. The effect of gp130/STAT signaling inhibition on LLC induced signaling. Fully differentiated C2C12 cells were treated with LCM with or without PDTC (STAT/NFκB inhibitor, 50μM), LLL12 (STAT3 specific inhibitor, 100nM) and gp130 receptor antibody (1:1000) for 4h (A) or 72h (B, C, D, E,F) A) p-STAT3 and total STAT3 protein expression was measured via western blot analysis after 4 hour treatment. B) Diameter of C2C12 myotubes after 72h of LLC, PDTC, LLL12 or gp130 antibody

administration. C) Relative protein synthesis rates were measured by the incorporation of puromycin into proteins after 72 hours of PDTC, LLL12 or gp130 antibody administration. D-F) C2C12 signaling proteins was measured after 72h of D), gp130 antibody, E) LLL12, or F) PDTC administration in the presence of LCM by western blot analysis. G) PDTC was administered for 1 week to mice bearing LLC tumors. Western blot analysis of LLC associated signaling including STAT3, P65, AMPK, P38, and Akt, were measured. Graphical representation is displayed as the ratio of phosphorylate to total protein levels. Values are the means ± SE. Cell culture data were analyzed with one-way ANOVA and *in vivo* data analyzed with t-test *:$p \leq 0.05$, **: $p \leq 0.01$, ***: $p \leq 0.005$, significant different from control group, #:$p \leq 0.05$, significant different from LLC group.

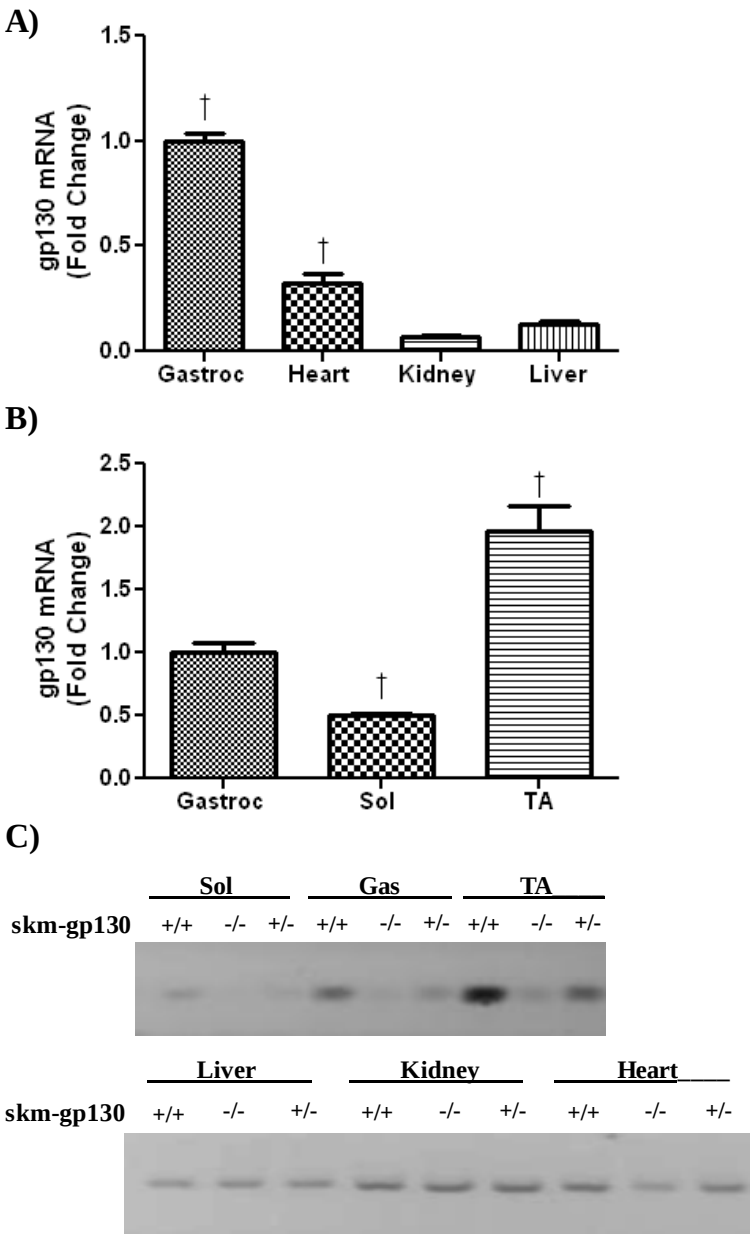
A)
gp130 mRNA (Fold Change)
1.5
1.0
0.5
0.0
†
†
Gastroc
Heart
Kidney
Liver
B)
gp130 mRNA (Fold Change)
2.5
2.0
1.5
1.0
0.5
0.0
†
†
Gastroc
Sol
TA
C)
Sol
Gas
TA
skm-gp130
+/+ -/- +/- +/+ -/- +/- +/+ -/- +/-
Liver
Kidney
Heart
skm-gp130
+/+ -/- +/- +/+ -/- +/- +/+ -/- +/-

Figure 5.1

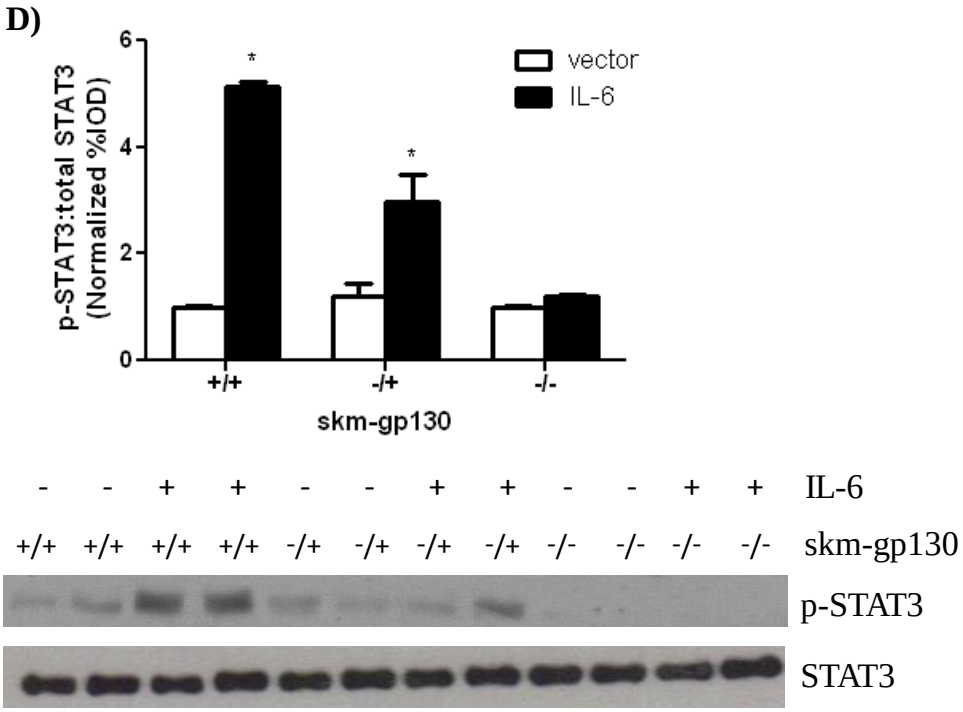

Figure 5.1. Mouse tissue expression of gp130. A) gp130 is differentially expressed in tissues. B) Differential expression of gp130 mRNA in the soleus (Sol), gastrocnemius (Gastroc), Tibialis anterior (TA) muscles of C57BL/6 mice. C) PCR analysis of gp130 mRNA (643bp product size) in the gastrocnemius (Gas), soleus (Sol),Tibialis anterior (TA) muscles, liver, kidney and heart of skm - gp130 +/+, skm-gp130$^{+/-}$ mice and skm-gp130$^{-/-}$ mice. D) STAT3 protein phosphorylation in heterozygous and homozygous skm- gp130 knockout after two weeks of IL-6 over-expression. All values are represented as Mean ± SEM. †Significantly different from all other comparisons. *Significantly different form genotype vector control, $p<0.05$.

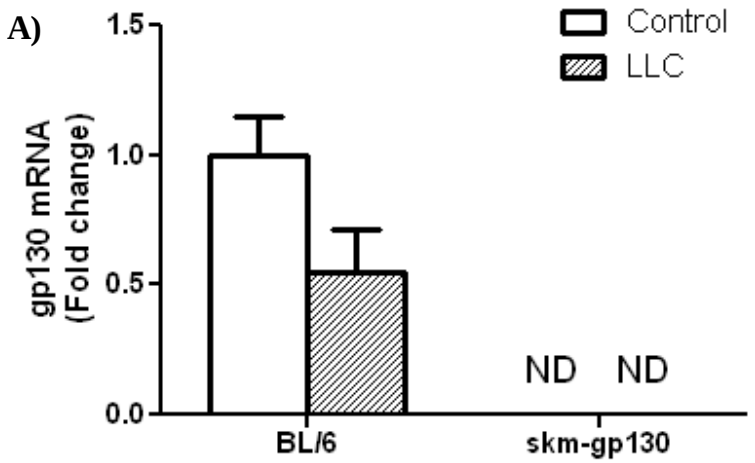
A)
Control
LLC
gp130 mRNA
(Fold change)
1.5
1.0
0.5
0.0
ND
ND
BL/6
skm-gp130

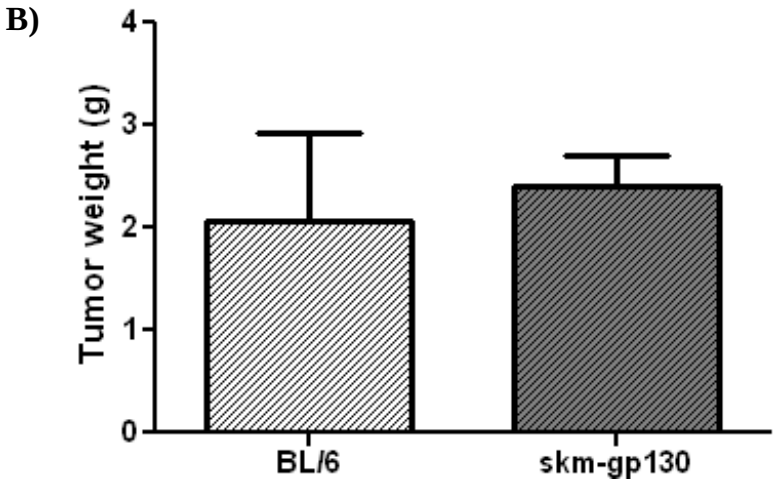
B)
Tumor weight (g)
4
3
2
1
0
BL/6
skm-gp130

Figure 5.2

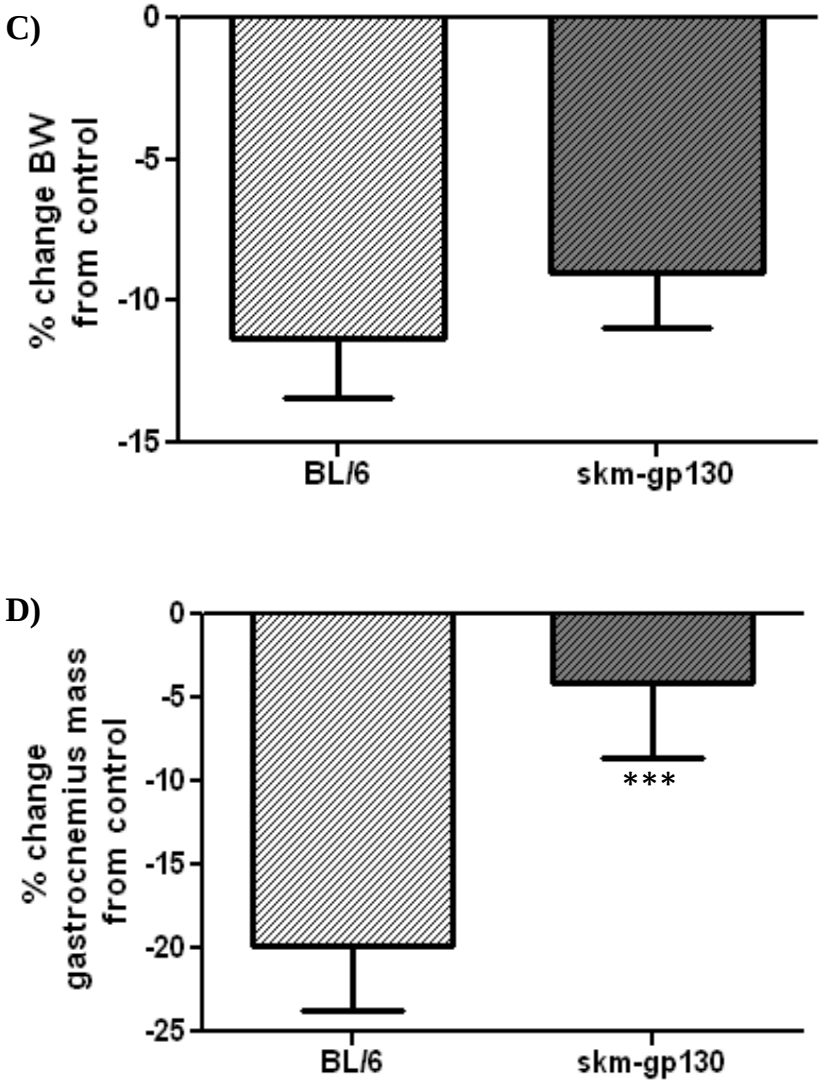

Figure 5.2. The effect of skm-gp130 on development of cancer induced cachexia. At 8 weeks of age wild-type BL/6 mice and skm-gp130$^{-/-}$ (skm-gp130) mice were implanted with LLC tumor cells. Tumors were allowed to grow until 13 weeks of age. A) Skeletal muscle gp130 expression changes with LLC induced cachexia in wild-type and skm-gp130 mice in the gastrocnemius (ND:not detected). B) Tumor mass was measured at the time of sacrifice C) Percent change in body weight (BW) from genotype control and D) percent change in gastrocnemius muscle mass were calculated from weights collected at the time of sacrifice. All values are represented as Mean ± SEM .***significantly different from BL/6 $p<0.05$.

A)

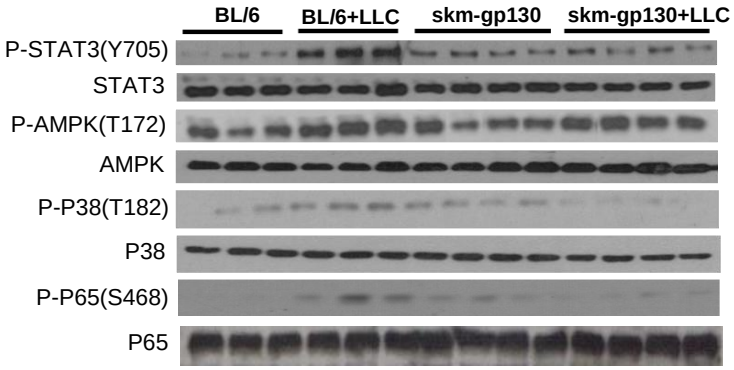
BL/6
BL/6+LLC
skm-gp130
skm-gp130+LLC
P-STAT3(Y705)
STAT3
P-AMPK(T172)
AMPK
P-P38(T182)
P38
P-P65(S468)
P65

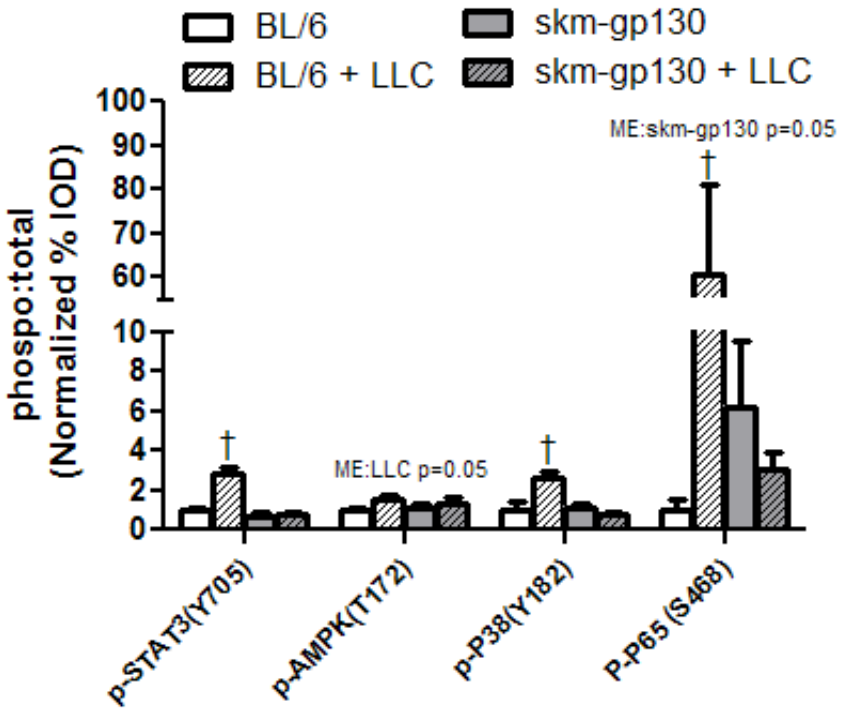
BL/6
BL/6 + LLC
skm-gp130
skm-gp130 + LLC
phospo:total
(Normalized % IOD)
ME:skm-gp130 p=0.05
ME:LLC p=0.05
p-STAT3(Y705)
p-AMPK(T172)
p-P38(Y182)
P-P65 (S468)

Figure 5.3.

B)

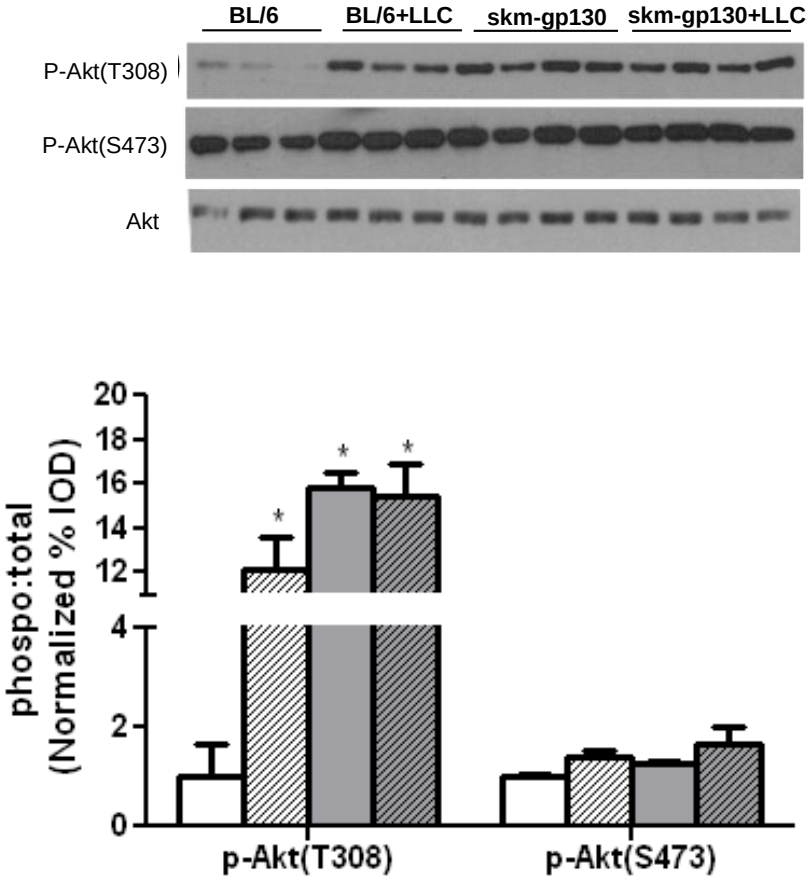

Figure 5.3 (continued).

C)

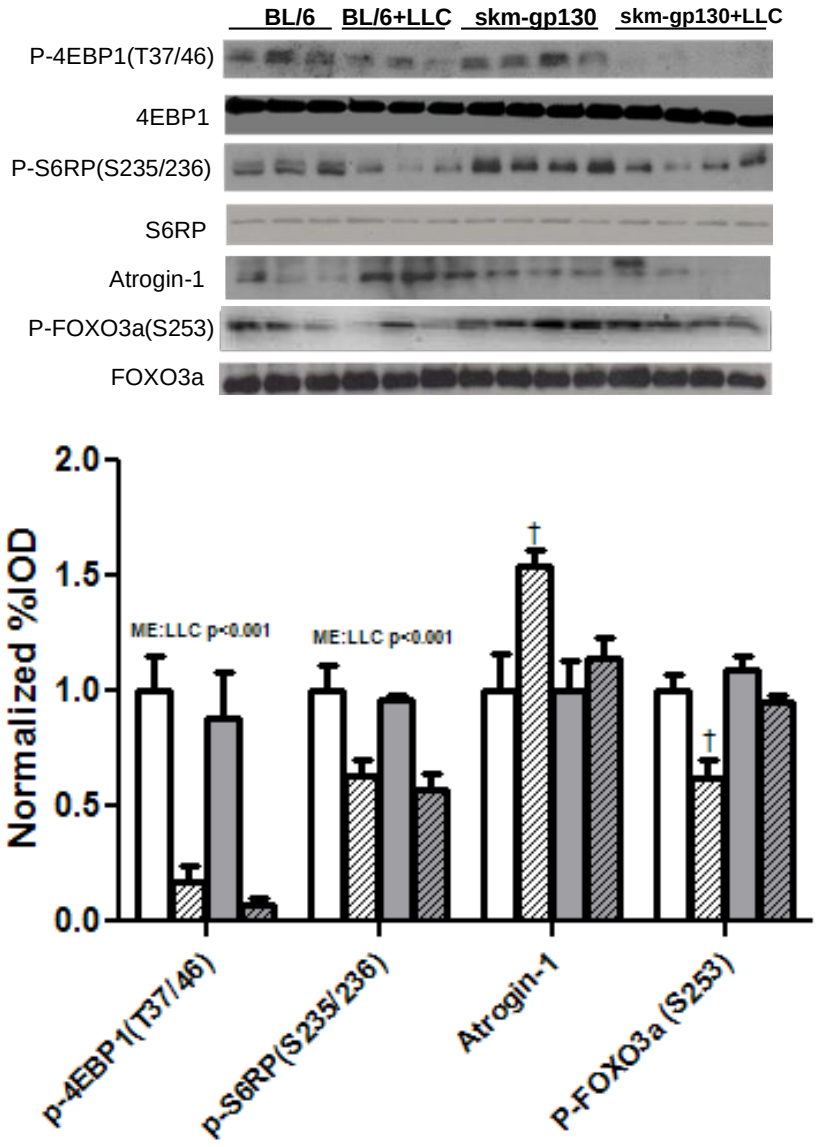

Figure 5.3. (continued)

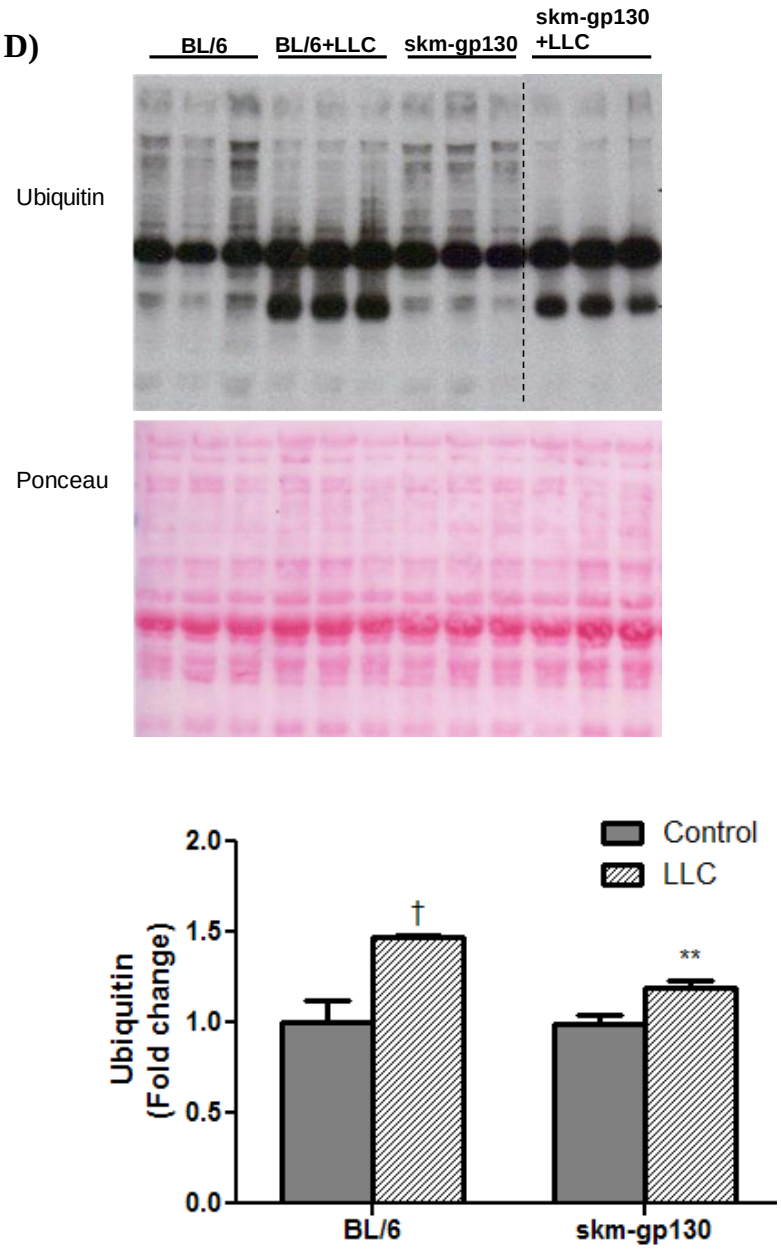

Figure 5.3 (continued).

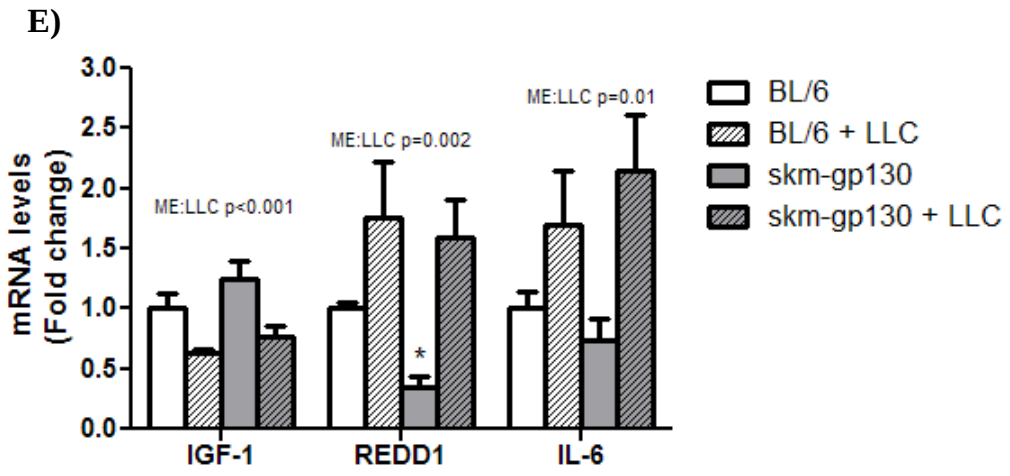

Figure 5.3. The effect of skm-gp130 on LLC induced signaling. A) Western blot analysis of p-STAT3, total STAT3, p-AMPK, total AMPK, p-p38, total p38 and p – NF - κB, total NF - κB protein expression. Ponceau stain was used to verify equal loading. B.) Western blot analysis of p-Akt(T308), p-Akt(S473), and total Akt, Graphical analysis of western blots are expressed as a ratio of phosphorylated to total protein levels. C) Western blot analysis of mTOR signaling proteins p-4EBP1, total 4EPB1, p-S6, total S6, p-FOXO3, total FOXO3, and Atrogin. Ponceau stain was used to ensure equal loading. Graphical analysis of phospho-proteins is expressed as a ratio of phosphorylated to total protein levels. D) Levels of ubiquinated proteins were quantified by western blot analysis. Dashed line indicates different sections of same gel. E) Skeletal muscle mRNA expression of IGF-1, REDD1, and IL-6 was measured in the gastrocnemius. All values are represented as Mean ± SEM. Two-way ANOVA was used to analyze the effect of skm-gp130 and LLC. †significantly different from all other comparisons, **significantly different from BL/6 LLC, *significantly different BL/6 control $p<0.05$.

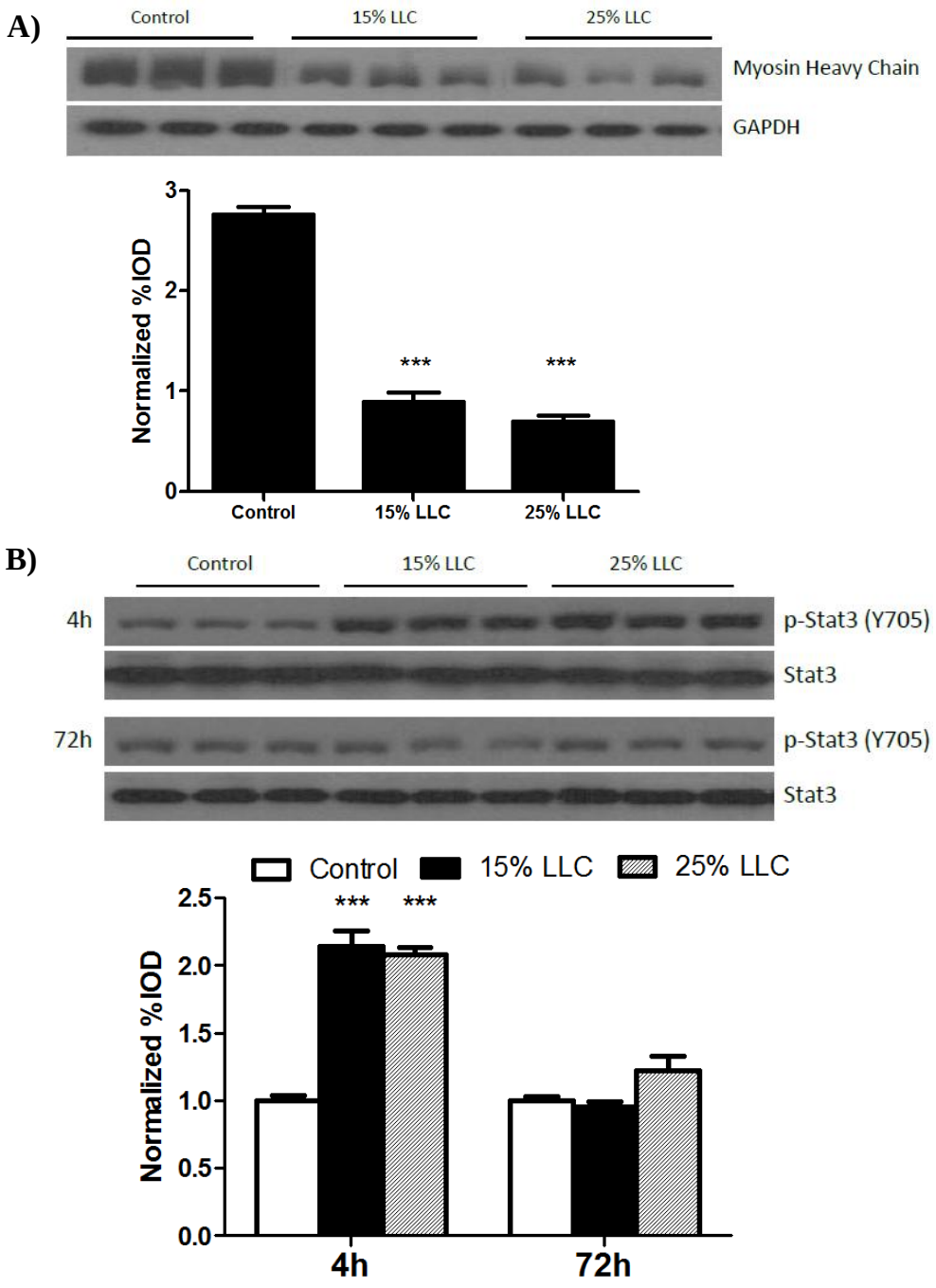
A)
Control
15% LLC
25% LLC
Myosin Heavy Chain
GAPDH
Normalized %IOD
3
2
1
0
***
***
Control
15% LLC
25% LLC
B)
Control
15% LLC
25% LLC
4h
p-Stat3 (Y705)
Stat3
72h
p-Stat3 (Y705)
Stat3
Control
15% LLC
25% LLC
Normalized %IOD
2.5
2.0
1.5
1.0
0.5
0.0
***
***
4h
72h

Figure 5.4.

C)

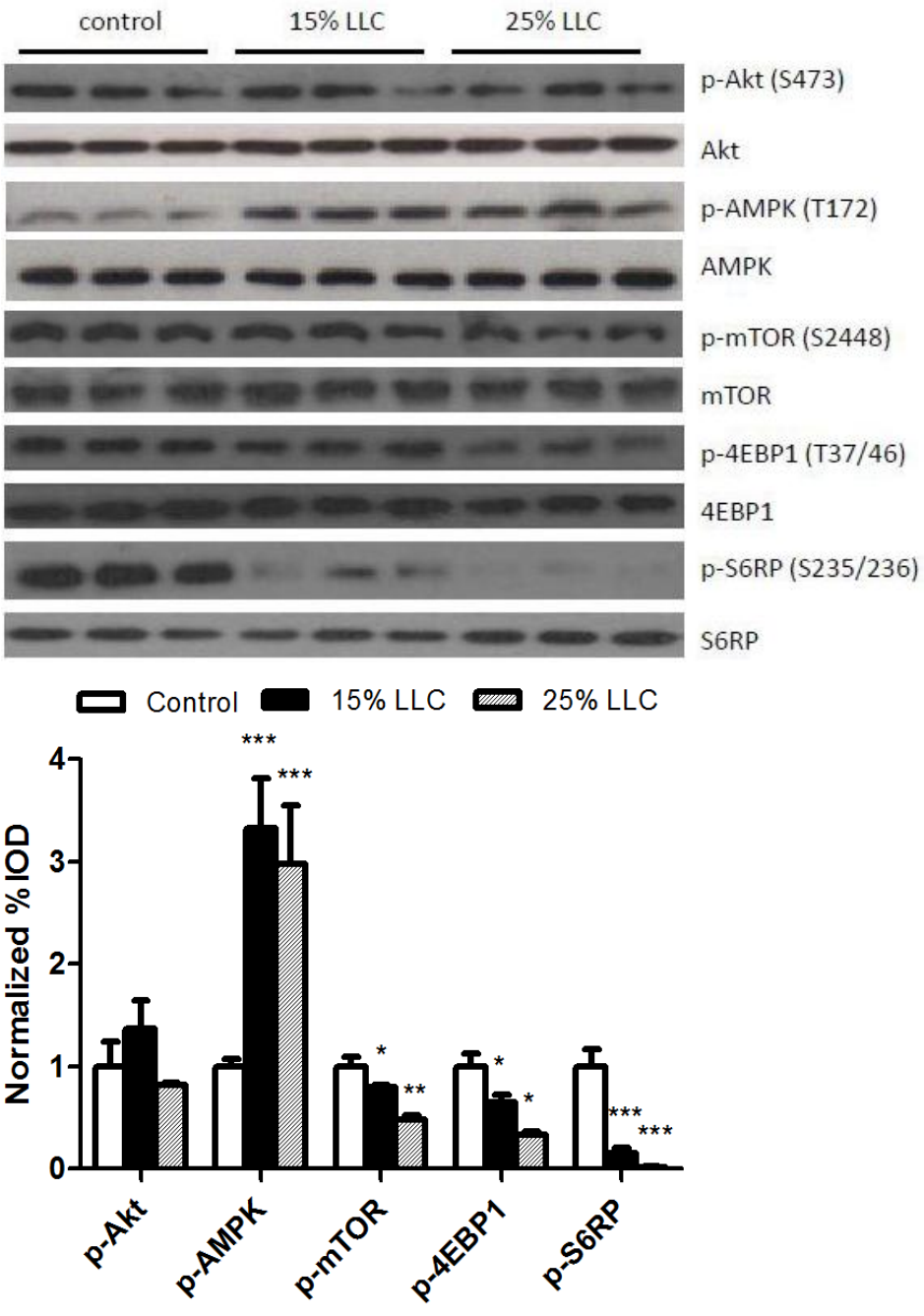

Figure 5.4 (Continued).

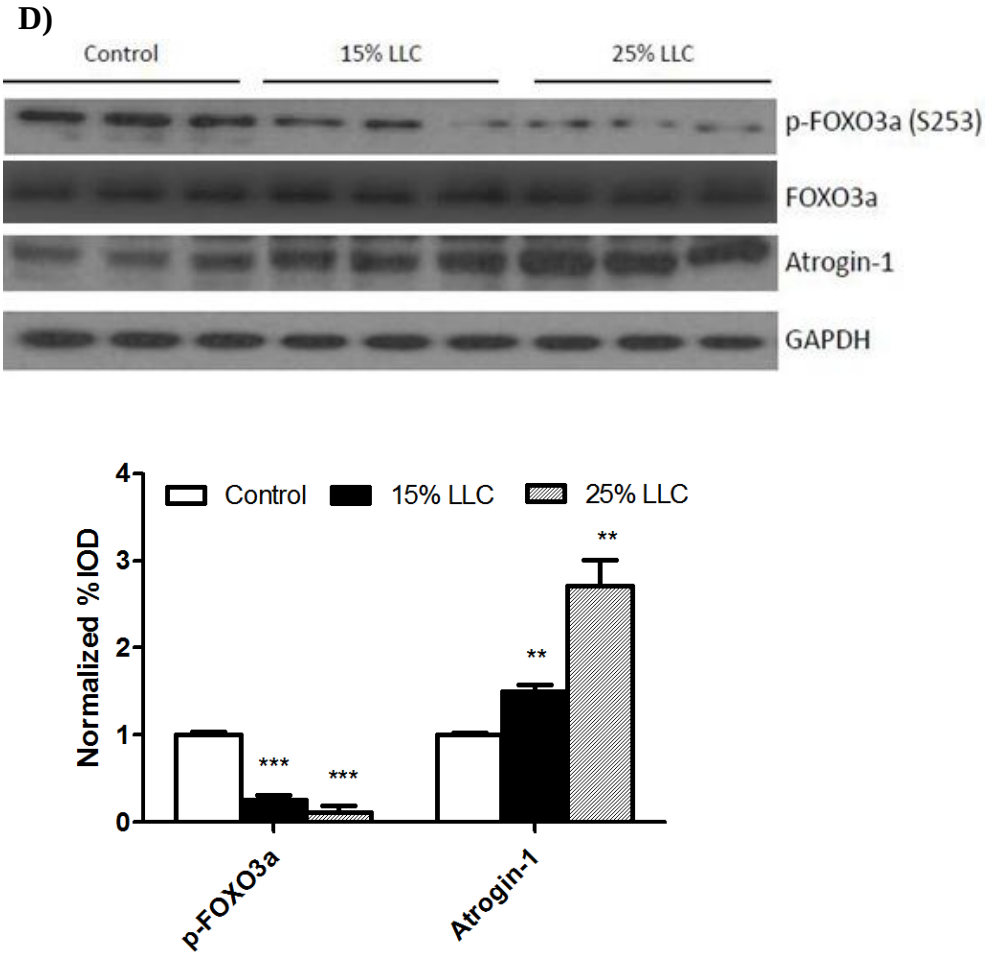

Figure 5.4. The effect of LLC conditioned media on Myosin Heavy Chain level, STAT3 signaling and protein turnover regulation in C2C12 myotubes. A) Myotube atrophy induced by 72h LCM was measured with protein levels of Myosin Heavy Chain. B) Inflammatory signaling, STAT3 induced by administration of LCM for 4 or 72h. C) Protein expression of p-AKT, total Akt, p-AMPK, total AMPK, p-mTOR, total mTOR, p-S6, total S6, p-4EBP1, and total 4EPB1 after 72h incubation with LCM was measured by western blots. Graphical analysis of mTOR signaling proteins are expressed as a ratio of phosphorylated to total protein levels. D) Protein expression of p-FOXO3, total FOXO3, Atrogin, and GAPDH was measured by western blots. Graphical analysis of AMPK and FOXO3 is expressed as a ratio of phosphorylated to total protein levels.. Values are the means ± SEM. Data were analyzed with one-way ANOVA. *:$p \leq 0.05$, **: $p \leq 0.01$, ***: $p \leq 0.005$, significant different from control group.

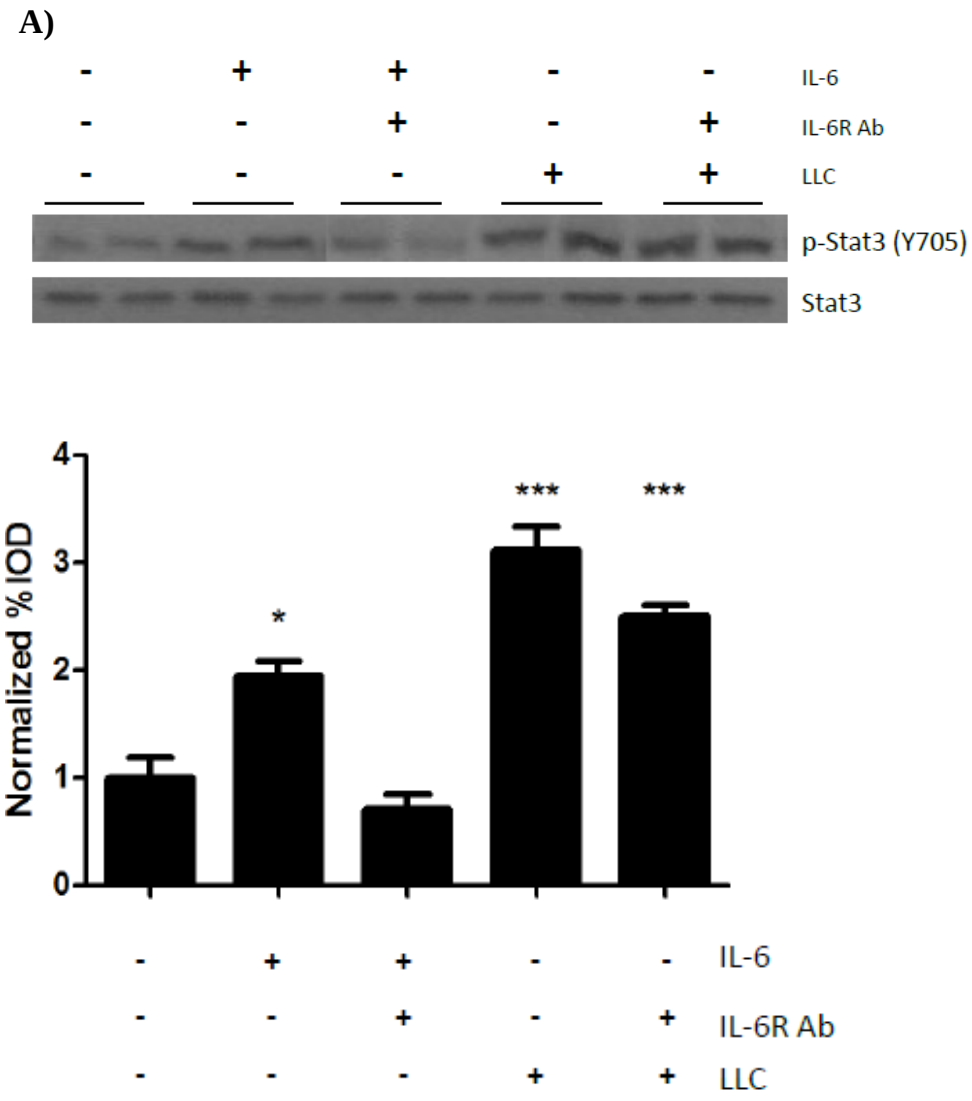
A)
- + + - - IL-6
- - + - + IL-6R Ab
- - - + + LLC
p-Stat3 (Y705)
Stat3
Normalized % IOD
0
1
2
3
4
*
***
***
- + + - - IL-6
- - + - + IL-6R Ab
- - - + + LLC

Figure 5.5.

B)

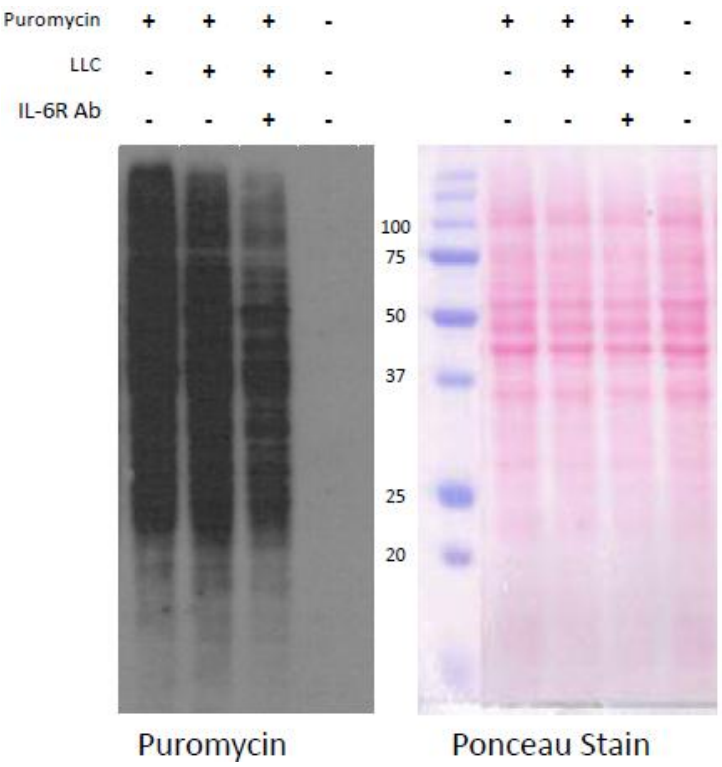

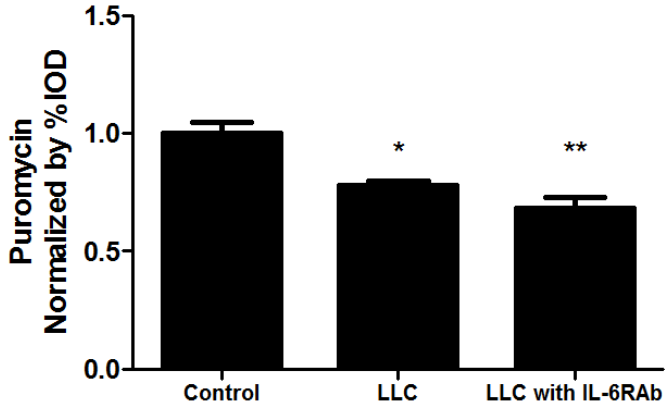

Figure 5.5 (continued).

C)

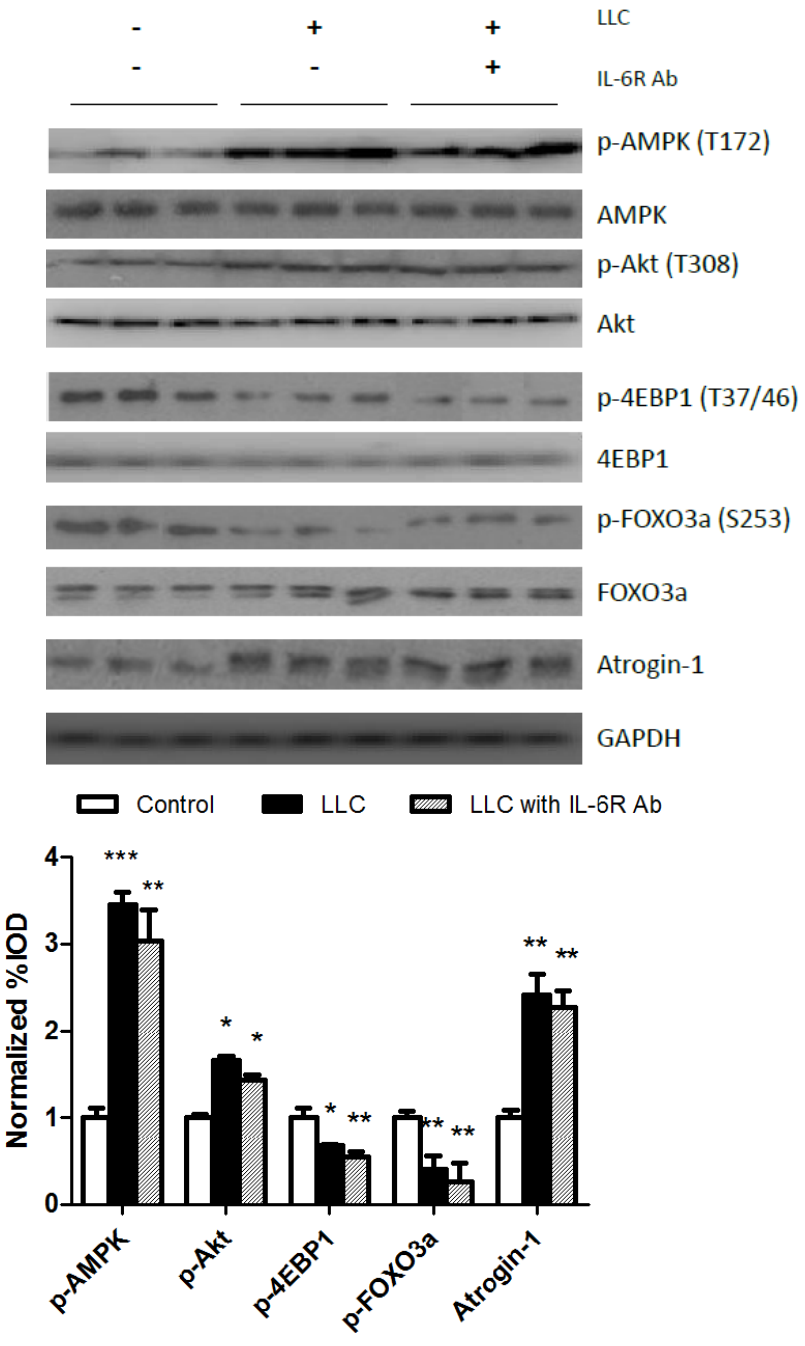

Figure 5.5 (continued).

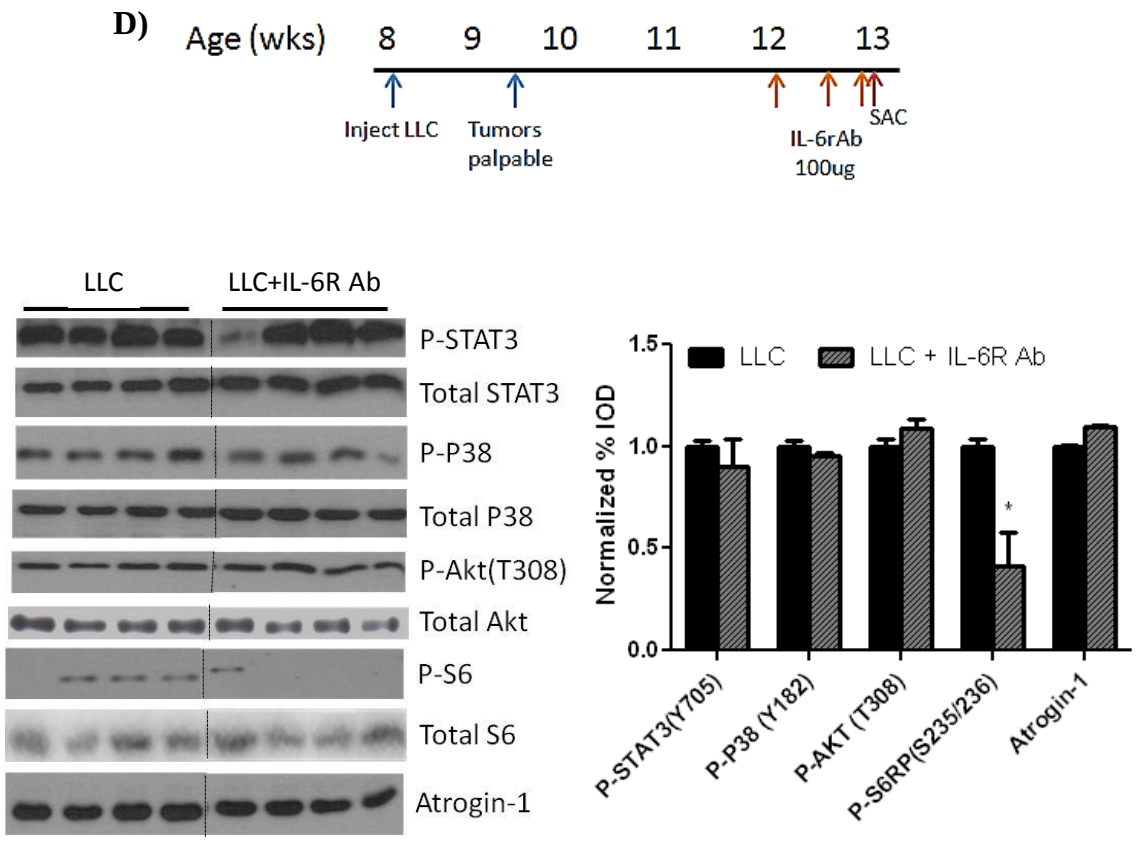

Figure 5.5 (continued).

E)

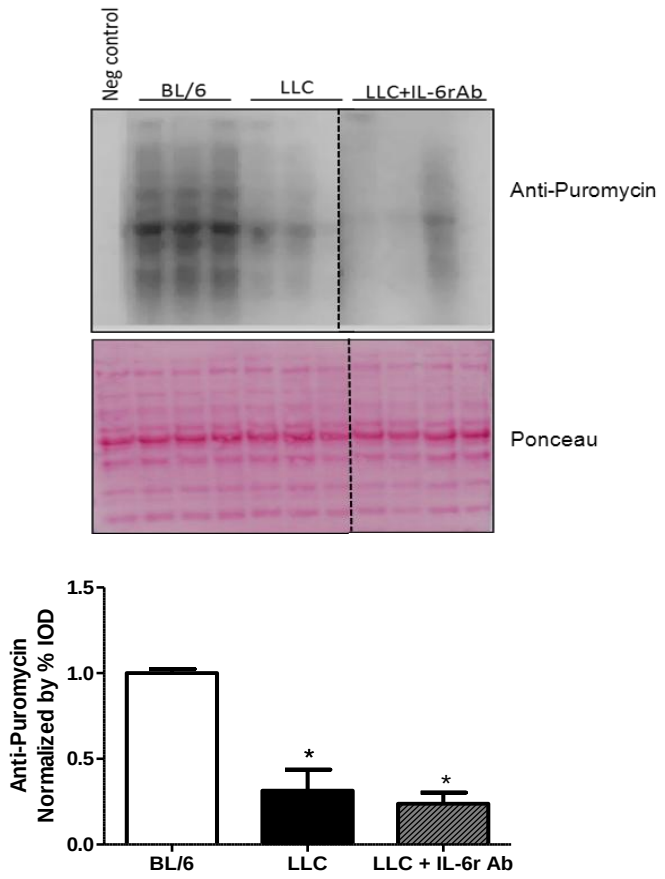

Figure 5.5. The effect of IL-6 inhibition on LLC induced signaling. A) p-STAT3 and total STAT3 protein expression was measured via western blot analysis in fully differentiated C2C12 cells treated with IL-6 (100ng/ml) or LCM (25%) with or without IL-6r Ab (1:1000) for 4h. B) Protein synthesis was measured by the incorporation of puromycin into proteins in C2C12 cells treated with LCM (25%) with or without IL-6r Ab (1:1000) for 72h. C) Protein expression of p-Akt, total Akt, p-AMPK, total AMPK, p-4EBP1, total 4EBP1, p-FOXO3, total FOXO3, Atrogin and GAPDH was measured by western blots in C2C12 cells treated with LCM (25%) with or without IL-6r Ab (1:1000) for 72h. Graphical analysis of Akt, AMPK, 4EBP1, and FOXO3 is expressed as a ratio of phosphorylated to total protein levels. D) IL-6r Ab was administered acutely *in vivo* in mice with LLC tumors for 1 week after tumor development. Western blot analysis of LLC associated signaling including STAT3, p38, Akt, S6RP, and atrogin-1 were measured. E) Protein synthesis was measured by incorporation of puromycin into the proteins 30 minutes after injection and measured by western blot. Dashed line indicates different sections of same gel. Values are the means ± SEM. Cell culture data were analyzed with one-way ANOVA and *in vivo* data analyzed with t-test. *:$p \leq 0.05$, **: $p \leq 0.01$, ***: $p \leq 0.005$, significant different from control group.

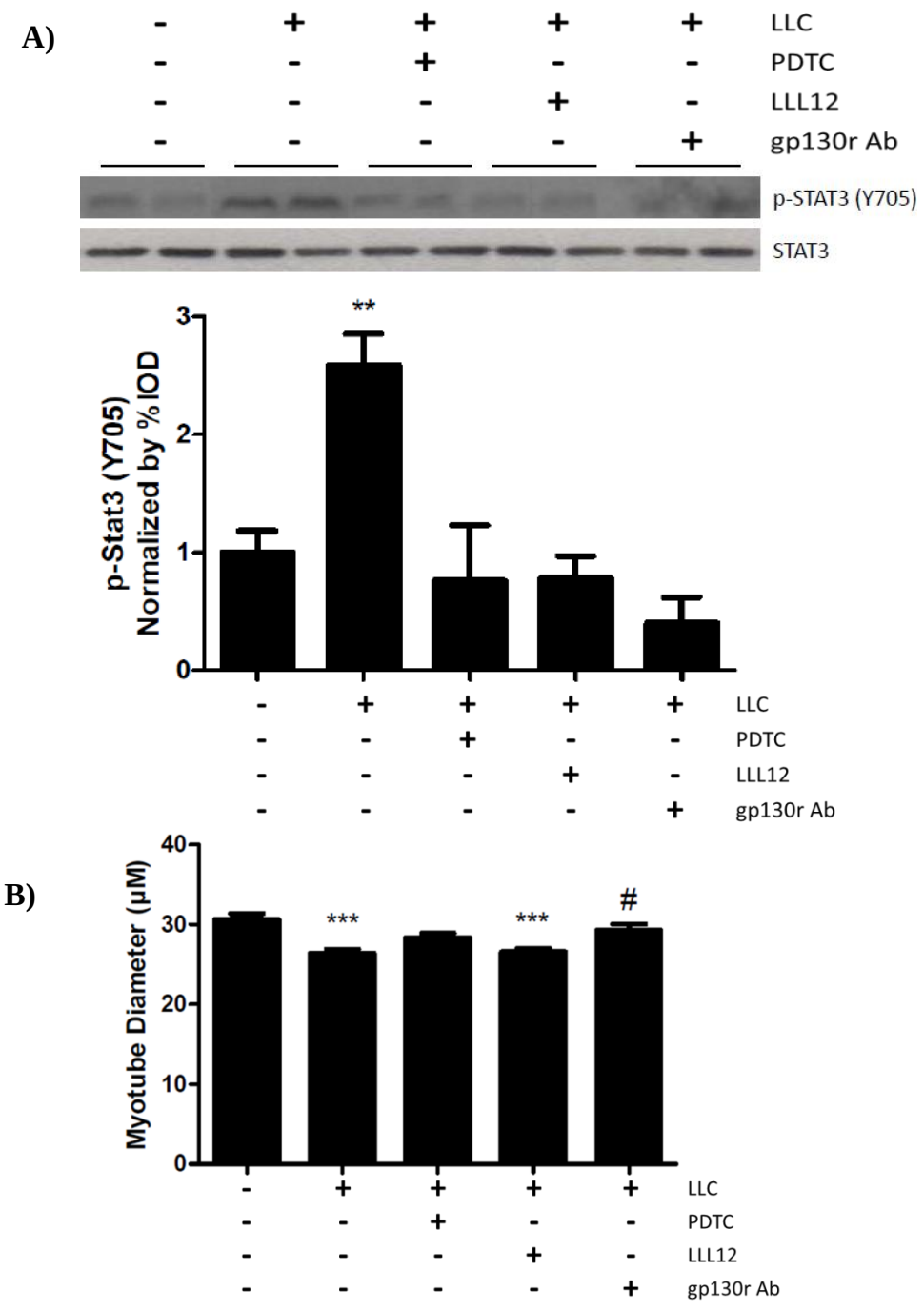

Figure 5.6 (continued).

Figure 5-6 (continued).

C)

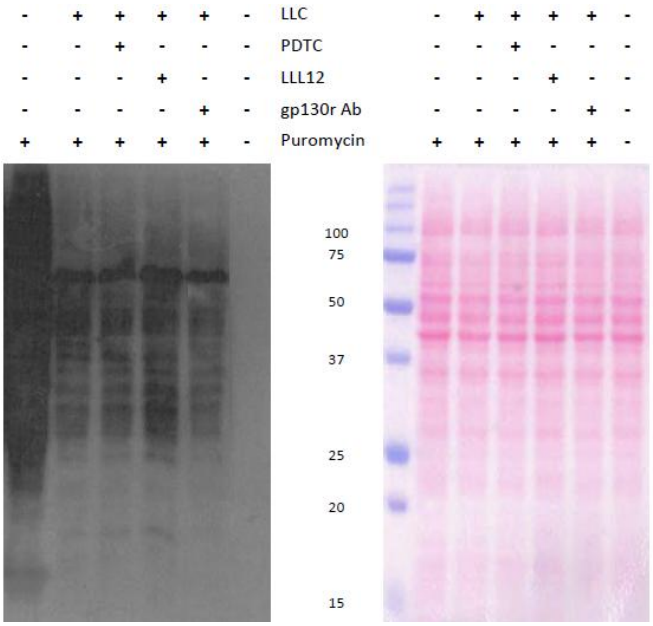

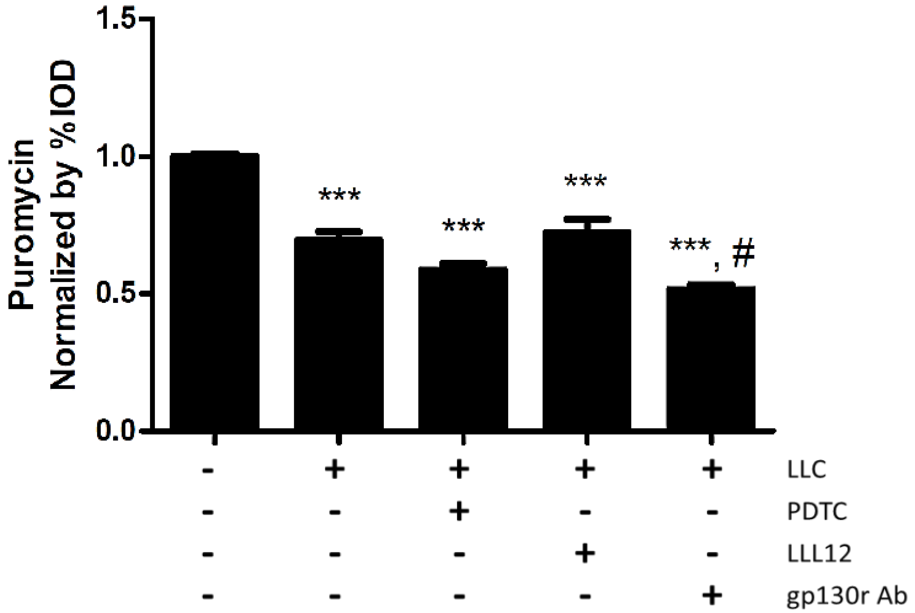

Figure 5-6 (continued).

D)

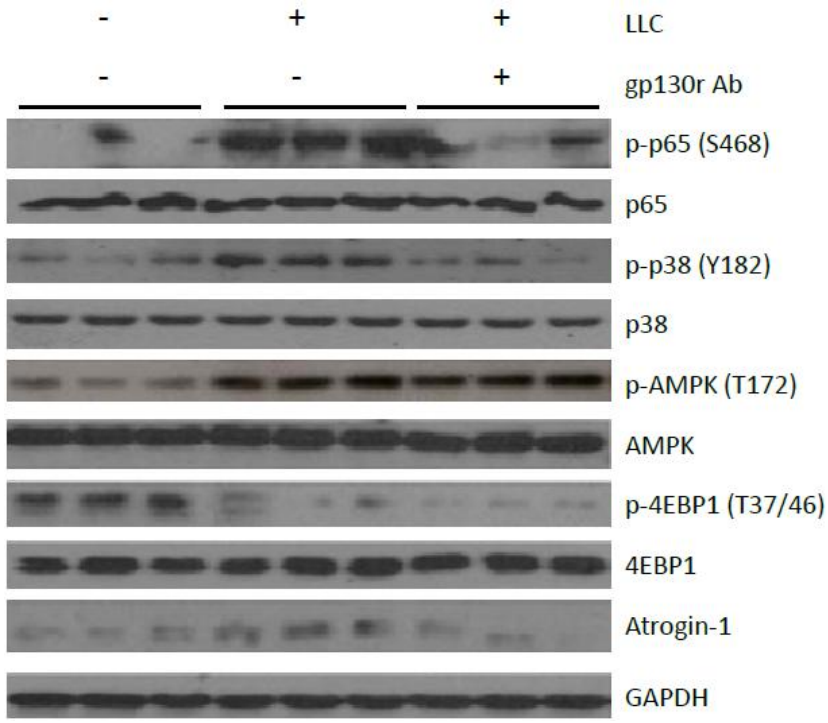

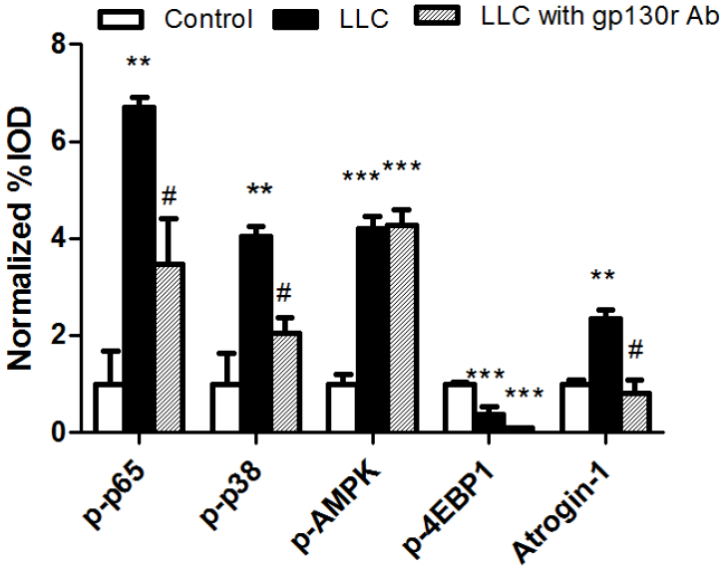

Figure 5-6 (continued).

E)

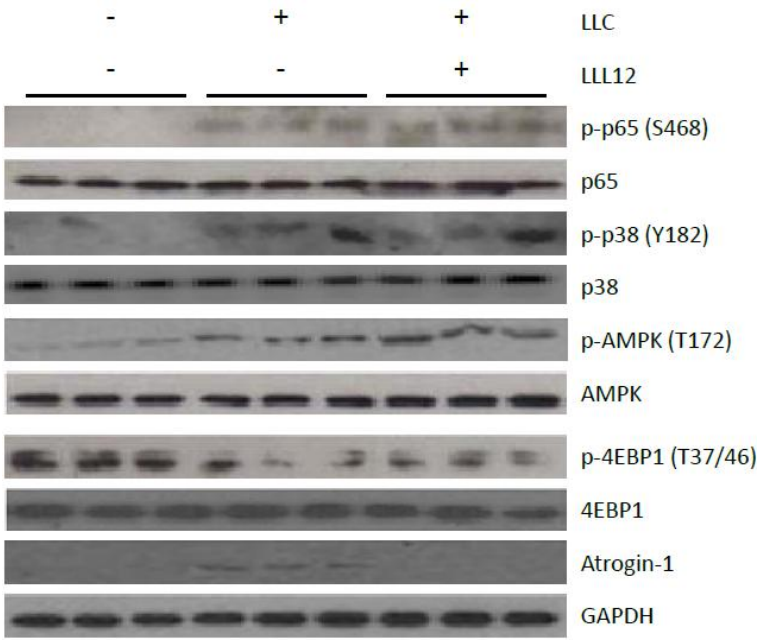

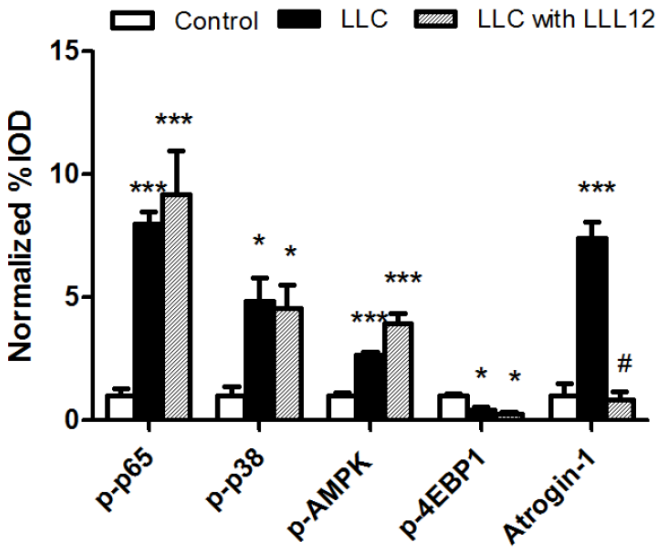

F)

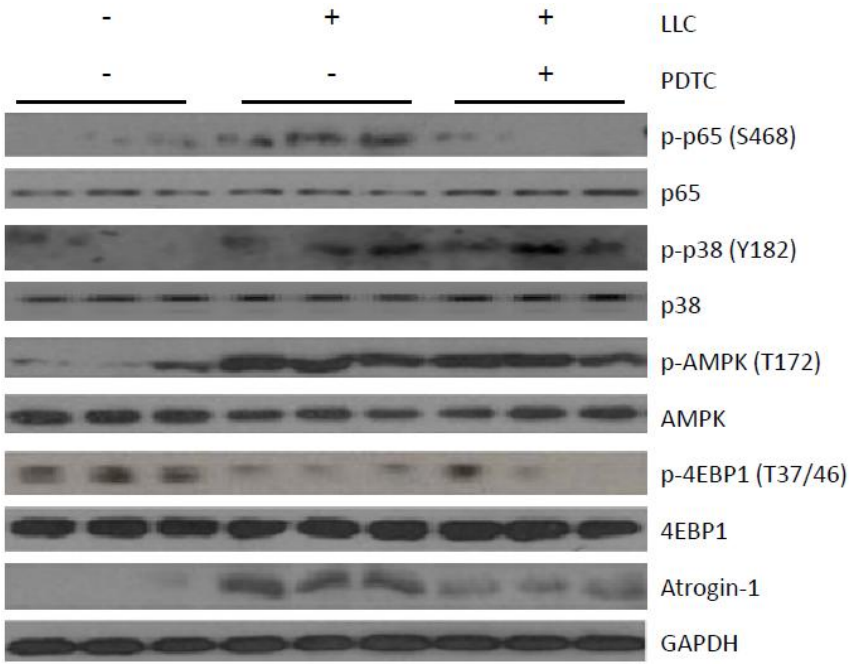

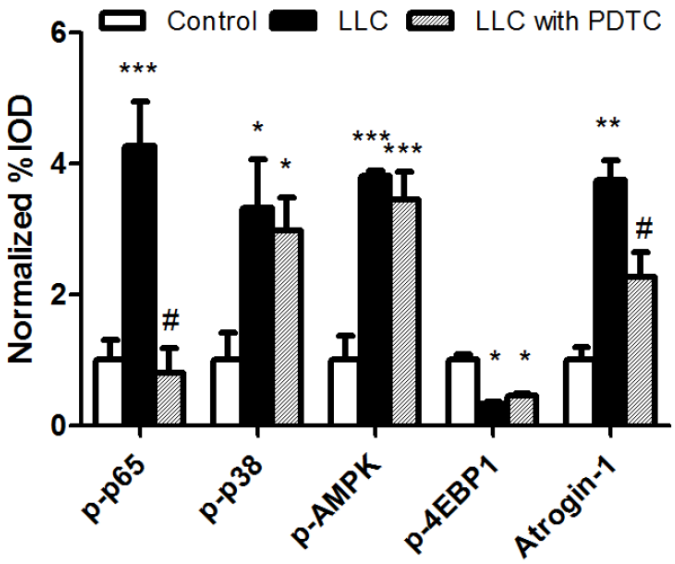

Figure 5.6 (continued).

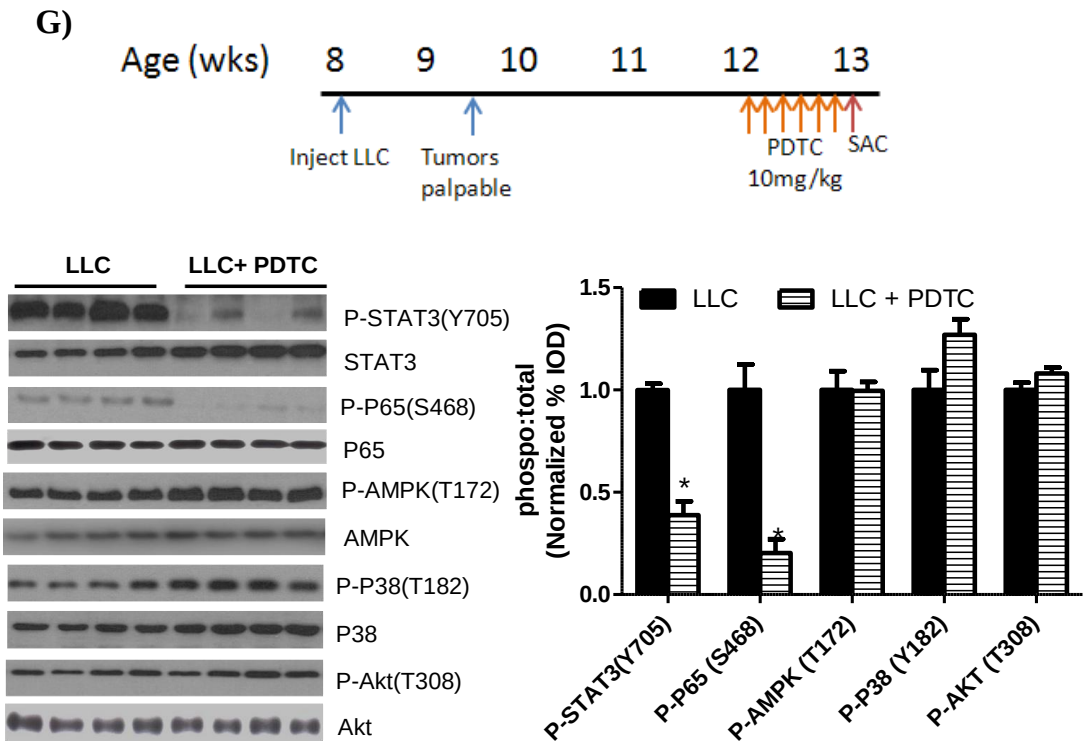

Figure 5.6. The effect of gp130/STAT signaling inhibition on LLC induced signaling. Fully differentiated C2C12 cells were treated with LCM with or without PDTC (STAT/NFκB inhibitor, 50μM), LLL12 (STAT3 specific inhibitor, 100nM) and gp130 receptor antibody (1:1000) for 4h (A) or 72h (B, C, D, E,F) A) p-STAT3 and total STAT3 protein expression was measured via western blot analysis after 4 hour treatment. B) Diameter of C2C12 myotubes after 72h of LLC, PDTC, LLL12 or gp130 antibody administration. C) Relative protein synthesis rates were measured by the incorporation of puromycin into proteins after 72 hours of PDTC, LLL12 or gp130 antibody administration. D-F) C2C12 signaling proteins was measured after 72h of D), gp130 antibody, E) LLL12, or F) PDTC administration in the presence of LCM by western blot analysis. G) PDTC was administered for 1 week to mice bearing LLC tumors. Western blot analysis of LLC associated signaling including STAT3, P65, AMPK, P38, and Akt, were measured. Graphical representation is displayed as the ratio of phosphorylate to total protein levels. Values are the means ± SE. Cell culture data were analyzed with one-way ANOVA and *in vivo* data analyzed with t-test *:$p \leq 0.05$, **: $p \leq 0.01$, ***: $p \leq 0.005$, significant different from control group, #:$p \leq 0.05$, significant different from LLC group.

CHAPTER 6

CACHECTIC SKELETAL MUSCLE RESPONSE TO A NOVEL BOUT OF LOW FREQUENCY STIMULATION[4]

[4] Melissa Puppa, Angela Murphy, Greg Hand, Raja Fayad, and James Carson. Submitted for publication in Journal of Applied Physiology.

6.1 Abstract

While exercise benefits have been well documented in patients with chronic diseases, the mechanistic understanding of contraction in cachectic muscle induced by cancer is largely unknown. We previously demonstrated that treadmill exercise training attenuates the initiation of cancer cachexia. However, the metabolic signaling response to a novel, acute bout of low frequency contraction in a muscle that is already cachectic is unknown. Therefore, the purpose of this study was to determine if severe cancer cachexia disrupts the acute contraction-induced response to low frequency muscle contraction (LoFS). The induction of metabolic genes and signaling was examined 3h after a novel 30-minute bout of contraction (10Hz) in cachectic $Apc^{Min/+}$ (Min) and C57BL/6 (BL-6) mice. Min mice exhibited cachexia at the time of stimulation that included body weight loss, decreased gastrocnemius muscle mass, decreased volitional strength, and decreased cage activity. Although Glut4 mRNA was decreased by cachexia, LoFS increased muscle Glut4 mRNA in both BL-6 and Min mice. LoFS also induced muscle PPARγ and PGC-1α mRNA. However, in Min mice LoFS was not able to induce muscle PGC-1α targets NRF-1 and TFAM mRNA. Muscle contraction induced P-S6 in BL-6 mice, but this induction was blocked by cachexia. Administration of PDTC for 24h, a general STAT and NFκB inhibitor, rescued contraction- induced P-S6 in cachectic muscle. Stimulation increased muscle p-AMPK and p38 in BL-6 and Min mice. These data demonstrate that cachexia alters the muscle metabolic response to acute low frequency muscle contraction; and inflammation-induced inhibition of protein translation may be important for this altered response.

KEY WORDS: Cachexia, contraction, low frequency stimulation, skeletal muscle, mitochondria

6.2 Introduction

Cachexia, an unintentional loss of 5% of body weight including muscle and fat mass given an underlying disease, is associated with many conditions including HIV-AIDS, renal failure, diabetes, chronic heart failure, and many cancers (Deans and Wigmore, 2005). The progression of the cachexia is associated with the degree of body weight loss, and is positively correlated with mortality (Evans et al., 2008). Cachexia accounts for approximately 20% of cancer deaths and approximately 40% of colon cancer related deaths (Tan and Fearon, 2008; Tisdale, 2003). Modeling cachexia in rodents has lead to a better understanding of the regulation of the wasting (Dianliang, 2009). However, an approved treatment for cachexia remains elusive. The lack of treatment options may relate to the underlying disease ultimately controlling the mechanisms regulating the initiation and progression of wasting (Carson and Baltgalvis, 2010).

The $Apc^{Min/+}$ mouse is an established model of intestinal cancer that develops a slowly progressing cachexia when compared to many other cancer cachexia models, and provides physiologic relevance to the human condition. A nonsense mutation in the Adenomatous polyposis coli (Apc) gene predisposes mice to intestinal adenomas (Moser et al., 1990). Cachexia is initiated around 14 weeks of age, and the average lifespan of these mice is approximately 20 weeks. Elevated circulating IL-6 levels are associated with the development of cachexia in $Apc^{Min/+}$ mice. Global knockout of IL-6 in $Apc^{Min/+}$ mice blocks cachexia development and IL-6 over-expression accelerates cachexia progression in $Apc^{Min/+}$ mice (Baltgalvis et al., 2008b). Exercise has shown to be beneficial for attenuating the initiation and progression of cachexia in $Apc^{Min/+}$ mice. With the progression of cachexia, there is an inverse relationship between voluntary wheel

running distance and cachexia development in $Apc^{Min/+}$ mice (Baltgalvis et al., 2010). However, regular treadmill exercise can reduce tumor growth in these mice (Mehl et al., 2005) and also prevent the initiation of cachexia even under conditions of chronically elevated IL-6 (Puppa et al., 2011d). While there are currently no approved pharmaceutical therapies for cachexia our laboratory and others have demonstrated the potential for exercise training to prevent muscle mass loss in the cachectic environment (Puppa et al., 2011d).

An acute bout of exercise alters skeletal muscle signaling and has been shown to benefit patients with many chronic diseases (Fentem, 1994). Contraction can regulate several signaling cascades including fatty acid oxidation (Vavvas et al., 1997), glucose transport (Hayashi et al., 1998), mitochondrial biogenesis (Bergeron et al., 2001; Hood et al., 2006), and protein synthesis (Nader and Esser, 2001). Many exercise responses in muscle have been related to AMPK activation; however, chronically elevated AMPK activation, as seen during the progression of cachexia in the $Apc^{Min/+}$ mouse, can suppress protein synthesis (White et al., 2013b). After an acute bout of exercise, PGC-1α is rapidly upregulated leading to a subsequent increase in mitochondrial associated gene transcription and mitochondrial biogenesis (Baar et al., 2002; Pilegaard et al., 2003). Upregulation of these genes can persist for up to 4 hours before returning to baseline levels (Pilegaard et al., 2000). Additionally, S6-kinase (S6K1), a target of mTOR signaling to increase protein translation, is suppressed in cachectic skeletal muscle (White et al., 2011b), and has been shown to be upregulated 3 hours after a bout of low frequency contraction in rodent skeletal muscle (Nader and Esser, 2001). However, it is

not known if severely cachectic skeletal muscle maintains the capacity to respond to acute contraction.

We have previously demonstrated that treadmill exercise training attenuates the initiation of cancer cachexia-induced muscle and body weight loss (Puppa et al., 2011d). Low frequency electrical stimulation (LoFS) has been shown to alter local metabolic signaling pathways in vivo, without altering the systemic environment as whole body exercise does (Nader and Esser, 2001). However, the metabolic signaling response to a novel, acute bout of low frequency contraction in a muscle that is already cachectic is unknown. Muscle contraction induces several signaling pathways that are suppressed with the progression of cancer cachexia, such as PGC-1α, and ribosomal protein S6 (Baar et al., 2002; Nader and Esser, 2001; White et al., 2011b; White et al., 2012b). Therefore, the purpose of this study was to determine if severe cancer cachexia disrupts the acute contraction response induced by low frequency muscle contraction. We hypothesized that an acute bout of low frequency contraction would stimulate metabolic signaling regulating mitochondrial biogenesis in cachectic skeletal muscle. To test this hypothesis, *Apc*$^{Min/+}$ mice were monitored until they had developed sustained weight loss. Mice then underwent an acute 30 minute bout of low-frequency electrical stimulation in which one leg was stimulated and the other served as an internal control. Hindlimb muscles were harvested three hours after the completion of the contraction and changes in mRNA expression levels and protein expression were measured in both BL-6 and *Apc*$^{Min/+}$ mouse muscle.

6.3 Materials and Methods

Animals. C57BL/6 (BL-6) and *Apc*$^{Min/+}$ (Min) mice were originally purchased from Jackson Laboratories. Mice were bred at the Animal Resource Facility at the University of South Carolina and genotyped for heterozygosity of the *Apc* gene. All animals were kept on a 12:12 light:dark cycle. Animals had *ad libitum* access to food and water during the course of the study. All animals were fasted for 5 hours prior to sacrifice. At 18-20 weeks of age male mice underwent an acute contraction stimulus. A subset of 18-20wk old Min mice received pyrrolidine dithiocarbamate (PDTC), 10mg/kg BW, a STAT3/NFκB inhibitor, 24h prior to acute low frequency stimulation. Three hours after the completion of the contraction protocol animals were anesthetized with a ketamine/ xylazine/ acepromazine cocktail, and tissues were removed, weighed, and frozen in liquid nitrogen. Tissues were stored at -80 °C until further analysis. All animal experimentation was approved by the University of South Carolina's Institutional Animal Care and Use Committee.

Grip strength. Combined hindlimb and forelimb rodent grip strength was measured prior to low frequency stimulation with the Grip Tester (Columbus Instruments, Columbus, OH). Mice were placed with all 4 limbs on a metal grid mounted at a 45° angle connected to a force transducer. Mice were pulled by the tail until they let go of the grid and the force was recorded. Each mouse went through a series of 2 sets of 5 repetitions of force measurements, with a 2-3 minute rest period between each set.

Cage activity monitoring. Two nights prior to stimulation, mice were single housed and placed in activity monitor cages (Opto-M3 Activity Meter, Columbus Instruments, Columbus, OH). Activity was measured for 12 hours during the dark cycle (7 PM -7 AM); the number of beams crossed in an X-Y plane was recorded for two consecutive nights. Food consumption was also recorded during this time given that the mice were single housed.

Low Frequency Stimulation: Low frequency stimulation was conducted as described by Nader and Esser (Nader and Esser, 2001) with slight modifications. Briefly, all animals were fasted for 5 hours prior to stimulation and food was restricted for the remainder of the study. Animals were anesthetized with Isoflurane in a chamber at 2-5% and remained anesthetized for the procedure via a nose cone that was connected tothe isoflurane/oxygen. Animals were placed on a heat pad and the left hind limb was shaved free of hair and cleaned with alcohol followed by betadine. Electrodes were placed on both sides of the peroneal nerve and stimulated via subcutaneous needle. Proper electrode position was confirmed by observing plantarflexion at the ankle joint. This protocol elicited an overall effect of plantar flexion resulting in tapping of the foot. The voltage was applied by a Grass S88 stimulator (Grass technologies). Stimulation was delivered at a frequency of 10 Hz, 5 V, 10-ms duration, 90-ms delay for a total time of 30 min. During the recovery period, animals remained on a heat pad. The right leg served as the control for each animal.

Western Blot analysis: Western blot analysis was performed as previously described (Puppa et al., 2011d). Briefly, gastrocnemius muscle was homogenized and protein concentration was determined by the Bradford method (Bradford, 1976). Homogenates were fractionated on 8-15% SDS-polyacrylamide gels and transferred overnight to PVDF membrane. Primary antibodies for P-S6, S6, P-AMPK, AMPK, TFAM, P-P65, P65, P-STAT3 and STAT3 (cell signaling), and PCG-1α (Santa Cruz) were incubated 1:1000 to 1:2000 for 1h at RT. Secondary antibodies were used at a concentration of 1:2000-1:5000. Enhanced chemiluminescence was used to visualize the antibody-antigen interactions and developed by autoradiography. Blots were analyzed by measuring the integrated optical density (IOD) of each band using ImageJ software. All Western blots were normalized to BL-6 controls run on the same gel unless otherwise noted.

RNA Isolation/PCR. RNA isolation, cDNA synthesis and real-time PCR were performed as previously described (White et al., 2013b) , using reagents from Applied Biosystems. GLUT4, PGC-1α, PGC-1β, PPARγ, NRF1/2, TFAM, Cytochrome B, and GAPDH primers were purchased from IDT. Real time PCR analysis was conducted using an ABI 7300 Sequence Detection System. Data were analyzed using the cycle threshold. All gene expression data were normalized to GAPDH.

Statistical analysis. All data are represented as mean ± SEM. A student t-test was used to determine systemic and baseline differences between BL-6 and Min mice and also between Min and PDTC treated mice. A repeated measure two-way ANOVA (LoFS & Genotype) was used to determine the effects of contraction and cachexia. To determine

the effects of PDTC on muscle mRNA expression a repeated measure two-way ANOVA was used (LoFS & PDTC). An intra-animal comparison of muscles from control and contracted legs from the same mouse was used as the repeated measure. Bonforroni post hoc analysis was used to examine interactions. Significance was set at $p \leq 0.05$.

6.4 Results

Cachexia in $Apc^{Min/+}$ mice.

Apc^{Min} mice (Min) lose body weight, skeletal muscle, and fat mass as cachexia progresses. As with our previous studies these Min mice had a 13.8% loss in body weight, while BL-6 mice did not demonstrate any weight loss. Body weight loss corresponded with a 35% decrease in gastrocnemius muscle mass and a 93% decrease in epidydimal fat mass when compared with BL-6 mice (Table 6.1). Body weight loss was not associated with alterations in food intake measured during the week prior to sacrifice (BL-6: 1.8±0.2 g/d Min: 1.6±0.4 g/d).

Human cancer patients exhibit decreased physical activity and increased fatigue with cachexia (Maddocks et al.; Mustian et al., 2007). We have previously reported that Min mice also demonstrate decrements in functional status and physical activity with the initiation and progression of cachexia (Baltgalvis et al., 2010). We extend these observations to demonstrate that Min mice have dramatically reduced cage activity with severe cachexia. There was a significant reduction in XY plane cage activity (Fig 6.1A) and a decrease in rearing activity (Fig 6.1B) during the active dark cycle. Volitional grip strength was decreased 27% in severely cachectic Min mice; however, the decrease in force may be attributed to an overall loss in body mass as no differences were seen when values are normalized with body weight (Table 6.2). These data demonstrate that with severe cachexia, the loss in body mass is accompanied by a dramatic decrease in activity level and voluntary force production. However, the capacity to contract skeletal muscle remains intact.

LoFS regulation of metabolic genes in cachectic mice

To examine if cachexia altered the capacity of LoFS to induce muscle expression of metabolic genes, mRNA expression was examined 3 hours after a novel bout of contraction (Fig 6.2). Contraction induced a 3-fold increase in GLUT4 mRNA levels in BL-6 mice (Fig 6.2A). Similarly, contraction induced a 4.7-fold increase in GLUT4 mRNA in cachectic skeletal muscle despite having basal expression suppressed by cachexia (Fig 6.2A). Peroxisome proliferator-activated receptor gamma (PPARγ), a regulator of lipid metabolism, was increased 3-fold by contraction in BL-6, and a similar increase was seen in cachectic muscle (Fig 6.2B). Contraction did not induce PGC-1α mRNA expression in BL-6 mice; however, it induced a 6-fold increase in PCG-1α mRNA in cachectic muscle despite suppressed basal expression (Fig 6.2C). Contraction suppressed PGC-1β mRNA expression 45% in wild type mice. Cachexia inhibited muscle PGC-1β expression 78% and contraction did not change PGC-1β in cachectic muscle (Fig 6.2D). These data demonstrate that cachectic skeletal muscle maintains the capacity for contraction-induction of some metabolic genes.

PGC-1α is known to upregulate the transcription of mitochondrial associated genes. To determine if the increase in PGC-1α leads to subsequent increases in mitochondrial associated gene transcription, we measured mRNA expression of PGC-1α target genes NRF-1, TFAM, and cytochrome B (Fig 6.3). Cachexia suppressed expression of NRF-1, TFAM, and cytochrome B mRNA (Fig 6.3). Contraction elicited a 2.2-fold increase in NRF-1mRNA expression in BL-6 mice; however, contraction was

unable to stimulate NRF-1 mRNA in cachectic muscle (Fig 6.3A). Similar to NRF-1, TFAM expression was induced 90% by contraction in BL-6 mice, whereas contraction was unable to induce TFAM expression in cachectic muscle (Fig 6.3B). We also measured the expression of a mitochondrial encoded gene, cytochrome B. Contraction induced a 2.4-fold increase in cytochrome B mRNA expression in BL-6 mice, which was inhibited by cachexia (Fig 6.3C). These data demonstrate that cachectic skeletal muscle displays altered induction of mitochondrial associated genes with acute contraction.

LoFS regulation of protein expression in cachectic mice

We examined if cachexia altered the capacity for LoFS contraction to increase signaling regulating protein synthesis. We measured the phosphorylation of S6 ribosomal protein as an indicator of mTOR signaling (Fig 6.4). Contraction induced an 8-fold increase in BL-6 muscle S6 phosphorylation; however, there was no contraction induced phosphorylation of S6 in cachectic muscle (Fig 6.4A). We next examined if cachexia altered contraction-induced expression of mitochondrial proteins (Fig 6.4). TFAM protein expression was not altered by cachexia (Fig 6.4B); however, cachexia suppressed the expression of muscle cytochrome c and PGC-1α protein expression (Fig 6.4C/D). Contraction induced a 30% increase in TFAM expression in BL-6 mice (Fig 6.4B), but there was no contraction-induced increase in cachectic muscle. Similarly, contraction increased cytochrome c expression 40% in BL-6 mice, but cachexia blocked the contraction-induction of cytochrome c protein (Fig 6.4C). PGC-1α protein expression was suppressed by cachexia (Fig 6.4D). Unlike TFAM and cytochrome c, there was a

main effect of contraction to increase muscle PGC-1α protein expression in both BL-6 and cachectic muscle (Fig 6.4D). These data demonstrate that cachectic muscle lacks contraction-induction of mTOR signaling. Although contraction did not induce mitochondrial protein expression in cachectic muscle, it did induce protein expression of the upstream regulator, PGC-1α.

Effect of Pyrrolidine dithiocarbamate on cachectic muscle response to LoFS

We next examined if the acute suppression of systemic inflammation altered cachectic muscle's response to contraction. Inflammation was suppressed by administration of pyrrolidine dithiocarbamate (PDTC), a STAT3/NFκB inhibitor, 24h prior to contraction. The phosphorylation of STAT3 was elevated in cachectic muscle (Fig 6.5A). There was a main effect of contraction to induce muscle STAT3 phosphorylation in all groups, regardless of cachexia and PDTC treatment. Contraction increased p65 phosphorylation in BL-6 mice, but not cachectic mice. However, the phosphorylation of p65 was increased by cachexia. PDTC administration blocked basal STAT3 and P65 phosphorylation in cachectic muscle. However, contraction-induced STAT3 and P65 phosphorylation was not altered by PDTC (Fig 6.5A). The administration of PDTC increased basal levels of PGC-1α target mRNAs NRF-1, TFAM, and cytochrome b in cachectic muscle; however, contraction did not increase PGC-1α target mRNAs (Fig 6.5B). The inability of contraction to induce p-S6 in cachectic muscle was rescued by the PTDC treatment (Fig 6.5C). Interestingly, PDTC treatment increased protein expression of TFAM and cytochrome c in cachectic muscle; however, the

contraction-induced increased in S6 phosphorylation was not associated with contraction-induced increases in protein levels of cytochrome c or TFAM with PDTC (Fig 6.5C). These data demonstrate that inhibition of inflammatory signaling in cachectic muscle recues the suppression of contraction-induced mTOR signaling, and reverses the cachexia-induced suppression of mitochondrial associated genes.

LoFS mediated regulation of mTOR

Finally, we examined if the induction of AMPK, p38 and Akt phosphorylation by contraction was altered in skeletal muscle from cachectic mice. These signaling pathways are known regulators of mTOR signaling. Cachexia increased muscle AMPK phosphorylation (Fig 6.6A), which has been previously reported (White et al., 2013b). The ability for contraction to increase muscle AMPK phosphorylation was not altered by cachexia. Contraction induced an 80% increase in muscle AMPK phosphorylation in BL-6 mice and a 50% increase in cachectic mice (Fig 6.6A). Neither basal nor contraction-induced muscle P38 phosphorylation was changed by cachexia (Fig 6.6B). Akt phosphorylation was elevated 4-fold in cachectic muscle (Fig 6.6C). Increases in Akt phosphorylation with cachexia have been previously reported (White et al., 2011b). Contraction elicited a 60% increase in Akt phosphorylation in BL-6 mice; however, contraction did not alter the phosphorylation in cachectic muscle (Fig 6.6C). These data demonstrate that the interaction of cachexia and contraction differentially regulate several signaling pathways that have the potential to control the muscle's metabolic response.

6.5 Discussion

While the development and progression of cachexia has a well-documented impact on cancer patient survival, there are currently no approved treatments that can block or attenuate this condition (Murphy and Lynch, 2012). Muscle contraction may have therapeutic value for the treatment and management of cachexia. Exercise has recognized benefits for the prevention of some cancers (Murphy and Lynch, 2012), and electrical muscle stimulation has beneficial effects in critically ill patients (Gerovasili et al., 2009). Several studies have suggested the use of exercise training to resolve muscle wasting in conditions of cachexia as reviewed by Zinna and Yarasheski (Zinna and Yarasheski, 2003). However, few studies to date have examined if severely cachectic skeletal muscle retains the metabolic plasticity to respond to exercise. Because many patients are not diagnosed until significant muscle and body mass have been lost (Tisdale, 2002), it is imperative that we understand the cachectic muscle response to therapeutic interventions in order to develop viable treatments. While we have demonstrated that treadmill exercise training in mice is beneficial for attenuating the initiation of cachexia, to our knowledge we present the first study to demonstrate that severely cachectic skeletal muscle has an altered metabolic response to a novel bout of contraction. While contraction was able to elicit expression of some metabolic genes and signaling pathways, there were deficiencies in the activation of mitochondrial biogenesis and mTOR signaling. The contraction induction of muscle PGC-1α gene targets was also inhibited by cachexia, even though PGC-1-α mRNA and protein expression was induced by contraction. Interestingly, chronic inflammation may have a role in the altered response of skeletal muscle to contraction, as administration of pyrrolidine

dithiocarbamate (PDTC) restored mTOR signaling in cachectic muscle. Further work is needed to determine the interaction between muscle inflammatory signaling and contraction-induced metabolic regulation.

Skeletal muscle contraction is widely considered advantageous for offsetting metabolic dysfunction, as it stimulates signaling pathways involved with glucose uptake, intra-cellular energy status, and calcium signaling (Hood et al., 2006). Activation of these signaling pathways can result in increased protein synthesis and enhanced mitochondrial biogenesis. AMPK and P38 are examples of signaling pathways activated by contraction that can regulate muscle metabolism, and we report that these pathways maintain the ability to be activated in severely cachectic muscle. Although AMPK and P38 MAPK are acutely regulated by contractile activity (Fernandez-Marcos and Auwerx, 2011), chronic activation of these pathways has been reported with muscle wasting (McClung et al., 2010; White et al., 2013b; Zhang et al., 2011). Acute activation of AMPK and P38 can induce post-translational modifications of proteins that regulate contraction-induced gene expression through the activity of nuclear transcription factors and transcriptional co-activators (Hood et al., 2006). Chronic activation of AMPK and P38 signaling are associated with muscle wasting (White et al., 2013b; Zhang and Li, 2012). Contraction-induced P38 activation increases the transcription of ATF2 and PGC-1α. Additionally, mice with constitutively active P38 demonstrate increased PGC-1α and cytochrome oxidase IV protein expression (Akimoto et al., 2005a). Chronic P38 activation is also associated with increased atrogene expression, which is involved in protein degradation (Zhang et al., 2011; Zhang et al., 2013). Prolonged AMPK activation is associated with decreased muscle protein synthesis through the suppression of mTOR (White et al.,

2013b). Contraction-induced activation of AMPK is associated with increased PGC-1α protein expression after low frequency contraction (Atherton et al., 2005). Contraction-induced metabolic homeostasis includes the regulation of GLUT4 for increased muscle glucose uptake in an insulin independent manner (Brozinick et al., 1992; King et al., 1993). We found that cachexia suppressed baseline skeletal muscle expression of GLUT4 mRNA. Translocation of AMPK into the nucleus is associated with increased GLUT4 mRNA expression and this is enhanced under conditions of low glycogen as seen after exercise (Steinberg et al., 2006). Similar to what is seen in type 2 diabetes (Kennedy et al., 1999), we demonstrate that acute contraction maintains the ability to increase GLUT4 mRNA expression despite the presences of severe cachexia.

PGC-1α is involved in the regulation of mitochondrial biogenesis. Both acute contraction and exercise training stimulate transcriptional co-activator PGC-1α expression (Baar et al., 2002). While PGC-1α gene expression can be increased after acute exercise in humans, the duration and intensity of the exercise may play a role in its induction (Russell et al., 2005). We found that LoFS contraction increased PGC-1α mRNA expression in cachectic mice, while there was only a trend for a change in wild type mice. However, contraction was able to increase PGC-1α protein expression independent of cachexia. The relative exercise intensity, the muscle's intrinsic oxidative capacity, and the fatigue-ability of the muscle may be responsible for the large contraction induction of PGC-1 α mRNA in cachectic mice. Interestingly, despite the contraction increase in PGC-1 α mRNA and protein in cachectic muscle there was not a corresponding induction of TFAM and NRF-1 mRNA levels, which are transcriptional targets of PGC-1 α. Cachexia is associated with preferential atrophy of glycolytic muscle

fibers (Julienne et al., 2012), and all fiber types have a reduction in muscle oxidative metabolism (White et al., 2011a). It is possible that the induction of PGC-1α expression without any changes in its target genes is related to mRNA stability;many important regulators of mitochondrial biogenesis such as PGC-1 and TFAM have relatively short mRNA half lives (D'Souza et al., 2012). Lai et al. have demonstrated accelerated mRNA turnover of PGC-1α and TFAM after chronic contraction (Lai et al., 2010). Recently D'souza et al. demonstrated that inherent muscle oxidative capacity could affect mRNA stability resulting in changes in mRNA turnover (D'Souza et al., 2012). The phosphorylation of PGC-1α by P38 has been shown to increase PGC-1 protein half life (Fernandez-Marcos and Auwerx, 2011). A decrease in the half life of PGC-1α protein during cachexia could explain why we did not observe any increases in PGC-1α targets that are known to induce mitochondrial biogenesis. Further work is necessary to identify why cachexia had a selective regulation of contraction sensitive gene expression related to regulators of mitochondria biogenesis and oxidative metabolism.

The process of mRNA translation related to protein synthesis is a necessary component of muscle metabolic plasticity. Muscle protein synthesis is regulated by many stimuli including; hormonal, nutrient, mechanical, and inflammatory inputs. mTOR signaling has an acknowledged role for the integration of stimuli regulating muscle protein synthesis (Dickinson et al., 2011; Hayashi and Proud, 2007; Lee and Hung, 2007; Parkington et al., 2003). Additionally, the regulation of skeletal muscle mitochondria and oxidative metabolism through PGC-1α and NRF1/2 has been shown to involve mTOR signaling (Cunningham et al., 2007; Risson et al., 2009). Dysregulation of mTOR has been identified in humans and in animal models during cancer cachexia (Tisdale, 2002;

Tisdale, 2009; White et al., 2013b; White et al., 2012b). We demonstrate that cachexia suppresses the ability of contraction to induce mTOR signaling. The phosphorylation of mTOR target S6 or NRF-1 mRNA levels was not induced by contraction in cachectic muscle. Interestingly, cachexia did not suppress the contraction-induction of PGC-1α or mechanical signaling through p38 phosphorylation. Further work is needed to determine the ramification of mTOR suppression and its relationship to the loss of oxidative capacity in cachectic muscle.

There is evidence to suggest that the inflammation associated with cachexia may be a potent mTOR suppressor, as IL-6 over-expression accelerates muscle atrophy and decreases mTOR signaling in *Apc*$^{Min/+}$ mice and C2C12 myotubes (White et al., 2013b). We now report that the acute suppression of systemic inflammatory signaling in *Apc*$^{Min/+}$ mice by PDTC administration can rescue contraction-induced S6 phosphorylation. This is an interesting finding since we have previously found in Lewis Lung Carcinoma-induced muscle wasting that inhibition of skeletal muscle gp130 and STAT3 is not sufficient to rescue mTOR signaling and muscle protein synthesis (Puppa et al., 2013a). Additionally, 2 weeks of systemic IL-6 inhibition during the initiation of cachexia in *Apc*$^{Min/+}$ mice did not rescue mTOR signaling and muscle protein synthesis (White et al., 2011b). These data question the role of IL-6 and STAT3 in the suppression of mTOR in cachectic muscle. However, PDTC is an inhibitor of both STAT3 and NFκB (He et al., 2006; Nai et al., 2007). NFκB may have a role in suppression of mTOR, as IL-6 overexpression in *Apc*$^{Min/+}$ mice and the progression of cachexia activate NFκB signaling (Puppa et al., 2011d). Although the induction of NFκB signaling with cachexia is commonly associated with protein catabolism, it is also induced by muscle contraction and has a role

in the regulation of muscle metabolism (Acharyya and Guttridge, 2007; Bakkar et al., 2008; Peterson and Guttridge, 2008). Further work is needed to identify the mechanisms by which inflammation may be mediating contraction-induced mTOR signaling in cachectic muscle.

To our knowledge we are the first to report that severe cancer cachexia can alter the metabolic plasticity of skeletal muscle to an acute bout of contraction. We report that acute low frequency stimulated contraction was able to induce PGC-1α and PPARγ mRNA expression in cachectic muscle. However, cachexia blocked contraction induced NRF-1 and TFAM mRNA expression, which are PGC-1α transcriptional targets. Coinciding with these findings, contraction-induced S6 phosphorylation, a target of mTOR signaling, was inhibited by cachexia. Inhibition of systemic inflammation related to NFκB and STAT3 signaling was sufficient to rescue contraction stimulated S6 phosphorylation in cachectic muscle, but not TFAM or cytochrome c protein expression. These data suggest that the response of cachectic muscle to a novel, acute bout of low frequency contraction is disrupted, and combinatorial therapeutic approaches involving exercise may prove beneficial for cachectic patients. Additionally, further research is needed to determine if multiple bouts of exercise or contraction improve the metabolic response of cachectic muscle to an acute bout of contraction.

Acknowledgements

The authors thank Ms. Tia Davis for technical assistance with the animal breeding.

Table 6.1. Cachexia in $Apc^{Min/+}$ (Min) mice is associated with muscle mass loss. There was no difference between the stimulated and non stimulated legs three hours post contraction. Body weight (BW) was monitored throughout the course of the study. Mass of gastrocnemius, epididymal fat (Epi fat), and spleen was weighed at the time of sacrifice. * Significantly different from BL-6, $p<0.05$

	BL-6 (n=5)	**Min** (n=5)
Max BW (g)	28.0±0.4	25.2±0.9
BW at Sacrifice (g)	28.0±0.4	21.7±.09*
% change BW	0.0±0.0	-13.8±2.9*
Gastrocnemius (mg)	137.0±3.0	88.3±5.4*
Epi Fat (mg)	468.5±40.9	29.6±12.2*
Spleen (mg)	85.8±3.0	437.8±54.0
Tibia Length (mm)	16.9±0.1	16.9±0.1

Table 6.2. Grip Strength in the Min mouse is decreased during severe cachexia. Volitional grip strength was measured in mice prior to stimulation. Grip strength was normalized to body weight (BW) taken at the time of testing. *Significantly different from BL-6, $p<0.05$

	BL-6 (n=5)	**Min** (n=5)
Avg Grip Strength (N)	2.27±0.07	1.66±0.19*
Max Grip Strength (N)	2.80±0.08	2.16±0.09*
Avg Grip Strength/BW (N/g)	0.079±0.002	0.068±0.006
Max Grip Strength/BW (N/g)	0.097±0.003	0.090±0.005

6.6 Figure Legend

Figure 6.1. Cage Activity during severe cachexia. Cage activity was measured for three consecutive nights during the active cycle (1900-0700h). All animals were single housed. A) XY ambulatory count, the number of times a new beam is interrupted, and B) total Z counts were analyzed. T-test was run to test for significance. *significantly different from BL-6 $p<0.001$.

Figure 6.2. Metabolic gene response to a novel bout of low frequency stimulated contraction. mRNA levels of A) GLUT4 B) PPARγ C) PGC-1α and D) PGC-1β three hours after a novel bout of contraction in healthy wild type (BL-6) and cachectic $Apc^{Min/+}$ (Min) mice *Significantly different from BL-6 control from pre-planned t-test. # main effect LoFS, & main effect genotype, † significantly different from all other comparisons, $p<0.05$.

Figure 6.3. Expression of PGC-1α targets in response to a novel bout of low frequency stimulated contraction. mRNA levels for the PGC-1α target A) Nuclear Respiratory Factor-1 (NRF-1) and B) Mitochondrial transcription factor A (TFAM) were measured in the gastrocnemius muscle of wild type (BL-6) and cachectic *ApcMin/+* (Min) mice. C) mitochondrial encoded cytochrome B mRNA was measured in the gastrocnemius, & main effect genotype, † significantly different from all other comparisons, $p<0.05$.

Figure 6.4. LoFS regulation of protein expression. A) The ratio of phosphorylated to total S6 in the gastrocnemius muscle was used as a marker of protein synthesis. The translational response of B) TFAM C) Cytochrome C and D) PGC-1α three hours after a novel bout of contraction in healthy wild type (BL-6) and cachectic $Apc^{Min/+}$ (Min) mice. Lanes connected by a bar in the representative western blots represent the control (C) and LoFS (L) leg from the same animal. All comparisons were run on the same gel. # main effect LoFS, & main effect genotype, † significantly different from all other comparisons, $p<0.05$.

Figure 6.5. Effect of Pyrrolidine dithiocarbamate on cachectic muscle response to LoFS. Inflammatory signaling was blocked 24h prior to stimulation by acute PDTC administration A) The ratio of phosphorylation:total STAT3 and P65 were measured 3h after acute contraction. B) mRNA targets of PGC-1α, Nuclear Respiratory Factor-1 (NRF-1) and Mitochondrial transcription factor A (TFAM), and cytochrome B (Cyto B) were measured in mice administered PDTC. Data were normalized to the levels seen in the control leg of $Apc^{Min/+}$ mice. The dotted line represents BL-6 control levels. C) The ratio of phosphorylated: total S6 was used as a marker of protein synthesis, and the protein levels of TFAM and cytochrome c (Cyto C) were measured by western blot analysis and normalized to Min controls run on the same gel. Lanes connected by a bar in the representative western blots represent the control (C) and LoFS (L) leg from the same animal. All comparisons were run on the same gel. * significantly different from Min based on pre-planned t-test. $ main effect PDTC, # main effect LoFS, & main effect genotype, ** significantly different from control leg within group, ^^ significantly

different from all other control groups, ∞ significantly different from all other LoFS comparisons, $p<0.05$.

Figure 6.6. LoFS mediated regulators of mTOR. Known activators and suppressors of mTOR were measured in gastrocnemius of BL-6 and Min mice 3 hours after LoFS. A) AMPK B) P-38 and C) Akt phosphorylation was measured and graphed as a ratio of phosphorylated to total protein. Lanes connected by a bar in the representative western blots represent the control (C) and LoFS (L) leg from the same animal. All comparisons were run on the same gel. # main effect LoFS, & main effect genotype, † significantly different from all other comparisons, $p<0.05$.

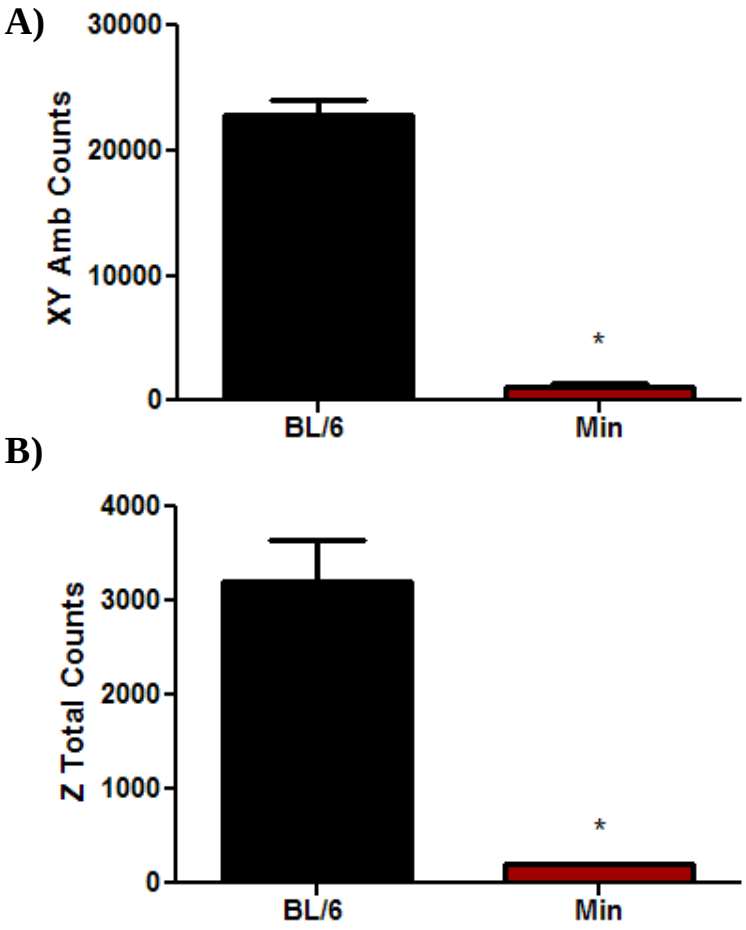

Figure 6.1. Cage Activity during severe cachexia. Cage activity was measured for three consecutive nights during the active cycle (1900-0700h). All animals were single housed. A) XY ambulatory count, the number of times a new beam is interrupted, and B) total Z counts were analyzed. T-test was run to test for significance. *significantly different from BL-6 $p<0.001$.

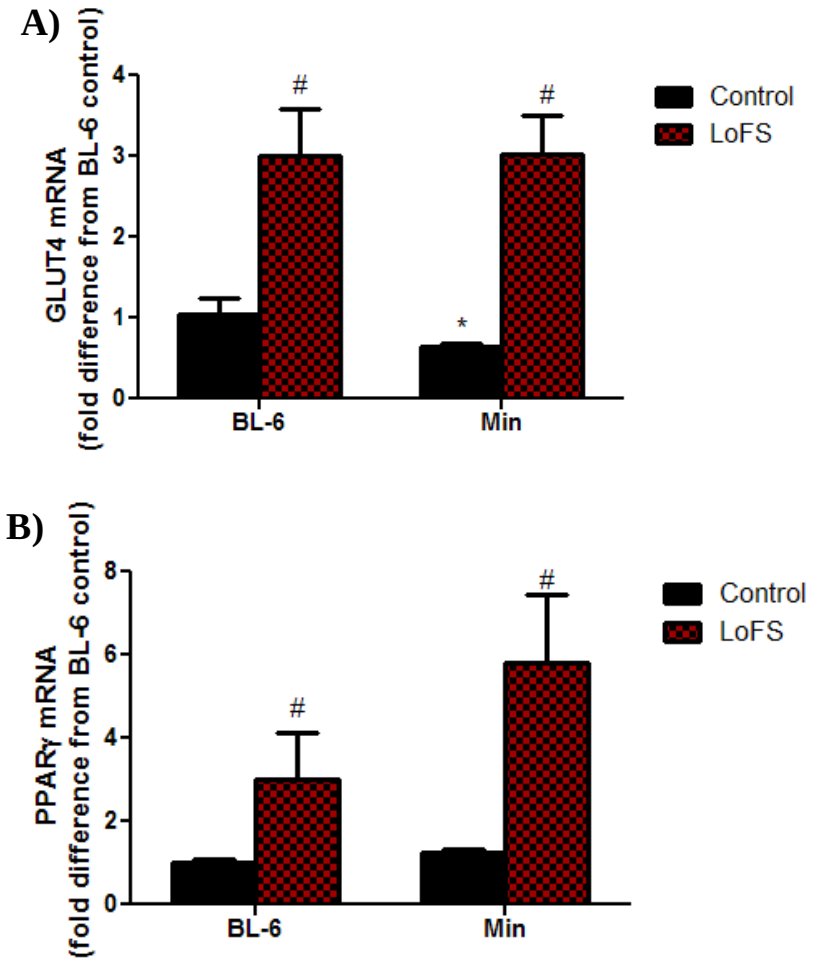
A)
GLUT4 mRNA
(fold difference from BL-6 control)
4
3
2
1
0
#
#
*
BL-6
Min
Control
LoFS
B)
PPARγ mRNA
(fold difference from BL-6 control)
8
6
4
2
0
#
#
BL-6
Min
Control
LoFS

Figure 6.2.

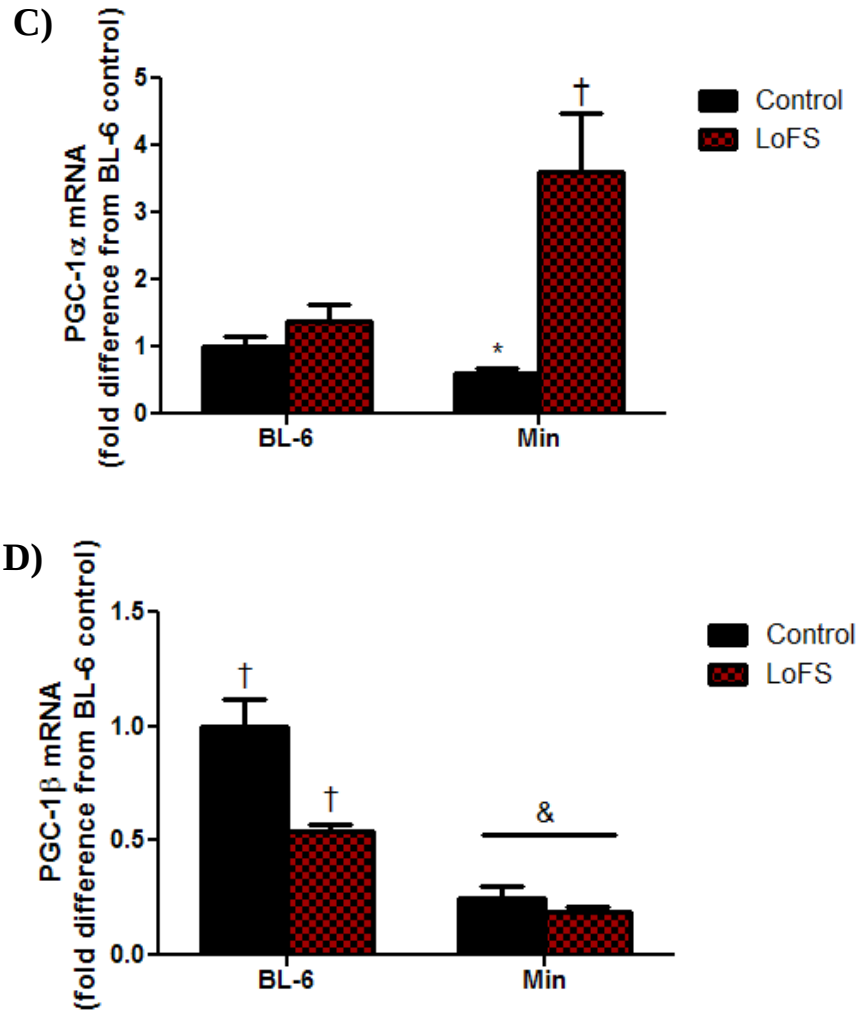

Figure 6.2. Metabolic gene response to a novel bout of low frequency stimulated contraction. mRNA levels of A) GLUT4 B) PPARγ C) PGC-1α and D) PGC-1β three hours after a novel bout of contraction in healthy wild type (BL-6) and cachectic *Apc*$^{Min/+}$ (Min) mice *Significantly different from BL-6 control from pre-planned t-test. # main effect LoFS, & main effect genotype, † significantly different from all other comparisons, $p<0.05$.

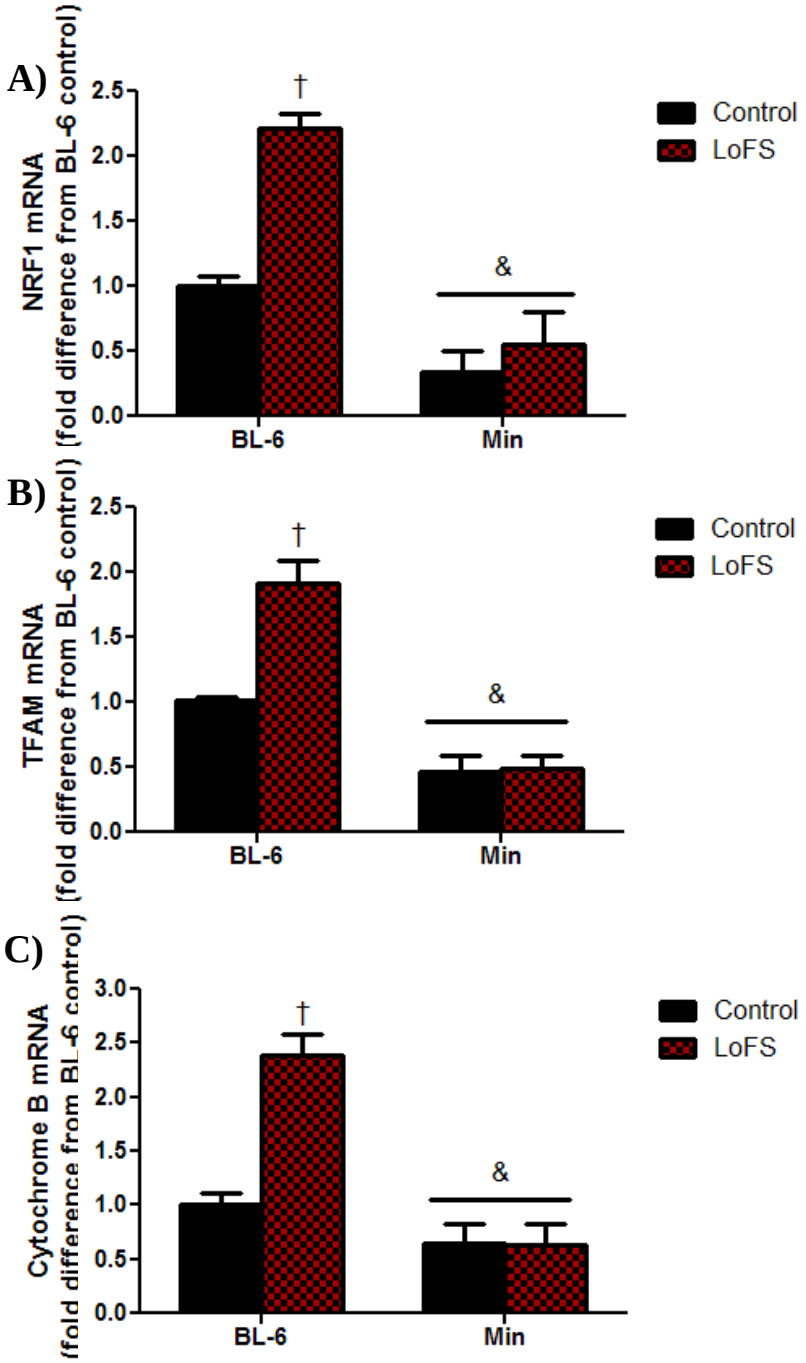

Figure 6.3. Expression of PGC-1α targets in response to a novel bout of low frequency stimulated contraction. mRNA levels for the PGC-1α target A) Nuclear Respiratory Factor-1 (NRF-1) and B) Mitochondrial transcription factor A (TFAM) were measured in the gastrocnemius muscle of wild type (BL-6) and cachectic *ApcMin/+* (Min) mice. C) mitochondrial encoded cytochrome B mRNA was measured in the gastrocnemius, & main effect genotype, † significantly different from all other comparisons, $p<0.05$.

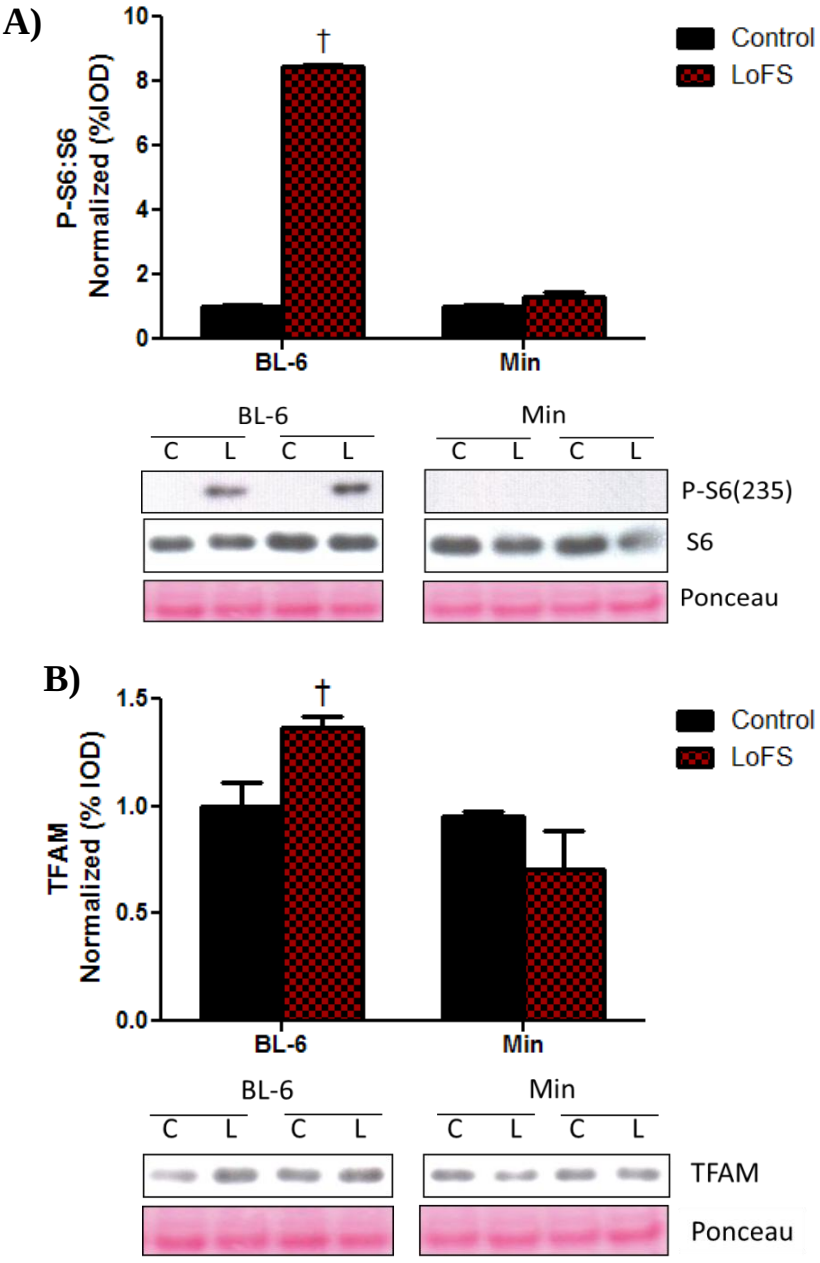
A)
P-S6:S6
Normalized (%IOD)
10
8
6
4
2
0
†
Control
LoFS
BL-6
Min
BL-6
Min
C L C L
C L C L
P-S6(235)
S6
Ponceau
B)
TFAM
Normalized (% IOD)
1.5
1.0
0.5
0.0
†
Control
LoFS
BL-6
Min
BL-6
Min
C L C L
C L C L
TFAM
Ponceau

Figure 6.4.

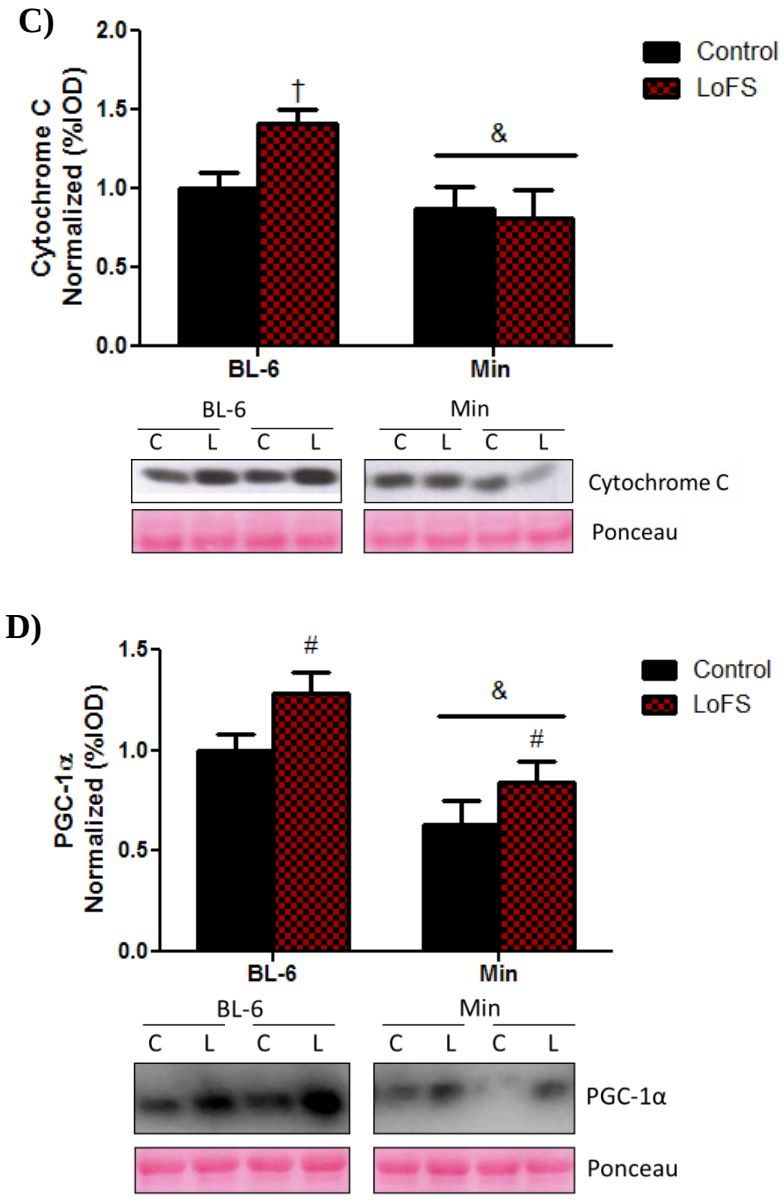

Figure 6.4. LoFS regulation of protein expression. A) The ratio of phosphorylated to total S6 in the gastrocnemius muscle was used as a marker of protein synthesis. The translational response of B) TFAM C) Cytochrome C and D) PGC-1α three hours after a novel bout of contraction in healthy wild type (BL-6) and cachectic $Apc^{Min/+}$ (Min) mice. Lanes connected by a bar in the representative western blots represent the control (C) and LoFS (L) leg from the same animal. All comparisons were run on the same gel. # main effect LoFS, & main effect genotype, † significantly different from all other comparisons, $p<0.05$.

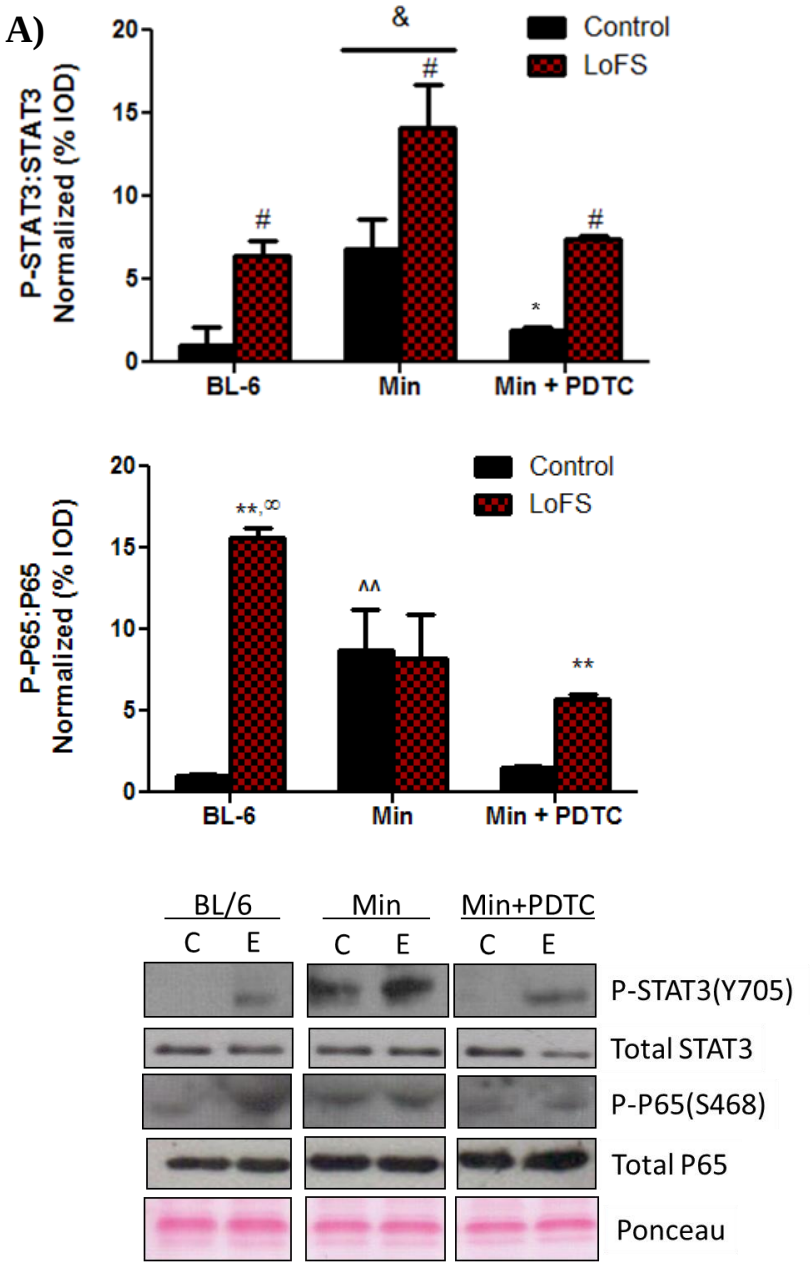
A)
P-STAT3:STAT3
Normalized (% IOD)
20
15
10
5
0
&
#
#
#
*
Control
LoFS
BL-6
Min
Min + PDTC
P-P65:P65
Normalized (% IOD)
**,∞
^^
**
Control
LoFS
BL-6
Min
Min + PDTC
BL/6
Min
Min+PDTC
C E C E C E
P-STAT3(Y705)
Total STAT3
P-P65(S468)
Total P65
Ponceau

Figure 6.5.

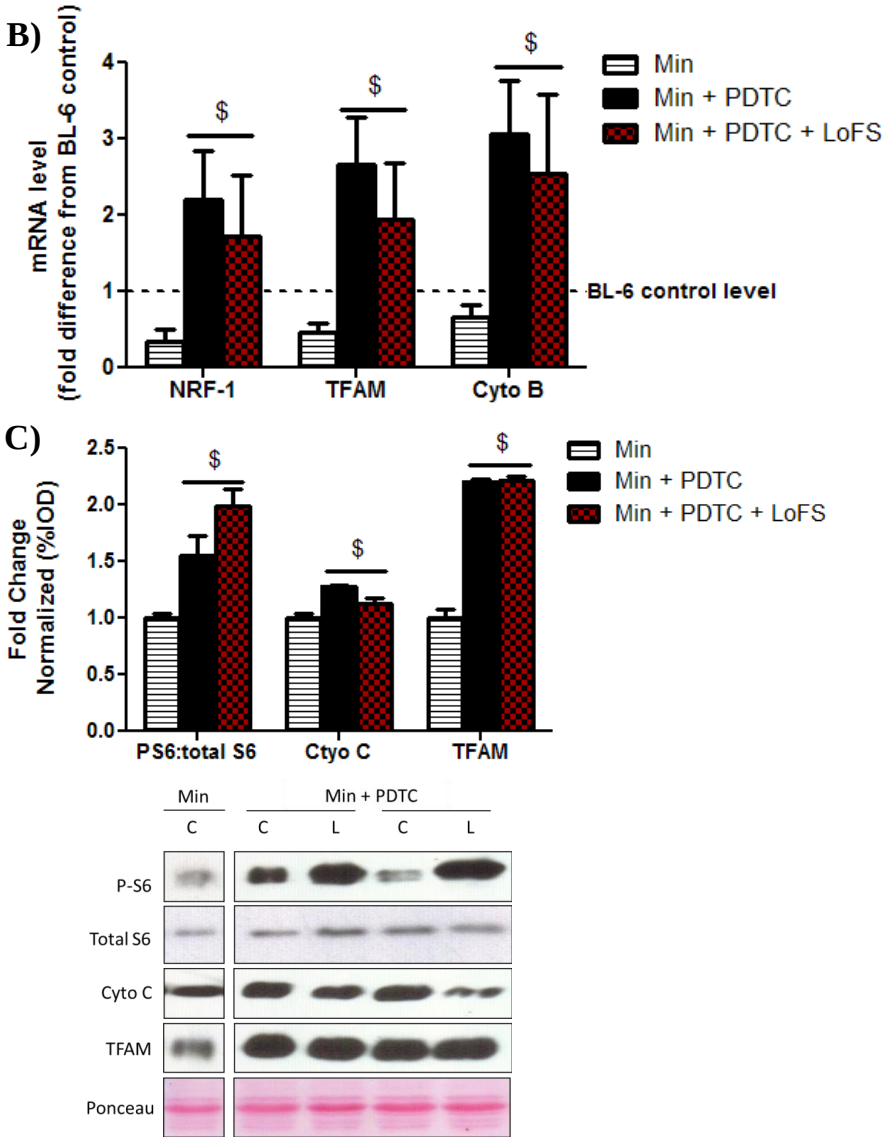

Figure 6.5. Effect of Pyrrolidine dithiocarbamate on cachectic muscle response to LoFS. Inflammatory signaling was blocked 24h prior to stimulation by acute PDTC administration A) The ratio of phosphorylation:total STAT3 and P65 were measured 3h after acute contraction. B) mRNA targets of PGC-1α, NRF-1, TFAM, and cytochrome B (Cyto B) were measured in mice administered PDTC. Data were normalized to the levels seen in the control leg of *Apc*$^{Min/+}$ mice. The dotted line represents BL-6 control levels. C) The ratio of phosphorylated: total S6 was used as a marker of protein synthesis, and the protein levels of TFAM and cytochrome c (Cyto C) were measured by western blot analysis and normalized to Min controls run on the same gel. Lanes connected by a bar represent the control (C) and LoFS (L) leg from the same animal. All comparisons were run on the same gel. * significantly different from Min based on pre-planned t-test. $ main effect PDTC, # main effect LoFS, & main effect genotype, ** significantly different from control leg within group, ^^ significantly different from all other control groups, ∞ significantly different from all other LoFS comparisons, $p<0.05$.

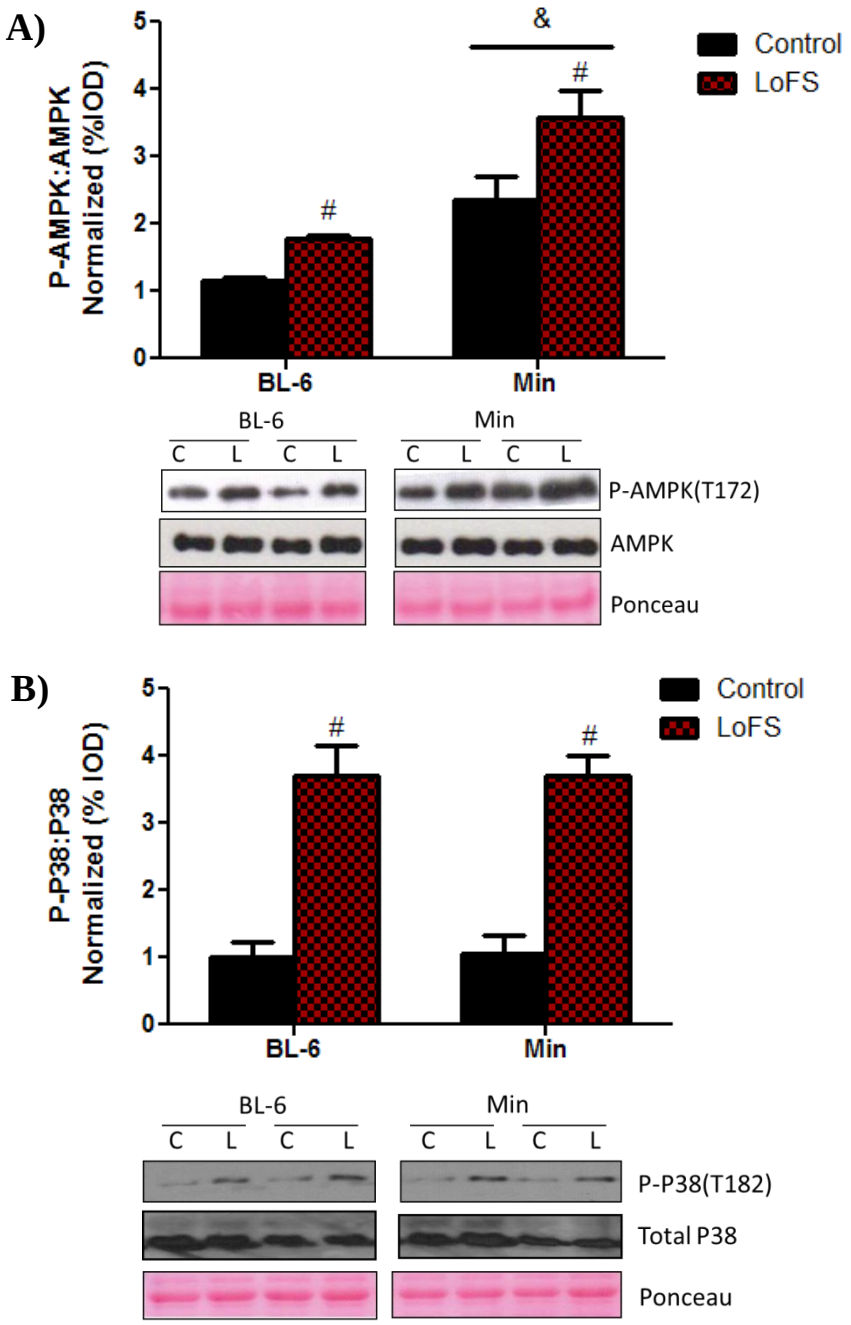
A)
P-AMPK:AMPK
Normalized (%IOD)
5
4
3
2
1
0
&
#
#
Control
LoFS
BL-6
Min
BL-6
Min
C L C L
C L C L
P-AMPK(T172)
AMPK
Ponceau
B)
P-P38:P38
Normalized (% IOD)
5
4
3
2
1
0
#
#
Control
LoFS
BL-6
Min
BL-6
Min
C L C L
C L C L
P-P38(T182)
Total P38
Ponceau

Figure 6.6.

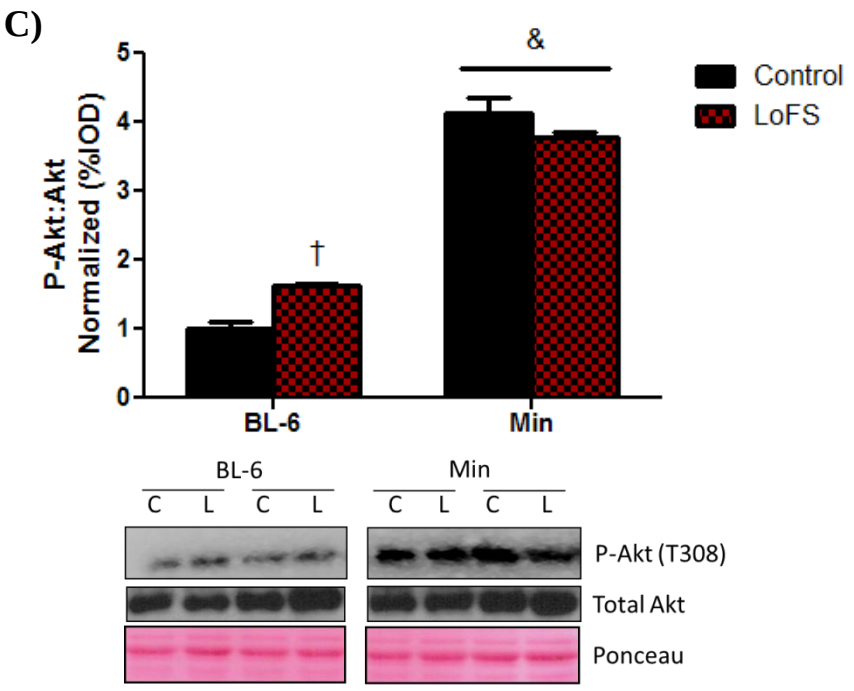

Figure 6.6. LoFS mediated regulators of mTOR. Known activators and suppressors of mTOR were measured in gastrocnemius of BL-6 and Min mice 3 hours after LoFS. A) AMPK B) P-38 and C) Akt phosphorylation was measured and graphed as a ratio of phosphorylated to total protein. Lanes connected by a bar in the representative western blots represent the control (C) and LoFS (L) leg from the same animal. All comparisons were run on the same gel. # main effect LoFS, & main effect genotype, † significantly different from all other comparisons, $p<0.05$.

CHAPTER 7

OVERALL DISCUSSION

Cachexia is defined as the unintentional loss of body weight including muscle mass with or without adipose tissue loss given an underlying condition (Batista et al., 2012; Bruera, 1997; Evans et al., 2008; Fearon et al., 2011). Cancer cachexia accounts for approximately 20% of all cancer related deaths and 40% of deaths related to colon cancer (Bruera, 1997; Tisdale, 2002). Given the complexity of the cachectic condition, it is not diagnosed until after significant muscle loss and there are currently no approved pharmaceutical interventions for the treatment of cachexia. While there are many models of cachexia there is an underlying increase in systemic inflammation that is associated with increased muscle protein degradation and functional decrements (Argiles et al., 2003; Argiles et al., 2012; Fearon et al., 2013; Fortunati et al., 2007; Strassmann et al., 1992; Strassmann and Kambayashi, 1995). Therefore the purpose of this dissertation was to determine the role of inflammatory signaling through gp130/STAT3 signaling on the regulation of muscle mass and mitochondrial content during cancer cachexia. We hypothesized that inhibition of systemic STAT3 signaling would attenuate muscle mass loss through inhibition of protein degradation and maintenance of mitochondria content and that inhibition of skeletal muscle gp130 signaling would be sufficient for muscle mass maintenance during cachexia.

The data presented support our hypothesis that inhibition of skeletal muscle gp130 signaling can attenuate skeletal muscle protein degradation and improve muscle oxidative capacity; however, muscle gp130 was unable to release cachexia-suppression of muscle protein synthesis or the induction of mitochondrial fission. Additionally, inhibition of trans IL-6 signaling attenuated cachexia and suppressed muscle inflammatory signaling and activation of protein degradation pathways. Trans IL-6

inhibition maintained muscle mitochondrial content and alleviated the increase of mitochondrial fission, but could not attenuate the suppression of mitochondrial fusion or the suppression of muscle protein synthesis. Similarly systemic inhibition of STAT3/NFκB signaling inhibited muscle protein degradation and mitochondrial loss; however, STAT3/NFκB inhibition through PDTC administration increased muscle protein synthesis in cachectic mice. Inhibition of STAT3 alone was unable to rescue protein synthesis in LLC induced muscle atrophy suggesting that it is the systemic actions of PDTC that act to improve muscle protein synthesis. Finally cachectic muscle has an altered response to acute contraction. While contraction was able to induce signaling which should increase muscle mitochondrial biogenesis, increases in mitochondrial biogenesis were blunted in cachectic muscle. Inhibition of inflammatory signaling attenuated the cachexia-block of contraction-induced mitochondrial biogenesis.

Regulation of mitochondrial biogenesis by inflammatory signaling during cachexia.

The loss of mitochondrial content and alterations in mitochondrial dynamics have been reported during cancer cachexia (Fermoselle et al., 2013; Julienne et al., 2012; Tisdale, 2002; Tzika et al., 2013; White et al., 2011a). Although cachexia is not associated with decrements in the ability of individual mitochondria to produce ATP (Julienne et al., 2012), the overall production is limited with the net loss of mitochondria. This decrease in ATP will inhibit energy using pathways such as protein synthesis and may ultimately lead to activation of energy saving/energy producing pathways such as protein degradation. We have previously demonstrated that inhibition of systemic IL-6 signaling can attenuate the progression of skeletal muscle loss after the initiation of cachexia and is associated with improved muscle mitochondrial content and dynamics

(White et al., 2013b; White et al., 2012c). Our initial studies blocked both classical and trans IL-6 signaling. We now show that trans IL-6 signaling can attenuate muscle mitochondrial loss potentially through the suppression of mitochondrial fission; however, trans signaling was unable to rescue mitochondrial fusion. Muscle specific gp130 signaling inhibition also attenuated mitochondrial loss and was associated with increases in mitochondrial fusion, but did not block mitochondrial fission. These data suggest that mitochondrial fusion may be regulated through a gp130 independent pathway and may be more closely related to alterations in systemic inflammatory signaling than muscle specific inflammatory signaling. Alternatively the suppression of mitochondrial fusion may be related to the disuse as activity generally declines prior to muscle loss in the Min mouse (Baltgalvis et al., 2010). Disuse of skeletal muscle as well as aging are associated with decreased mitochondrial fusion and increased fission (Iqbal et al., 2013). Long term decreases in mitochondrial fusion are detrimental to skeletal muscle as fusion is required for mitochondrial DNA stability and function and loss of MFN1/2 is associated with mitochondrial myopathies and muscle loss (Chen et al., 2010). Further work is necessary to understand the role of altered mitochondrial fusion on the progression of cachexia.

Increases in muscle mitochondrial fission are associated with inflammatory signaling (White et al., 2012b). Additionally mitochondrial fission can regulate the induction of protein degradation (Romanello et al., 2010; Romanello and Sandri, 2010) and the suppression of mitochondrial fission may be one mechanism through which repression of inflammation is acting to decrease protein degradation. While we see inhibition of IL-6 trans signaling suppressed mitochondrial fission, the suppression of systemic STAT3 and muscle gp130 signaling were unable to prevent FIS induction.

Interestingly inhibition of inflammatory signaling by all three methods resulted in attenuation of muscle degradation signaling. One possible explanation for the induction of fission and fusion with PDTC treatment and muscle gp130 inhibition is that there may be higher mitochondrial turnover with these treatments. Interestingly inhibition of STAT3 and muscle gp130 were not sufficient to suppress mitochondrial fission, suggesting that the induction of mitochondrial fission may be independent of inflammatory signaling and may not be regulating muscle protein breakdown during cancer cachexia. Further work is necessary to determine the mechanism by which PDTC administration and muscle gp130 inhibition attenuate protein degradation independently of increases in mitochondrial fission.

Interestingly, mice over-expressing PGC-1α are not protected from the rapid induction of muscle mass loss induced by LLC cachexia (Wang et al., 2012). A limitation to this study was that circulating IL-6 was increased in animals with muscle over-expression of PGC-1α, but not in wild type tumor bearing mice, and the suppression of muscle mitochondrial content with cachexia was not demonstrated. Over-expression of muscle PGC-1α4 can prevent LLC induced muscle wasting demonstrating the need for further research examining the role of mitochondrial content in muscle wasting (Ruas et al., 2012). We have shown that exercise training prior to development of cachexia can increase mitochondrial capacity and attenuate cachexia induced fission and suppression of fusion (White et al., 2012b). Acute contraction after the initiation of cachexia was unable to increase markers of mitochondrial biogenesis; however, when basal inflammation was suppressed mitochondrial biogenesis was increased. Inflammatory signaling is a potent regulator of muscle mitochondrial content during cachexia, and

exercise has been shown to decrease inflammation. Although increased mitochondrial content is not sufficient for the prevention of cachexia, it is unknown if the mitochondria are functional. A buildup of dysfunctional mitochondria may be detrimental to the cachectic condition. Further work is necessary to determine if functional increases in muscle mitochondrial content can attenuate muscle loss associated with increased inflammation and if exercise training after the initiation of cachexia can attenuate further mitochondrial and muscle mass loss.

Regulation of muscle protein turnover by inflammatory signaling during cachexia

Much of the focus of cachexia research has been aimed towards the suppression of cachexia induced muscle protein degradation. Inhibition of potential cachectic mediators such as myostatin (Busquets et al., 2012; Murphy et al., 2011), FOXO (Reed et al.), C/EBPβ (Zhang et al., 2011), mitochondrial fission (Romanello et al., 2010; Romanello and Sandri, 2010), and STAT3 (Bonetto et al., 2012) have been shown to attenuate muscle mass loss through suppression of protein catabolism pathways. We further this research demonstrating that inhibition of systemic STAT3/NFκB signaling, IL-6 trans signaling, and of muscle gp130 signaling can also attenuate the cachexia-induction of muscle protein degradation pathways. Skeletal muscle gp130 may be inhibiting degradation through a combination of STAT3 inhibition and inhibition of P38 which have both been implicated in muscle protein breakdown in models of cachexia (Bonetto et al., 2012; Zhang and Li, 2012). Inhibition of muscle gp130 was sufficient to inhibit muscle mass loss in the LLC model of cachexia, but not the Min model. The induction of atrogin was suppressed in both models, and the suppression of protein synthesis was unaltered by gp130 inhibition. Because the LLC is a rapid model of

cachexia, it is possible that the long term suppression of muscle protein synthesis in the Min model is responsible for the overall muscle mass loss, whereas in the LLC there was only a short term suppression of protein synthesis. Further work needs to be done to determine if the inhibition of muscle gp130 delays the onset of cachexia in the Min mouse. Many of the models currently used for cachexia research develop cachexia within a matter of days-weeks suggesting that the effectiveness of many of the treatments studied may only be beneficial for delaying the onset of cachexia in a slower model. Further research needs to be done to examine the effectiveness of long term inhibition on muscle protein degradation without improvements in synthesis for the prevention of muscle loss with cachexia.

Induction of muscle protein degradation is one mechanism inducing the loss of muscle mass with cachexia that has received much attention; however, cachexia is also associated with a suppression of muscle protein synthesis which could independently decrease muscle mass (Atherton et al., 2005; Dworzak et al., 1998; Goodman et al., 2011b; Risson et al., 2009; White et al., 2011b). To date no treatments aside from exercise have been shown to release the cachexia-suppression of muscle protein synthesis and most studies have focused solely on protein breakdown. We have previously demonstrated that exercise training prior to cachexia development can prevent IL-6 suppression of IGF-1 and mTOR signaling (White et al., 2013b). Our lab has also shown that high frequency stimulation, mimicking resistance exercise, in muscle after the initiation of cachexia can increase muscle protein synthesis (Sato, 2012).

One potential mechanism in which cachexia may be suppressing protein synthesis is through the up regulation of AMPK. Inflammation has been shown to

increase AMPK activation in skeletal muscle. Interestingly we found inhibition of AMPK activation in the Min mouse with skm-gp130 deletion, but did not see this in the LLC model of cachexia. This may be due to the IL-6 dependent nature of the cachexia in the Min mouse, whereas the LLC model has been shown to be dependent on either IL-6 or TNFα which act through different signaling mechanism. Suppression of AMPK through administration of IL-6r Ab, inhibition of gp130 signaling, or inhibition of IL-6 trans signaling was not associated with improvements in muscle protein synthesis. REDD1 can suppress protein synthesis regulator, mTORC1, through the dissociation of TSC2/14-3-3 complex (Ho et al., 2005) and REDD1 can suppress mTOR independently of AMPK (Frost and Lang). The inhibition of skeletal muscle gp130 signaling did not alter cachexia-induced REDD1 expression.

Another potential suppressor of protein synthesis could be through the up regulation of glucocorticoids. Glucocorticoids have been shown to be increased during cachexia and are implicated in muscle atrophy (Braun et al., 2013; Rivadeneira et al., 1999; Schakman et al., 2013). Additionally glucocorticoids have been shown to suppress protein synthesis (Kim and Kim, 1975). Global inhibition of glucocorticoids does not prevent wasting; however, inhibition of muscle glucocorticoid receptor can attenuate muscle mass loss (Braun et al., 2013; Rivadeneira et al., 1999). Not only did the muscle deletion of the glucocorticoid receptor inhibit activation of protein degradation pathways, it also prevented cachexia and LPS induction of REDD1. The role of glucocorticoids in the suppression of muscle protein synthesis during cachexia requires further investigation. Combination therapies in which glucocorticoid and inflammation levels are suppressed may be crucial for long term protection from cancer-induced muscle wasting.

Interestingly we found that PDTC administration increased muscle protein synthesis in wild type and cachectic mice. PDTC has been shown to decrease tumor development as well at suppress atrogin expression in skeletal muscle of tumor bearing mice (Nai et al., 2007; Puppa et al., 2013b). Additionally PDTC has been implicated in the regulation of protein synthesis pathways (Song et al., 2011). Because of the inhibition of degradation and the improvements in muscle protein synthesis, PDTC has promise as a therapeutic intervention for the treatment of cachexia. Combination therapies that include exercise may be the most beneficial for improved patient survival and quality of life. Further work is necessary to identify potential pathways that PDTC may be acting through to relieve the inhibition of muscle protein synthesis with cachexia.

Summary

In summary, we demonstrate that inhibition of gp130/STAT3 signaling may be able to delay the onset of cachexia through suppression of muscle protein degradation and improved muscle oxidative capacity, but were ineffective at improving muscle protein synthesis. Additionally, the blunted exercise response seen in cachectic muscle was attenuated with inhibition of inflammatory signaling. The mechanism through which PDTC was able to abrogate the contraction response requires further investigation. Further work is necessary to determine if these improvements are sufficient for long term survival and quality of life in the cancer patient. Decreases in muscle atrogin expression were associated with inhibition of STAT3 signaling. Further work is needed to identify the regulation of alternative degradation pathways by gp130/STAT signaling during cachexia and the long term implications of gp130/STAT3 inhibition on skeletal muscle health.

Table 7.1. Summary of gp130/STAT3 regulation of muscle mass during cachexia.

	Cachexia	skm-gp130	sgp130Fc	PDTC
STAT3	↑	↓	↓	↓
AMPK	↑	↓/↔	↓	↓
Protein degradation	↑	↓	↓	↓
Protein synthesis	↓	↔	↔	↑
Mitochondrial content	↓	↑	↑	↑
Mito fission	↑	↔	↓	↔
Mito fusion	↓	↑	↔	↑

Future Directions

The data collected for this dissertation has revealed several novel aspects in the regulation of skeletal muscle mass by gp130/STAT3 during cancer cachexia; however, there are still gaps in our understanding of the suppression of muscle protein synthesis and the differential roles of systemic and muscle specific gp130 signaling on the progression of cachexia. We demonstrated that improvements in mitochondrial content as well as suppression of muscle degradation pathways and inflammation through gp130 is not sufficient to prevent long term muscle wasting; however, it appears to delay muscle loss in short term models. Further work is necessary to assess the mechanism through which muscle wasting can still occur when muscle inflammatory signaling is inhibited. Additionally, further work is required to understand if inhibitions of muscle inflammatory signaling can enhance the anabolic response of cachectic muscle to contraction. We found that PDTC administration was able to improve muscle protein synthesis in cachectic mice; however the mechanism through which PDTC is acting is not well understood. Understanding how PDTC is improving muscle protein synthesis may lead to the development of pharmacological interventions for the treatment of cachexia.

REFERENCES

Acharyya, S. and Guttridge, D. C. (2007). Cancer Cachexia Signaling Pathways Continue to Emerge Yet Much Still Points to the Proteasome. *Clinical Cancer Research* **13**, 1356-1361.

Agustsson, T., Ryden, M., Hoffstedt, J., van Harmelen, V., Dicker, A., Laurencikiene, J., Isaksson, B., Permert, J. and Arner, P. (2007). Mechanism of increased lipolysis in cancer cachexia. *Cancer Res* **67**, 5531-7.

Akimoto, T., Pohnert, S. C., Li, P., Zhang, M., Gumbs, C., Rosenberg, P. B., Williams, R. S. and Yan, Z. (2005a). Exercise stimulates Pgc-1alpha transcription in skeletal muscle through activation of the p38 MAPK pathway. *J Biol Chem* **280**, 19587-93.

Akimoto, T., Pohnert, S. C., Li, P., Zhang, M., Gumbs, C., Rosenberg, P. B., Williams, R. S. and Yan, Z. (2005b). Exercise stimulates Pgc-1α transcription in skeletal muscle through activation of the p38 MAPK pathway. *Journal of Biological Chemistry* **280**, 19587-19593.

al-Majid, S. and McCarthy, D. O. (2001). Cancer-induced fatigue and skeletal muscle wasting: the role of exercise. *Biol Res Nurs* **2**, 186-97.

Ando, K., Takahashi, F., Motojima, S., Nakashima, K., Kaneko, N., Hoshi, K. and Takahashi, K. (2013). Possible role for tocilizumab, an anti-interleukin-6 receptor antibody, in treating cancer cachexia. *J Clin Oncol* **31**, e69-72.

Argiles, J. M., Busquets, S. and Lopez-Soriano, F. J. (2003). Cytokines in the pathogenesis of cancer cachexia. *Curr Opin Clin Nutr Metab Care* **6**, 401-6.

Argiles, J. M., Lopez-Soriano, F. J. and Busquets, S. (2012). Counteracting inflammation: a promising therapy in cachexia. *Crit Rev Oncog* **17**, 253-62.

Asp, M. L., Tian, M., Wendel, A. A. and Belury, M. A. (2010). Evidence for the contribution of insulin resistance to the development of cachexia in tumor-bearing mice. *Int J Cancer* **126**, 756-63.

Atherton, P. J., Babraj, J., Smith, K., Singh, J., Rennie, M. J. and Wackerhage, H. (2005). Selective activation of AMPK-PGC-1alpha or PKB-TSC2-mTOR signaling can explain specific adaptive responses to endurance or resistance training-like electrical muscle stimulation. *FASEB J* **19**, 786-8.

Atreya, R., Mudter, J., Finotto, S., Mullberg, J., Jostock, T., Wirtz, S., Schutz, M., Bartsch, B., Holtmann, M., Becker, C. et al. (2000). Blockade of interleukin 6 trans signaling suppresses T-cell resistance against apoptosis in chronic intestinal inflammation: evidence in crohn disease and experimental colitis in vivo. *Nature Medicine* **6**, 583-8.

Aulino, P., Berardi, E., Cardillo, V. M., Rizzuto, E., Perniconi, B., Ramina, C., Padula, F., Spugnini, E. P., Baldi, A., Faiola, F. et al. (2010). Molecular, cellular and

physiological characterization of the cancer cachexia-inducing C26 colon carcinoma in mouse. *BMC Cancer* **10**, 363.

Baar, K., Wende, A. R., Jones, T. E., Marison, M., Nolte, L. A., Chen, M., Kelly, D. P. and Holloszy, J. O. (2002). Adaptations of skeletal muscle to exercise: rapid increase in the transcriptional coactivator PGC-1. *FASEB J* **16**, 1879-86.

Baeza-Raja, B. and Muñoz-Cánoves, P. (2004). p38 MAPK-induced nuclear factor-κB activity is required for skeletal muscle differentiation: role of interleukin-6. *Molecular biology of the cell* **15**, 2013-2026.

Bakkar, N., Wang, J., Ladner, K. J., Wang, H., Dahlman, J. M., Carathers, M., Acharyya, S., Rudnicki, M. A., Hollenbach, A. D. and Guttridge, D. C. (2008). IKK/NF-kappaB regulates skeletal myogenesis via a signaling switch to inhibit differentiation and promote mitochondrial biogenesis. *J Cell Biol* **180**, 787-802.

Baltgalvis, K. A., Berger, F. G., Pena, M. M., Davis, J. M. and Carson, J. A. (2008a). Effect of exercise on biological pathways in ApcMin/+ mouse intestinal polyps. *J Appl Physiol* **104**, 1137-43.

Baltgalvis, K. A., Berger, F. G., Pena, M. M., Davis, J. M. and Carson, J. A. (2009a). The interaction of a high-fat diet and regular moderate intensity exercise on intestinal polyp development in Apc Min/+ mice. *Cancer Prev Res (Phila)* **2**, 641-9.

Baltgalvis, K. A., Berger, F. G., Pena, M. M., Davis, J. M., Muga, S. J. and Carson, J. A. (2008b). Interleukin-6 and cachexia in ApcMin/+ mice. *Am J Physiol Regul Integr Comp Physiol* **294**, R393-401.

Baltgalvis, K. A., Berger, F. G., Pena, M. M., Davis, J. M., White, J. P. and Carson, J. A. (2009b). Muscle wasting and interleukin-6-induced atrogin-I expression in the cachectic Apc (Min/+) mouse. *Pflugers Arch* **457**, 989-1001.

Baltgalvis, K. A., Berger, F. G., Pena, M. M., Mark Davis, J., White, J. P. and Carson, J. A. (2010). Activity level, apoptosis, and development of cachexia in Apc(Min/+) mice. *J Appl Physiol* **109**, 1155-61.

Barkhausen, T., Tschernig, T., Rosenstiel, P., van Griensven, M., Vonberg, R. P., Dorsch, M., Mueller-Heine, A., Chalaris, A., Scheller, J., Rose-John, S. et al. Selective blockade of interleukin-6 trans-signaling improves survival in a murine polymicrobial sepsis model. *Crit Care Med* **39**, 1407-13.

Barton, B. E. and Murphy, T. F. (2001). Cancer cachexia is mediated in part by the induction of IL-6-like cytokines from the spleen. *Cytokine* **16**, 251-7.

Batista, M. L., Jr., Peres, S. B., McDonald, M. E., Alcantara, P. S., Olivan, M., Otoch, J. P., Farmer, S. R. and Seelaender, M. (2012). Adipose tissue inflammation and cancer cachexia: Possible role of nuclear transcription factors. *Cytokine* **57**, 9-16.

Beck, S. A., Mulligan, H. D. and Tisdale, M. J. (1990). Lipolytic factors associated with murine and human cancer cachexia. *J Natl Cancer Inst* **82**, 1922-6.

Benard, G. and Karbowski, M. (2009). Mitochondrial fusion and division: Regulation and role in cell viability. *Semin Cell Dev Biol* **20**, 365-74.

Benrick, A., Wallenius, V. and Wernstedt Asterholm, I. (2012). Interleukin-6 mediates exercise-induced increase in insulin sensitivity in mice. *Exp Physiol*.

Bergeron, R., Ren, J. M., Cadman, K. S., Moore, I. K., Perret, P., Pypaert, M., Young, L. H., Semenkovich, C. F. and Shulman, G. I. (2001). Chronic activation of AMP kinase results in NRF-1 activation and mitochondrial biogenesis. *Am J Physiol Endocrinol Metab* **281**, E1340-6.

Bing, C., Brown, M., King, P., Collins, P., Tisdale, M. J. and Williams, G. (2000). Increased gene expression of brown fat uncoupling protein (UCP)1 and skeletal muscle UCP2 and UCP3 in MAC16-induced cancer cachexia. *Cancer Res* **60**, 2405-10.

Bing, C., Taylor, S., Tisdale, M. J. and Williams, G. (2001). Cachexia in MAC16 adenocarcinoma: suppression of hunger despite normal regulation of leptin, insulin and hypothalamic neuropeptide Y. *J Neurochem* **79**, 1004-12.

Bo, H., Zhang, Y. and Ji, L. L. Redefining the role of mitochondria in exercise: a dynamic remodeling. *Ann N Y Acad Sci* **1201**, 121-8.

Bolster, D. R., Crozier, S. J., Kimball, S. R. and Jefferson, L. S. (2002). AMP-activated protein kinase suppresses protein synthesis in rat skeletal muscle through down-regulated mammalian target of rapamycin (mTOR) signaling. *J Biol Chem* **277**, 23977-80.

Bonetto, A., Aydogdu, T., Jin, X., Zhang, Z., Zhan, R., Puzis, L., Koniaris, L. G. and Zimmers, T. A. (2012). JAK/STAT3 pathway inhibition blocks skeletal muscle wasting downstream of IL-6 and in experimental cancer cachexia. *Am J Physiol Endocrinol Metab*.

Bonetto, A., Aydogdu, T., Kunzevitzky, N., Guttridge, D. C., Khuri, S., Koniaris, L. G. and Zimmers, T. A. (2011). STAT3 activation in skeletal muscle links muscle wasting and the acute phase response in cancer cachexia. *PLoS One* **6**, e22538.

Bothe, G. W., Haspel, J. A., Smith, C. L., Wiener, H. H. and Burden, S. J. (2000). Selective expression of Cre recombinase in skeletal muscle fibers. *Genesis* **26**, 165-6.

Bradford, M. M. (1976). A rapid and sensitive method for the quantitation of microgram quantities of protein utilizing the principle of protein-dye binding. *Anal Biochem* **72**, 248-54.

Bradley, R. L., Jeon, J. Y., Liu, F. F. and Maratos-Flier, E. (2008). Voluntary exercise improves insulin sensitivity and adipose tissue inflammation in diet-induced obese mice. *Am J Physiol Endocrinol Metab* **295**, E586-94.

Braun, T. P., Grossberg, A. J., Krasnow, S. M., Levasseur, P. R., Szumowski, M., Zhu, X. X., Maxson, J. E., Knoll, J. G., Barnes, A. P. and Marks, D. L. (2013). Cancer- and endotoxin-induced cachexia require intact glucocorticoid signaling in skeletal muscle. *FASEB J* **27**, 3572-82.

Briso, E. M., Dienz, O. and Rincon, M. (2008). Cutting edge: soluble IL-6R is produced by IL-6R ectodomain shedding in activated CD4 T cells. *J Immunol* **180**, 7102-6.

Brozinick, J. T., Jr., Etgen, G. J., Jr., Yaspelkis, B. B., 3rd and Ivy, J. L. (1992). Contraction-activated glucose uptake is normal in insulin-resistant muscle of the obese Zucker rat. *J Appl Physiol* **73**, 382-7.

Bruera, E. (1997). ABC of palliative care. Anorexia, cachexia, and nutrition. *BMJ* **315**, 1219-22.

Busquets, S., Toledo, M., Orpi, M., Massa, D., Porta, M., Capdevila, E., Padilla, N., Frailis, V., Lopez-Soriano, F. J., Han, H. Q. et al. (2012). Myostatin blockage using actRIIB antagonism in mice bearing the Lewis lung carcinoma results in the improvement of muscle wasting and physical performance. *J Cachexia Sarcopenia Muscle* **3**, 37-43.

Cai, D., Frantz, J. D., Tawa Jr, N. E., Melendez, P. A., Oh, B.-C., Lidov, H. G., Hasselgren, P.-O., Frontera, W. R., Lee, J. and Glass, D. J. (2004a). IKKβ/NF-κB activation causes severe muscle wasting in mice. *Cell* **119**, 285-298.

Cai, D., Frantz, J. D., Tawa, N. E., Jr., Melendez, P. A., Oh, B. C., Lidov, H. G., Hasselgren, P. O., Frontera, W. R., Lee, J., Glass, D. J. et al. (2004b). IKKbeta/NF-kappaB activation causes severe muscle wasting in mice. *Cell* **119**, 285-98.

Carbo, N., Busquets, S., van Royen, M., Alvarez, B., Lopez-Soriano, F. J. and Argiles, J. M. (2002). TNF-alpha is involved in activating DNA fragmentation in skeletal muscle. *Br J Cancer* **86**, 1012-6.

Carson, J. A. and Baltgalvis, K. A. (2010). Interleukin 6 as a Key Regulator of Muscle Mass during Cachexia. *Exercise and Sport Sciences Reviews* **38**, 168-176.

Cartoni, R., Leger, B., Hock, M. B., Praz, M., Crettenand, A., Pich, S., Ziltener, J. L., Luthi, F., Deriaz, O., Zorzano, A. et al. (2005). Mitofusins 1/2 and ERRalpha expression are increased in human skeletal muscle after physical exercise. *J Physiol* **567**, 349-58.

Catalano, M. G., Fortunati, N., Arena, K., Costelli, P., Aragno, M., Danni, O. and Boccuzzi, G. (2003). Selective up-regulation of tumor necrosis factor receptor I in tumor-bearing rats with cancer-related cachexia. *Int J Oncol* **23**, 429-36.

Chabicovsky, M., Prieschl-Grassauer, E., Seipelt, J., Muster, T., Szolar, O. H., Hebar, A. and Doblhoff-Dier, O. (2010). Pre-clinical safety evaluation of pyrrolidine dithiocarbamate. *Basic Clin Pharmacol Toxicol* **107**, 758-67.

Chen, H., Vermulst, M., Wang, Y. E., Chomyn, A., Prolla, T. A., McCaffery, J. M. and Chan, D. C. (2010). Mitochondrial fusion is required for mtDNA stability in skeletal muscle and tolerance of mtDNA mutations. *Cell* **141**, 280-9.

Chomentowski, P., Coen, P. M., Radikova, Z., Goodpaster, B. H. and Toledo, F. G. Skeletal muscle mitochondria in insulin resistance: differences in intermyofibrillar versus subsarcolemmal subpopulations and relationship to metabolic flexibility. *J Clin Endocrinol Metab* **96**, 494-503.

Costelli, P., Carbo, N., Tessitore, L., Bagby, G. J., Lopez-Soriano, F. J., Argiles, J. M. and Baccino, F. M. (1993). Tumor necrosis factor-alpha mediates changes in tissue protein turnover in a rat cancer cachexia model. *J Clin Invest* **92**, 2783-9.

Costelli, P., Muscaritoli, M., Bossola, M., Penna, F., Reffo, P., Bonetto, A., Busquets, S., Bonelli, G., Lopez-Soriano, F. J., Doglietto, G. B. et al. (2006). IGF-1 is downregulated in experimental cancer cachexia. *Am J Physiol Regul Integr Comp Physiol* **291**, R674-83.

Cunningham, J. T., Rodgers, J. T., Arlow, D. H., Vazquez, F., Mootha, V. K. and Puigserver, P. (2007). mTOR controls mitochondrial oxidative function through a YY1-PGC-1alpha transcriptional complex. *Nature* **450**, 736-40.

Cuzzocrea, S., Chatterjee, P. K., Mazzon, E., Dugo, L., Serraino, I., Britti, D., Mazzullo, G., Caputi, A. P. and Thiemermann, C. (2002). Pyrrolidine dithiocarbamate attenuates the development of acute and chronic inflammation. *Br J Pharmacol* **135**, 496-510.

D'Souza, D., Lai, R. Y., Shuen, M. and Hood, D. A. (2012). mRNA stability as a function of striated muscle oxidative capacity. *Am J Physiol Regul Integr Comp Physiol* **303**, R408-17.

Das, S. K., Eder, S., Schauer, S., Diwoky, C., Temmel, H., Guertl, B., Gorkiewicz, G., Tamilarasan, K. P., Kumari, P., Trauner, M. et al. (2011). Adipose triglyceride lipase contributes to cancer-associated cachexia. *Science* **333**, 233-8.

De Larichaudy, J., Zufferli, A., Serra, F., Isidori, A. M., Naro, F., Dessalle, K., Desgeorges, M., Piraud, M., Cheillan, D., Vidal, H. et al. (2012). TNF-alpha- and tumor-induced skeletal muscle atrophy involves sphingolipid metabolism. *Skelet Muscle* **2**, 2.

Deans, C. and Wigmore, S. J. (2005). Systemic inflammation, cachexia and prognosis in patients with cancer. *Curr Opin Clin Nutr Metab Care* **8**, 265-9.

Dehoux, M., Gobier, C., Lause, P., Bertrand, L., Ketelslegers, J. M. and Thissen, J. P. (2007). IGF-I does not prevent myotube atrophy caused by proinflammatory cytokines despite activation of Akt/Foxo and GSK-3beta pathways and inhibition of atrogin-1 mRNA. *Am J Physiol Endocrinol Metab* **292**, E145-50.

Dianliang, Z. (2009). Probing cancer cachexia-anorexia: recent results with knockout, transgene and polymorphisms. *Curr Opin Clin Nutr Metab Care* **12**, 227-31.

Dickinson, J. M., Fry, C. S., Drummond, M. J., Gundermann, D. M., Walker, D. K., Glynn, E. L., Timmerman, K. L., Dhanani, S., Volpi, E. and Rasmussen, B. B. (2011). Mammalian target of rapamycin complex 1 activation is required for the stimulation of human skeletal muscle protein synthesis by essential amino acids. *J Nutr* **141**, 856-62.

Ding, H., Jiang, N., Liu, H., Liu, X., Liu, D., Zhao, F., Wen, L., Liu, S., Ji, L. L. and Zhang, Y. Response of mitochondrial fusion and fission protein gene expression to exercise in rat skeletal muscle. *Biochim Biophys Acta* **1800**, 250-6.

Dumas, J. F., Goupille, C., Pinault, M., Fandeur, L., Bougnoux, P., Servais, S. and Couet, C. (2010). n-3 PUFA-enriched diet delays the occurrence of cancer cachexia in rat with peritoneal carcinosis. *Nutr Cancer* **62**, 343-50.

Duncan, G. E., Perri, M. G., Theriaque, D. W., Hutson, A. D., Eckel, R. H. and Stacpoole, P. W. (2003). Exercise training, without weight loss, increases insulin sensitivity and postheparin plasma lipase activity in previously sedentary adults. *Diabetes Care* **26**, 557-62.

Dworzak, F., Ferrari, P., Gavazzi, C., Maiorana, C. and Bozzetti, F. (1998). Effects of cachexia due to cancer on whole body and skeletal muscle protein turnover. *Cancer* **82**, 42-8.

Ernst, M. and Jenkins, B. J. (2004). Acquiring signalling specificity from the cytokine receptor gp130. *Trends Genet* **20**, 23-32.

Esper, D. H. and Harb, W. A. (2005). The cancer cachexia syndrome: a review of metabolic and clinical manifestations. *Nutr Clin Pract* **20**, 369-76.

Evans, W. J., Morley, J. E., Argiles, J., Bales, C., Baracos, V., Guttridge, D., Jatoi, A., Kalantar-Zadeh, K., Lochs, H., Mantovani, G. et al. (2008). Cachexia: a new definition. *Clin Nutr* **27**, 793-9.

Faldt, J., Wernstedt, I., Fitzgerald, S. M., Wallenius, K., Bergstrom, G. and Jansson, J. O. (2004). Reduced exercise endurance in interleukin-6 deficient mice. *Endocrinology* **145**, 2680-2686.

Fearon, K., Arends, J. and Baracos, V. (2013). Understanding the mechanisms and treatment options in cancer cachexia. *Nat Rev Clin Oncol* **10**, 90-9.

Fearon, K., Strasser, F., Anker, S. D., Bosaeus, I., Bruera, E., Fainsinger, R. L., Jatoi, A., Loprinzi, C., MacDonald, N., Mantovani, G. et al. (2011). Definition and classification of cancer cachexia: an international consensus. *Lancet Oncol* **12**, 489-95.

Febbraio, M. A. (2007). Gp130 receptor ligands as potential therapeutic targets for obesity. *Journal of Clinical Investigation* **117**, 841-849.

Febbraio, M. A. and Pedersen, B. K. (2005). Contraction-induced myokine production and release: is skeletal muscle an endocrine organ? *Exerc Sport Sci Rev* **33**, 114-9.

Fentem, P. H. (1994). ABC of sports medicine. Benefits of exercise in health and disease. *BMJ* **308**, 1291-5.

Fermoselle, C., Garcia-Arumi, E., Puig-Vilanova, E., Andreu, A. L., Urtreger, A. J., de Kier Joffe, E. D., Tejedor, A., Puente-Maestu, L. and Barreiro, E. (2013). Mitochondrial dysfunction and therapeutic approaches in respiratory and limb muscles of cancer cachectic mice. *Exp Physiol* **98**, 1349-65.

Fernandez-Marcos, P. J. and Auwerx, J. (2011). Regulation of PGC-1alpha, a nodal regulator of mitochondrial biogenesis. *Am J Clin Nutr* **93**, 884S-90.

Figueras, M., Busquets, S., Carbo, N., Almendro, V., Argiles, J. M. and Lopez-Soriano, F. J. (2005). Cancer cachexia results in an increase in TNF-alpha receptor gene expression in both skeletal muscle and adipose tissue. *Int J Oncol* **27**, 855-60.

Fortunati, N., Manti, R., Birocco, N., Pugliese, M., Brignardello, E., Ciuffreda, L., Catalano, M. G., Aragno, M. and Boccuzzi, G. (2007). Pro-inflammatory cytokines and oxidative stress/antioxidant parameters characterize the bio-humoral profile of early cachexia in lung cancer patients. *Oncol Rep* **18**, 1521-7.

Fox, K. M., Brooks, J. M., Gandra, S. R., Markus, R. and Chiou, C. F. (2009). Estimation of Cachexia among Cancer Patients Based on Four Definitions. *J Oncol* **2009**, 693458.

Frost, R. A., Huber, D., Pruznak, A. and Lang, C. H. (2009). Regulation of REDD1 by insulin-like growth factor-I in skeletal muscle and myotubes. *J Cell Biochem* **108**, 1192-202.

Frost, R. A. and Lang, C. H. mTor signaling in skeletal muscle during sepsis and inflammation: where does it all go wrong? *Physiology* **26**, 83-96.

Frost, R. A., Lang, C. H. and Gelato, M. C. (1997). Transient exposure of human myoblasts to tumor necrosis factor-alpha inhibits serum and insulin-like growth factor-I stimulated protein synthesis. *Endocrinology* **138**, 4153-9.

Fujita, J., Tsujinaka, T., Ebisui, C., Yano, M., Shiozaki, H., Katsume, A., Ohsugi, Y. and Monden, M. (1996). Role of interleukin-6 in skeletal muscle protein breakdown and cathepsin activity in vivo. *Eur Surg Res* **28**, 361-6.

Gallagher, I. J., Stephens, N. A., MacDonald, A. J., Skipworth, R. J., Husi, H., Greig, C. A., Ross, J. A., Timmons, J. A. and Fearon, K. C. (2012). Suppression of skeletal muscle turnover in cancer cachexia: evidence from the transcriptome in sequential human muscle biopsies. *Clin Cancer Res* **18**, 2817-27.

Garnier, A., Fortin, D., Zoll, J., N'Guessan, B., Mettauer, B., Lampert, E., Veksler, V. and Ventura-Clapier, R. (2005). Coordinated changes in mitochondrial function and biogenesis in healthy and diseased human skeletal muscle. *FASEB J* **19**, 43-52.

Gerovasili, V., Stefanidis, K., Vitzilaios, K., Karatzanos, E., Politis, P., Koroneos, A., Chatzimichail, A., Routsi, C., Roussos, C. and Nanas, S. (2009). Electrical muscle stimulation preserves the muscle mass of critically ill patients: a randomized study. *Crit Care* **13**, R161.

Glass, D. J. (2005). Skeletal muscle hypertrophy and atrophy signaling pathways. *Int J Biochem Cell Biol* **37**, 1974-84.

Goodman, C. A., Frey, J. W., Mabrey, D. M., Jacobs, B. L., Lincoln, H. C., You, J. S. and Hornberger, T. A. The role of skeletal muscle mTOR in the regulation of mechanical loadâ€ • induced growth. *The Journal of physiology* **589**, 5485-5501.

Goodman, C. A. and Hornberger, T. A. Measuring protein synthesis with SUnSET: a valid alternative to traditional techniques? *Exerc Sport Sci Rev*.

Goodman, C. A., Kotecki, J. A., Jacobs, B. L. and Hornberger, T. A. (2012). Muscle fiber type-dependent differences in the regulation of protein synthesis. *PLoS One* **7**, e37890.

Goodman, C. A., Mabrey, D. M., Frey, J. W., Miu, M. H., Schmidt, E. K., Pierre, P. and Hornberger, T. A. (2011a). Novel insights into the regulation of skeletal muscle protein synthesis as revealed by a new nonradioactive in vivo technique. *FASEB J* **25**, 1028-39.

Goodman, C. A., Mayhew, D. L. and Hornberger, T. A. (2011b). Recent progress toward understanding the molecular mechanisms that regulate skeletal muscle mass. *Cell Signal* **23**, 1896-906.

Goodyear, L. J., Giorgino, F., Sherman, L. A., Carey, J., Smith, R. J. and Dohm, G. L. (1995). Insulin receptor phosphorylation, insulin receptor substrate-1 phosphorylation, and phosphatidylinositol 3-kinase activity are decreased in intact skeletal muscle strips from obese subjects. *J Clin Invest* **95**, 2195-204.

Gordon, J. W., Rungi, A. A., Inagaki, H. and Hood, D. A. (2001). Effects of contractile activity on mitochondrial transcription factor A expression in skeletal muscle. *J Appl Physiol* **90**, 389-96.

Grossberg, A. J., Scarlett, J. M. and Marks, D. L. (2010). Hypothalamic mechanisms in cachexia. *Physiol Behav* **100**, 478-89.

Grosvenor, M., Bulcavage, L. and Chlebowski, R. T. (1989). Symptoms potentially influencing weight loss in a cancer population. Correlations with primary site, nutritional status, and chemotherapy administration. *Cancer* **63**, 330-4.

Guttridge, D. C., Mayo, M. W., Madrid, L. V., Wang, C. Y. and Baldwin, A. S., Jr. (2000). NF-kappaB-induced loss of MyoD messenger RNA: possible role in muscle decay and cachexia. *Science* **289**, 2363-6.

Haan, C., Heinrich, P. C. and Behrmann, I. (2002). Structural requirements of the interleukin-6 signal transducer gp130 for its interaction with Janus kinase 1: the receptor is crucial for kinase activation. *Biochem J* **361**, 105-11.

Haddad, F., Zaldivar, F., Cooper, D. M. and Adams, G. R. (2005). IL-6-induced skeletal muscle atrophy. *J Appl Physiol* **98**, 911-7.

Handberg, A., Vaag, A., Damsbo, P., Beck-Nielsen, H. and Vinten, J. (1990). Expression of insulin regulatable glucose transporters in skeletal muscle from type 2 (non-insulin-dependent) diabetic patients. *Diabetologia* **33**, 625-7.

Hariri, G., Yan, H., Wang, H., Han, Z. and Hallahan, D. E. (2010). Radiation-guided drug delivery to mouse models of lung cancer. *Clin Cancer Res* **16**, 4968-77.

Hawley, J. A. (2004). Exercise as a therapeutic intervention for the prevention and treatment of insulin resistance. *Diabetes Metab Res Rev* **20**, 383-93.

Hawley, J. A. and Lessard, S. J. (2008). Exercise training-induced improvements in insulin action. *Acta Physiol (Oxf)* **192**, 127-35.

Hayashi, A. A. and Proud, C. G. (2007). The rapid activation of protein synthesis by growth hormone requires signaling through mTOR. *Am J Physiol Endocrinol Metab* **292**, E1647-55.

Hayashi, T., Hirshman, M. F., Kurth, E. J., Winder, W. W. and Goodyear, L. J. (1998). Evidence for 5' AMP-activated protein kinase mediation of the effect of muscle contraction on glucose transport. *Diabetes* **47**, 1369-73.

He, H. J., Zhu, T. N., Xie, Y., Fan, J., Kole, S., Saxena, S. and Bernier, M. (2006). Pyrrolidine dithiocarbamate inhibits interleukin-6 signaling through impaired STAT3 activation and association with transcriptional coactivators in hepatocytes. *J Biol Chem* **281**, 31369-79.

Heinrich, P. C., Behrmann, I., Haan, S., Hermanns, H. M., Muller-Newen, G. and Schaper, F. (2003). Principles of interleukin (IL)-6-type cytokine signalling and its regulation. *Biochem J* **374**, 1-20.

Heinrich, P. C., Behrmann, I., Muller-Newen, G., Schaper, F. and Graeve, L. (1998). Interleukin-6-type cytokine signalling through the gp130/Jak/STAT pathway. *Biochem J* **334 (Pt 2)**, 297-314.

Hirata, H., Tetsumoto, S., Kijima, T., Kida, H., Kumagai, T., Takahashi, R., Otani, Y., Inoue, K., Kuhara, H., Shimada, K. et al. (2013). Favorable Responses to Tocilizumab in Two Patients With Cancer-Related Cachexia. *J Pain Symptom Manage*.

Ho, R. C., Hirshman, M. F., Li, Y., Cai, D., Farmer, J. R., Aschenbach, W. G., Witczak, C. A., Shoelson, S. E. and Goodyear, L. J. (2005). Regulation of IκB kinase and NF-κB in contracting adult rat skeletal muscle. *American Journal of Physiology-Cell Physiology* **289**, C794-C801.

Holloszy, J. O. (1967). Biochemical adaptations in muscle. Effects of exercise on mitochondrial oxygen uptake and respiratory enzyme activity in skeletal muscle. *J Biol Chem* **242**, 2278-82.

Holloszy, J. O. and Coyle, E. F. (1984). Adaptations of skeletal muscle to endurance exercise and their metabolic consequences. *J Appl Physiol* **56**, 831-8.

Hood, D. A., Irrcher, I., Ljubicic, V. and Joseph, A. M. (2006). Coordination of metabolic plasticity in skeletal muscle. *J Exp Biol* **209**, 2265-75.

Hoppeler, H. (1986). Exercise-induced ultrastructural changes in skeletal muscle. *Int J Sports Med* **7**, 187-204.

Houmard, J. A., Shaw, C. D., Hickey, M. S. and Tanner, C. J. (1999). Effect of short-term exercise training on insulin-stimulated PI 3-kinase activity in human skeletal muscle. *Am J Physiol* **277**, E1055-60.

Huang, J., Kaminski, P. M., Edwards, J. G., Yeh, A., Wolin, M. S., Frishman, W. H., Gewitz, M. H. and Mathew, R. (2008). Pyrrolidine dithiocarbamate restores endothelial cell membrane integrity and attenuates monocrotaline-induced pulmonary artery hypertension. *Am J Physiol Lung Cell Mol Physiol* **294**, L1250-9.

Iqbal, S., Ostojic, O., Singh, K., Joseph, A. M. and Hood, D. A. (2013). Expression of mitochondrial fission and fusion regulatory proteins in skeletal muscle during chronic use and disuse. *Muscle Nerve* **48**, 963-70.

Iwase, S., Murakami, T., Saito, Y. and Nakagawa, K. (2004). Steep elevation of blood interleukin-6 (IL-6) associated only with late stages of cachexia in cancer patients. *Eur Cytokine Netw* **15**, 312-6.

Jager, S., Handschin, C., St-Pierre, J. and Spiegelman, B. M. (2007). AMP-activated protein kinase (AMPK) action in skeletal muscle via direct phosphorylation of PGC-1alpha. *Proc Natl Acad Sci U S A* **104**, 12017-22.

James, D. E., Burleigh, K. M., Kraegen, E. W. and Chisholm, D. J. (1983). Effect of acute exercise and prolonged training on insulin response to intravenous glucose in vivo in rat. *J Appl Physiol* **55**, 1660-4.

James, D. E., Kraegen, E. W. and Chisholm, D. J. (1984). Effect of exercise training on whole-body insulin sensitivity and responsiveness. *J Appl Physiol* **56**, 1217-22.

Jones, S. A., Horiuchi, S., Topley, N., Yamamoto, N. and Fuller, G. M. (2001). The soluble interleukin 6 receptor: mechanisms of production and implications in disease. *FASEB J* **15**, 43-58.

Jones, S. A., Scheller, J. and Rose-John, S. (2011). Therapeutic strategies for the clinical blockade of IL-6/gp130 signaling. *J Clin Invest* **121**, 3375-83.

Julienne, C. M., Dumas, J. F., Goupille, C., Pinault, M., Berri, C., Collin, A., Tesseraud, S., Couet, C. and Servais, S. (2012). Cancer cachexia is associated with a decrease in skeletal muscle mitochondrial oxidative capacities without alteration of ATP production efficiency. *J Cachexia Sarcopenia Muscle* **3**, 265-75.

Kahn, B. B. (1992). Facilitative glucose transporters: regulatory mechanisms and dysregulation in diabetes. *J Clin Invest* **89**, 1367-74.

Kalra, P. R. and Tigas, S. (2002). Regulation of lipolysis: natriuretic peptides and the development of cachexia. *Int J Cardiol* **85**, 125-32.

Kamoshida, S., Watanabe, K., Suzuki, M., Mizutani, Y., Sakamoto, K., Sugimoto, Y., Oka, T., Fukushima, M. and Tsutsumi, Y. (2006). Expression of cancer cachexia-related factors in human cancer xenografts: an immunohistochemical analysis. *Biomed Res* **27**, 275-81.

Kelly, M., Keller, C., Avilucea, P. R., Keller, P., Luo, Z. J., Xiang, X. Q., Giralt, M., Hidalgo, J., Saha, A. K., Pedersen, B. K. et al. (2004). AMPK activity is diminished in tissues of IL-6 knockout mice: the effect of exercise. *Biochem Biophys Res Commun* **320**, 449-454.

Kennedy, J. W., Hirshman, M. F., Gervino, E. V., Ocel, J. V., Forse, R. A., Hoenig, S. J., Aronson, D., Goodyear, L. J. and Horton, E. S. (1999). Acute exercise induces GLUT4 translocation in skeletal muscle of normal human subjects and subjects with type 2 diabetes. *Diabetes* **48**, 1192-7.

Kim, S., Takahashi, H., Lin, W. W., Descargues, P., Grivennikov, S., Kim, Y., Luo, J. L. and Karin, M. (2009). Carcinoma-produced factors activate myeloid cells through TLR2 to stimulate metastasis. *Nature* **457**, 102-6.

Kim, Y. S. and Kim, Y. (1975). Glucocorticoid inhibition of protein synthesis in vivo and in vitro. *J Biol Chem* **250**, 2293-8.

King, P. A., Betts, J. J., Horton, E. D. and Horton, E. S. (1993). Exercise, unlike insulin, promotes glucose transporter translocation in obese Zucker rat muscle. *Am J Physiol* **265**, R447-52.

Kishimoto, T., Akira, S., Narazaki, M. and Taga, T. (1995). Interleukin-6 family of cytokines and gp130. *Blood* **86**, 1243-54.

Klover, P. J., Zimmers, T. A., Koniaris, L. G. and Mooney, R. A. (2003). Chronic exposure to interleukin-6 causes hepatic insulin resistance in mice. *Diabetes* **52**, 2784-9.

Kondo, T., Kobayashi, I. and Murakami, M. (2006). Effect of exercise on circulating adipokine levels in obese young women. *Endocr J* **53**, 189-95.

Koshiba, T., Detmer, S. A., Kaiser, J. T., Chen, H., McCaffery, J. M. and Chan, D. C. (2004). Structural basis of mitochondrial tethering by mitofusin complexes. *Science* **305**, 858-62.

La Rosa, G., Cardali, S., Genovese, T., Conti, A., Di Paola, R., La Torre, D., Cacciola, F. and Cuzzocrea, S. (2004). Inhibition of the nuclear factor-kappaB activation with pyrrolidine dithiocarbamate attenuating inflammation and oxidative stress after experimental spinal cord trauma in rats. *J Neurosurg Spine* **1**, 311-21.

Lai, R. Y., Ljubicic, V., D'Souza, D. and Hood, D. A. Effect of chronic contractile activity on mRNA stability in skeletal muscle. *Am J Physiol Cell Physiol* **299**, C155-63.

Lai, R. Y., Ljubicic, V., D'Souza, D. and Hood, D. A. (2010). Effect of chronic contractile activity on mRNA stability in skeletal muscle. *Am J Physiol Cell Physiol* **299**, C155-63.

Lantier, L., Mounier, R., Leclerc, J., Pende, M., Foretz, M. and Viollet, B. Coordinated maintenance of muscle cell size control by AMP-activated protein kinase. *The FASEB Journal* **24**, 3555-3561.

Lanza, I. R. and Nair, K. S. (2009). Functional assessment of isolated mitochondria in vitro. *Methods Enzymol* **457**, 349-72.

Lee, D. F. and Hung, M. C. (2007). All roads lead to mTOR: integrating inflammation and tumor angiogenesis. *Cell Cycle* **6**, 3011-4.

Li, P., Waters, R. E., Redfern, S. I., Zhang, M., Mao, L., Annex, B. H. and Yan, Z. (2007). Oxidative phenotype protects myofibers from pathological insults induced by chronic heart failure in mice. *Am J Pathol* **170**, 599-608.

Liesa, M., Borda-d'Agua, B., Medina-Gomez, G., Lelliott, C. J., Paz, J. C., Rojo, M., Palacin, M., Vidal-Puig, A. and Zorzano, A. (2008). Mitochondrial fusion is increased by the nuclear coactivator PGC-1beta. *PLoS One* **3**, e3613.

Liesa, M., Palacin, M. and Zorzano, A. (2009). Mitochondrial dynamics in mammalian health and disease. *Physiol Rev* **89**, 799-845.

Lin, L., Hutzen, B., Li, P. K., Ball, S., Zuo, M., DeAngelis, S., Foust, E., Sobo, M., Friedman, L., Bhasin, D. et al. (2010). A novel small molecule, LLL12, inhibits STAT3 phosphorylation and activities and exhibits potent growth-suppressive activity in human cancer cells. *Neoplasia* **12**, 39-50.

Lin, L., Liu, A., Peng, Z., Lin, H. J., Li, P. K., Li, C. and Lin, J. (2011). STAT3 is necessary for proliferation and survival in colon cancer-initiating cells. *Cancer Res* **71**, 7226-37.

Llovera, M., Garcia-Martinez, C., Lopez-Soriano, J., Carbo, N., Agell, N., Lopez-Soriano, F. J. and Argiles, J. M. (1998). Role of TNF receptor 1 in protein turnover during cancer cachexia using gene knockout mice. *Mol Cell Endocrinol* **142**, 183-9.

Lo, C. W., Chen, M. W., Hsiao, M., Wang, S., Chen, C. A., Hsiao, S. M., Chang, J. S., Lai, T. C., Rose-John, S., Kuo, M. L. et al. (2011). IL-6 trans-signaling in formation and progression of malignant ascites in ovarian cancer. *Cancer Res* **71**, 424-34.

Lorite, M. J., Cariuk, P. and Tisdale, M. J. (1997). Induction of muscle protein degradation by a tumour factor. *Br J Cancer* **76**, 1035-40.

Maddocks, M., Byrne, A., Johnson, C. D., Wilson, R. H., Fearon, K. C. and Wilcock, A. Physical activity level as an outcome measure for use in cancer cachexia trials: a feasibility study. *Support Care Cancer* **18**, 1539-44.

Matthys, P., Heremans, H., Opdenakker, G. and Billiau, A. (1991). Anti-interferon-gamma antibody treatment, growth of Lewis lung tumours in mice and tumour-associated cachexia. *Eur J Cancer* **27**, 182-7.

Mattusch, F., Dufaux, B., Heine, O., Mertens, I. and Rost, R. (2000). Reduction of the plasma concentration of C-reactive protein following nine months of endurance training. *Int J Sports Med* **21**, 21-4.

McClung, J. M., Judge, A. R., Powers, S. K. and Yan, Z. (2010). p38 MAPK links oxidative stress to autophagy-related gene expression in cachectic muscle wasting. *Am J Physiol Cell Physiol* **298**, C542-9.

Mehl, K. A., Davis, J. M., Clements, J. M., Berger, F. G., Pena, M. M. and Carson, J. A. (2005). Decreased intestinal polyp multiplicity is related to exercise mode and gender in ApcMin/+ mice. *J Appl Physiol* **98**, 2219-25.

Menshikova, E. V., Ritov, V. B., Fairfull, L., Ferrell, R. E., Kelley, D. E. and Goodpaster, B. H. (2006). Effects of exercise on mitochondrial content and function in aging human skeletal muscle. *J Gerontol A Biol Sci Med Sci* **61**, 534-40.

Mingrone, G., Manco, M., Calvani, M., Castagneto, M., Naon, D. and Zorzano, A. (2005). Could the low level of expression of the gene encoding skeletal muscle mitofusin-2 account for the metabolic inflexibility of obesity? *Diabetologia* **48**, 2108-14.

Mole, P. A., Oscai, L. B. and Holloszy, J. O. (1971). Adaptation of muscle to exercise. Increase in levels of palmityl Coa synthetase, carnitine palmityltransferase, and palmityl Coa dehydrogenase, and in the capacity to oxidize fatty acids. *J Clin Invest* **50**, 2323-30.

Monitto, C. L., Berkowitz, D., Lee, K. M., Pin, S., Li, D., Breslow, M., O'Malley, B. and Schiller, M. (2001). Differential gene expression in a murine model of cancer cachexia. *Am J Physiol Endocrinol Metab* **281**, E289-97.

Mori, M., Yamaguchi, K., Honda, S., Nagasaki, K., Ueda, M., Abe, O. and Abe, K. (1991). Cancer cachexia syndrome developed in nude mice bearing melanoma cells producing leukemia-inhibitory factor. *Cancer Res* **51**, 6656-9.

Morino, K., Petersen, K. F. and Shulman, G. I. (2006). Molecular mechanisms of insulin resistance in humans and their potential links with mitochondrial dysfunction. *Diabetes* **55 Suppl 2**, S9-S15.

Moser, A. R., Pitot, H. C. and Dove, W. F. (1990). A dominant mutation that predisposes to multiple intestinal neoplasia in the mouse. *Science* **247**, 322-4.

Mulligan, H. D., Mahony, S. M., Ross, J. A. and Tisdale, M. J. (1992). Weight loss in a murine cachexia model is not associated with the cytokines tumour necrosis factor-alpha or interleukin-6. *Cancer Lett* **65**, 239-43.

Murphy, K. T., Chee, A., Gleeson, B. G., Naim, T., Swiderski, K., Koopman, R. and Lynch, G. S. Antibody-directed myostatin inhibition enhances muscle mass and function in tumor-bearing mice. *American Journal of Physiology-Regulatory, Integrative and Comparative Physiology* **301**, R716-R726.

Murphy, K. T., Chee, A., Gleeson, B. G., Naim, T., Swiderski, K., Koopman, R. and Lynch, G. S. (2011). Antibody-directed myostatin inhibition enhances muscle mass and function in tumor-bearing mice. *Am J Physiol Regul Integr Comp Physiol* **301**, R716-26.

Murphy, K. T. and Lynch, G. S. (2009). Update on emerging drugs for cancer cachexia. *Expert Opin Emerg Drugs* **14**, 619-32.

Murphy, K. T. and Lynch, G. S. (2012). Editorial update on emerging drugs for cancer cachexia. *Expert Opin Emerg Drugs* **17**, 5-9.

Muscaritoli, M., Anker, S. D., Argiles, J., Aversa, Z., Bauer, J. M., Biolo, G., Boirie, Y., Bosaeus, I., Cederholm, T., Costelli, P. et al. (2010). Consensus definition of

sarcopenia, cachexia and pre-cachexia: joint document elaborated by Special Interest Groups (SIG) "cachexia-anorexia in chronic wasting diseases" and "nutrition in geriatrics". *Clin Nutr* **29**, 154-9.

Mustian, K. M., Morrow, G. R., Carroll, J. K., Figueroa-Moseley, C. D., Jean-Pierre, P. and Williams, G. C. (2007). Integrative nonpharmacologic behavioral interventions for the management of cancer-related fatigue. *Oncologist* **12 Suppl 1**, 52-67.

Nachlas, M. M., Tsou, K. C., De Souza, E., Cheng, C. S. and Seligman, A. M. (1957). Cytochemical demonstration of succinic dehydrogenase by the use of a new p-nitrophenyl substituted ditetrazole. *J Histochem Cytochem* **5**, 420-36.

Nader, G. A. and Esser, K. A. (2001). Intracellular signaling specificity in skeletal muscle in response to different modes of exercise. *J Appl Physiol* **90**, 1936-42.

Nai, Y. J., Jiang, Z. W., Wang, Z. M., Li, N. and Li, J. S. (2007). Prevention of cancer cachexia by pyrrolidine dithiocarbamate (PDTC) in colon 26 tumor-bearing mice. *JPEN J Parenter Enteral Nutr* **31**, 18-25.

Nechemia-Arbely, Y., Barkan, D., Pizov, G., Shriki, A., Rose-John, S., Galun, E. and Axelrod, J. H. (2008). IL-6/IL-6R axis plays a critical role in acute kidney injury. *J Am Soc Nephrol* **19**, 1106-15.

Niehof, M., Streetz, K., Rakemann, T., Bischoff, S. C., Manns, M. P., Horn, F. and Trautwein, C. (2001). Interleukin-6-induced tethering of STAT3 to the LAP/C/EBPbeta promoter suggests a new mechanism of transcriptional regulation by STAT3. *J Biol Chem* **276**, 9016-27.

Nowell, M. A., Richards, P. J., Horiuchi, S., Yamamoto, N., Rose-John, S., Topley, N., Williams, A. S. and Jones, S. A. (2003). Soluble IL-6 receptor governs IL-6 activity in experimental arthritis: blockade of arthritis severity by soluble glycoprotein 130. *J Immunol* **171**, 3202-9.

O'Gorman, P., McMillan, D. C. and McArdle, C. S. (1998). Impact of weight loss, appetite, and the inflammatory response on quality of life in gastrointestinal cancer patients. *Nutr Cancer* **32**, 76-80.

Oh, H. M., Yu, C. R., Dambuza, I., Marrero, B. and Egwuagu, C. E. (2012). STAT3 protein interacts with Class O Forkhead transcription factors in the cytoplasm and regulates nuclear/cytoplasmic localization of FoxO1 and FoxO3a proteins in CD4(+) T cells. *J Biol Chem* **287**, 30436-43.

Ohe, Y., Podack, E. R., Olsen, K. J., Miyahara, Y., Miura, K., Saito, H., Koishihara, Y., Ohsugi, Y., Ohira, T., Nishio, K. et al. (1993). Interleukin-6 cDNA transfected Lewis lung carcinoma cells show unaltered net tumour growth rate but cause weight loss and shortened survival in syngeneic mice. *Br J Cancer* **67**, 939-44.

Oscai, L. B. and Holloszy, J. O. (1971). Biochemical adaptations in muscle. II. Response of mitochondrial adenosine triphosphatase, creatine phosphokinase, and adenylate kinase activities in skeletal muscle to exercise. *J Biol Chem* **246**, 6968-72.

Parkington, J. D., Siebert, A. P., LeBrasseur, N. K. and Fielding, R. A. (2003). Differential activation of mTOR signaling by contractile activity in skeletal muscle. *Am J Physiol Regul Integr Comp Physiol* **285**, R1086-90.

Penna, F., Busquets, S., Pin, F., Toledo, M., Baccino, F. M., Lopez-Soriano, F. J., Costelli, P. and Argiles, J. M. Combined approach to counteract experimental cancer cachexia: eicosapentaenoic acid and training exercise. *J Cachexia Sarcopenia Muscle* **2**, 95-104.

Persson, C. and Glimelius, B. (2002). The relevance of weight loss for survival and quality of life in patients with advanced gastrointestinal cancer treated with palliative chemotherapy. *Anticancer Res* **22**, 3661-8.

Petersen, A. M. and Pedersen, B. K. (2005). The anti-inflammatory effect of exercise. *J Appl Physiol* **98**, 1154-62.

Peterson, J. M. and Guttridge, D. C. (2008). Skeletal muscle diseases, inflammation, and NF-kappaB signaling: insights and opportunities for therapeutic intervention. *Int Rev Immunol* **27**, 375-87.

Pfeilschifter, W., Czech, B., Hoffmann, B. P., Sujak, M., Kahles, T., Steinmetz, H., Neumann-Haefelin, T. and Pfeilschifter, J. Pyrrolidine dithiocarbamate activates p38 MAPK and protects brain endothelial cells from apoptosis: a mechanism for the protective effect in stroke? *Neurochemical research* **35**, 1391-1401.

Pilegaard, H., Ordway, G. A., Saltin, B. and Neufer, P. D. (2000). Transcriptional regulation of gene expression in human skeletal muscle during recovery from exercise. *Am J Physiol Endocrinol Metab* **279**, E806-14.

Pilegaard, H., Saltin, B. and Neufer, P. D. (2003). Exercise induces transient transcriptional activation of the PGC-1alpha gene in human skeletal muscle. *J Physiol* **546**, 851-8.

Puppa, M., Gao, S., Narsale, A. and Carson, J. (2013a). Skeletal muscle glycoprotein 130's role in Lewis Lung Carcinoma induced cachexia. *FASEB J* **(in press)**.

Puppa, M. J., Gao, S., Narsale, A. A. and Carson, J. A. (2013b). Skeletal muscle glycoprotein 130's role in Lewis lung carcinoma-induced cachexia. *FASEB J*.

Puppa, M. J., White, J. P., Baltgalvis, K. A., Sato, S., Baynes, J. W. and Carson, J. A. (2011a). The effect of exercise on IL-6 induced cachexia in the ApcMin/+ mouse. *J cachexia, Sarcopenia, and Muscle*.

Puppa, M. J., White, J. P., Sato, S., Cairns, M., Baynes, J. W. and Carson, J. A. (2011b). Gut barrier dysfunction in the Apc(Min/+) mouse model of colon cancer cachexia. *Biochim Biophys Acta* **1812**, 1601-6.

Puppa, M. J., White, J. P., Sato, S., M.A., C., Baynes, J. W. and Carson, J. A. (2011c). Gut barrier dysfunction in the ApcMin/+ mouse model of colon cancer cachexia. *Biochemica et Biophysica Acta*.

Puppa, M. J., White, J. P., Velazquez, K. T., Baltgalvis, K. A., Sato, S., Baynes, J. W. and Carson, J. A. (2011d). The effect of exercise on IL-6-induced cachexia in the Apc (Min/+) mouse. *J Cachexia Sarcopenia Muscle*.

Qiu, H., Lizano, P., Laure, L., Sui, X., Rashed, E., Park, J. Y., Hong, C., Gao, S., Holle, E., Morin, D. et al. (2011). H11 kinase/heat shock protein 22 deletion impairs both nuclear and mitochondrial functions of STAT3 and accelerates the transition into heart failure on cardiac overload. *Circulation* **124**, 406-15.

Ramaswamy, S., Nakamura, N., Sansal, I., Bergeron, L. and Sellers, W. R. (2002). A novel mechanism of gene regulation and tumor suppression by the transcription factor FKHR. *Cancer Cell* **2**, 81-91.

Reed, S. A., Sandesara, P. B., Senf, S. M. and Judge, A. R. Inhibition of FoxO transcriptional activity prevents muscle fiber atrophy during cachexia and induces hypertrophy. *FASEB J* **26**, 987-1000.

Reed, S. A., Sandesara, P. B., Senf, S. M. and Judge, A. R. (2012). Inhibition of FoxO transcriptional activity prevents muscle fiber atrophy during cachexia and induces hypertrophy. *FASEB J* **26**, 987-1000.

Risson, V., Mazelin, L., Roceri, M., Sanchez, H., Moncollin, V., Corneloup, C., Richard-Bulteau, H., Vignaud, A., Baas, D., Defour, A. et al. (2009). Muscle inactivation of mTOR causes metabolic and dystrophin defects leading to severe myopathy. *J Cell Biol* **187**, 859-74.

Rivadeneira, D. E., Naama, H. A., McCarter, M. D., Fujita, J., Evoy, D., Mackrell, P. and Daly, J. M. (1999). Glucocorticoid blockade does not abrogate tumor-induced cachexia. *Nutr Cancer* **35**, 202-6.

Rodriguez, C., Grosgeorge, J., Nguyen, V. C., Gaudray, P. and Theillet, C. (1995). Human gp130 transducer chain gene (IL6ST) is localized to chromosome band 5q11 and possesses a pseudogene on chromosome band 17p11. *Cytogenet Cell Genet* **70**, 64-7.

Romanello, V., Guadagnin, E., Gomes, L., Roder, I., Sandri, C., Petersen, Y., Milan, G., Masiero, E., Del Piccolo, P., Foretz, M. et al. Mitochondrial fission and remodelling contributes to muscle atrophy. *EMBO J* **29**, 1774-85.

Romanello, V., Guadagnin, E., Gomes, L., Roder, I., Sandri, C., Petersen, Y., Milan, G., Masiero, E., Del Piccolo, P., Foretz, M. et al. (2010). Mitochondrial fission and remodelling contributes to muscle atrophy. *EMBO J* **29**, 1774-85.

Romanello, V. and Sandri, M. Mitochondrial biogenesis and fragmentation as regulators of muscle protein degradation. *Curr Hypertens Rep* **12**, 433-9.

Romanello, V. and Sandri, M. (2010). Mitochondrial biogenesis and fragmentation as regulators of muscle protein degradation. *Curr Hypertens Rep* **12**, 433-9.

Rose-John, S. (2003). Interleukin-6 biology is coordinated by membrane bound and soluble receptors. *Acta Biochim Pol* **50**, 603-11.

Rose-John, S. (2012). IL-6 trans-signaling via the soluble IL-6 receptor: importance for the pro-inflammatory activities of IL-6. *Int J Biol Sci* **8**, 1237-47.

Rose-John, S., Scheller, J., Elson, G. and Jones, S. A. (2006). Interleukin-6 biology is coordinated by membrane-bound and soluble receptors: role in inflammation and cancer. *J Leukoc Biol* **80**, 227-36.

Ruas, J. L., White, J. P., Rao, R. R., Kleiner, S., Brannan, K. T., Harrison, B. C., Greene, N. P., Wu, J., Estall, J. L., Irving, B. A. et al. (2012). A PGC-1alpha isoform induced by resistance training regulates skeletal muscle hypertrophy. *Cell* **151**, 1319-31.

Russell, A. P., Hesselink, M. K., Lo, S. K. and Schrauwen, P. (2005). Regulation of metabolic transcriptional co-activators and transcription factors with acute exercise. *FASEB J* **19**, 986-8.

Saini, A., Al-Shanti, N. and Stewart, C. E. (2006). Waste management - cytokines, growth factors and cachexia. *Cytokine Growth Factor Rev* **17**, 475-86.

Saito, M., Yoshida, K., Hibi, M., Taga, T. and Kishimoto, T. (1992). Molecular cloning of a murine IL-6 receptor-associated signal transducer, gp130, and its regulated expression in vivo. *J Immunol* **148**, 4066-71.

Sato, S. (2012). The effect of sex and exercise training during the progression of cancer cachexia in the apc min/+ mouse. In *Exercise Science*, vol. PhD (ed., pp. 310. Columbia: University of South Carolina.

Schakman, O., Kalista, S., Barbe, C., Loumaye, A. and Thissen, J. P. (2013). Glucocorticoid-induced skeletal muscle atrophy. *Int J Biochem Cell Biol* **45**, 2163-72.

Schiaffino, S. and Mammucari, C. (2011). Regulation of skeletal muscle growth by the IGF1-Akt/PKB pathway: insights from genetic models. *Skelet Muscle* **1**, 4.

Schieke, S. M., Phillips, D., McCoy, J. P., Jr., Aponte, A. M., Shen, R. F., Balaban, R. S. and Finkel, T. (2006). The mammalian target of rapamycin (mTOR) pathway

regulates mitochondrial oxygen consumption and oxidative capacity. *J Biol Chem* **281**, 27643-52.

Schmidt, E. K., Clavarino, G., Ceppi, M. and Pierre, P. (2009). SUnSET, a nonradioactive method to monitor protein synthesis. *Nat Methods* **6**, 275-7.

Schreck, R., Meier, B., Mannel, D. N., Droge, W. and Baeuerle, P. A. (1992). Dithiocarbamates as potent inhibitors of nuclear factor kappa B activation in intact cells. *J Exp Med* **175**, 1181-94.

Schwantner, A., Dingley, A. J., Ozbek, S., Rose-John, S. and Grotzinger, J. (2004). Direct determination of the interleukin-6 binding epitope of the interleukin-6 receptor by NMR spectroscopy. *J Biol Chem* **279**, 571-6.

Scott, H. R., McMillan, D. C., Brown, D. J., Forrest, L. M., McArdle, C. S. and Milroy, R. (2003). A prospective study of the impact of weight loss and the systemic inflammatory response on quality of life in patients with inoperable non-small cell lung cancer. *Lung Cancer* **40**, 295-9.

Serrano, A. L., Baeza-Raja, B., Perdiguero, E., Jardi, M. and Munoz-Cinoves, P. (2008). Interleukin-6 is an essential regulator of satellite cell-mediated skeletal muscle hypertrophy. *Cell Metabolism* **7**, 33-44.

Shi, X., Leonard, S. S., Wang, S. and Ding, M. (2000). Antioxidant properties of pyrrolidine dithiocarbamate and its protection against Cr(VI)-induced DNA strand breakage. *Ann Clin Lab Sci* **30**, 209-16.

Siddiqui, R. A., Hassan, S., Harvey, K. A., Rasool, T., Das, T., Mukerji, P. and DeMichele, S. (2009). Attenuation of proteolysis and muscle wasting by curcumin c3 complex in MAC16 colon tumour-bearing mice. *Br J Nutr* **102**, 967-75.

Soda, K., Kawakami, M., Kashii, A. and Miyata, M. (1995). Manifestations of cancer cachexia induced by colon 26 adenocarcinoma are not fully ascribable to interleukin-6. *Int J Cancer* **62**, 332-6.

Solheim, T. S., Fearon, K. C., Blum, D. and Kaasa, S. (2013). Non-steroidal anti-inflammatory treatment in cancer cachexia: A systematic literature review. *Acta Oncol* **52**, 6-17.

Song, S., Abdelmohsen, K., Zhang, Y., Becker, K. G., Gorospe, M. and Bernier, M. (2011). Impact of pyrrolidine dithiocarbamate and interleukin-6 on mammalian target of rapamycin complex 1 regulation and global protein translation. *J Pharmacol Exp Ther* **339**, 905-13.

Soriano, F. X., Liesa, M., Bach, D., Chan, D. C., Palacin, M. and Zorzano, A. (2006). Evidence for a mitochondrial regulatory pathway defined by peroxisome proliferator-activated receptor-gamma coactivator-1 alpha, estrogen-related receptor-alpha, and mitofusin 2. *Diabetes* **55**, 1783-91.

Stahl, N., Boulton, T. G., Farruggella, T., Ip, N. Y., Davis, S., Witthuhn, B. A., Quelle, F. W., Silvennoinen, O., Barbieri, G., Pellegrini, S. et al. (1994). Association and activation of Jak-Tyk kinases by CNTF-LIF-OSM-IL-6 beta receptor components. *Science* **263**, 92-5.

Steinberg, G. R., Watt, M. J., McGee, S. L., Chan, S., Hargreaves, M., Febbraio, M. A., Stapleton, D. and Kemp, B. E. (2006). Reduced glycogen availability is associated with increased AMPKalpha2 activity, nuclear AMPKalpha2 protein abundance, and GLUT4 mRNA expression in contracting human skeletal muscle. *Appl Physiol Nutr Metab* **31**, 302-12.

Stitt, T. N., Drujan, D., Clarke, B. A., Panaro, F., Timofeyva, Y., Kline, W. O., Gonzalez, M., Yancopoulos, G. D. and Glass, D. J. (2004). The IGF-1/PI3K/Akt pathway prevents expression of muscle atrophy-induced ubiquitin ligases by inhibiting FOXO transcription factors. *Mol Cell* **14**, 395-403.

Strassmann, G., Fong, M., Freter, C. E., Windsor, S., D'Alessandro, F. and Nordan, R. P. (1993). Suramin interferes with interleukin-6 receptor binding in vitro and inhibits colon-26-mediated experimental cancer cachexia in vivo. *J Clin Invest* **92**, 2152-9.

Strassmann, G., Fong, M., Kenney, J. S. and Jacob, C. O. (1992). Evidence for the involvement of interleukin 6 in experimental cancer cachexia. *J Clin Invest* **89**, 1681-4.

Strassmann, G. and Kambayashi, T. (1995). Inhibition of experimental cancer cachexia by anti-cytokine and anti-cytokine-receptor therapy. *Cytokines Mol Ther* **1**, 107-13.

Tan, B. H. and Fearon, K. C. (2008). Cachexia: prevalence and impact in medicine. *Curr Opin Clin Nutr Metab Care* **11**, 400-7.

Tazaki, E., Shimizu, N., Tanaka, R., Yoshizumi, M., Kamma, H., Imoto, S., Goya, T., Kozawa, K., Nishina, A. and Kimura, H. (2011). Serum cytokine profiles in patients with prostate carcinoma. *Exp Ther Med* **2**, 887-891.

Tessitore, L., Bonelli, G. and Baccino, F. M. (1987). Early development of protein metabolic perturbations in the liver and skeletal muscle of tumour-bearing rats. A model system for cancer cachexia. *Biochem J* **241**, 153-9.

Tisdale, M. J. (2001). Cancer anorexia and cachexia. *Nutrition* **17**, 438-42.

Tisdale, M. J. (2002). Cachexia in cancer patients. *Nat Rev Cancer* **2**, 862-71.

Tisdale, M. J. (2003). The 'cancer cachectic factor'. *Support Care Cancer* **11**, 73-8.

Tisdale, M. J. (2005). Molecular pathways leading to cancer cachexia. *Physiology (Bethesda)* **20**, 340-8.

Tisdale, M. J. (2009). Mechanisms of cancer cachexia. *Physiol Rev* **89**, 381-410.

Toledo-Corral, C. M. and Banner, L. R. Early changes of LIFR and gp130 in sciatic nerve and muscle of diabetic mice. *Acta Histochem* **114**, 159-65.

Tzika, A. A., Fontes-Oliveira, C. C., Shestov, A. A., Constantinou, C., Psychogios, N., Righi, V., Mintzopoulos, D., Busquets, S., Lopez-Soriano, F. J., Milot, S. et al. (2013). Skeletal muscle mitochondrial uncoupling in a murine cancer cachexia model. *Int J Oncol* **43**, 886-94.

Uguccioni, G. and Hood, D. A. The importance of PGC-1alpha in contractile activity-induced mitochondrial adaptations. *Am J Physiol Endocrinol Metab* **300**, E361-71.

Vavvas, D., Apazidis, A., Saha, A. K., Gamble, J., Patel, A., Kemp, B. E., Witters, L. A. and Ruderman, N. B. (1997). Contraction-induced changes in acetyl-CoA carboxylase and 5'-AMP-activated kinase in skeletal muscle. *J Biol Chem* **272**, 13255-61.

von Haehling, S., Lainscak, M., Springer, J. and Anker, S. D. (2009). Cardiac cachexia: a systematic overview. *Pharmacol Ther* **121**, 227-52.

Waetzig, G. H. and Rose-John, S. (2012). Hitting a complex target: an update on interleukin-6 trans-signalling. *Expert Opin Ther Targets* **16**, 225-36.

Wallenius, V., Wallenius, K., Ahren, B., Rudling, M., Carlsten, H., Dickson, S. L., Ohlsson, C. and Jansson, J. O. (2002). Interleukin-6-deficient mice develop mature-onset obesity. *Nature Medicine* **8**, 75-79.

Walsh, D., Donnelly, S. and Rybicki, L. (2000). The symptoms of advanced cancer: relationship to age, gender, and performance status in 1,000 patients. *Support Care Cancer* **8**, 175-9.

Wang, X., Pickrell, A. M., Zimmers, T. A. and Moraes, C. T. (2012). Increase in muscle mitochondrial biogenesis does not prevent muscle loss but increased tumor size in a mouse model of acute cancer-induced cachexia. *PLoS One* **7**, e33426.

Wang, X. H., Du, J., Klein, J. D., Bailey, J. L. and Mitch, W. E. (2009). Exercise ameliorates chronic kidney disease-induced defects in muscle protein metabolism and progenitor cell function. *Kidney Int* **76**, 751-9.

Washington, T. A., White, J. P., Davis, J. M., Wilson, L. B., Lowe, L. L., Sato, S. and Carson, J. A. (2011). Skeletal muscle mass recovery from atrophy in IL-6 knockout mice. *Acta Physiol (Oxf)* **202**, 657-69.

Watt, M. J., Dzamko, N., Thomas, W. G., Rose-John, S., Ernst, M., Carling, D., Kemp, B. E., Febbraio, M. A. and Steinberg, G. R. (2006). CNTF reverses obesity-induced insulin resistance by activating skeletal muscle AMPK. *Nature Medicine* **12**, 541-548.

White, J., Puppa, M., Gao, S., Sato, S., Welle, S. and Carson, J. (2012a). Disrupted mTOR Signaling During Cancer Cachexia. *American Journal of Physiology - Endocrinology and Metabolism* **(in review)**.

White, J. P., Baltgalvis, K. A., Puppa, M. J., Sato, S., Baynes, J. W. and Carson, J. A. Muscle oxidative capacity during IL-6-dependent cancer cachexia. *Am J Physiol Regul Integr Comp Physiol* **300**, R201-11.

White, J. P., Baltgalvis, K. A., Puppa, M. J., Sato, S., Baynes, J. W. and Carson, J. A. (2011a). Muscle oxidative capacity during IL-6-dependent cancer cachexia. *Am J Physiol Regul Integr Comp Physiol* **300**, R201-11.

White, J. P., Baynes, J. W., Welle, S. L., Kostek, M. C., Matesic, L. E., Sato, S. and Carson, J. A. (2011b). The regulation of skeletal muscle protein turnover during the progression of cancer cachexia in the Apc(Min/+) mouse. *PLoS One* **6**, e24650.

White, J. P., Gao, S., Puppa, M. J., Sato, S., Welle, S. L. and Carson, J. A. (2013a). Testosterone regulation of Akt/mTORC1/FoxO3a signaling in skeletal muscle. *Mol Cell Endocrinol* **365**, 174-86.

White, J. P., Puppa, M. J., Gao, S., Sato, S., Welle, S. L. and Carson, J. A. (2013b). Muscle mTORC1 suppression by IL-6 during cancer cachexia: A role for AMPK. *Am J Physiol Endocrinol Metab*.

White, J. P., Puppa, M. J., Sato, S., Gao, S., Price, R. L., Baynes, J. W., Kostek, M. C., Matesic, L. E. and Carson, J. A. (2012b). IL-6 regulation on skeletal muscle mitochondrial remodeling during cancer cachexia in the ApcMin/+ mouse. *Skelet Muscle* **2**, 14.

White, J. P., Reecy, J. M., Washington, T. A., Sato, S., Le, M. E., Davis, J. M., Wilson, L. B. and Carson, J. A. (2009). Overload-induced skeletal muscle extracellular matrix remodelling and myofibre growth in mice lacking IL-6. *Acta Physiologica* **197**, 321-332.

White, J. P., Sato, S., Puppa, M., Baynes, J. W., Kostek, M. C., Matesic, L. E. and Carson, J. A. (2012c). IL-6 Regulation of Muscle Mitochondrial Biogenesis and Fission/Fusion Dynamics During the Progression of Cacner Cachexia. *Skelet Muscle* **In Press**.

Widegren, U., Jiang, X. J., Krook, A., Chibalin, A. V., Björnholm, M., Tally, M., Roth, R. A., Henriksson, J., Wallberg-henriksson, H. and Zierath, J. R. (1998). Divergent effects of exercise on metabolic and mitogenic signaling pathways in human skeletal muscle. *The FASEB Journal* **12**, 1379-1389.

Wu, Z., Puigserver, P., Andersson, U., Zhang, C., Adelmant, G., Mootha, V., Troy, A., Cinti, S., Lowell, B., Scarpulla, R. C. et al. (1999). Mechanisms controlling mitochondrial biogenesis and respiration through the thermogenic coactivator PGC-1. *Cell* **98**, 115-24.

Wu, Z., Woodring, P. J., Bhakta, K. S., Tamura, K., Wen, F., Feramisco, J. R., Karin, M., Wang, J. Y. and Puri, P. L. (2000). p38 and extracellular signal-regulated kinases regulate the myogenic program at multiple steps. *Molecular and cellular biology* **20**, 3951-3964.

Yaffe, M. P. (1999). The machinery of mitochondrial inheritance and behavior. *Science* **283**, 1493-7.

Yoshida, K., Taga, T., Saito, M., Suematsu, S., Kumanogoh, A., Tanaka, T., Fujiwara, H., Hirata, M., Yamagami, T., Nakahata, T. et al. (1996). Targeted disruption of gp130, a common signal transducer for the interleukin 6 family of cytokines, leads to myocardial and hematological disorders. *Proc Natl Acad Sci U S A* **93**, 407-11.

Zhang, G., Jin, B. and Li, Y. P. (2011). C/EBPbeta mediates tumour-induced ubiquitin ligase atrogin1/MAFbx upregulation and muscle wasting. *EMBO J* **30**, 4323-35.

Zhang, G. and Li, Y. P. (2012). p38beta MAPK upregulates atrogin1/MAFbx by specific phosphorylation of C/EBPbeta. *Skelet Muscle* **2**, 20.

Zhang, G., Lin, R. K., Kwon, Y. T. and Li, Y. P. (2013). Signaling mechanism of tumor cell-induced up-regulation of E3 ubiquitin ligase UBR2. *FASEB J* **27**, 2893-901.

Zhang, P., Chen, X. and Fan, M. (2007). Signaling mechanisms involved in disuse muscle atrophy. *Med Hypotheses* **69**, 310-21.

Zhao, L., Hart, S., Cheng, J., Melenhorst, J. J., Bierie, B., Ernst, M., Stewart, C., Schaper, F., Heinrich, P. C., Ullrich, A. et al. (2004). Mammary gland remodeling depends on gp130 signaling through Stat3 and MAPK. *J Biol Chem* **279**, 44093-100.

Zinna, E. M. and Yarasheski, K. E. (2003). Exercise treatment to counteract protein wasting of chronic diseases. *Curr Opin Clin Nutr Metab Care* **6**, 87-93.

Zinzalla, V., Stracka, D., Oppliger, W. and Hall, M. N. (2011). Activation of mTORC2 by association with the ribosome. *Cell* **144**, 757-68.

Zong, H., Ren, J. M., Young, L. H., Pypaert, M., Mu, J., Birnbaum, M. J. and Shulman, G. I. (2002). AMP kinase is required for mitochondrial biogenesis in skeletal muscle in response to chronic energy deprivation. *Proc Natl Acad Sci U S A* **99**, 15983-7.

APPENDIX A

SUPPLEMENTAL DATA

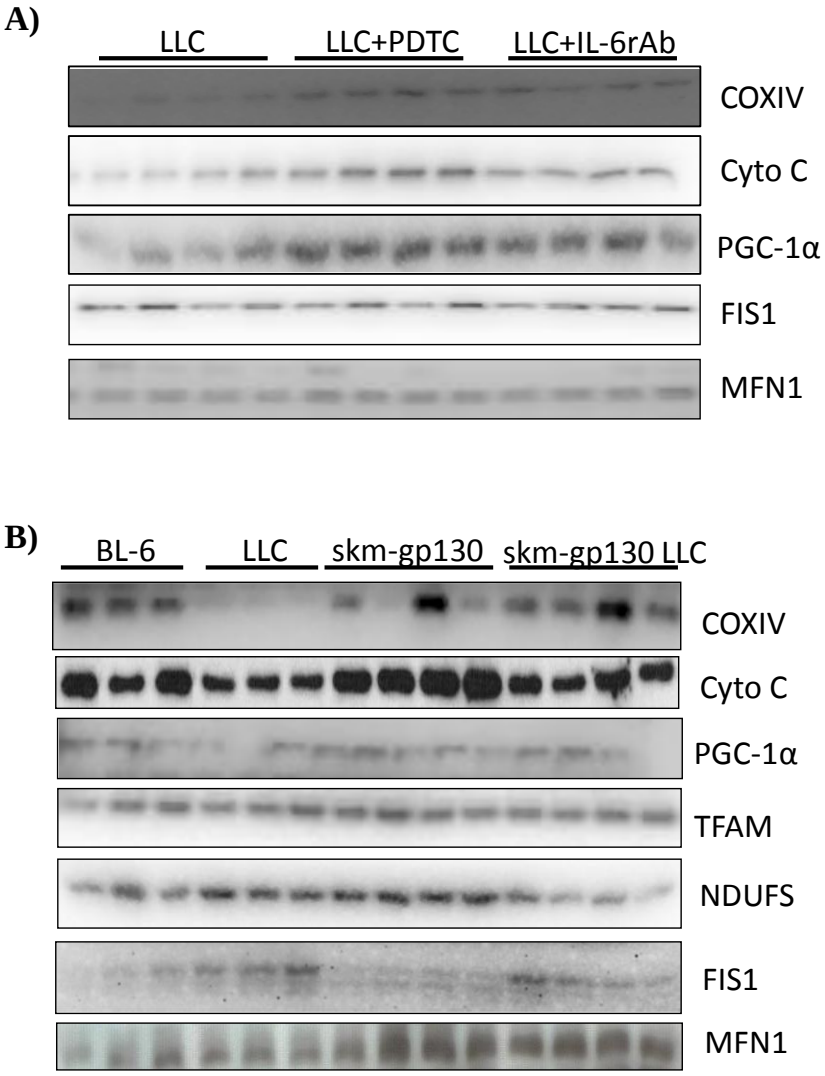

Figure A.1. Effect of inflammation inhibition on the regulation of muscle oxidative capacity in LLC-induced cachexia. Western blot analysis of mitochondrial content and dynamics markers in LLC mice treated with A) acute IL-6r Ab or PDTC for one week after tumor development, and B) in mice lacking skeletal muscle gp130.

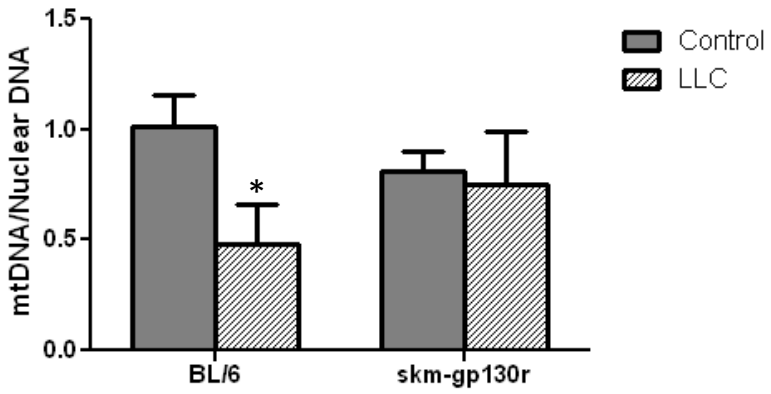

Figure A.2. Effect of skm-gp130 inhibition on mitochondrial content in LLC-induced cachexia. Skeletal muscle mitochondrial content was measured as the ratio of mitochondrial DNA to genomic DNA. Two-way ANOVA was run to determine the effects of LLC x skm-gp130. Pre-planned t-test was used to determine the effects of LLC in BL/6 mice. * significant from BL/6 control, $P<0.05$.

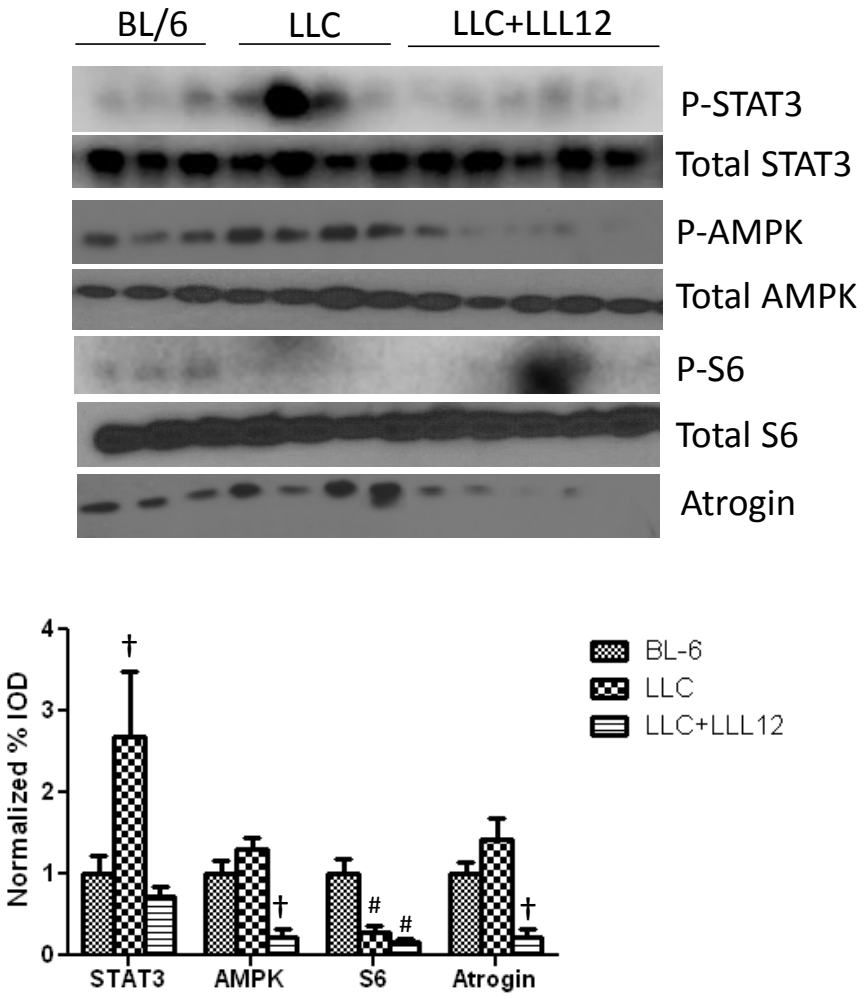

Figure A.3. Effect of LLL12 on LLC-induced muscle signaling. Skeletal muscle STAT3 was blocked for one week after 4 weeks of tumor growth. Skeletal muscle signaling was measured by western blot analysis. A One-Way ANOVA was run. †Different from all other comparisons, # different from BL-6, $p<0.05$.

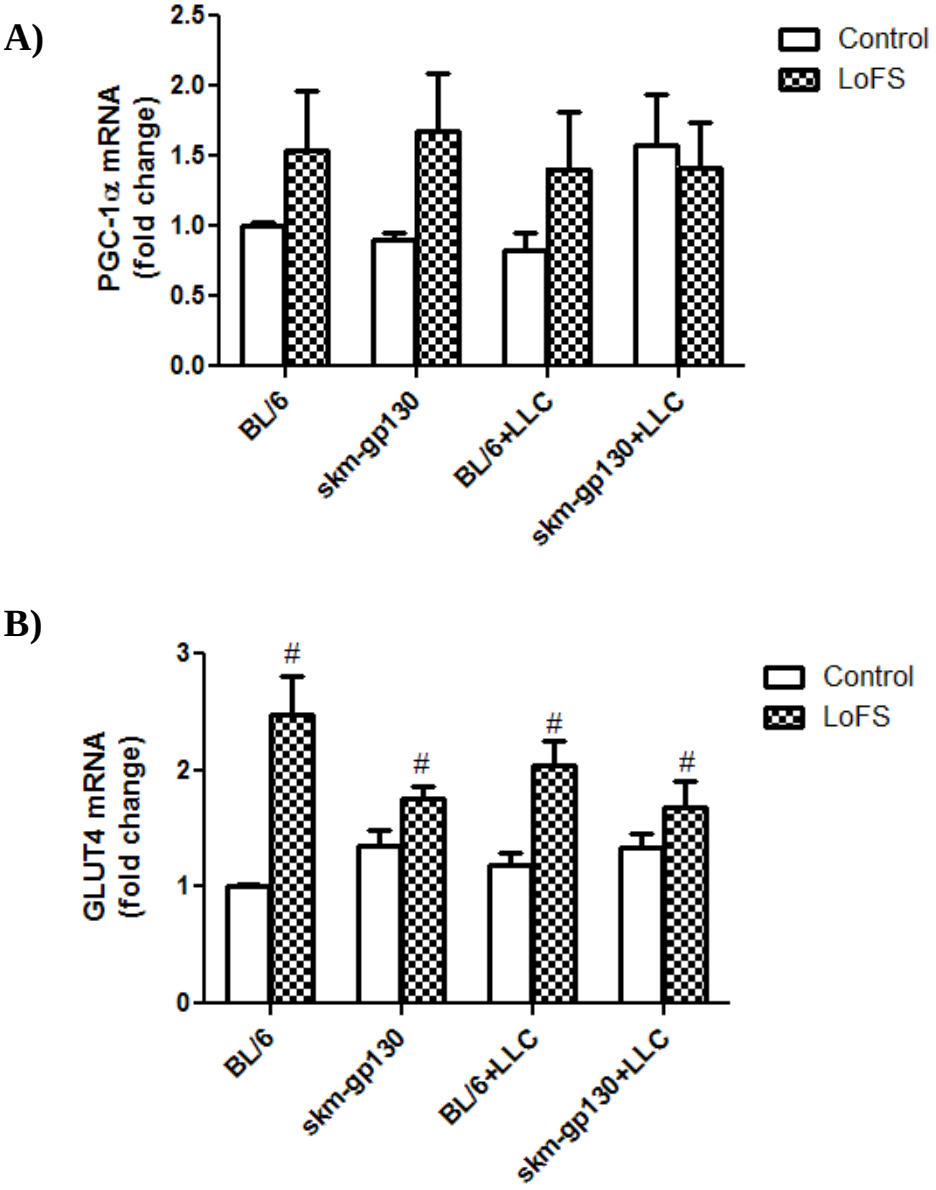

Figure A.4. Effect of skm-gp130 inhibition on LoFS induced PGC-1α and GLUT4 mRNA in LLC-induced cachexia. Skeletal muscle A) PGC-1α and B) GLUT4 mRNA was measured in gastrocnemius of mice 3h post a novel bout of low frequency stimulated contraction. Repeated measures two-way ANOVA was used to examine gp130 x LLC in control and LoFS muscle. # signifies main effect of LoFS, $p<0.05$.

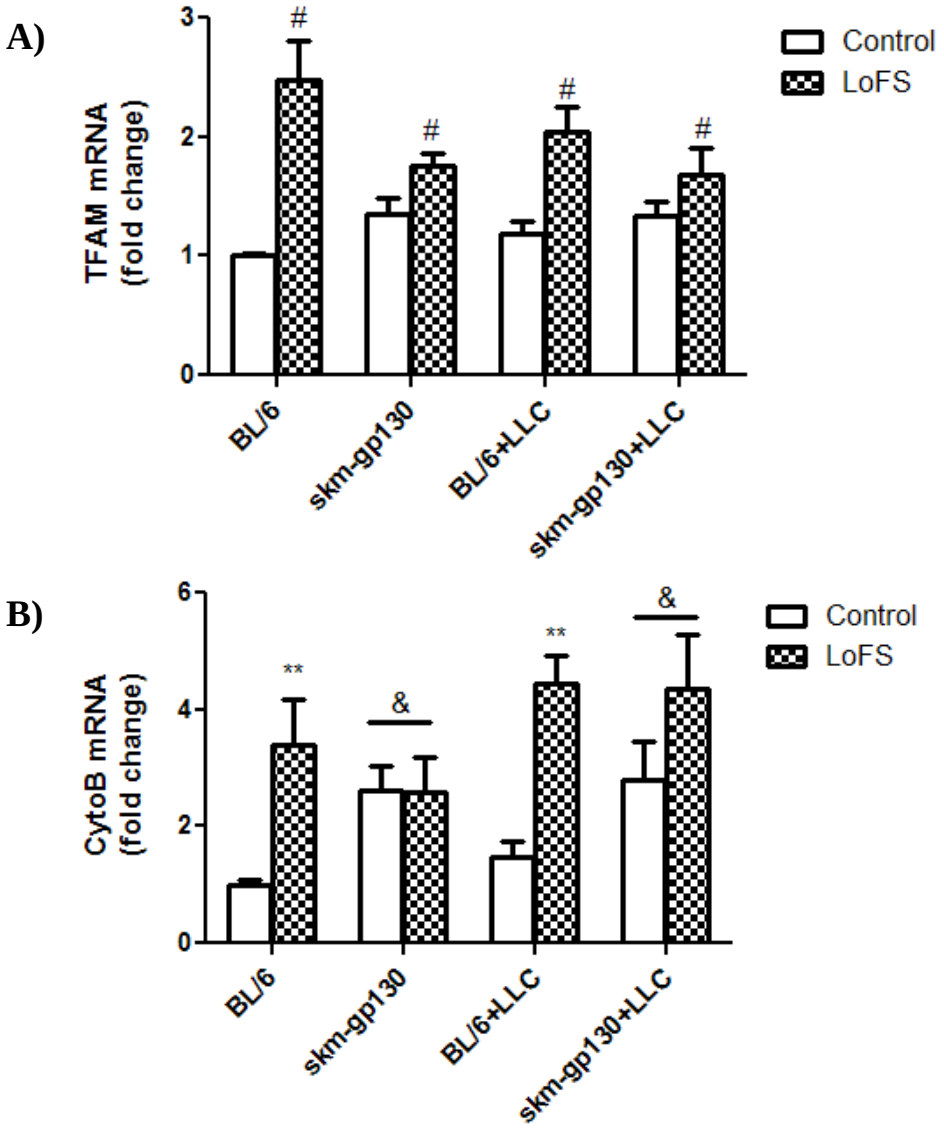
A)
TFAM mRNA (fold change)
Control
LoFS
BL/6
skm-gp130
BL/6+LLC
skm-gp130+LLC
B)
CytoB mRNA (fold change)
Control
LoFS
BL/6
skm-gp130
BL/6+LLC
skm-gp130+LLC

Figure A.5.

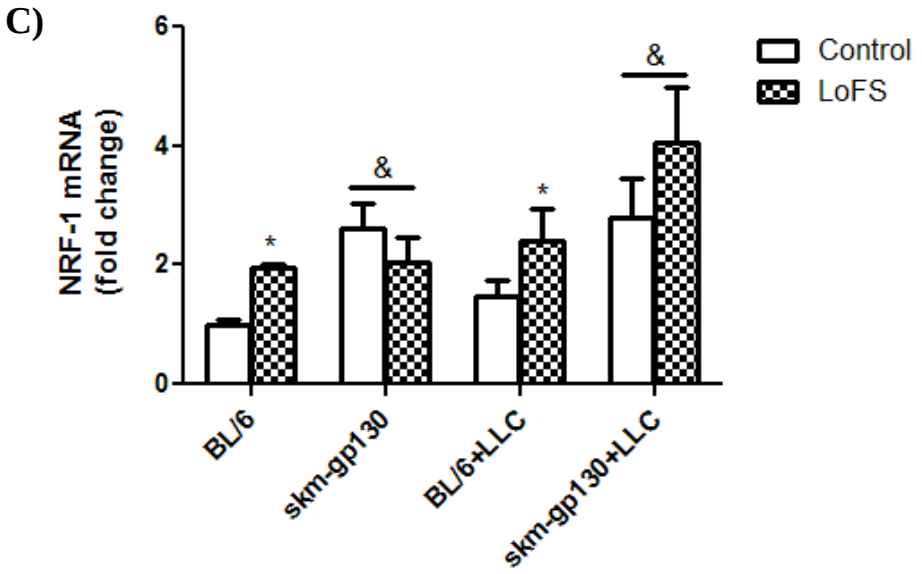

Figure A.5. Effect of skm-gp130 inhibition on LoFS induced PGC-1α targets in LLC-induced cachexia. Skeletal muscle A) TFAM B) cytochrome B and C) NRF-1 mRNA was measured in gastrocnemius of mice 3h post a novel bout of low frequency stimulated contraction. Repeated measures two-way ANOVA was used to examine gp130 x LLC in control and LoFS muscle. # signifies main effect of LoFS, & signifies main effect of skm-gp130, * different from BL/6 control, ** different from control leg within group, $p<0.05$.

APPENDIX B

DETAILED PROTOCOLS

RNA Isolation

1. Clean work area thoroughly with alcohol
2. Label 3 sets of sterile RNAase free 1.5mL eppendorf tubes
3. Homogenize samples in 1mL of Trizol on ice using the polytron
4. Transfer homogenate to a sterile 1.5mL tube
5. Let samples sit at RT for 5 minutes
6. Add 200ul of chloroform to each tube
7. Shake tubes **(DO NOT VORTEX)** for 15-30s (should be the color of pepto bismal)
8. Let samples sit at RT for 2-3min
9. Spin samples at max speed for 15 minutes at 4°C
10. **Clean gloves** and pipette with RNAase AWAY
11. Transfer clear supernatant to new tube **(Do NOT disturb the protein interface, white layer)**
12. Add 500ul of isopropanol and invert to mix
13. Incubate on ice for 20-30 minutes
14. Spin samples at max speed for 15 minutes at 4°C
15. Dump the supernatant being careful not to lose the pellet
16. Add 1mL 75% EtOH in DEPC to RNA pellet invert to break loose
17. Spin at 9500rpm for 5 min at 4°C
18. Dump supernatant and remove all liquid with pipette
19. Repeat steps 18-20 once or twice

20. Air dry tubes upside down in hood for 10-20 minutes
21. Add ~20ul of DEPC water to dissolve pellet **(Keep track of the amount of DEPC added)**
22. Pipette to mix
23. Heat in dry bath at 60°C for 10 minutes
24. Pipette to mix
25. Read on spec(1-2ul RNA+800ul dH_2O) in quartz cuvette/NANO DROP and record 260/280/and 230 measurements
26. Calculate RNA concentration

    RNA= (OD260*40*0.8)/ volume RNA added to cuvette
27. Do not use samples with 260/280 below 1.6

RNA Gel

1. Label a set of 200ul tubes
2. Prepare 100ml 1% agarose gel as follows:
    a. Measure 1.0g Agarose
    b. Add to 72 mL dH_2O
    c. Melt agarose in dH_2O in microwave
    d. Add 10mL of 10X MOPS
    e. Allow to cool under hood
    f. Add 18mL of 37% Formaldehyde
    g. Pour gel
3. Prepare 1X MOPS for running buffer
4. Prepare sample buffer

Reagent	**ul/sample**
10X MOPS	1.5
37% Formaldehyde	2.6
Formamide	7.5
EtBr	0.2
Total	11.8

5. Pull out 1ul of RNA and dilute with DEPC water to load total of 0.5 - 1ug of RNA
6. Add sample buffer 11.8ul/sample + 3.2ul RNA
7. Heat samples at 65 for 15 minutes then **quickly ice**
8. Add 2ul of RNA loading dye to each tube
9. Centrifuge to collect sample to bottom
10. Load and run gel at 80V for ~1h

cDNA synthesis

1.) Prepare reverse transcriptase cocktail as follows and keep on ice:

Reagent	ul/sample
DEPC	4.2
10X RT bx	2.0
dNTP mix	0.8
10X Random Primers	2.0
Reverse Transcriptase	1.0
Total	10.0

2.) In a cold block add 3ug of RNA in a 200ul PCR tube and volume to 10ul with DEPC water

3.) Add 10ul of reverse transcriptase cocktail to each tube

4.) Put in thermocycler on Program #25

   a. 25°C for 10 min

   b. 42°C for 50 min

   c. 70°C for 15 min

   d. 4°C Hold

5.) Store all samples in -20°C

RT PCR

1. Dilute cDNA 1:10 and 1:100
2. Fill out plate template so samples are in duplicate
3. Prepare master mix solutions

Reagent	**ul/sample**
Syber Green Mix	12.5
Forward Primer (20uM)	1.0
Reverse Primer (20uM)	1.0
Sterile dH_2O	0.5
Total	15.0

4. Load 15ul of Master Mix solution
5. Load 10ul of cDNA to each well as per template and pipette to mix
6. Cover plate with plate cover sheet
7. Spin plate in centrifuge in environmental genomics core
8. Put plate RT machine (Dr. Davis Lab)
9. Add dissociation step and set volume to 25ul
10. Start analysis
11. Turn OFF machine when finished

PCR on thermocycler

1. Dilute cDNA 1:10 and 1:100

2. Prepare master mix solutions

Reagent	**ul/sample**
Go Taq	10
Forward Primer (20uM)	0.4
Reverse Primer (20uM)	0.4
Sterile dH_2O	9.2
Total	20.0

3. Load 5ul of cDNA

4. Load 10ul Master Mix

5. Pipette to mix

6. Spin in centrifuge to collect all sample

7. Place in thermocycler on appropriate cycle setting

DNA Gel (PCR Product)

1. Make 1X TAE for running buffer
2. Make 1% agarose gel as follows:
    a. Use autoclave tape to tape sides of plastic mold
    b. Test mold with water to ensure good seal and pour out water
    c. Mix 1g agarose with 100mL 1xTAE in a 150mL flask
    d. Microwave for 30s swirl
    e. Repeat step d
    f. Add 5ul of EtBr and swirl
    g. Repeat step d
    h. Allow Flask to cool to the touch
    i. Pour gel into mold and insert comb
    j. Allow to sit until solidified (approximately 20 min)
3. Prepare samples with loading buffer
    a. Add 5ul of 6X loading buffer and 5ul of sample to a 200ul tube
    b. Vortex and spin to collect sample
4. Load gel
5. Run at 80V for ~ 30min (Gel runs from Black to Red)
6. Use UV imager to take a picture of the gel
7. Save picture, log off computer, and turn off UV light

DNA Isolation

1. Homogenize sample in 1mL DNAzol on ice using glass on glass (or Teflon) for ~5-10s
2. Centrifuge samples at room temperature 10G for 10 minutes
3. In a new sterile set of tubes transfer the supernatant, discard the pellet
4. Add 500ul of 95% EtOH to each sample and mix by gentle inversion (DO NOT VORTEX or PIPETTE VIGEROUSLY)
5. Allow to sit at room temperature for at least 5 minutes (DNA will be a cloudy precipitate).
6. Centrifuge samples at room temperature for 10 min at 4G
7. Discard the supernatant, be sure not to lose the pellet
8. Add 1mL of 75% EtOH to the tubes containing the DNA pellet, and mix by gentle inversion.
9. Centrifuge for 5 min at 4G at room temp
10. Repeat steps 7-9
11. Air dry the samples after removing the supernatant
12. Re-suspend the DNA in 8mM NaOH and pipette gently to mix.
13. Read on spec(1-2ul DNA+1mL 8mM NaOH) in quartz cuvette/NANO DROP and record 260/280/and 230 measurements
14. Calculate DNA concentration if used spec

    DNA= (OD260*50*1)/ volume DNA added to cuvette
15. Store in -20°C

Primer Dilution

1. Find the nMol concentration from the tube, it should be in the range of ~33 nMol.
2. Add TE bx to the tube by a factor of 10. (Ex for a 33.20 nMol primer as 330ul of TE bx.) This will result in the primer concentration to be 100uM.
3. Dilute primers to working concentration of 20uM. Do this by combining 20 ul of the 100uM primer with 80 ul of dH20. This is a 1:5 dilution giving you the working 20uM stock.
4. Place the 100uM primer in the appropriate box, most likely Mouse Primers and put the 20uM stock solution in the clear plastic box named 20uM working primers.

TE bx reagents

300ml solution

1ml Tris HCl 1M

200ul EDTA 0.5M

98.8ul dH20

pH to 8.0

Protein Isolation

1. Make Mueller and Diluent buffer
2. Weigh out the samples to be used and place weighted portion into an ependorf tube labeled with the sample and M.
3. Add 10ul/mg tissue of Mueller buffer to the homogenization tube and add sample.
4. Homogenize in glass on glass tissue homogenizer keeping the sample in ice while homogenizing. (homogenize ~30s check sample repeat if needed)
5. Transfer solution back to ependorf tube
6. Spin samples at 13,000rpm for 10min at 4°C
7. Transfer supernatant to clean ependorf tube labeled with sample and D, discard the pellet
8. Add 5ul/mg tissue of Diluent buffer to the D tube and vortex
9. Run protein assay
10. Dilute samples down to a working concentration in a new tube labeled with the sample and the working concentration. Keep the D tube.

Muller Buffer	Stock concentration	Desired concentration	Volume of stock needed(ul)
Hepes	500mM	50mM	600
Triton-X	100%	0.10%	6
EGTA (pH 8.0)	500mM	4mM	48
EDTA (pH 8.0)	500mM	10mM	120
$Na_4P_2O_7$	100mM	15mM	900
β-glycerophosphate	2M	100mM	300
NaF	500mM	25mM	300
$NaVO_4$	1M	5mM	30
dH_2O	-	-	3585
Protease Inhibitor	-	-	60

Diluent Buffer	Stock concentration	Desired concentration	Volume of stock needed(ul)
glycerol	100%	50%	1500
$Na_4P_2O_7$	100mM	50mM	1500
EGTA (pH 8.0)	500mM	2.5mM	15
β-mercaptoethanol	500mM	1mM	6
Protease Inhibitor	-	-	30

Protein Assay (Bradford Assay)

1. Make a stock of 1mg/ml BSA in PBS
2. In a clear flat bottom 96 well plate create a standard curve with the 1ug/ul BSA solution from 0-14ug in duplicate or triplicate
3. Dilute samples 1:5 in a new tube with water (5ul sample: 20ul dH20)
4. Add 5ul of the diluted samples to the wells of the plate being sure to run them in duplicate or triplicate
5. Make a 1:5 dilution of Bradford reagent. You will need enough for 300ul/well Be sure to clean the glassware well before you use it with soap and water.
6. Add 300ul of diluted Bradford reagent to each well.
7. Let sit in dark drawer for 15 minutes
8. Read in plate reader at 595nm
9. Calculate protein concentration based on standard curve
    a. Create curve being sure to subtract out the zero value from both curve and samples.
    b. Calculate protein concentration using y=mx+b equation (sample=con*slope+intercept -> con=(sample-intercept)/slope)

SDS Page/Western Blot

SDS Page

1. Make gel. Base the % off of what molecular weight the protein of interest is.
2. Prepare samples
    a. Pipette desired amount of protein into ependorf stub
    b. Add equal volume of 2x SDS loading dye
    c. Vortex and do a quick spin
    d. Heat in heat block at 100°C or in boiling water for 5 minutes
    e. Quick spin
3. Load 4ul of protein ladder to the 1st lane in the gel
4. Load all of sample on gel
5. Run gel at 200V for ~1h or until samples have run through the gel

Transfer

6. Prepare 750ml of transfer buffer
7. Prepare membrane by placing in a small amount of methanol for 1 minute
8. Pour methanol into the transfer buffer and wash membranes with the transfer buffer
9. Set up the transfer with the black side of the holder facing down, sponge, blotting paper, gel, membrane (be sure there are absolutely no bubbles between the gel and the membrane), blotting paper, sponge, white/clear side.
10. Carefully close the sandwich and place in the transfer box black side to black side and clear side facing the red side of the transfer box.
11. Place ice pack in the box and pour remaining transfer buffer into the box.

12. Transfer either overnight at 70mA or for 200min at 200mA making sure to pack well with ice.

Probing

13. Prepare 5% milk in TBST solution
14. Remove membrane from transfer and place in ponceau solution for 3-5 minutes
15. Rinse off excess ponceau with dH2O and place membrane in plastic sheet and scan into computer
16. Wash off ponceau with 1XTBST
17. Block the membrane for 1h in 5% TBST milk solution (made in step 13)
18. Incubate in primary antibody in milk solution
19. Wash membranes 3x with 1xTBST for 5 minutes each
20. Incubate in secondary antibody in milk solution for 1 hour
21. Wash membranes 3x with 1xTBST for 5 minutes each
22. Develop with ECL or ECL quantum

Protocol for IHC (vibratome sections) Puromycin

1. Mount sections in acrylamide block and wait 30-60 minutes for block to set
2. Cut sections at 150um-300um thick sections
3. Wash 3x in PBS/0.01M Glycine/0.1% triton-X, 30 min each wash
4. Block in 5% BSA/PBS for 1h
5. Block in 5% Normal Goat Serum in 1%BSA/PBS for 1h
6. Block in FAB (1:100) in 1% BSA/PBS for 1h
7. Incubate in Primary antibody (1:100) ON @ 4°C
8. Wash samples 2x with 1%BSA/PBS, 15 min each wash
9. Block samples in 5% Normal Goat Serum in 1%BSA/PBS for 1h

   From this point forward keep samples covered with foil
10. Incubate samples with Secondary antibody Cy3_Alexa 488 IgG2a (1:100) in 1% BSA/PBS for 1h @37°C
11. Wash 2x with 1%BSA/PBS, 15 min each wash
12. Wash 1x in 1xPBS for 15 min
13. Incubate for 15 minutes in DAPI in PBS (1:5000)
14. Wash 2x in 1xPBS for 15 min each
15. Mount with Dabco
    a. Using glass shards place a shard on either side of the sample
    b. Add ~80ul of Dabco on top of the sample
    c. Very slowly add the cover slip making sure that there are NO BUBBLES and the Dabco goes all the way to the edges
    d. Seal coverslip with nail polish (be liberal to get very good seal)
    e. Store in a sealed container (keep in the dark) @ 4°C

Protocol for SDH Staining

1. Prepare stock solutions

    a. Succinic dehydrogenase solution

        0.59 g Succinic acid
        10 ml dH_2O
        Adjust pH to 7.0 (use low heat to get into solution if necessary

    b. NBT (must be made fresh each time)

        10 mg Nitroblue tetrazolium (NBT)
        2.5 ml dH_2O

2. Using slides cut at 10µm, remove slides from -80°C freezer and air dry for 10 minutes (make up the incubation solution during this time)

    a. Incubation solution

        2.5 ml Nitroblue tetrazolium (NBT)
        3.5 ml dH_2O
        2.5 ml Tris buffer (0.2M, pH 7.4)
        0.5 ml $MgCl_2$ (0.1M)
        1.0 ml Succinic dehydrogenase solution

3. Place slides on a tray and incubate slides in incubation solution at 37°C for 45 minutes
4. Wash slides in running tap water for 3 minutes (do not let the water hit directly on the samples on the slide
5. Dehydrate slides in 50% EtOH for 2 minutes
6. Mount with mounting media and dry
7. Take pictures of slides once media is dry (Next day)
8. Count SDH positive fibers (dark stained) as any that are 2x above the standard deviation of the background

Protocol for IHC (vibratome sections) Myosin Heavy Chain 2A

1. Wash 3x in PBS/0.01M Glycine/0.1% triton-X, 30 min each wash
2. Block in 5% BSA/PBS for 1h
3. Block in 5% Normal Horse Serum in 1%BSA/PBS for 1h
4. Incubate in Primary antibody (1:5) ON @ 4°C
5. Wash samples 2x with 1%BSA/PBS, 15 min each wash
6. Block samples in 5% Normal Goat Serum in 1%BSA/PBS for 1h

   From this point forward keep samples covered with foil
7. Incubate samples with Secondary antibody Cy3 IgG (1:100) in 1% BSA/PBS for 1h @37°C
8. Wash 2x with 1%BSA/PBS, 15 min each wash
9. Wash 1x in 1xPBS for 15 min
10. Incubate for 15 minutes in DAPI in PBS (1:5000)
11. Wash 2x in 1xPBS for 15 min each
12. Mount with Dabco
    a. Using glass shards place a shard on either side of the sample
    b. Add ~80ul of Dabco on top of the sample
    c. Very slowly add the cover slip making sure that there are NO BUBBLES and the Dabco goes all the way to the edges
    d. Seal coverslip with nail polish (be liberal to get very good seal)
    e. Store in a sealed container (keep in the dark) @ 4°C

Mouse Tailing/Genotyping

Print out a Genotyping log sheet

Materials needed:

Genotyping sheet. cages, food, water, cage lids, cage cards/card holders, ear puncher, scissors, 1.5ml ependorf tubes, 15ml falcon tube, PCR tubes, Pipettes (p1000, p100, p20), pipette tips, primers, master mix, nuclease free water, thermocycler.

1. Turn on a water bath to approximately 55 ºC with 1-2 inch of water in the bottom
2. Wean pups- once mice are 4-5 weeks of age wean the pups by separating the male and the females into new cages (limit 5 mice/ cage).
3. On the genotyping sheet fill out the date of birth and the cross that the pups came from. Also write out animal numbers for the mice.
4. Punch the ear of the mouse and write down the ear and mouse number on both the genotyping sheet and the cage card.
5. Once the ear is punched, pinch the tip of the tail and snip just above your finger nails (do not take more than 2-4mm) and put into an ependorf tube labeled with the animal number (not the ear punch).
6. Once this is complete for all of the animals make up the tail digest buffer. In a large (15ml) falcon tube add 200ul of tail buffer/ sample
   and 5ul of proteinase K/ sample. Mix by inversion.
7. Add 200ul of tail digest buffer to each ependorf tube containing the tail and place in a blue tube rack.
8. Place tube rack in the water bath over night (be sure the water covers the bottom of the tubes)

9. Turn Dri-bath to 95ºC
10. Label PCR tubes
11. Once bath is at 95 place ependorf tubes with tail digest into heat block for 10 minutes.
12. Set up PCR reaction.

gp130 Flox	Amount/sample
Master Mix (Go Taq)	12.5ul
Forward Primer- ACGTCACAGAGCTGAGTGATGCAC	0.5ul
Reverse Primer-GGCTTTTCCTCTGGTTCTTG	0.5ul
dH2O	10.5ul
Tail digest (DNA)	1ul

Load 24ul of the PCR reaction and 1ul of DNA

95°C-5 min
35X 95°C-30s
60°C-1 min
72°C-30s
5X 72°C-30s
95°C-30s
72°C- 10 min
4°C hold

Cre reaction: To determine mlc cre heterozygosity two seperate pcr reactions must be run.

mlc Cre F+R	Amount/sample
Master Mix (Go Taq)	12.5ul
Forward Primer- AAGCCCTGACCCTTTAGATTCCATTT	0.5ul
Reverse Primer- AAAACGCCTGGCGATCCCTGAAC	0.5ul
dH2O	10.5ul
Tail digest (DNA)	1ul

mlc cre F+WT	Amount/sample
Master Mix (Go Taq)	12.5ul
Forward Primer- AAGCCCTGACCCTTTAGATTCCATT	0.5ul
WT Primer- GCGGGCTTCTTCACGTCTTTCTTT	0.5ul
dH2O	10.5ul
Tail digest (DNA)	1ul

For each of the two reactions add 24 ul of PCR reaction and 1ul of tail digest (DNA)

94°C-2 min
35X 94°C-1 min
56°C-1 min
72°C-1 min

72°C- 1 min
4°C hold

IL-6 Electroporation

1. Prepare plasmids. They are typically at a concentration of 2-3 ug/ul. Dilute to 1 ug/ul in sterile saline. You will need 50 ug of plasmid per injection.
2. Start anesthesia with Isoflurane at 1-2%/1L O2. (Change percentage of isoflurane based on the level of consciousness of the mice.)
3. Add mice to the anesthesia box.
4. Place mouse under nose cone. Shave top of quad. Alcohol off skin and betadyne.
5. Sterilize Scissors with bead sterilizer and alcohol. Make a small vertical snip with scissors over quad.
6. Inject plasmid (50 ug at 1 ug/ul=50 ul) VERY SLOWLY in the middle of the quad using insulin syringe.
7. Electroporate with default setting. 100 mV; 50 ms; 8 pulses. Make sure electrodes are under the skin, next to the quad. Touch foot pedal once to start the electrical current.
8. Close the incision with a wound clip.
9. Return mouse to cage.
10. Remove wound clip in 7-10 days.

Rotorod Protocol:

1. Make sure that the rotorod is plugged into the computer. Turn on computer then turn on the rotorod
2. Open Rotomex program. Go to **Experimen**t then **Run** then check that the program is correct
3. Program:

   Start Speed: 1rpm

   End Speed: 25rpm

   Acceleration: 0.5rpm/ 2 sec

   Duration: 180sec

   Keep delay set at 2 sec.
4. Record what mouse is in each lane
5. Click **Start Experiment** on computer
6. On rotorod push button for each lane that has a mouse in it then hit Enter on the rotorod and the rotorod will start
7. Record **Total Time** and **Max speed** from the computer on the log for each mouse
8. Move mouse to a new lane and run the trial again do this for a total of 3 trials
9. Clean rotorod with sponge or paper towel and turn off computer and rotorod

Grip Strength Protocol:

1. Weigh mice to get current body weight
2. Plug in and turn on meter
3. Zero out the meter
4. Place mouse on the top of the bars and gently pull down at a constant velocity
5. Record measure and move to the next mouse
6. Once through the mice in a cage (4-5 mice) go back through the mice in the same order
7. Repeat this for a total of 2 runs of 5 trials each
8. Turn off meter
9. Clean up any mess

Fasting Glucose:

1. Fast the mice for 5hours (8am-1pm).
2. Snip a small portion of the tail with clean scissors
3. Get a full drop of blood and measure glucose on the handheld glucometer (make sure the blood goes all the way up the strip to get an accurate reading)
4. Using a plastic capillary tube, collect a sample of blood and put in tube labeled with the mouse number and the age of the mouse. (If doing a vet scan use the vet scan tubes)
5. Keep tubes on ice until all mice are completed.
6. Inject mice with 0.5mL sterile PBS
7. Feed mice and put back in room 14
8. Spin blood in 4°C centrifuge at 10G for 10minutes
9. Separate plasma into a new ependorf tube labeled with the mouse number and the age of the mouse.
10. Store in -80°C chest freezer in a box labeled with experiment, group of mice, age of mice, date, and initials

Glucose gavage:

1. Fast the mice for 5hours (8am-1pm)
2. Make a fresh tube of 20% glucose (2g D+ Glucose volume up in sterile water and filtered with 2um syringe)
3. Snip a small portion of the tail with clean scissors
4. Get a full drop of blood and measure glucose on the handheld glucometer (make sure the blood goes all the way up the strip to get an accurate reading)
5. Using a plastic capillary tube, collect a sample of blood and put in tube labeled with the mouse number and the age of the mouse. (If doing a vet scan use the vet scan tubes)
6. Place a small amount of isofluorane into a bell jar on a paper towel
7. Put mouse in bell jar until just is knocked out (too long will kill the mouse)
8. Using a gavage needle gavage the mouse with 2g/kg of glucose (made is step 2)
9. Wait 30 minutes
10. Wipe of tip of tail and repeat step 4-5
11. Inject mouse with 0.5ml of sterile PBS.
12. Feed mice and put back in room 14.
13. Spin blood in 4°C centrifuge at 10G for 10minutes
14. Separate plasma into a new ependorf tube labeled with the mouse number and the age of the mouse.
15. Store in -80°C chest freezer in a box labeled with experiment, group of mice, age of mice, date, and initials

DEXA protocol:

1. Plug in the DEXA machine and connect to the computer
2. Turn on the DEXA and then turn on the computer
3. Open PIXIMUS software
4. Calibrate the DEXA machine
    a. Place the phantom mouse on the scanner
    b. Press F6 for quality control
    c. Press F3 and then click ok (this will run the quality control)
    d. Exit the room and wait until the scan is completed
5. Anesthetize mice in the isoflurane chamber for several minutes on ~2.5% isoflurane/L O_2/min
6. Set up nose cone so that it is on the edge of the scanning platform
7. Place mouse belly down with the four limbs spread out and the nose in the nose cone, be sure to keep the mouse within the designated area
8. Select "analyze new subject" or press F3
9. Enter in the subject ID and the body weight and press ok
10. Press F3 to start the scan
11. Exit the room and wait until the scan is complete (a colored outline will appear on the computer screen when the scan is complete.
12. To adjust the region of interest press the F3 key twice
13. Use the arrow keys to adjust the green circle (the area excluded from the results)
14. Press enter

15. Record your data in your lab notebook

16. Press F8 twice to go back to the main menu for the next scan

*Calibration only needs to be done prior to the first mouse measurement

Run to Fatigue:

1. Acclimate mice to the treadmill by placing mice in the lanes 10-15 minutes prior to the start of the warm-up
2. Run the warm-up protocol

   5min at 5m/min, 5min at 10m/min, 5min at 15m/min
3. Start the fatigue test running mice at 20m/min
4. After 30 minutes increase the speed to 25m/min
5. Use gentle hand prodding to keep mice running
6. Fatigue will be defined as the time at which mice are **no longer able or willing to keep up** with the treadmill despite gentle hand prodding **for a period of 1min**.
7. Clean the treadmill and the area around it with a sponge or paper towels. Sweep the floor around the treadmills. There should be no feces on the treadmill, the treadmill cart, or the floor when you leave.

APPENDIX C

DOCTORAL DISSERTATION PROPOSAL

The regulation of skeletal muscle mass and mitochondrial biogenesis by gp130/STAT signaling during cancer cachexia

by

Melissa J Puppa

March 31, 2013

C.1 Specific Aims

Cancer cachexia accounts for approximately 20% of all cancer related deaths and about 40% of deaths related to colon cancer (Bruera, 1997; Tisdale, 2002). Cachexia is defined as the unintentional loss of body weight with an underlying disease present (Evans et al., 2008; Fearon et al., 2011; Muscaritoli et al., 2010). While cachexia consists of the loss of both skeletal muscle and adipose tissue, maintenance of skeletal muscle mass has proven to be of importance. A potential mediator of skeletal muscle mass during cachexia is the inflammatory cytokine interleukin 6 (IL-6). Inflammation is a prominent feature during the promotion and progression of colon cancer cachexia, and high IL-6 levels are correlated with cachexia in late stage cancer patients (Iwase et al., 2004). Over-expression of IL-6 in tumor bearing mice can decrease skeletal muscle mass in a dose dependent manner (White et al., 2012a). Inhibition of IL-6 signaling via an IL-6 receptor antibody or by knocking out IL-6 attenuates skeletal muscle wasting in the $Apc^{Min/+}$ mouse model of cachexia; however it is unclear whether these actions are from the systemic inhibition of IL-6 signaling or whether they are dependent on the local inhibition of IL-6 signaling in the muscle itself (Baltgalvis et al., 2008b; White et al., 2011b).

IL-6 is a pleotropic cytokine secreted from many different tissues including skeletal muscle. IL-6 has both pro-inflammatory and anti-inflammatory properties as well as the ability to activate target genes for cell proliferation, differentiation, and apoptosis (Heinrich et al., 2003). During cachexia, IL-6 may act on the tumors, stimulating growth and differentiation, or IL-6 may act directly on peripheral tissues, such as skeletal muscle, that are atrophying. The initiation and progression of cachexia in both of these models is

directly related to tumor burden and circulating IL-6 levels (Baltgalvis et al., 2008b; White et al., 2011b). IL-6 signals through the glycoprotein 130 (gp130/CD130) receptor to activate downstream signaling. This occurs by binding with the membrane IL-6 receptor and forming a complex with the gp130 receptor to activate downstream signaling including the JAK/STAT, RAS/ERK, and MAPK pathways during classical signaling (Ernst and Jenkins, 2004). Alternatively it can bind the soluble IL-6 receptor and interact with the membrane bound gp130 receptor which is called trans signaling. Trans signaling can activate downstream signaling in tissues that do not express the IL-6 receptor, or express IL-6 receptor in very low levels such as the kidney (Nechemia-Arbely et al., 2008), as well as enhance the actions of IL-6 on tissues that express the IL-6 receptor. Bonetto et. al. showed that muscle STAT3 signaling, a downstream mediator of inflammatory and IL-6-gp130 signaling, is sufficient for inflammation and cancer-induced muscle wasting in some tumor bearing mice (Bonetto et al., 2012; Bonetto et al., 2011). STAT3 inhibition can attenuate muscle loss suggesting that the JAK/STAT pathway is an important downstream effector of IL-6-gp130 signaling in skeletal muscle during cachexia (8). The role of classical and trans IL-6 signaling and whether IL-6 is acting through local or systemic STAT3 activation during cancer cachexia remains uninvestigated.

Mitochondrial biogenesis and function, is associated with a muscle's metabolic capacity and substrate utilization flexibility (Chomentowski et al.). Muscle mitochondrial function is related to muscle apoptosis, autophagy, and protein turnover thus mediating skeletal muscle mass (Romanello and Sandri, 2010). We have shown that when IL-6 is administered to C2C12 myotubes mitochondrial content decreases and, mitochondrial

fission increases (White et al., 2012c). There is also an IL-6 induced decrease in myotube diameter (White et al., 2012c). Mitochondria are dysregulated in the skeletal muscle of rodents with cancer cachexia (White et al., 2011a; White et al., 2012c). Many studies have shown that the dysregulation of muscle mitochondrial signaling including decreased mitochondrial biogenesis, altered dynamics, and decreased function can lead to muscle loss (Romanello et al., 2010). These results have been extended to the cachexia field by our experiments in the $Apc^{Min/+}$ mouse which show a loss of mitochondrial content with the progression of cachexia and IL-6 overexpression (White et al., 2011a; White et al., 2012c). We have shown that systemic inhibition of IL-6 signaling after the initiation of cachexia can attenuate mitochondrial dysfunction in the $Apc^{Min/+}$ mouse (White et al., 2012c). Exercise training, which is known to increase mitochondrial plasticity, can prevent mitochondrial dysfunction even in the presence of increased circulating IL-6 (Puppa et al., 2011d). While IL-6 signaling appears to be a regulator of mitochondrial function during cachexia, it is unclear whether these actions involve direct signaling in the muscle through the gp130 or if IL-6 action on alternative tissues leads to dysregulation of skeletal muscle mitochondria.

Inhibition of either STAT3 or IL-6 attenuates muscle loss with cancer (Baltgalvis et al., 2008b; Bonetto et al., 2012; Bonetto et al., 2011; White et al., 2011b; White et al., 2012c). While there is evidence showing that IL-6 inhibition preserves skeletal muscle quality related to mitochondrial biogenesis and function, it is unclear if these actions are from local inhibition at the level of the skeletal muscle or if systemic inhibition of IL-6 signaling is important for the protection of muscle quality. While STAT3 inhibition preserves skeletal muscle mass during cancer cachexia, STAT3 regulation of muscle

mitochondrial plasticity during cancer cachexia remains to be established. The overall goal of this proposal is to determine the regulation of skeletal muscle mass and mitochondrial biogenesis by IL-6 signaling and muscle contraction during cancer cachexia. Our *central hypothesis* is that IL-6 signaling through gp130 and STAT3 will suppress muscle mass and mitochondrial biogenesis during cachexia, and gp130/STAT3 inhibition will attenuate muscle mass loss and increase mitochondrial plasticity resulting in an enhanced response to contraction.

Specific Aim #1 will determine if attenuation of systemic trans IL-6 signaling/STAT3 or local IL-6 signaling through gp130 can prevent mitochondrial loss and altered mitochondrial dynamics during cancer cachexia.

Rational: We have previously shown that systemic inhibition of IL-6 signaling in the $Apc^{Min/+}$ mouse can repress increases in mitochondrial fission and attenuate the loss of mitochondrial content (White et al., 2012c). We have also shown that inhibition of IL-6 signaling decreases protein degradation, but does not appear to have a potent affect on protein synthesis (White et al., 2011b). Thus we would like to investigate if the actions of IL-6 inhibition are due to attenuation of systemic trans IL-6 signaling.

Hypothesis #1: The inhibition of systemic IL-6 trans signaling/STAT3 in Min mice will increase mitochondrial fusion and decrease fission and prevent the loss of oxidative capacity.

Hypothesis #2: The inhibition of skeletal muscle gp130 signaling Min mice will attenuate the loss of skeletal mitochondrial oxidative capacity and inhibited mitochondrial biogenesis.

Hypothesis #3: The inhibition of IL-6 trans signaling will attenuate the induction of muscle protein degradation, but will have no effect on skeletal muscle protein synthesis.

Specific Aim #2 will determine if IL-6 signaling through muscle gp130 receptor/ STAT3 regulates the disruption of muscle mass in the cachectic muscle.

Rational: We have previously shown the induction of skeletal muscle protein degradation and suppression of protein synthesis during IL-6 induced cachexia (White et al., 2011b; White et al., 2013b). Additionally, STAT3, a downstream mediator of IL-6/gp130 signaling, can attenuate skeletal muscle wasting in cancer-induced cachexia (Bonetto et al., 2012; Bonetto et al., 2011); however the actions of local IL-6 signaling and the role of systemic STAT3 signaling on muscle mass regulation during cachexia is unknown. IL-6 and STAT3 clearly regulate muscle mass during cachexia, but it is unclear whether these actions are from systemic activation or local activation of the gp130/STAT3 pathway.

Hypothesis #1: The loss of skeletal muscle gp130 receptor signaling will prevent cachexia-induced decreases in skeletal muscle protein synthesis attenuated increases in protein degradation during cancer cachexia.

Hypothesis #2: The inhibition of systemic STAT3 signaling will suppress cachexia-induced decreases in skeletal muscle protein synthesis attenuated increases in protein degradation.

Hypothesis #3: The loss of STAT3 signaling will attenuate increased protein degradation, but not alter protein synthesis during cancer cachexia.

Specific Aim #3 will determine if the transcription and translation of proteins regulating mitochondrial biogenesis are altered with acute contraction during cachexia.

Rational: We have previously shown that exercise training prior to the initiation of cachexia attenuates the loss of skeletal muscle mitochondrial content in the $Apc^{Min/+}$ mouse (Puppa et al., 2011d). Our preliminary data suggests that cachectic muscle has the capacity to up-regulate nuclear encoded mitochondrial gene (NUGEMPs) transcription after a novel bout of contraction, but this increase in transcription is not associated with an increase in translation of the proteins. It is unclear if cachectic skeletal muscle has altered mitochondrial plasticity in response to an acute contraction bout. Understanding the ability of cachectic muscle to respond to contraction will have therapeutic value for the treatment of cachectic patients.

Hypothesis #1: The translational response of NUGEMPs and mitochondrial proteins to an acute endurance-like contraction bout will be blunted in cachectic mice, while the transcriptional response of NUGEMPSs and mitochondrial genes will remain unaltered.

Hypothesis #2: Inhibition of systemic inflammation will alleviate the suppression of NUGEMP translation after an acute contraction bout.

C.2 Limitations and Pitfalls

1) The use of a soluble gp130 fusion protein allows for the examination of inhibition of IL-6 trans signaling; however, there are currently no muscle specific knockouts of the membrane bound IL-6 receptor to determine the effects of classical IL-6 signaling during cancer cachexia.
2) The use of the gp130 fusion protein inhibits global trans signaling. Results from these experiments must be interpreted as such since IL-6 signaling will be repressed in multiple tissue types which could have effects on skeletal muscle mitochondrial biogenesis and dynamics.
3) A muscle specific IL-6 receptor knockout mouse has not yet been developed, so we chose to develop a muscle specific gp130 knockout mouse. Many cytokines act through the gp130, several which are elevated during cancer cachexia including IL-6, leukemia inhibitory factor (LIF), and ciliary neurotrophic factor (CNTF). The inhibition of all IL-6 family of cytokines must be taken into consideration when interpreting the results from these experiments.
4) The use of the compound PDTC has been shown to decrease the production of IL-6 as well as inhibit STAT3 activation and NFκB activation. While we are less interested in the inhibition of NFκB it must be considered when interpreting the results.
5) STAT3 signaling will be globally inhibited by PDTC administration. Further experiments would be needed to examine the direct role of STAT3 on skeletal muscle mitochondrial biogenesis and dynamics.

6) Only one time point will be used to examine the acute effects of contraction on skeletal muscle mitochondrial plasticity. Further experiments would be needed to determine if a delayed response is present.
7) It is unknown if mice with a skeletal muscle deletion of gp130 will respond to acute contraction normally. Experiments using IL-6KO mice have shown a differential response to contraction compared to wild type animals. While an altered response in the wild type mice would prove interesting they would have to be taken into consideration since the aim of the study is to determine if there are improvements with cancer cachexia.
8) Only the effects of the treatments on mitochondrial biogenesis and dynamics will be assessed. Conclusions pertaining to mitochondrial function can only be made related to these variables although it is likely that changes in mitochondrial respiration and ATP production may exist.

C.3 Preliminary Data

The role of IL-6 on cachexia development and skeletal muscle protein turnover has been studied extensively by our lab. We have characterized the progression of cachexia in the Min model of colon cancer cachexia in relation to protein turnover and skeletal muscle mitochondrial content (White et al., 2011b; White et al., 2013b). The Min mouse displays increases in muscle protein degradation, decreases in muscle protein synthesis and mitochondrial content, and alterations in mitochondrial dynamics with the progression cachexia (White et al., 2011a; White et al., 2013b; White et al., 2012c). Importantly we have shown that the Min mouse develops and IL-6 dependent cachexia and inhibition of IL-6 prevents the progression of cachexia (Baltgalvis et al., 2008b; Baltgalvis et al., 2009b).

We have published that global inhibition, that is both inhibition of classical and trans IL-6 signaling together, can attenuate muscle mass loss and mitochondrial dysfunction in the ApcMin/+ mouse (White et al., 2011a; White et al., 2012c). We have preliminary data showing increases in the soluble IL-6 receptor prior to weight loss (Figure C.1) leading us to believe that IL-6 trans signaling is playing a vital role in the progression of cachexia. Dr. Rose-John has successfully developed a fusion protein to specifically inhibit IL-6 trans signaling both in vitro and in vivo (Atreya et al., 2000; Barkhausen et al.; Jones et al., 2011; Lo et al., 2011; Nechemia-Arbely et al., 2008; Nowell et al., 2003; Rose-John, 2012; Waetzig and Rose-John, 2012). To further explore the role of IL-6 signaling on skeletal muscle mass regulation we have developed a mouse

with a muscle specific knockout of the gp130 (Figure C.2). We have previously initiated studies using the Lewis lung carcinoma model of cachexia in collaboration with Dr. Mark Davis's lab to examine the effects of nutraceuticals on cachexia development. We have preliminary data in the LLC model of cancer cachexia showing attenuation of skeletal muscle mass loss without alterations in tumor burden or systemic inflammation in the skeletal muscle gp130 knockout mouse, skm-gp130 (Figure C.3). Associated with the decreases in skeletal muscle mass are decreased in mitochondrial content as measured by Cytochrome C which is attenuated in the skm-gp130 mice with LLC tumors (Figure C.4). We have successfully crossed the skm-gp130 mouse with the Min mouse and are in the process of breeding and aging these animals.

Our lab has previously published that activity in the Min mouse decreases prior to initial declines in muscle mass and body weight and regular moderate exercise can attenuate cancer cachexia progression in the Min mouse (Baltgalvis et al., 2008a; Baltgalvis et al., 2009a; Baltgalvis et al., 2010; Puppa et al., 2011d). Preliminary data supports the hypothesis that inhibition of skeletal muscle gp130 attenuates losses in skeletal muscle endurance capacity as the skm-gp130 Min mouse has an increased time to fatigue on a treadmill running test when compared to the Min mouse at 12 weeks of age (Fig C.5). To further investigate the role of muscle gp130 in the progression and prevention of cachexia we want to explore if inhibition of gp130 signaling can improve the mitochondrial transcriptional and translational responses to contractions. We have previously published that exercise or inhibition of IL-6 signaling can attenuate decrease in mitochondrial content and alterations in mitochondrial dynamics in the Min mouse; however, the combination of the two therapies has not been explored (Puppa et al.,

2011d; White et al., 2011a; White et al., 2012c). We have preliminary data showing that skeletal muscle of cachectic mice is capable of responding to an acute bout of contraction through increased gene expression (Figure C.6); however, it is unknown if an acute bout of contraction is capable of increasing genes regulating mitochondrial biogenesis in cachectic muscle and if the increases in gene expression result in increases in the protein levels.

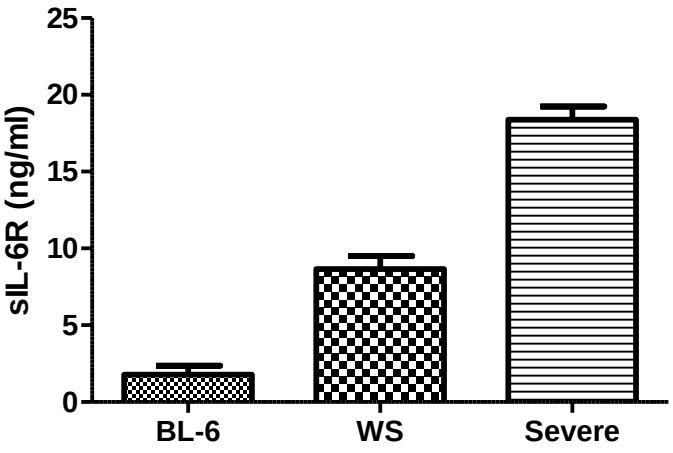

Figure C.1. Plasma sIL-6R levels in the Min mouse. Soluble IL-6 receptor (sIL-6R) was measured in plasma taken from wild type BL-6 mice, weight stable Min mice at 12 weeks of age (WS), and severely cachectic mice at 20 weeks of age (Severe).

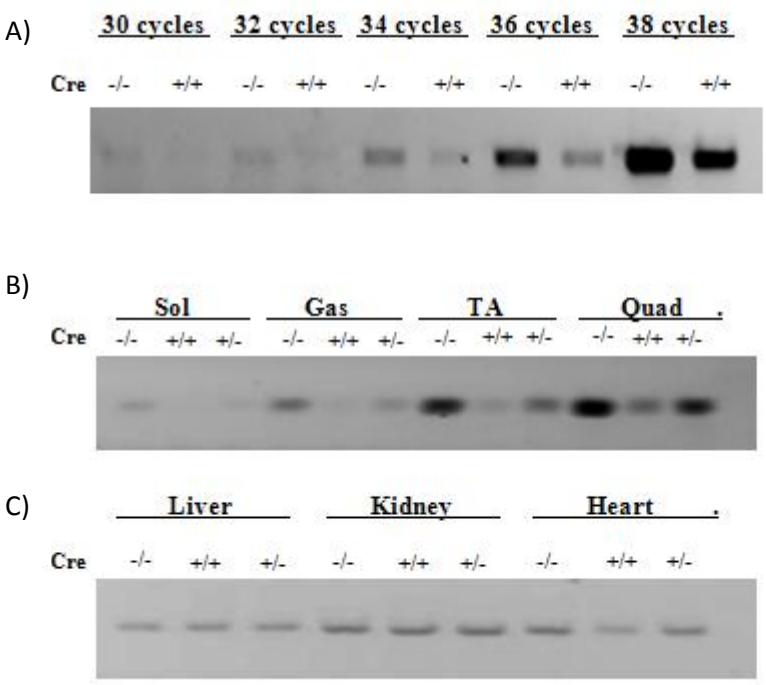

Figure C.2. Characterization of the muscle specific gp130 receptor knockout mouse (skm-gp130). A) PCR analysis of gp130 mRNA (643bp product size) in quadriceps muscle of wild type (Cre -/-) and skm-gp13 (cre +/+) mice. B) Differential expression of gp130 mRNA in the soleus (sol), gastrocnemius (gas), tibialis anterior (TA), and quadriceps (Quad) muscles of gp130 floxed mice with heterozygous or homozygous cre expression. C) gp130 mRNA expression in the liver, kidney and heart.

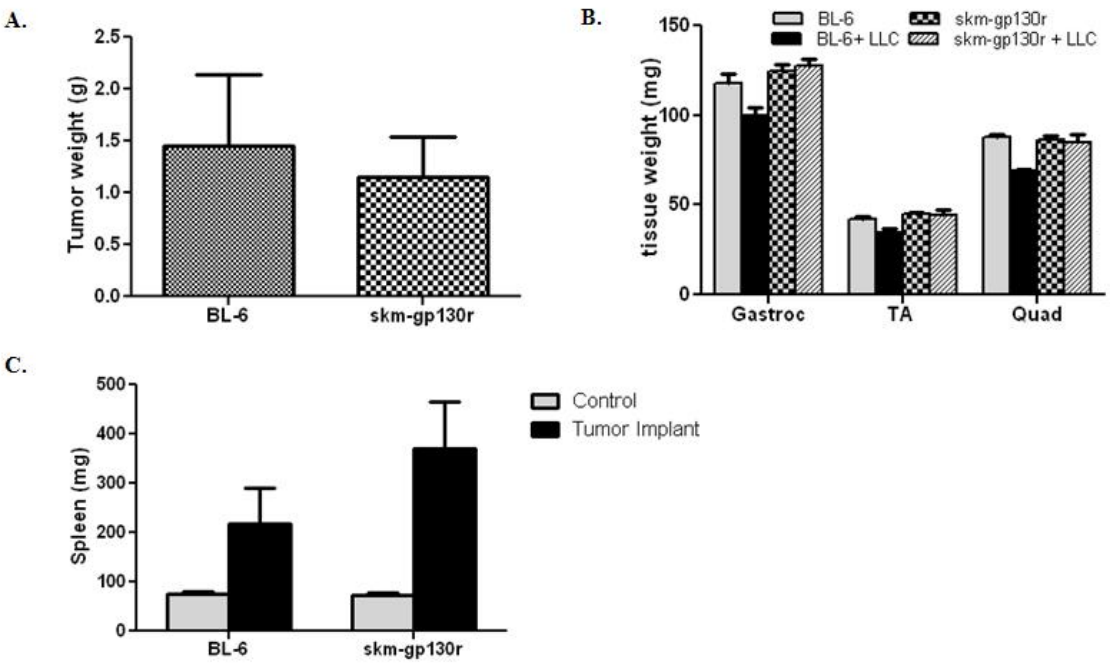

Figure C.3. The effect of skm-gp130 on development of cancer induced cachexia. At 8 weeks of age wild type BL-6 mice and skm-gp130 mice expressing heterozygous cre (skm-gp130) were implanted with LLC tumor cells. Tumors were allowed to grow until 13 weeks of age. A) tumor weights and B) muscle mass of gastrocnemius (gastroc), tibialis anterior (TA) and quadriceps (quad) and C) spleen weight were measured at the time of sacrifice.

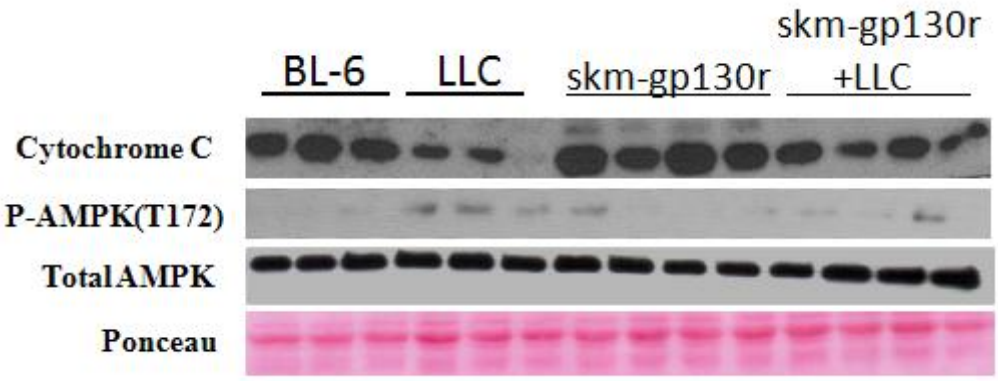

Figure C.4. The effect of skm-gp130 on muscle mitochondrial capacity in the LLC tumor implant model. Western blots of cytochrome C, P-AMPK, total AMPK and ponceau stain.

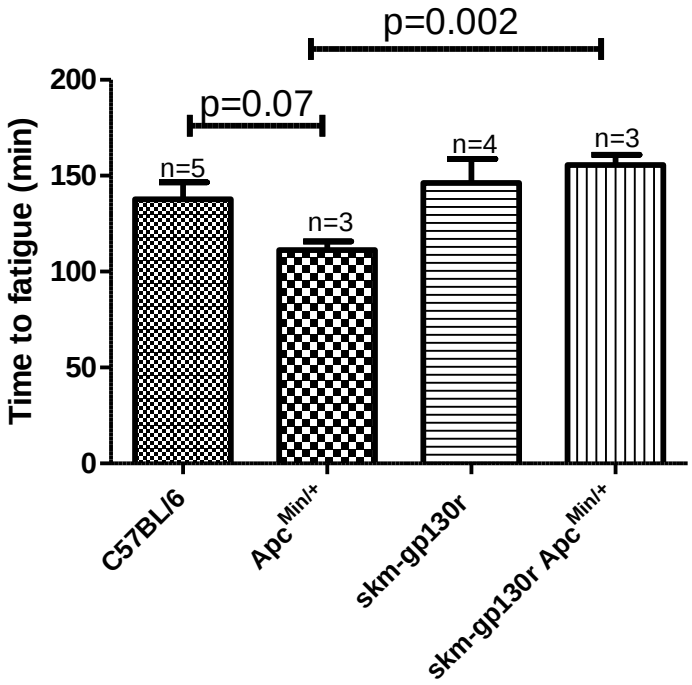

Figure C.5. Run to fatigue in Min mice lacking skm-gp130. At 12 weeks of age mice underwent a run to fatigue test. Mice were acclimated to the treadmill for 30 minutes prior to the test. The warm up consisted to 15 minutes of running (5min @ 5m/min, 5min@ 10m/min, and 5min@ 15m/min). The time started when the treadmill speed was increased to 20m/min. Mice ran at 20m/min for 30min and then 25m/min for the remainder of the test. Mice were removed when they no longer ran for a duration of 1min despite gentle hand prodding.

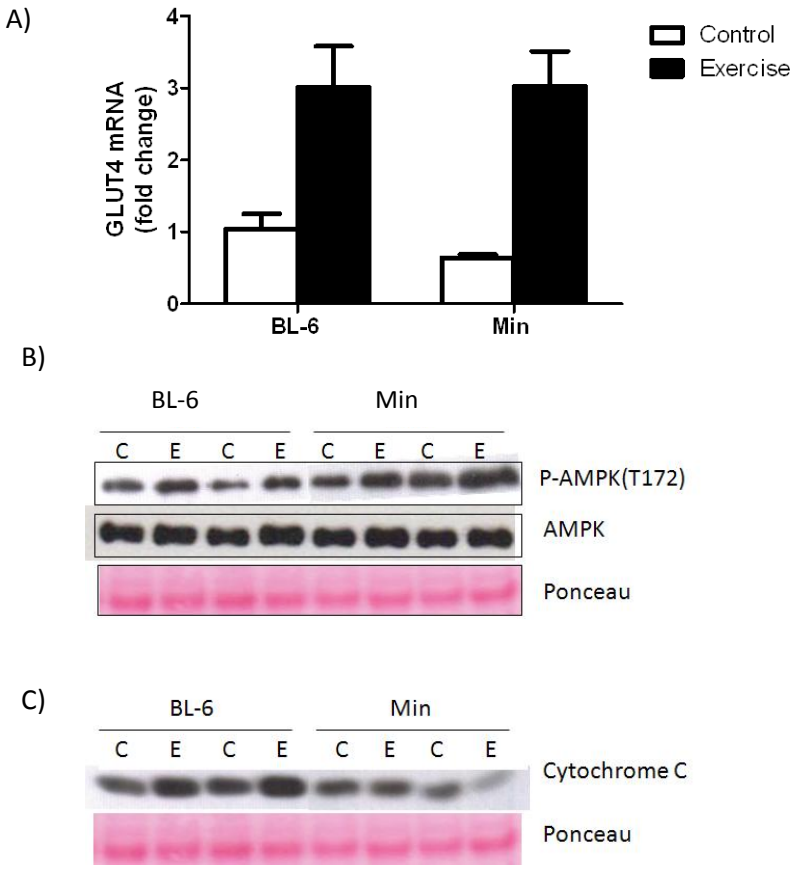

Figure C.6. The effects of an acute bout of contraction on skeletal muscle in Wild type (BL-6) and ApcMin/+ (Min) mice. Mice received a single 30 minute bout of low frequency stimulation. 3 hours after the completion of the stimulus animals were sacrificed. A) Skeletal muscle glucose transporter (GLUT4) mRNA levels were measured in the gastrocnemius to validate a skeletal muscle response to the contraction. B) Western blot analysis of AMPK activation was measured to further validate the model. C) Cytochrome C, a marker of mitochondrial content was measured in the gastrocnemius by western blot analysis.

C.4 Research Design and Methods

Specific Aim #1 will determine if attenuation of trans IL-6 signaling can prevent the loss of mitochondrial biogenesis and altered mitochondrial dynamics associated with cancer cachexia.

Rational: We have previously shown that systemic inhibition of IL-6 signaling through administration of an IL-6 receptor antibody in the $Apc^{Min/+}$ mouse can repress increases in mitochondrial fission and attenuate the loss of mitochondrial content (White et al., 2012c). Because the IL-6 receptor antibody blocks both classical and trans IL-6 signaling it is unknown if the inhibition of classical or trans signaling is responsible for the improvements in skeletal muscle mitochondrial content in cachectic mice. Inhibition of IL-6 trans signaling has been shown to decrease tumor formation in cancer (Lo et al., 2011; Rose-John et al., 2006); however the mechanisms underlying this are unknown. It is also unknown if inhibition after the formation of the tumors and initiation of cachexia will be protective. In this aim we would like to investigate if the actions of improved mitochondrial biogenesis and dynamics, and suppressed protein degradation during cachexia are due to attenuation of trans IL-6 signaling.

Experimental design for specific aim #1. Experiment 1 will determine the role of IL-6 trans signaling on skeletal muscle mitochondrial biogenesis and dynamics during cachexia.

At approximately age 16wk of age mice will be randomized to a control group or treatment group. An IL-6 fusion protein (sgp130Fc) will be injected once weekly for two weeks starting at approximately 16wk of age. Control mice will receive an injection of

sterile PBS once weekly for two weeks. Min mice have initiated body weight loss by 15-16 weeks of age making it an ideal time point to the role of IL-6 trans signaling on cachexia progression. All mice will be housed in standard cages until the time of sacrifice. Body weight food consumption and body temperature will be measured before and during treatment with sgp130Fc or PBS. At sacrifice skeletal muscles, epidydimal fat, intestines, plasma, and tibia will be collected. Skeletal muscle will be weighted and frozen for tissue analysis of mitochondrial content, dynamics, and biogenesis by protein, RNA, and enzyme activity via succinate dehydrogenase (SDH) staining. Polyp counts of the intestines will be conducted to determine tumor burden. Tibia length will be measured to normalize mice to body size.

Experiment #1 will determine if inhibition of IL-6 trans signaling in $Apc^{Min/+}$ mice will increase mitochondrial fusion decrease fission and improve mitochondrial oxidative capacity.

Animals. *$Apc^{Min/+}$* male mice on a C57BL/6 background will be bred with female C57BL/6 mice in the USC animal resource facility. Animals will be genotyped as heterozygous for the *Apc* gene. All mice will be provided with standard rodent chow (Harlan Teklad Rodent Diet, #8604, Madison, WI) and water ad libitum. Body weights will be measured weekly throughout the course of the study. At 16 weeks of age mice will be assigned to one of two groups; control or sgp130Fc. A soluble gp130 fusion protein, provided by Dr. Stefan Rose-John (Conaris, Germany), will be used to inhibit IL-6 trans signaling and sterile PBS will be used as a control. sgp130Fc will be administered to mice intraparotaneally once weekly at a dose of 150ug in a volume of 100ul per mouse for a total of two weeks. All mice will be sacrificed at 18 weeks of age after two weeks of

the respective treatment. Based on data using the IL-6 receptor antibody 6 mice per group is sufficient to detect a 5% difference in markers of mitochondrial fission. A subset of wild type C57BL/6 mice (n=3/group) will receive an acute exposure to LPS, which has been shown to induce IL-6 trans signaling, with or without the Sgp130Fc. LPS has been extensively published to rely on IL-6 trans signaling. The kidney will be used as a control to show that IL-6 trans signaling is suppressed as the kidney has very low expression levels of the IL-6 receptor.

Table C-1. Animal treatment groups for experiment #1.

Strain	Treatment	Age (weeks)	n
C57BL/6	PBS	16-18	5-6
C57BL/6	sgp130Fc	16-18	5-6
C57BL/6	skm-gp130	16-18	5-6
$Apc^{Min/+}$	PBS	16-18	5-6
$Apc^{Min/+}$	sgp130Fc	16-18	5-6
$Apc^{Min/+}$	skm-gp130	16-18	5-6

Primary outcomes:

Mitochondrial Biogenesis:

Mitochondrial Biogenesis will be measured by examining the levels of PGC-1α, a co-activator of many genes regulating mitochondrial biogenesis, and Mitochondrial Transcription Factor A (TFAM). An upstream regulator of PGC-1 that is known to be altered during cachexia is AMP-activated protein kinase (AMPK) and will be measured at the phosporylation site T172 as well as total levels.

Mitochondrial Content:

Mitochondrial content will be measured by examining levels of mitochondrial electron

transport chain complex COX IV or cytochrome c via western blot analysis. Content will be further validated by measurement of mitochondrial DNA (cytochrome B gene) normalized to genomic DNA (GAPDH gene). Succinate dehydrogenase staining of myofibers will be used to analyze the percentage of highly oxidative fibers, an indicator of mitochondrial content, in the tibialis anterior muscle.

Mitochondrial Dynamics:

Mitochondrial dynamics will be measured using western blot analysis of mitofusin 1 (MFN1), a marker of mitochondrial fusion, and mitochondrial fission 1 (FIS), a marker of mitochondrial fission as well as mRNA levels of MFN1/2 and FIS1.

Secondary outcomes:

Protein turnover: Markers of protein synthesis including p-S6: total S6 will be measured via western blot analysis as well as incorporation of puromycin into muscle protein. Atrogin-1 will be measured as a marker of protein degradation.

Inflammation: Markers of skeletal muscle inflammation p-STAT3:STAT3 and p-AMPK:AMPK will be measured via western blot analysis.

Specific Methodology Aim #1:

Animals. *Apc*$^{Min/+}$ male mice on a C57BL/6 background will be bred with the gp130 fl/fl mice provided by Dr. Colin Stuart's lab in collaboration with Dr. Hennighausen (NCI) (Zhao et al., 2004). Fl/fl *Apc*$^{Min/+}$ male mice will then be bred with cre-expressing mice driven by myosin light chain which were secured from Dr. Steven Burden (NYU) (Bothe et al., 2000). The resulting fl/fl cre/cre and fl/fl cre/cre *Apc*$^{Min/+}$ mice will have a skeletal

muscle deletion of the gp130 protein. $Apc^{Min/+}$ and C57BL/6 males will be used for controls. Offspring will be genotyped for cre recombinase, floxed gp130, and the *Apc* by taking tail snips at the time of weaning. All animals will be housed in standard cages and the room will be maintained on a 12:12 light:dark cycle with the light period starting at 0700. Mice will be provided with ad libitum access to water and standard rodent chow (Harlan Teklad Rodent Diet #8604). Food consumption will be monitored during the course of the study. Body weight will be measured weekly and animals losing more than 20% body weight will be promptly removed from the study and euthanized. All animal experimentation is approved by the University of South Carolina's Institutional Animal Care and Use Committee.

Genotyping: All animals will be genotyped using a tail snip. At 4-5 weeks of age animals a weaned, numbered, and a small tail snip (~1-2mm) collected. The tail snip is digested in 200ul of tail digest buffer and 5ul of proteinase K. Tails are incubated overnight in a water bath set at 37°C. After incubation samples are heat shocked at 95°C in a dri-bath for 10 minutes. Heterozygousity of the *Apc* gene will be determined via a PCR reaction (*Apc* forward 5' TGAGAAAGACAGAAGTTA 3", reverse 5' TTCCACTTTGGCATAAGGC 3'). PCR products are run out on a 1% agarose gel and exposed to UV light. Presence of a band indicates heterozygosity of the *Apc* gene.

Tissue Collection: Mice will be anesthetized with a subcutaneous injection of ketamine/acepromazine/xylazine cocktail (1.4mL/kg BW). Blood will be collected from the retro-orbital sinus using a capillary tube. Blood will be spun at 4°C, 10,000rpm, for 10 minutes. Plasma will then be pipetted off and stored at -80°C until analysis. Gastrocnemius (gas), plantaris (pla), soleus (sol), tibialis anterior (TA), extensor

digitorum longus (EDL), and quadriceps (quad) will be excised rinsed in PBS, weighed, snap frozen in liquid nitrogen, and stored at -80°C until further analysis. Epididymal fat pads and tibia length will also be measured. Tibia length will be used as a measure of body size and a correction factor for skeletal muscle and body weight measures. The small intestine will be dissected distally to the stomach and proximal to the cecum. Intestine will be cut into four sections rinsed with PBS and opened longitudinally. Sections will be fixed in 10% formalin for 24h and stored in 70% ethanol and used for tumor counts in the $Apc^{Min/+}$ mice.

Plasma IL-6: Plasma IL-6 will be measured using a mouse specific ELISA kit. Approximately 25-50ul of plasma will be incubated. A standard curve will be used to determine the levels of circulating IL-6 in all samples before and after treatment with the sgp130Fc. An ELISA plate will be coated with capture antibody using a coating buffer and set to incubate in 4°C overnight. After washing the plate 100ul of blocking solution is added for 1h. After three washes 100ul of standard or diluted sample is added to the wells in duplicate and incubated for 2 hours at room temperature. After washes 100ul of the detector antibody solution is added and incubated for 1h. After 7 washes 100ul of TMB cocktail is added to each well and stored in the dark for 30 minutes. Fifty microliters of Stop solution is added to the wells and the plate is read at 450nm and 570nm according to the manufacturer's instructions.

Polyp count: Intestinal polyps will be performed as previously described (Baltgalvis et al., 2008b). At the time of sacrifice intestines will be carefully dissected out and mesenteric fat will be removed. Intestines will be cleaned in PBS cut into 5 sections from the proximal to the distal end and opened longitudinally. All sections will be laid flat and

fixed in formalin for 24 hours and stored in 70% ethanol until analyzed. Sections will be stained with 0.1% methylene blue. Using a dissecting microscope and tweezers all intestinal polyps will be counted and categorized as <1mm, 1-2mm, >2mm in size.

mtDNA: Mitochondrial DNA will be used to determine relative mitochondrial number. DNA will be isolated from 20-30mg of skeletal muscle using DNAzol (Invitrogen) and resuspended in 8mM NaOH. Purity and quantity of DNA will be determined from the 260/280 ratio. PCR will be run with the DNA sample with cytochrome B forward: 5′-ATT CCT TCA TGT CGG ACG AG-3′; cytochrome B reverse: 5′-ACT GAG AAG CCC CCT CAA AT-3′; Gapdh forward: 5′-TTG GGT TGT ACA TCC AAG CA-3′; Gapdh reverse, 5′-CAA GAA ACA GGG GAG CTG AG-3′.

RNA isolation: RNA will be isolated from skeletal muscle using TRIzol reagent (Life Technologies, Grand Island, NY). Isolated RNA absorbance will be measured at 260nm and 280nm to determine RNA purity and quantity. RNA quality will be analyzed by running samples out on an agarose gel. CDNA will be synthesized using 1ug of RNA in a 10ul volume will be added to 10ul of cocktail consisting of 10X RT buffer, dNTP mix, 10X random primers, and reverse transcriptase.

Real-time PCR: Real time PCR will be used to measure mRNA levels of genes related to mitochondrial biogenesis, dynamics, and content. All real-time PCR reactions will be carried out in 25ul reactions consisting of 2x SYBR green PCR buffer 0.1ul cDNA, RNase free water and 60nM of each primer. Samples will be run using ABI 7300 Sequence detection system. Reactions will be incubated for 2 minutes at 50 and 10 min at 95 then 50 cycles of 15s denaturing at 95 1-minute annealing at 60. Cycle threshold (C_T)

will be calculated using the ABI software and is the cycle at which the SYBR emission if halfway between detection level and saturation level.

Gene	Forward Primer	Reverse Primer	Size (bps)	Reference
PGC-1α	5′-GAC CAC AAA CGA TGA CCC TCC-3′	5′-CCT GAG AGA GAC TTT GGA GGC-3′	635	(Lai et al.)
PGC-1β	5′-AAC CCA ACC AGT CTC ACA GG-3′	5′-TGC TGC TGT CCT CAA ATA CG-3′	371	(Uguccioni and Hood)
TFAM	5′-ATG GCG CTG TTC CGG GGA ATG TGG G-3′	5′-TTA ATT CTC AGA GAT GTC TCC CGG G-3′	735	(Lai et al.)
NRF-1	5′-GTA GCG CAG CCG CTC TGA GG-3′	5′-GGG TCA CTC CGT GCT CCT CC-3′	201	(Uguccioni and Hood)
MFN1	5’-TGT TTT GGT CGC AAA CTC TG-3’	5’-CTG TCT GCG TAC GTC TTC CA-3’	88	
FIS1	5’-AAG TAT GTG CGA GGG CTG T-3’	5’-TGC CTA CCA GTC CAT CTT TC -3’		(Romanello et al., 2010)

Protein extraction: Skeletal muscle samples will be weighted and homogenized using a glass on glass homogenization system. Müller buffer will be used (10ul/mg of tissue) to homogenize samples in. Following centrifugation for 10 minutes at 13,000rmp at 4°C supernatant is placed in a new ependorf tube and diluent buffer is added at 5ul/mg of tissue. Protein content is determined using the Bradford Assay (Bradford, 1976). All samples are diluted to a working concentration of 3ug/ul using a solution of 2:1 müller buffer: diluent buffer and stored at -80°C.

Western blot: Protein extracts will be run out on SDS-page gels and transferred to PVDF membrane. FIS, MFN1, Cytochrome C, AMPK, STAT3, and PGC-1 will be probed for. Muscle homogenates, 20-40 µg are fractionated on 6% to 12% SDS-polyacrylamide gels. The gels are transferred to PVDF membrane overnight at 70mA then stained with

ponceau to ensure equal loading. Membranes are blocked in 5% Tris-buffered saline with 0.1% Tween 20 (TBST) milk for 1 h at room temperature and placed in primary antibody at dilutions of 1:1000 to 1:5000 in 1% TBST milk overnight at 4°C overnight. Secondary anti-rabbit or anti-mouse IgG-conjugated secondary antibodies are incubated with the membranes at 1:2,000 to 1:5,000 dilutions for 1 h in 1% TBST milk at room temperature. Enhanced chemiluminescence is used to visualize the antibody-antigen interactions and develop the blot by autoradiography. Digitally scanned blots are analyzed by measuring the integrated optical density (IOD) of each band using digital imaging software (Scion Image, Frederick, MD).

Succinate Dehydrogenase Staining Transverse sections (~10 μm) will be cut from the midbelly of the tibialis anterior on a cryostat at −20°C, and slides stored at −80°C until SDH staining. The frozen sections will be dried at room temperature for 10 min. Sections will be incubated in a solution made up of 0.2 M phosphate buffer (pH 7.4), 0.1 M MgCl2, 0.2 M succinic acid, and 2.4 mM nitroblue tetrazolium at 37°C for 45 min. The sections will then be washed in deionized water for 3 min, dehydrated in 50% ethanol for 2 min, and mounted for viewing with mounting media. Digital photographs will be taken from each section at a ×200 magnification with a Nikon spot camera, and fibers traced with imaging software (Scion Image, Frederick, MD). Approximately 150 fibers/animal will be traced at a ×25 magnification in a blinded fashion. The percentage of SDH positive fibers will be determined based on a criteria integrated optical density value and categorized as stained or non-stained.

Specific Aim #2. To determine if IL-6 signaling through muscle gp130 receptor/ STAT3 regulates the disruption of muscle mass in the cachectic muscle.

Rationale. We have previously shown the induction of skeletal muscle protein degradation and suppression of protein synthesis during IL-6 induced cachexia (White et al., 2011b; White et al., 2013b). Additionally, STAT3, a downstream mediator of IL-6/gp130 signaling, can attenuate skeletal muscle wasting in cancer-induced cachexia (Bonetto et al., 2012; Bonetto et al., 2011); however the actions of local IL-6 signaling and the role of systemic STAT3 signaling on muscle mass regulation during cachexia is unknown. IL-6 and STAT3 clearly regulate muscle mass during cachexia, but it is unclear whether these actions are from systemic activation or local activation of the gp130/STAT3 pathway.

Experimental design for specific aim #2.

Experiment 2 will examine if loss of the skeletal muscle gp130 prevents the disruption of protein degradation and protein synthesis during cachexia in the LLC model of cancer cachexia. The LLC tumor implanted mice will have tumors implanted for 30 days after which they will be sacrificed and tissues harvested. At sacrifice skeletal muscles, epididymal fat, intestines, plasma, and tibia will be collected. Skeletal muscle will be weighted and frozen for tissue analysis including protein, RNA, and SDH staining. Tumors will be weighted from the LLC mice to indicate tumor burden. Tibia length will be measured to normalize mice to body size.

Experiment #2 will determine if the inhibition of muscle gp130 or systemic IL-6/STAT3 signaling can attenuate cancer cachexia in the LLC model.

Animals. Mice on a C57BL/6 background will be bred with the gp130 fl/fl mice provided by Dr. Colin Stuart's lab in collaboration with Dr. Hennighausen (NCI) (Zhao et al., 2004). Fl/fl mice will then be bred with cre-expressing mice driven by myosin light chain which were secured from Dr. Steven Burden (NYU) (Bothe et al., 2000). The resulting fl/fl cre/cre mice will have a skeletal muscle deletion of the gp130 protein. fl/fl or C57BL/6 males will be used for controls. Offspring will be genotyped for cre recombinase and floxed gp130 by taking tail snips at the time of weaning. All animals will be housed in standard cages and the room will be maintained on a 12:12 light:dark cycle with the light period starting at 0700. Mice will be provided with ad libitum access to water and standard rodent chow (Harlan Teklad Rodent Diet #8604). Food consumption will be monitored during the course of the study. Body weight will be measured weekly and animals losing more than 20% body weight will be promptly removed from the study and euthanized. All animal experimentation is approved by the University of South Carolina's Institutional Animal Care and Use Committee.

Table C-2. Animal treatment groups for experiment #2.

Strain/Treatment	Age (weeks)	n
C57BL/6	8-13	6-8
C57BL/6 LLC	8-13	6-8
skm-gp130	8-13	6-8
skm-gp130 LLC	8-13	6-8

Table C-3. Animal treatment groups for experiment #2b.

Strain	Treatment	Age (weeks)	n
C57BL/6	LLC	8-13	5
C57BL/6	LLC+PDTC	8-13	5
C57BL/6	LLC+IL-6r Ab	8-13	5

Experiment #2b will determine if loss of STAT3 signaling will attenuate decreases in muscle mass during cachexia or alter protein turnover.

Animals. Body weights will be measured weekly throughout the course of the study. At 13 weeks of age mice will be assigned to one of three groups; control, IL-6r Ab, or PDTC. PDTC will be used to inhibit global STAT3 signaling and will be administered to mice daily at a dose of 100ug/mg BW for 1 week in LLC mice. As a control a subset of mice will receive the specific STAT3 inhibitor LLL12 (Lin et al., 2010) administered at a dose of 5mg/kg BW as previously reported in vivo (Lin et al., 2011) for one week in LLC implanted mice. All mice will be sacrificed after the respective treatment at ~13 weeks of age. All animals will be housed in standard cages and the room will be maintained on a 12:12 light:dark cycle with the light period starting at 0700. Mice will be provided with ad libitum access to water and standard rodent chow (Harlan Teklad Rodent Diet #8604). Food consumption will be monitored during the course of the study. Body weight will be measured weekly and animals losing more than 20% body weight will be promptly removed from the study and euthanized. All animal experimentation is approved by the University of South Carolina's Institutional Animal Care and Use Committee.

Primary outcomes:

Cachexia:

Cachexia will be measured as the loss in body weight and muscle mass over the course of the study. Body weigh will be measured weekly to monitor the health of the animal. DEXA measurements will be conducted before tumor implantation and that the time of sacrifice as an indicator of fat loss. Fat and muscle will be measured at the time of sacrifice and tumor free body weight will be measured.

Inflammatory Signaling:

Markers of skeletal muscle inflammation pSTAT3:STAT3, pAMPK:AMPK, pP65:P65 and pP38:P38 will be measured by western blot analysis. Circulating IL-6 will be measured in LLC implanted mice.

Protein Turnover: Markers of protein synthesis p-S6: total S6 will be measured via western blot analysis. FOXO and Atrogin-1 will be measured as a marker of protein degradation.

Specific Methodology Aim #2

Genotyping: All animals will be genotyped using a tail snip. At 4-5 weeks of age animals a weaned, numbered, and a small tail snip collected. The tail snip is digested in 200ul of tail digest buffer and 5ul of proteinase K. Tails are incubated overnight in a water bath set at 37°C. After incubation samples are heat shocked at 95°C in a dri-bath for 10 minutes. A separate PCR reaction is used to determine the presence or absence of floxed gp130 and cre recombinase. Offspring will be genotyped for cre recombinase (forward 5' AAG CCC TGA CCC TTT AGA TTC CAT TT 3', reverse 5' AAA ACG CCT GGC GAT

CCC TGA AC 3', wild type 5' GCGGGCTTCTTCACGTCTTTCTTT 3'), floxed gp130 (forward 5' ACG TCA CAG AGC TGA GTG ATG CAC 3', reverse 5' GGC TTT TCC TCT GGT TCT TG 3'), and the Apc gene (forward 5' TGAGAAAGACAGAAGTTA 3", reverse 5' TTCCACTTTGGCATAAGGC 3') by taking tail snips at the time of weaning.

Tissue Collection: Mice will be anesthetized with a subcutaneous injection of ketamine/acepromazine/xylazine cocktail (1.4mL/kg BW). Blood will be collected from the retro-orbital sinus using a capillary tube. Blood will be spun at 4°C, 10,000rpm, for 10 minutes. Plasma will then be pipetted off and stored at -80°C until analysis. Gastrocnemius (gas), plantaris (pla), soleus (sol), tibialis anterior (TA), extensor digitorum longus (EDL), quadriceps (quad), and tumors from the LLC mice will be excised rinsed in PBS, weighed, snap frozen in liquid nitrogen, and stored at -80°C until further analysis. Epididymal fat pads and tibia length will also be measured. Tibia length will be used as a measure of body size and a correction factor for skeletal muscle and body weight measures.

Plasma IL-6: Plasma IL-6 will be measured using a mouse specific ELISA kit. A high sensitivity IL-6 ELISA (Invitrogen) will be used to analyze the data from the LLC study. The assay will be carried out according to the manufacturer's instructions. IL-6 will be measured as described in Aim 1.

RNA isolation: RNA will be isolated from skeletal muscle using TRIzol reagent as described in Aim 1.

Real-time PCR: Real time PCR will be used to measure mRNA levels of genes related to mitochondrial biogenesis, and dynamics as described in Aim 1.

Protein extraction: Skeletal muscle samples will be weighted and homogenized using a glass on glass homoginazation system as described in Aim 1. Protein content will be determined using the Bradford Assay.

Western blot: Protein extracts will be run out on SDS-page gels and transferred to PVDF membrane. FIS, MFN1, Cytochrome C, COXIV, TFAM, PGC-1, p-S6, p-STAT3, and p-AMPK will be probed for as described in Aim 1.

Protein synthesis: To directly measure protein synthesis mice will be injected with phenylalanine or puromycin (0.04mM/kg) 30 minutes prior to sacrifice. Muscle homogenates will be analyzed via western blot when appropriate using an anti-puromycin antibody for alterations in the amount of puromycin incorporated into the proteins. This method has been widely published as a valid measurement of the rate of protein synthesis (Goodman and Hornberger; Goodman et al., 2012; Goodman et al., 2011a; Schmidt et al., 2009).

Specific Aim #3 will determine if the transcription and translation of proteins regulating mitochondrial biogenesis are altered with acute contraction during cachexia.

Specific Aim #3 Rational: We have previously shown that exercise training prior to the initiation of cachexia attenuates the loss of skeletal muscle mitochondrial content in the Min mouse (Puppa et al., 2011d). Our preliminary data suggests that cachectic muscle has the capacity to up-regulate nuclear encoded mitochondrial gene (NUGEMPs) transcription after a novel bout of contraction, but this increase in transcription is not associated with an increase in translation of the proteins. It is unclear if cachectic skeletal

muscle has decreased mitochondrial plasticity to an acute contraction bout, and if inhibition of inflammation can regulate contraction mediated mitochondrial plasticity in cachectic muscle.

Experimental Design for specific aim #3: In this experimental aim C57BL/6 mice and $Apc^{Min/+}$ will be used. Mice will be implanted with aged to approximately 18-20 weeks old at which point Min mice will have lost significant body weight and will be cachectic. To inhibit inflammatory signaling, PDTC will be administered to a subset of Min mice 24 hours prior to stimulation. All mice will undergo an acute 30 minute bout of low frequency electrical stimulation (10Hz, 90ms delay, 1ms pulse) at 18-20 weeks of age. The stimulation will mimic an acute endurance bout of exercise. Only the left leg will be stimulated and the right leg will serve as an internal control. All mice will be sacrificed 3 hours after the completion of the 30 minutes exercise bout. Mice will be housed in standard cages until the time of sacrifice. At sacrifice skeletal muscles, epididymal fat, intestines, plasma, and tibia will be collected. Skeletal muscle will be weighted and frozen for tissue analysis including protein, and RNA. Tibia length will be measured to normalize mice to body size. Five animals will be used for each group to give a power of 99.4% with a 5% probability of incorrectly rejecting the null hypothesis that there is no difference in transcription of PGC-1α with stimulation. Analysis is based on preliminary data from $Apc^{Min/+}$ mice.

Table 1-4. Animal treatment groups for experiment #3.

Strain	Age (wks)	Treatment		n
		Right leg	Left Leg	
C57BL/6	13	Stim	Con	5-7
$Apc^{Min/+}$	13	Stim	Con	5-7
$Apc^{Min/+}$ +PDTC	13	Stim	Con	5-7

Primary Outcomes:

Transcriptional response of NUGEMPs: The transcriptional response of NUGEMPs will be measured by real time PCR. TFAM, a prominent nuclear gene encoding a mitochondrial protein, will be measured as well as PGC-1 and NRF1 which are known regulators of NUGEMP transcription.

Translational response of NUGEMPs: Skeletal muscle translational response of NUGEMPs will be measured by western blot analysis of several proteins. TFAM and PGC-1 protein content will be measured in muscle three hours after the contraction bout. Changes in AMPK activation will be used to examine upstream regulation of NUGEMP transcription and translation. Activation of S6 ribosomal protein will be measured as a marker of protein synthesis which should be increased during translation of proteins. The incorporation of puromycin will be used to directly measure protein synthesis *in vivo*.

Specific Methodology Aim #3

Genotyping: All animals will be genotyped using a tail snip. At 4-5 weeks of age animals a weaned, numbered, and a small tail snip collected. The tail snip is digested in 200ul of tail digest buffer and 5ul of proteinase K. Tails are incubated overnight in a water bath set

at 37°C. After incubation samples are heat shocked at 95°C in a dri-bath for 10 minutes. A separate PCR reaction is used to determine the presence or absence of floxed gp130 and cre recombinase.

Electrical Stimulation: Prior to stimulation food will be restricted for 5 hours, but animals will have ad libitum access to water. Animal will be anesthetized with Isoflurane in a chamber at 2-5% and remained anesthetized using a cone hooked up to the isoflurane/oxygen. Gas will be scavenged using carbon filters that will be replaced after an increase of 50g in weight. Animals will be placed on a heat pad and the left hind limb will be shaved free of hair and cleaned with alcohol followed by betadine. Electrodes will be placed on both sides of the siatic nerve and stimulated posterior to the knee via subcutaneous needle. The stimulating electrode will be positioned proximal to the bifurcation of the sciatic nerve, thus contractions occurred in all compartments of the leg. Proper electrode position will be confirmed by observing plantarflexion at the ankle joint. This protocol will elicit an overall effect of plantar flexion and will result in tapping of the foot. The voltage will be applied by Grass S88 stimulator (Grass technologies, RI). Stimulation will be delivered at a frequency of 10 Hz, 5 V, 10-ms duration, 90-ms delay, there will be 1s stimulation followed by 1s rest for a total time of 30 min. During recovery period, animals will remain on a heat pad and be closely monitored.

Tissue Collection: Mice will be anesthetized with a subcutaneous injection of ketamine/acepromazine/xylazine cocktail (1.4mL/kg BW). Blood will be collected from the retro-orbital sinus using a capillary tube. Blood will be spun at 4°C, 10,000rpm, for 10 minutes. Plasma will then be pipetted off and stored at -80°C until analysis. Gastrocnemius (gas), plantaris (pla), soleus (sol), tibialis anterior (TA), and extensor

digitorum longus (EDL) will be excised rinsed in PBS, weighed, snap frozen in liquid nitrogen, and stored at -80°C until further analysis. Epididymal fat pads and tibia length will also be measured. Tibia length will be used as a measure of body size and a correction factor for skeletal muscle and body weight measures. The tumor will be dissected away and weighed to give the tumor burden.

RNA isolation: RNA will be isolated from skeletal muscle using Trizol reagent. Isolated RNA absorbance will be measured at 260nm and 280nm to determine RNA purity and quantity. RNA quality will be analyzed by running samples out on an agarose gel.

Real-time PCR: Real time PCR will be used to measure mRNA levels of genes related to mitochondrial biogenesis.

Protein extraction: Skeletal muscle samples will be weighted and homogenized using a glass on glass homoginazation system. Müller buffer will be used (10ul/mg of tissue) to homogenize samples in. Protein content will be determined using the Bradford Assay.

Western blot: Protein extracts will be run out on SDS-page gels and transferred to PVDF membrane as described in Aim 1. Cytochrome C, COXIV, TFAM, AMPK, S6 ribosomal protein, and PGC-1 will be probed for using dilutions of 1:1000-1:5000 in 1% TBST milk.

Protein synthesis: To directly measure protein synthesis mice will be injected with phenylalanine 30 minutes prior to sacrifice. Muscle homogenates will be analyzed via western blot using an anti-puromycin antibody for alterations in the amount of puromycin incorporated into the proteins. This method has been widely published as a valid measurement of the rate of protein synthesis.

APPENDIX D

RAW DATA

Mouse	Geno	Treatment	Peak BW	Post BW	R.Sol	L.Sol		R. Plant	L. Plant		R. Gas	L. Gas		R. EDL	L. EDL		R. TA	L. TA		R. RF	L. RF	
2831	BL/6	control	25.4	25.4	7	8	7.5	16	16	16	117	122	119.5	10	10	10	47	47	47	93	na	93
2832	BL/6	control	24.7	24.7	8	8	8	13	16	14.5	115	126	120.5	10	8	9	39	47	43	98	112	105
2833	BL/6	control	26.9	26.9	8	9	8.5	16	19	17.5	136	135	135.5	12	13	12.5	46	50	48	117	105	111
2622	BL/6	control	29.3	29.3	12	11	11.5	22	23	22.5	153	147	150	14	12	13	48	52	50	118	119	118.5
2662	BL/6	control	27.4	27.4	9	10	9.5	20	22	21	144	140	142	15	13	14	41	44	42.5	123	101	112
2628	BL/6	control	27.4	27.4	9	9	9	21	23	22	147	156	151.5	10	7	8.5	61	57	59	103	107	105
2784	BL/6	control	27.5	27.5	11	12	11.5	19	23	21	139	146	142.5	15	15	15	54	52	53	102	103	102.5
2785	BL/6	control	28.7	28.7	12	10	11	24	20	22	152	141	146.5	13	12	12.5	53	56	54.5	116	111	113.5
2624	BL/6	control	28.7	28.7	13	10	11.5	21	20	20.5	140	146	143	12	9	10.5	52	53	52.5	104	105	104.5
		mean	**27.3**	**27.3**			**9.8**			**19.7**			**139.0**			**11.7**			**49.9**			**107.2**
		stdev	**1.5**	**1.5**			**1.6**			**2.9**			**11.8**			**2.3**			**5.4**			**7.5**
		se	**0.5**	**0.5**			**0.5**			**1.0**			**3.9**			**0.8**			**1.8**			**2.5**
3207	BL/6	sgp130 Fc	28.5	27.4	7	9	8	20	17	18.5	145	139	142	12	10	11	54	52	53	101	98	99.5
3209	BL/6	sgp130 Fc	27.7	27.7	11	11	11	18	19	18.5	138	142	140	11	11	11	54	61	57.5	99	106	102.5
3218	BL/6	sgp130 Fc	25.9	25.8	10	10	10	18	21	19.5	134	139	136.5	14	14	14	47	54	50.5	102	100	101
3221	BL/6	sgp130 Fc	27.9	27.9	11	9	10	21	21	21	144	143	143.5	13	11	12	50	55	52.5	97	104	100.5
		mean	**27.5**	**27.2**			**9.8**			**19.4**			**140.5**			**12.0**			**53.4**			**100.9**
		stdev	**1.1**	**1.0**			**1.3**			**1.2**			**3.0**			**1.4**			**3.0**			**1.3**
		se	**0.56**	**0.48**			**0.63**			**0.59**			**1.51**			**0.71**			**1.48**			**0.63**
2803	BL/6	skm-gp130	28.5	28.5	13	11	12	21	23	22	136	135	135.5	13	15	14	55	56	55.5	106	113	109.5
2804	BL/6	skm-gp130	26.3	26.3	12	11	11.5	18	20	19	121	124	122.5	12	12	12	52	47	49.5	89	88	88.5
2805	BL/6	skm-gp130	28.4	28.4	11	12	11.5	21	24	22.5	146	146	146	14	14	14	51	48	49.5	107	111	109
2854	BL/6	skm-gp130	31.4	31.4	12	11	11.5	22	22	22	161	166	163.5	14	14	14	61	66	63.5	121	123	122
2855	BL/6	skm-gp130	24.2	24.2	9	8	8.5	14	17	15.5	129	131	130	12	10	11	45	45	45	94	83	88.5
		mean	**27.8**	**27.8**			**11.0**			**20.2**			**139.5**			**13.0**			**52.6**			**103.5**
		stdev	**2.7**	**2.7**			**1.4**			**3.0**			**15.9**			**1.4**			**7.1**			**14.7**
		se	**1.2**	**1.2**			**0.6**			**1.3**			**7.1**			**0.6**			**3.2**			**6.6**

Mouse	Geno	Treatment	Liver	Spleen	Epi Fat	Testes	Heart	TL(mm)
2831	BL/6	control	1302	75	337	204	120	17.2
2832	BL/6	control	1200	67	261	210	118	16.9
2833	BL/6	control	1233	70	408	216	123	17.2
2622	BL/6	control	1143	96	709	199	114	17.2
2662	BL/6	control	1087	89	583	170	110	17.1
2628	BL/6	control	1037	81	345	210	112	17
2784	BL/6	control	1153	91	565	209	120	17
2785	BL/6	control	1134	143	406	207	102	17.4
2624	BL/6	control	1120	85	569	212	106	17.1
		mean	**1156.6**	**88.6**	**464.8**	**204.1**	**113.9**	**17.1**
		stdev	**79.1**	**22.6**	**147.2**	**13.7**	**7.0**	**0.1**
		se	**26.4**	**7.5**	**49.1**	**4.6**	**2.3**	**0.0**
3207	BL/6	sgp130Fc	1303	84	309	203	110	17
3209	BL/6	sgp130Fc	1226	86	420	201	110	17.2
3218	BL/6	sgp130Fc	1153	86	301	214	103	16.9
3221	BL/6	sgp130Fc	1167	79	432	211	116	16.7
		mean	**1212.3**	**83.8**	**365.5**	**207.3**	**109.8**	**17.0**
		stdev	**68.3**	**3.3**	**70.1**	**6.2**	**5.3**	**0.2**
		se	**34.14**	**1.65**	**35.05**	**3.12**	**2.66**	**0.10**
2803	BL/6	skm-gp130	1512	111	480	227	142	17.3
2804	BL/6	skm-gp131	1354	88	456	234	110	16.8
2805	BL/6	skm-gp132	1525	136	373	226	128	17.1
2854	BL/6	skm-gp133	1388	93	392	245	134	17.5
2855	BL/6	skm-gp134	1133	60	295	216	116	17
		mean	**1382.4**	**97.6**	**399.2**	**229.6**	**126.0**	**17.1**
		stdev	**158.2**	**28.2**	**73.1**	**10.7**	**13.0**	**0.3**
		se	**70.8**	**12.6**	**32.7**	**4.8**	**5.8**	**0.1**

MouseGeno	Treat	Peak BW	Sac BW	% change
2896Min	control	23.0	19.3	-16%
660Min	control	24.6	19.6	-20%
2919Min	control	25.8	21.8	-16%
659Min	control	24.3	21.6	-11%
663Min	control	23.1	18.3	-21%
2741Min	control	23.1	18.8	-18.6%
2740Min	control	23.6	17.2	-27.1%
2626Min	control	26.1	19.7	-24.5%
2830Min	control	23	17	-26.1%
2829Min	control	23.1	20	-13.4%
2623Min	control	26.1	23.5	-10.0%
	mean	**24.2**	**19.7**	**-18.50%**
	stdev	**1.3**	**2.0**	**5.87%**
	se	**0.4**	**0.6**	**1.77%**
3049Min	sgp130Fc	24.4	22.1	1.4%
3112Min	sgp130Fc	23.2	23.4	2.6%
3113Min	sgp130Fc	22.7	22	3.3%
3114Min	sgp130Fc	25.9	25.3	1.2%
3111Min	sgp130Fc	23	18.2	-12.5%
3137Min	sgp130Fc	25.3	25.8	2.0%
	mean	**24.1**	**22.8**	**-0.3%**
	stdev	**1.3**	**2.8**	**6.0%**
	se	**0.54**	**1.12**	**2.5%**
2758Min	skm-gp130	22.4	21.9	-2.2%
2759Min	skm-gp130	25.9	23.5	-9.3%
2902Min	skm-gp130	23.2	19.4	-16.4%
3058Min	skm-gp130	21.4	17.1	-20.1%
3035Min	skm-gp130	20.5	18.3	-10.7%
3059Min	skm-gp130	25.8	21.7	-15.9%
		23.2	**20.3**	**-12.43%**
		2.2	**2.4**	**6.37%**
		0.9	**1.0**	**2.6%**

Mouse	Geno	Treat	R. Sol	L. Sol	avg sol	R. Plant	L. Plant	avg Plant	R. Gas	L. Gas	avg Gas	R. EDL	L. EDL	avg EDL	R. TA	L. TA	avg TA	R. RF	L. RF	avg RF
2896	Min	control	6	5	5.5	7	10	8.5	51	56	53.5	5	6	5.5	21	22	21.5	37	36	36.5
660	Min	control	8	7	7.5	15	13	14	93	92	92.5	8	9	8.5	30	34	32	70	74	72
2919	Min	control	6	6	6	9	9	9	72	68	70	5	6	5.5	20	21	20.5	48	44	46
659	Min	control	8	7	7.5	12	11	11.5	91	89	90	6	7	6.5	29	34	31.5	63	66	64.5
663	Min	control	8	7	7.5	13	13	13	92	91	91.5	6	4	5	36	34	35	75	65	70
2741	Min	control	8	7	7.5	13	13	13	88	82	85	7	5	6	29	30	29.5	49	47	48
2740	Min	control	6	7	6.5	9	10	9.5	63	68	65.5	6	6	6	24	20	22	45	42	43.5
2626	Min	control	6	4	5	8	10	9	70	73	71.5	4	6	5	21	22	21.5	50	38	44
2830	Min	control	6	6	6	12	10	11	91	73	82	6	6	6	34	31	32.5	62	59	60.5
2829	Min	control	6	7	6.5	10	10	10	77	-	77	5	5	5	23	31	27	55	48	51.5
2623	Min	control	8	8	8	11	13	12	86	82	84	8	6	7	30	31	30.5	62	67	64.5
		mean			**6.7**			**11.0**			**78.4**			**6.0**			**27.6**			**54.6**
		stdev			**1.0**			**1.9**			**12.2**			**1.0**			**5.3**			**12.1**
		se			**0.3**			**0.6**			**3.7**			**0.3**			**1.6**			**3.6**
3049	Min	sgp130Fc	8	8	8	13	11	12	82	84	83	7	7	7	31	33	32	61	63	62
3112	Min	sgp130Fc	7	6	6.5	14	15	14.5	104	118	111	11	10	10.5	37	torn	37	73	na	73
3113	Min	sgp130Fc	8	9	8.5	15	13	14	106	82	94	9	7	8	32	33	32.5	72	74	73
3114	Min	sgp130Fc	9	8	8.5	14	12	13	114	108	111	9	6	7.5	32	22	27	77	67	72
3111	Min	sgp130Fc	5	5	5	8	8	8	93	94	93.5	7	5	6	26	24	25	51	47	49
3137	Min	sgp130Fc	5	8	6.5	19	17	18	132	132	132	10	5	7.5	40	30	35	97	101	
		mean			**7.2**			**13.3**			**104.1**			**7.8**			**31.4**			**65.8**
		stdev			**1.4**			**3.3**			**17.5**			**1.5**			**4.6**			**10.5**
		se			**0.57**			**1.34**			**7.15**			**0.62**			**1.88**			**4.68**
2758	Min	skm-gp130	11	7	9	14	12	13	83	70	76.5	5	6	5.5	34	28	31	51	45	48
2759	Min	skm-gp130	8	8	8	9	10	9.5	64	67	65.5	5	4	4.5	36	32	34	51	38	44.5
2902	Min	skm-gp130	8	8	8	10	10	10	63	71	67	8	7	7.5	29	32	30.5	50	48	49
3058	Min	skm-gp130	6	6	6	8	8	8	60	55	57.5	5	na	5		24	24	35	31	33
3035	Min	skm-gp130	7	6	6.5	9	10	9.5	68	71	69.5	7	6	6.5	22	24	23	48	43	45.5
3059	Min	skm-gp130	6	7	6.5	10	9	9.5	55	64	59.5	7	6	6.5	30	27	28.5	45	43	44
		mean			**7.3**			**9.9**			**65.9**			**5.9**			**28.5**			**44.0**
		stdev			**1.2**			**1.7**			**6.9**			**1.1**			**4.3**			**5.7**
		se			**0.5**			**0.7**			**2.8**			**0.5**			**1.7**			**2.3**

Mouse	Geno	Treatment	liver	Spleen	epi fat	testes	heart	Tibia Length
2896	Min	control	1405	645	0	40	100	16.1
660	Min	control	1161	296	0	170	102	17.2
2919	Min	control	1399	590	0	101	130	16.1
659	Min	control	1447	521	0	180	113	16.8
663	Min	control	1635	628	0	178	116	16.8
2741	Min	control	1082	530	0	136	107	16.3
2740	Min	control	756	210	0	85	96	17
2626	Min	control	889	386	0	108	90	16.6
2830	Min	control	992	207	0	153	91	16.8
2829	Min	control	1399	528	0	139	93	16.7
2623	Min	control	1777	430	52	178	131	17
		mean	**1267.5**	**451.9**	**4.7**	**133.5**	**106.3**	**16.7**
		stdev	**317.3**	**158.6**	**15.7**	**45.5**	**14.7**	**0.4**
		se	**95.7**	**47.8**	**4.7**	**13.7**	**4.4**	**0.1**
3049	Min	sgp130Fc	1656	696	52	158	101	16.6
3112	Min	sgp130Fc	1571	338	179	191	112	16.5
3113	Min	sgp130Fc	1429	492	138	194	102	16.4
3114	Min	sgp130Fc	1604	528	39	197	122	17
3111	Min	sgp130Fc	1099	344	0	104	121	16.5
3137	Min	sgp130Fc	1372	318	319	211	122	16.6
		mean	**1455.2**	**452.7**	**121.2**	**175.8**	**113.3**	**16.6**
		stdev	**205.1**	**148.0**	**117.5**	**39.3**	**9.9**	**0.2**
		se	**83.7**	**60.4**	**48.0**	**16.0**	**4.0**	**0.09**
2758	Min	skm-gp130	1379	438	13	133	160	16.7
2759	Min	skm-gp130	1560	714	10	149	120	16.5
2902	Min	skm-gp130	989	492	0	156	100	16
3058	Min	skm-gp130	1043	494	0	50	120	16.4
3035	Min	skm-gp130	1158	424	0	109	122	16.6
3059	Min	skm-gp130	1258	480	0	87	123	17
		mean	**1231**	**507.0**	**3.8**	**114.0**	**124.2**	**16.5**
		stdev	**215**	**105.5**	**6.0**	**40.5**	**19.5**	**0.3**
		se	**88**	**43.1**	**2.5**	**16.5**	**8.0**	**0.1**

Sample	cyto B	GAPDH	dct	ddct		2^ddct	normalized
2662	10.68	20.16	-9.48	0.80	-0.80	0.57	0.55
2628	13.35	23.84	-10.49	-0.21	0.21	1.16	1.10
2785	13.39	24.29	-10.90	-0.62	0.62	1.54	1.46
2622	13.00	23.12	-10.12	0.16	-0.16	0.90	0.85
2624	12.64	23.05	-10.41	-0.13	0.13	1.09	1.04
2855	11.34	23.59	-12.25	-1.97	1.97	3.92	3.73
2803	12.10	23.59	-11.49	-1.21	1.21	2.31	2.20
2854	12.07	22.64	-10.57	-0.29	0.29	1.22	1.16
2805	11.83	23.38	-11.55	-1.27	1.27	2.41	2.29
2804	10.19	23.37	-13.18	-2.90	2.90	7.46	7.10
2829	19.95	27.92	-7.97	2.31	-2.31	0.20	0.19
2626	14.16	23.18	-9.02	1.26	-1.26	0.42	0.40
2741	12.74	20.77	-8.03	2.25	-2.25	0.21	0.20
2537	13.02	23.16	-10.14	0.14	-0.14	0.91	0.86
2830	17.76	26.63	-8.87	1.41	-1.41	0.38	0.36
2902	10.45	21.02	-10.57	-0.29	0.29	1.22	1.16
3136	12.67	23.05	-10.38	-0.10	0.10	1.07	1.02
3155	14.56	22.21	-7.65	2.63	2.63	6.19	5.89
3120	14.26	24.12	-9.86	0.42	-0.42	0.75	0.71

mtDNA:gDNA	Mean	SEM
BL-6	1.00	0.15
Min	0.44	0.12
skm-gp130	3.30	1.03
skm-gp130Min	2.20	1.10

Sample	PGC-1α	GAPDH	dct	ddct	2^ddct	normalized
2622	23.16	19.3	3.86	-0.81	0.57	0.53
2628	23.06	18.46	4.6	-0.07	0.95	0.88
2784	22.31	16.73	5.58	0.91	1.87	1.74
2785	21.61	17.05	4.56	-0.11	0.92	0.86
2624	22.37	17.6	4.77	0.10	1.07	0.99
2758	22.13	18.52	3.61	-1.06	0.48	0.44
2759	23.41	18.6	4.81	0.14	1.10	1.02
2902	21.19	19.28	1.91	-2.76	0.15	0.14
3058	23.05	18.14	4.91	0.24	1.18	1.09
3059	23.16	18.91	4.25	-0.42	0.75	0.69
2803	23.53	17.87	5.66	0.99	1.98	1.84
2805	22.66	17.75	4.91	0.24	1.18	1.09
2854	21.3	16.98	4.32	-0.35	0.78	0.73
2855	23.29	18.07	5.22	0.55	1.46	1.36
2537	22.69	17.58	5.11	0.44	1.35	1.26
2741	22.67	20	2.67	-2.00	0.25	0.23
2626	22.09	20.17	1.92	-2.75	0.15	0.14
2829	22.07	19.89	2.18	-2.49	0.18	0.16
2627	22.29	19.48	2.81	-1.86	0.27	0.26

PGC-1α	Mean	SEM
BL-6	1.00	0.20
Min	0.20	0.02
skm-gp130	1.25	0.18
skm-gp130Min	0.68	0.18

Sample	TFAM	GAPDH	dct	ddct	2^ddct	normalized
2622	27.17	19.3	7.87	-0.27	0.83	0.81
2628	26.49	18.46	8.03	-0.11	0.93	0.91
2784	25.09	16.73	8.36	0.22	1.17	1.14
2785	25.68	17.05	8.63	0.49	1.41	1.37
2624	25.39	17.6	7.79	-0.35	0.79	0.77
2758	25.52	18.52	7	-1.14	0.46	0.44
2759	26.27	18.6	7.67	-0.47	0.72	0.71
2902	26.14	19.28	6.86	-1.28	0.41	0.40
3058	26.11	18.14	7.97	-0.17	0.89	0.87
3059	27.04	18.91	8.13	-0.01	1.00	0.97
2803	25.6	17.87	7.73	-0.41	0.75	0.74
2805	25.34	17.75	7.59	-0.55	0.68	0.67
2854	25.52	16.98	8.54	0.40	1.32	1.29
2855	26.05	18.07	7.98	-0.16	0.90	0.88
2537	25.87	17.58	8.29	0.15	1.11	1.09
2741	26.16	20	6.16	-1.98	0.25	0.25
2626	26.08	20.17	5.91	-2.23	0.21	0.21
2829	26.09	19.89	6.2	-1.94	0.26	0.26
2627	26.22	19.48	6.74	-1.40	0.38	0.37

TFAM	Mean	SEM
BL-6	1.00	0.11
Min	0.27	0.03
skm-gp130	0.93	0.11
skm-gp130Min	0.68	0.11

Sample	TFAM	GAPDH	dct	ddct	2^ddct	normalized
121	22.31	19.97	2.34	-0.64	0.64	0.36
123	22.26	19.58	2.68	-0.30	0.81	0.45
122	22.27	19.9	2.37	-0.61	0.65	0.36
124	21.33	16.79	4.54	1.56	2.94	1.64
2833	23.08	18.12	4.96	1.98	3.94	2.19
663	21.95	19.12	2.83	-0.15	0.90	0.50
2896	21.3	16.82	4.48	1.50	2.82	1.57
2916	23.16	19.2	3.96	0.98	1.97	1.10
659	20.81	17.15	3.66	0.68	1.60	0.89
660	22.26	18.7	3.56	0.58	1.49	0.83
3209	21.12	17.03	4.09	1.11	2.15	1.20
3207	22.18	17.24	4.94	1.96	3.88	2.16
3218	22.31	18.46	3.85	0.87	1.82	1.02
3221	22.07	17.6	4.47	1.49	2.80	1.56
3111	21.01	17.18	3.83	0.85	1.80	1.00
3113	21.38	16.85	4.53	1.55	2.92	1.63
3112	22.44	18.85	3.59	0.61	1.52	0.85
3114	21.4	17.03	4.37	1.39	2.62	1.46
3049	22.02	16.5	5.52	2.54	5.81	3.23
3137	22.34	17.58	4.76	1.78	3.43	1.91

TFAM	Mean	SEM
BL-6	1.00	0.38
BL-6+sgp130Fc	1.48	0.25
Min	0.98	0.18
min+sgp130Fc	1.68	0.35

Sample	PGC-1α	18S	dCT	ddCT	2^ddct	Normalized
121	30.395	21.43	8.965	-0.12	0.92	0.90
123	29.855	20.435	9.42	0.34	1.26	1.24
122	30.015	20.62	9.395	0.31	1.24	1.22
124	29.485	20.66	8.825	-0.26	0.84	0.82
2833	28.08	19.26	8.82	-0.26	0.83	0.82
663	29.2	23.22	5.98	-3.11	0.12	0.11
2916	29.08	26.65	2.43	-6.66	0.01	0.01
659	27.555	21.27	6.285	-2.80	0.14	0.14
660	28.225	23.665	4.56	-4.53	0.04	0.04
3209	29.965	20.18	9.785	0.70	1.62	1.60
3207	30.54	21.045	9.495	0.41	1.33	1.31
3218	28.955	20.495	8.46	-0.63	0.65	0.64
3221	29.24	20.495	8.745	-0.34	0.79	0.78
3111	17.825	18.935	9.34	0.26	1.19	1.17
3112	28.445	19.485	8.96	-0.12	0.92	0.90
3113	28.37	20.905	7.465	-1.62	0.33	0.32
3114	28.615	18.89	9.725	0.64	1.56	1.53

PGC-1α	Mean	SEM
BL-6	1.00	0.23
Min	0.08	0.03
BL-6 + sgp130Fc	1.08	0.22
Min + sgp130Fc	1.01	0.26

Sample	FIS	GAPDH	dct	ddct	2^ddct	normalized
121	26.88	19.96	6.92	0.27	1.20	1.18
123	25.9	19.69	6.21	-0.44	0.74	0.72
122	25.92	19.85	6.07	-0.58	0.67	0.65
124	24.59	17.18	7.41	0.76	1.69	1.65
2833	26.02	19.65	6.37	-0.28	0.82	0.80
663	26.68	17.62	9.06	2.41	5.31	5.18
2896	25.72	16.16	9.56	2.91	7.50	7.33
2916	26.94	18.91	8.03	1.38	2.60	2.54
659	25.08	17.37	7.71	1.06	2.08	2.03
660	26.05	18.15	7.9	1.25	2.37	2.32
3209	24.49	17.42	7.07	0.42	1.34	1.30
3207	24.44	17.39	7.05	0.40	1.32	1.29
3218	25.67	18.56	7.11	0.46	1.37	1.34
3221	25.13	17.75	7.38	0.73	1.66	1.62
3111	24.26	17.02	7.24	0.59	1.50	1.47
3113	24.25	17.1	7.15	0.50	1.41	1.38
3112	25.44	19.18	6.26	-0.39	0.76	0.74
3114	24.48	17.22	7.26	0.61	1.52	1.49
3049	24.58	16.56	8.02	1.37	2.58	2.52
3137	24.4	17.97	6.43	-0.22	0.86	0.84

FIS	Mean	SEM
BL-6	1.00	0.19
BL-6+sgp130Fc	1.39	0.08
Min	3.88	1.03
min+sgp130Fc	1.41	0.26

Sample	MFN	18S	dCT	ddCT	2^ddct	Normalized
121	24.84	20.58	4.26	-4.83	0.035	1.91
123	24.11	21.14	2.98	-6.11	0.014	0.78
122	23.64	20.58	3.07	-6.02	0.015	0.83
124	22.34	19.27	3.08	-6.01	0.016	0.84
2833	23.50	20.81	2.69	-6.40	0.012	0.64
663	23.97	22.59	1.38	-7.71	0.005	0.26
2896	22.76	20.04	2.72	-6.37	0.012	0.66
2916	23.04	21.01	2.03	-7.06	0.008	0.41
659	23.12	21.84	1.28	-7.81	0.004	0.24
660	25.29	24.05	1.24	-10.33	0.001	0.04
3209	22.59	19.85	2.74	-6.35	0.012	0.66
3207	24.33	21.24	3.09	-5.99	0.016	0.85
3218	24.24	21.50	2.74	-6.35	0.012	0.66
3221	23.22	20.55	2.67	-6.42	0.012	0.63
3111	24.01	21.87	2.14	-6.95	0.008	0.44
3112	23.49	20.69	2.80	-6.29	0.013	0.69
3113	24.36	22.03	2.33	-6.76	0.009	0.50
3114	23.89	22.18	1.72	-7.37	0.006	0.33
3049	22.71	19.93	2.79	-6.30	0.013	0.69
3137	24.19	22.70	1.49	-7.60	0.005	0.28

MFN1	Mean	SEM
BL-6	1.00	0.23
Min	0.32	0.10
BL-6 + sgp130Fc	0.70	0.05
Min + sgp130Fc	0.49	0.07

PGC-1	PGC-1	-bg	Normalized	PGC-1	PGC-1	-bg	Normalized			
B6	153.446	13.536	1.118	B6	155.964	26.56	1.22			
B6	154.586	14.676	1.212	B6	150.323	20.92	0.96		Mean	SEM
B6	145.382	5.472	0.452	B6	143.623	14.22	0.65	BL-6	1.000	0.08
Min	148.029	8.119	0.670	Min	137.052	7.65	0.35	Min	0.365	0.06
Min	141.564	1.654	0.137	Min	133.325	3.92	0.18	Fc	0.889	0.14
Min	145.77	5.860	0.484	Min	139.175	9.77	0.45	skm	1.181	0.05
skm	153.117	13.207	1.091	Fc	141.202	11.80	0.54	skmMin	1.235	0.18
skm	155.67	15.760	1.301	Fc	146.918	17.51	0.80	FcMin	0.998	0.07
skm	153.427	13.517	1.116	Fc	159.03	29.63	1.36			
skmMin	157.346	17.436	1.440	FcMin	153.009	23.60	1.08			
skmMin	149.576	9.666	0.798	FcMin	152.673	23.27	1.07			
skmMin	158.962	19.052	1.573	FcMin	147.275	17.87	0.82			
B6	152.615	12.705	1.049	B6	149.905	20.50	0.94			
B6	154.076	14.166	1.170	B6	155.993	26.59	1.22			
Min	147.503	7.593	0.627	Min	139.071	9.67	0.44			
Min	141.598	1.688	0.139	Min	133.068	3.66	0.17			
skm	155.602	15.692	1.296	Fc	145.941	16.54	0.76			
skm	153.231	13.321	1.100	Fc	150.623	21.22	0.98			
skmMin	149.5	9.590	0.792	FcMin	154.675	25.27	1.16			
skmMin	158.959	19.049	1.573	FcMin	147.907	18.50	0.85			

Sample	Cyto B	GAPDH	dct		ddct	2^ddct	Normalized
122	9.93	18.61	-8.68	8.68	0.52	1.43	1.40
123	10.28	18.34	-8.06	8.06	-0.10	0.93	0.91
124	9.04	17.16	-8.12	8.12	-0.04	0.97	0.95
2832	9.57	17.36	-7.79	7.79	-0.38	0.77	0.75
598	10.68	18.28	-7.60	7.60	-0.56	0.68	0.66
610	9.01	16.79	-7.78	7.78	-0.38	0.77	0.75
611	11.52	19.83	-8.32	8.32	0.15	1.11	1.08
658	10.84	17.92	-7.08	7.08	-1.09	0.47	0.46
8	10.19	17.89	-7.70	7.70	-0.46	0.73	0.71
659	18.14	22.20	-4.06	4.06	-4.11	0.06	0.06
660	11.63	18.47	-6.85	6.85	-1.32	0.40	0.39
684	10.11	14.15	-4.04	4.04	-4.13	0.06	0.06
2916	12.37	18.50	-6.13	6.13	-2.04	0.24	0.24
2919	15.14	20.36	-5.23	5.23	-2.94	0.13	0.13
3048	7.49	18.29	-10.80	10.80	2.64	6.23	6.07
3051	13.49	17.54	-4.05	4.05	-4.11	0.06	0.06
3052	7.06	18.01	-10.95	10.95	2.79	6.91	6.73
3085	7.95	16.37	-8.42	8.42	0.26	1.20	1.17
3086	8.02	18.33	-10.31	10.31	2.15	4.43	4.32
3049	10.01	18.12	-8.11	8.11	-0.05	0.97	0.94
3112	8.16	18.45	-10.29	10.29	2.13	4.37	4.26
3113	12.54	20.01	-7.48	7.48	-0.69	0.62	0.61
3114	9.31	17.65	-8.34	8.34	0.17	1.13	1.10
3207	10.02	18.26	-8.24	8.24	0.08	1.06	1.03
3209	10.49	18.26	-7.77	7.77	-0.39	0.76	0.74
3218	11.49	21.41	-9.92	9.92	1.76	3.38	3.30
3221	9.18	18.44	-9.26	9.26	1.10	2.14	2.09

mtDNA:gDNA	**Mean**	**SEM**
BL-6	1.00	0.14
BL-6+PDTC	3.67	1.32
BL-6+sgp130Fc	1.79	0.58
Min	0.17	0.06
Min+PDTC	0.73	0.10
Min+sgp130Fc	1.73	1.19

Cyto C		-bg	Normalized	Cyto C		-bg	Normalized			
B6	144.424	73.654	0.863	B6	185.36	56.66	1.066			
B6	147.951	77.181	0.905	B6	174.151	45.451	0.855		Mean	SEM
B6	175.874	105.104	1.232	B6	188.745	60.045	1.129	BL-6	1.000	0.05
Min	91.685	20.915	0.245	Min	140.939	12.239	0.230	Min	0.462	0.11
Min	92.42	21.65	0.254	Min	157.445	28.745	0.541	Fc	1.222	0.06
Min	87.102	16.332	0.191	Min	188.933	60.233	1.133	skm	0.860	0.03
skm	149.66	78.89	0.925	Fc	196.015	67.315	1.266	skmMin	0.695	0.02
skm	140.177	69.407	0.814	Fc	186.64	57.94	1.090	FcMin	1.074	0.11
skm	142.703	71.933	0.843	Fc	199.795	71.095	1.337			
skmMin	134.99	64.22	0.753	FcMin	202.745	74.045	1.393			
skmMin	126.158	55.388	0.649	FcMin	173.773	45.073	0.848			
skmMin	129.044	58.274	0.683	FcMin	195.547	66.847	1.257			
				B6	174.151	45.451	0.855			
				B6	186.92	58.22	1.095			
				Min	165.218	36.518	0.687			
				Min	150.892	22.192	0.417			
				Fc	185.91	57.21	1.076			
				Fc	200.074	71.374	1.342			
				FcMin	182.099	53.399	1.004			
				FcMin	174.782	46.082	0.867			

MFN		-bg	Normalized	MFN		-bg	Normalized			
B6	205.32	66.78	1.65	B6	162.58	28.21	1.23			
B6	177.90	39.36	0.97	B6	163.99	29.62	1.29		Mean	SEM
B6	167.08	28.54	0.70	B6	145.30	10.94	0.48	BL-6	1.000	0.13
Min	141.11	2.58	0.06	Min	139.66	5.30	0.23	Min	0.413	0.07
Min	164.24	25.70	0.63	Min	142.90	8.53	0.37	Fc	2.154	0.36
Min	155.65	17.11	0.42	Min	148.01	13.65	0.60	skm	1.032	0.09
skm	173.72	35.18	0.87	Fc	180.78	46.41	2.02	skmMin	0.913	0.11
skm	185.75	47.22	1.16	Fc	199.14	64.78	2.83	FcMin	0.366	0.10
skm	192.24	53.70	1.33	Fc	171.32	36.95	1.61			
skmMin	181.18	42.64	1.05	FcMin	141.13	6.77	0.30			
skmMin	181.11	42.57	1.05	FcMin	139.98	5.61	0.24			
skmMin	157.08	18.54	0.46	FcMin	147.16	12.80	0.56			
B6	177.89	39.35	0.97							
B6	167.14	28.60	0.71							
Min	164.85	26.32	0.65							
Min	151.99	13.46	0.33							
skm	173.92	35.39	0.87							
skm	176.19	37.66	0.93							
skmMin	180.34	41.80	1.03							
skmMin	177.95	39.41	0.97							

FIS		-bg	Normalized	FIS		-bg	Normalized			
B6	88.004	17.27	1.16	B6	153.619	19.26	0.90			
B6	80.798	10.06	0.67	B6	150.154	15.79	0.74		Mean	SEM
B6	87.396	16.66	1.11	B6	163.683	29.32	1.37	BL-6	1.000	0.09
Min	150.25	79.51	5.32	Min	159.215	24.85	1.16	Min	5.034	1.39
Min	193.273	122.54	8.20	Min	177.273	42.91	2.00	Fc	0.783	0.12
Min	230.887	160.15	10.72	Min	165.115	30.75	1.43	skm	2.853	0.29
skm	123.844	53.11	3.55	Fc	149.087	14.73	0.69	skmMin	4.348	0.51
skm	104.023	33.29	2.23	Fc	148.096	13.73	0.64	FcMin	0.358	0.13
skm	112.238	41.50	2.78	Fc	156.319	21.96	1.02			
skmMin	141.091	70.35	4.71	FcMin	145.35	10.99	0.51			
skmMin	152.369	81.63	5.46	FcMin	144.252	9.89	0.46			
skmMin	116.5	45.76	3.06	FcMin	136.531	2.17	0.10			
B6	86.517	15.78	1.06							
Min	166.401	95.66	6.40							
skm	107.402	36.66	2.45							
skmMin	132.817	62.08	4.16							

Atrogin		-bg	Normalized	**Atrogin**		-bg	Normalized			
B6	110.094	19.03	0.82	B6	93.917	2.86	0.52			
B6	115.139	24.08	1.04	B6	95.047	3.99	0.72		Mean	SEM
B6	117.691	26.63	1.15	B6	100.764	9.70	1.76	BL-6	1.000	0.14
Min	162.956	71.90	3.10	Min	136.821	45.76	8.30	Min	5.248	1.10
Min	166.068	75.01	3.24	Min	143.883	52.82	9.58	Fc	1.872	0.96
Min	140.822	49.76	2.15	Min	130.366	39.31	7.13	skm	0.780	0.02
skm	109.857	18.80	0.81	Fc	98.371	7.31	1.33	skmMin	1.110	0.09
skm	108.091	17.03	0.73	Fc	111.702	20.64	3.74	FcMin	1.734	1.18
skm	109.462	18.40	0.79	Fc	94.077	3.02	0.55			
skmMin	122.723	31.66	1.37	FcMin	113.487	22.43	4.07			
skmMin	114.48	23.42	1.01	FcMin	96.166	5.11	0.93			
skmMin	117.156	26.10	1.13	FcMin	92.215	1.16	0.21			
B6	114.019	22.96	0.99							
Min	166.401	75.34	3.25							
skm	107.402	16.34	0.71							
skmMin	112.817	21.76	0.94							

S6	Phospho	Total	Phos: total	Normalized	**S6**	Phospho	Total	Phos: total	Normalized			
B6	38.15	149.22	0.26	0.96	B6	12.33	49.49	0.25	0.53			
B6	35.55	160.44	0.22	0.83	B6	26.43	42.64	0.62	1.32		Mean	SEM
B6	48.91	151.11	0.32	1.21	B6	20.85	38.59	0.54	1.15	BL-6	1.000	0.12
Min	5.84	160.47	0.04	0.14	Min	6.06	30.40	0.20	0.42	Min	0.396	0.08
Min	16.98	150.66	0.11	0.42	Min	9.03	31.48	0.29	0.61	Fc	1.000	0.34
Min	7.82	167.77	0.05	0.17	Min	9.52	33.24	0.29	0.61	skm	0.708	0.16
skm	16.67	155.77	0.11	0.40	Fc	13.69	31.99	0.43	0.91	skmMin	0.250	0.12
skm	32.39	152.97	0.21	0.79	Fc	5.34	24.73	0.22	0.46	FcMin	0.520	0.16
skm	37.67	151.90	0.25	0.93	Fc	15.28	19.98	0.76	1.63			
skmMin	21.09	162.52	0.13	0.49	FcMin	7.12	33.60	0.21	0.45			
skmMin	5.54	163.29	0.03	0.13	FcMin	14.02	36.38	0.39	0.82			
skmMin	5.90	163.29	0.04	0.14	FcMin	4.54	33.58	0.14	0.29			

Mouse#	Geno	Treatment	Peak BW	Pre BW	Post BW	%change peak to pre	%change peak to sac	% change pre to sac
121	BL/6	control	28.9	28.1	28.9	-3%	0%	3%
122	BL/6	control	27.4	27	27.4	-1%	0%	1%
123	BL/6	control	22.0	21.5	22.0	-2%	0%	2%
702	BL/6	control	24.4	24.5	24.4	0%	0%	0%
124	BL/6	control	26.0	25.6	26.0	-2%	0%	2%
		average	**25.7**	**25.3**	**25.7**		**0.0%**	**1.6%**
		stdev	**2.7**	**2.5**	**2.7**		**0.0%**	**1.2%**
		se	**1.2**	**1.1**	**1.2**		**0.0%**	**0.6%**
3051	BL/6	PDTC	27.1	26	27.1	-4%	0%	4%
3086	BL/6	PDTC	28.7	27.4	28.7	-5%	0%	5%
3052	BL/6	PDTC	31.6	31.2	31.6	-1%	0%	1%
3085	BL/6	PDTC	25.4	25	25.4	-2%	0%	2%
3048	BL/6	PDTC	26.3	26.3	26.3	0%	0%	0%
		average	**27.8**	**27.2**	**27.8**		**0.0%**	**2.4%**
		stdev	**2.4**	**2.4**	**2.4**		**0.0%**	**2.0%**
		se	**1.1**	**1.1**	**1.1**		**0.0%**	**0.9%**
3050	Min	control	23.5	22.6	22.3	-4%	-5%	-1%
2537	Min	control	23.8	21.9	19.5	-8%	-18.1%	-11%
684	Min	control	23.1	22.2	20.3	-4%	-12%	-9%
2916	Min	control	25.8	23.3	20.9	-10%	-19%	-10%
2974	Min	control	24.0	22.2	20.5	-8%	-15%	-8%
			24.0	**22.4**	**20.7**	**-6.6%**	**-13.8%**	**-7.8%**
			1.0	**0.5**	**1.0**	**-7.1%**	**-15.5%**	**-9.0%**
			0.52	**0.27**	**0.46**	**-6.6%**	**-13.8%**	**-7.8%**
5	Min	PDTC	25.1	23	25.2	-8%	0%	10%
8	Min	PDTC	27.2	26	25.4	-4%	-7%	-2%
598	Min	PDTC	25.8	24.2	24.7	-6%	-4%	2%
611	Min	PDTC	25.8	24.1	24.7	-7%	-4%	2%
610	Min	PDTC	24.2	22.3	23.8	-8%	-2%	7%
658	Min	PDTC	24.5	22.9	24	-7%	-2%	5%
		average	**25.4**	**23.8**	**24.6**	**-6.7%**	**-3.1%**	**3.9%**
		stdev	**1.1**	**1.3**	**0.6**	**1.4%**	**2.5%**	**4.1%**
		se	**0.44**	**0.54**	**0.26**	**0.6%**	**1.0%**	**1.7%**

#	Geno	Treat	R.Sol	L.Sol		R. Plant	L. Plant		R. Gas	L. Gas		R. EDL	L. EDL		R. TA	L. TA		R. RF	L. RF	
121	BL/6	control	10	10	10	19	18	18.5	149	134	141.5	14	14	14	57	51	54	113	100	106.5
122	BL/6	control	8	9	8.5	19	14	16.5	139	137	138	12	11	11.5	39	48	43.5	100	95	97.5
123	BL/6	control	6	6	6	15	15	15	111	109	110	10	10	10	38	40	39	65	78	71.5
702	BL/6	control	9	8	8.5	17	17	17	124	126	125	10	11	10.5	44	43	43.5	81	81	81
124	BL/6	control	10	8	9	17	17	17	133	137	135	11	12	11.5	46	49	47.5	104	115	109.5
		average			**8.4**			**16.8**			**129.9**			**11.5**			**45.5**			**93.2**
		stdev			**1.5**			**1.3**			**12.7**			**1.5**			**5.6**			**16.4**
		se			**0.7**			**0.6**			**5.7**			**0.7**			**2.5**			**7.4**
3051	BL/6	PDTC	11	12	11.5	22	22	22	155	159	157	15	14	14.5	57	51	54	120	122	121
3086	BL/6	PDTC	11	13	12	20	23	21.5	146	144	145	14	12	13	53	55	54	100	96	98
3052	BL/6	PDTC	12	13	12.5	23	24	23.5	155	145	150	16	15	15.5	56	56	56	115	107	111
3085	BL/6	PDTC	11	11	11	19	17	18	126	129	127.5	12	13	12.5	51	49	50	96	89	92.5
3048	BL/6	PDTC	10	10	10	19	18	18.5	129	131	130	11	12	11.5	46	49	47.5	90	91	90.5
		average			**11.4**			**20.7**			**141.9**			**13.4**			**52.3**			**102.6**
		stdev			**1.0**			**2.4**			**12.8**			**1.6**			**3.5**			**13.0**
		se			**0.43**			**1.06**			**5.71**			**0.71**			**1.55**			**5.83**
3050	Min	control	7	8	7.5	16	15	15.5	98	100	99	8	7	7.5	37	36	36.5	75	76	75.5
2537	Min	control	5	6	5.5	10	8	9	75	73	74	6	9	7.5	29	33	31	56	na	56
684	Min	control	7	7	7	12	11	11.5	68	75	71.5	7	6	6.5	27	28	27.5	53	51	52
2916	Min	control	8	8	8	14	13	13.5	91	89	90	8	7	7.5	36	31	33.5	67	67	67
2974	Min	control	6	7	6.5	11	10	10.5	79	82	80.5	6	7	6.5	31	34	32.5	58	54	56
		average			**6.9**			**12.0**			**83.0**			**7.1**			**32.2**			**62.6**
		stdev			**1.0**			**2.5**			**11.5**			**0.5**			**3.3**			**10.7**
		se			**0.43**			**1.14**			**5.12**			**0.24**			**1.48**			**4.77**
5	Min	PDTC	7	9	8	12	15	13.5	85	94	89.5	8	9	8.5	27	39	33	63	68	65.5
8	Min	PDTC	9	8	8.5	16	14	15	112	106	109	10	9	9.5	43	na	43	73	66	69.5
598	Min	PDTC	8	7	7.5	13	13	13	91	90	90.5	9	8	8.5	37	37	37	60	54	57
611	Min	PDTC	7	7	7	15	16	15.5	104	104	104	7	8	7.5	34	38	36	67	69	68
610	Min	PDTC	8	6	7	18	13	15.5	94	84	89	7	7	7	30	29	29.5	71	64	67.5
658	Min	PDTC	8	7	7.5	15	14	14.5	98	100	99	9	7	8	31	32	31.5	76	87	81.5
		average			**7.6**			**14.5**			**96.8**			**8.2**			**35.0**			**68.2**
		stdev			**0.6**			**1.0**			**8.5**			**0.9**			**4.8**			**7.9**
		se			**0.24**			**0.43**			**3.46**			**0.36**			**1.96**			**3.22**

Mouse#	Geno	Treatment	Liver	Spleen	Epi Fat	Testes	Heart	Mes Fat	TL(mm)
121	BL/6	control	913	119	299	197	117	406	16.7
122	BL/6	control	1149	78	330	218	107	329	17.1
123	BL/6	control	953	151	146	178	93	258	16.5
702	BL/6	control	1198	86	267	192	97		16.6
124	BL/6	control	964	97	394	199	113	334	16.4
		average	**1035.4**	**106.2**	**287.2**	**196.8**	**105.4**	**331.8**	**16.7**
		stdev	**128.7**	**29.4**	**91.8**	**14.4**	**10.2**	**60.5**	**0.3**
		se	**57.5**	**13.2**	**41.1**	**6.4**	**4.6**	**30.2**	**0.1**
3051	BL/6	PDTC	1548	114	535	230	133	501	17.5
3086	BL/6	PDTC	1215	88	415	208	115	391	17.1
3052	BL/6	PDTC	1442	94	528	215	128	425	17.4
3085	BL/6	PDTC	1149	73	275	193	104	349	17
3048	BL/6	PDTC	1113	73	393	184	119	366	17
		average	**1293.4**	**88.4**	**429.2**	**206.0**	**119.8**	**406.4**	**17.2**
		stdev	**191.3**	**17.0**	**107.5**	**18.1**	**11.3**	**60.1**	**0.2**
		se	**85.57**	**7.62**	**48.09**	**8.11**	**5.07**	**26.89**	**0.10**
3050	Min	control	1072	219	203	198	96	233	16.6
2537	Min	control	1338	427	0	177	91	230	16.7
684	Min	control	1512	642	0	126	107	228	16
2916	Min	control	1439	397	0	174	110	276	17
2974	Min	control	1327	436	0	169	101	227	16.7
		average	**1337.6**	**424.2**	**40.6**	**168.8**	**101.0**	**238.8**	**16.6**
		stdev	**166.8**	**150.4**	**90.8**	**26.4**	**7.8**	**20.9**	**0.4**
		se	**74.62**	**67.24**	**40.60**	**11.79**	**3.48**	**9.36**	**0.16**
5	Min	PDTC	2058	662	157	102	125	337	16.7
8	Min	PDTC	1999	678	336	167	145	162	16.5
598	Min	PDTC	1594	674	34	131	156	317	17
611	Min	PDTC	1905	604	106	185	127	308	17
610	Min	PDTC	1879	701	92	156	151	248	16.8
658	Min	PDTC	1718	648	86	158	111	326	17.1
		average	**1858.8**	**661.2**	**135.2**	**149.8**	**135.8**	**283.0**	**16.9**
		stdev	**174.3**	**33.1**	**106.0**	**29.3**	**17.5**	**67.0**	**0.2**
		se	**71.14**	**13.51**	**43.27**	**11.94**	**7.15**	**27.33**	**0.09**

		-bg	Norm	P:total	
PSTAT	BL-6	122.175	4.10	0.84	0.93
	BL-6	124.971	6.90	1.41	1.37
	BL-6	121.719	3.64	0.75	0.70
	BL-6+PDTC	122.086	4.01	0.82	0.55
	BL-6+PDTC	119.768	1.69	0.35	0.38
	BL-6+PDTC	120.602	2.53	0.52	0.35
	Min	126.097	8.02	1.64	1.81
	Min	138.388	20.31	4.16	4.48
	Min	130.061	11.99	2.46	2.81
	Min	132.059	13.98	2.87	3.62
	Min+PDTC	124.047	5.97	1.22	1.50
	Min+PDTC	121.018	2.94	0.60	0.93
	Min+PDTC	120.17	2.09	0.43	0.37
	Min+PDTC	123.541	5.47	1.12	1.20
Total STAT3	BL-6	99.748	13.17	0.91	
	BL-6	101.56	14.98	1.03	
	BL-6	102.049	15.47	1.06	
	BL-6+PDTC	108.306	21.73	1.49	
	BL-6+PDTC	99.896	13.32	0.92	
	BL-6+PDTC	108.04	21.46	1.48	
	Min	99.766	13.19	0.91	
	Min	100.087	13.51	0.93	
	Min	99.294	12.72	0.87	
	Min	98.102	11.52	0.79	
	Min+PDTC	98.449	11.87	0.82	
	Min+PDTC	95.963	9.39	0.65	
	Min+PDTC	103.23	16.65	1.15	
	Min+PDTC	100.157	13.58	0.93	

			-bg	norm	phos:total	norm
PAMPK	BL-6	109.007	0.80	0.40	0.54	0.57
	BL-6	109.844	1.64	0.82	0.73	0.77
	BL-6	111.739	3.53	1.77	1.58	1.67
	BL-6+PDTC	109.45	1.24	0.63	0.36	0.38
	BL-6+PDTC	116.723	8.52	4.28	6.78	7.14
	BL-6+PDTC	114.074	5.87	2.95	2.79	2.94
	Min	129.468	21.26	10.68	8.84	9.32
	Min	134.588	26.38	13.25	12.08	12.72
	Min	145.193	36.99	18.58	11.83	12.46
	Min	123.8	15.59	7.83	6.88	7.25
	Min+PDTC	110.257	2.05	1.03	1.36	1.44
	Min+PDTC	111.118	2.91	1.46	0.98	1.03
	Min+PDTC	108.824	0.62	0.31	0.29	0.30
	Min+PDTC	108.803	0.60	0.30	0.24	0.25

TAMPK	BL-6	84.106	5.84	0.75
	BL-6	87.074	8.81	1.13
	BL-6	87.022	8.76	1.12
	BL-6+PDTC	91.923	13.66	1.75
	BL-6+PDTC	83.187	4.92	0.63
	BL-6+PDTC	86.504	8.24	1.06
	Min	87.686	9.42	1.21
	Min	86.824	8.56	1.10
	Min	90.514	12.25	1.57
	Min	87.142	8.88	1.14
	Min+PDTC	84.161	5.89	0.76
	Min+PDTC	89.948	11.68	1.50
	Min+PDTC	86.671	8.40	1.08
	Min+PDTC	87.957	9.69	1.24

			-bg	norm		Mean	SEM
Atrogin	BL-6	150.773	18.57	1.21	BL-6	1.00	0.27
	BL-6	152.718	20.52	1.33	BL-6+PDTC	0.59	0.11
	BL-6	139.281	7.08	0.46	Min	1.87	0.14
	BL-6+PDTC	139.151	6.95	0.45	Min+PDTC	0.71	0.25
	BL-6+PDTC	140.18	7.98	0.52			
	BL-6+PDTC	144.672	12.47	0.81			
	Min	160.432	28.23	1.83			
	Min	165.272	33.07	2.15			
	Min	163.25	31.05	2.02			
	Min	155.108	22.91	1.49			
	Min+PDTC	144.834	12.64	0.82			
	Min+PDTC	152.346	20.15	1.31			
	Min+PDTC	141.968	9.77	0.63			
	Min+PDTC	133.642	1.44	0.09			

			-bg	Norm		Mean	SEM
puromycin	BL-6	133.59	67.748	0.797733	BL-6	1.00	0.12
	BL-6	149.425	83.583	0.98419	BL-6+PDTC	1.31	0.02
	BL-6	169.288	103.446	1.218077	Min	0.41	0.06
	BL-6+PDTC	176.093	110.251	1.298206	Min+PDTC	0.90	0.10
	BL-6+PDTC	179.97	114.128	1.343858			
	BL-6+PDTC	175.439	109.597	1.290505			
	Min	87.5	21.658	0.255023			
	Min	107.642	41.8	0.492195			
	Min	106.985	41.143	0.484459			
	Min	101.962	36.12	0.425313			
	Min+PDTC	115.336	49.494	0.582792			
	Min+PDTC	152.724	86.882	1.023036			
	Min+PDTC	147.7	81.858	0.963878			
	Min+PDTC	151.67	85.828	1.010625			

			Normalized
MFN	BL-6	152.26	1.01
	BL-6	150.27	0.99
	BL-6	151.83	1.00
	BL-6+PDTC	137.70	0.91
	BL-6+PDTC	165.84	1.09
	BL-6+PDTC	183.64	1.21
	Min	146.35	0.97
	Min	129.52	0.86
	Min	130.29	0.86
	Min+PDTC	159.89	1.06
	Min+PDTC	180.88	1.19
	Min+PDTC	174.37	1.15

	Mean	SEM
BL-6	1.00	0.00
BL-6+PDTC	1.07	0.09
Min	0.89	0.04
Min+PDTC	1.13	0.04

FIS	BL-6	59.35	0.94
	BL-6	61.72	0.98
	BL-6	68.69	1.09
	BL-6+PDTC	68.11	1.08
	BL-6+PDTC	66.83	1.06
	BL-6+PDTC	71.96	1.14
	Min	69.63	1.10
	Min	74.51	1.18
	Min	73.46	1.16
	Min+PDTC	73.21	1.16
	Min+PDTC	71.14	1.12
	Min+PDTC	68.37	1.08

	Mean	SEM
BL-6	1.00	0.04
BL-6+PDTC	1.09	0.02
Min	1.15	0.02
Min+PDTC	1.12	0.02

CytoC	BL-6	189.13	0.95
	BL-6	205.99	1.04
	BL-6	201.25	1.01
	BL-6+PDTC	205.73	1.03
	BL-6+PDTC	197.90	1.00
	BL-6+PDTC	183.23	0.92
	Min	127.00	0.64
	Min	154.23	0.78
	Min	128.37	0.65
	Min+PDTC	185.33	0.93
	Min+PDTC	199.57	1.00
	Min+PDTC	196.84	0.99

	Mean	SEM
BL-6	1.00	0.03
BL-6+PDTC	0.98	0.03
Min	0.69	0.04
Min+PDTC	0.98	0.02

Mouse#	Geno	Treatment	8wk BW	Pre BW	Post BW	Sac-tumor	BW change
110	BL/6 + LLC	Control	20.6	23.5	28.1	21.583	4.8
3143	BL/6 + LLC	Control	22.1	22.9	22.4	20.337	-8.0
3138	BL/6 + LLC	Control	23.1	24.7	26	22.455	-2.8
3142	BL/6 + LLC	Control	21.4	20.1	17.1	16.14	-24.6
		avg	**21.8**	**22.8**	**23.4**	**20.1**	**-7.6**
		stdev	**1.1**	**1.9**	**4.8**	**2.8**	**12.4**
		n	**4.0**	**4.0**	**4.0**	**4.0**	**4.0**
		se	**0.5**	**1.0**	**2.4**	**1.4**	**6.2**

Mouse#	Geno	Treatment	8wk BW	Pre BW	Post BW	Sac-tumor	BWchange
108	BL/6 + LLC	PDTC	21.6	22.8	27.9	22.75	5.3
3103	BL/6 + LLC	PDTC	21.2	23.2	23.6	22.259	5.0
3104	BL/6 + LLC	PDTC	24.3	24.5	24.4	23.58	-3.0
3110	BL/6 + LLC	PDTC	20.8	21.0	21.7	19.957	-4.1
		avg	**22.0**	**22.9**	**24.4**	**22.1**	**0.8**
		stdev	**1.6**	**1.4**	**2.6**	**1.6**	**5.0**
		n	**4.0**	**4.0**	**4.0**	**4.0**	**4.0**
		se	**0.8**	**0.7**	**1.3**	**0.8**	**2.5**

Mouse#	Geno	Treatment	8wk BW	Pre BW	Post BW	Sac-tumor	BWchange
105	BL/6 + LLC	IL-6rAb	24.9	26.2	27.2	24.115	-3.2
109	BL/6 + LLC	IL-6rAb	22.1	24.6	27.8	22.082	-0.1
3149	BL/6 + LLC	IL-6rAb	23.8	24.9	26.2	24.15	1.5
3148	BL/6 + LLC	IL-6rAb	24.7	25.9	23.6	22.115	-10.5
		avg	**23.9**	**25.4**	**26.2**	**23.1**	**-3.1**
		stdev	**1.3**	**0.8**	**1.9**	**1.2**	**5.3**
		n	**4.0**	**4.0**	**4.0**	**4.0**	**4.0**
		se	**0.6**	**0.4**	**0.9**	**0.6**	**2.6**

0.523

Mouse#	Geno	Treatment	8wk BW	Pre BW	Post BW	Sac-tumor	BWchange
116fc	BL/6 + LLC	sgp130Fc	22.2	23.7	21.8	20.655	-7.0
166fc	BL/6 + LLC	sgp130Fc	22.4	24.6	23.8	20.389	-9.0
167fc	BL/6 + LLC	sgp130Fc	21.9	23.1	24.4	21.43	-2.1
118fc	BL/6 + LLC	sgp130Fc	21.5	23.4	23	21.174	-1.5
120fc	BL/6 + LLC	sgp130Fc	22.9	26.3	27.3	23.674	3.4
		avg	**22.2**	**24.2**	**24.1**	**21.5**	**-3.2**
		stdev	**0.5**	**1.3**	**2.1**	**1.3**	**4.9**
		n	**5.0**	**5.0**	**5.0**	**5.0**	**5.0**
		se	**0.2**	**0.6**	**0.9**	**0.6**	**2.2**

Mouse#	Geno	Treatment	8wk BW	Pre BW	Post BW	Sac-tumor	BWchange
3175	BL/6 + LLC	LLL12	25.2	26.1	25.8	21.709	-13.9
3182	BL/6 + LLC	LLL12	22	23.7	22.6	22.267	1.2
3185	BL/6 + LLC	LLL12	23.9	23.2	22.3	21.229	-11.2
3184	BL/6 + LLC	LLL12	23.9	23.9	23.5	21.329	-10.8
3183	BL/6 + LLC	LLL12	23	25.1	21.8	21.148	-8.1
3176	BL/6 + LLC	LLL12	24.2	23.3	24	22.35	-7.6
		avg	**23.7**	**24.2**	**23.3**	**21.7**	**-8.4**
		stdev	**1.1**	**1.1**	**1.5**	**0.5**	**5.2**
		n	**6.0**	**6.0**	**6.0**	**6.0**	**6.0**
		se	**0.4**	**0.5**	**0.6**	**0.2**	**2.1**

Mouse#	R.Sol	L.Sol	R. Plant	L. Plant	R. Gas	L. Gas	R. EDL	L. EDL	R. TA	L. TA	R. RF
110	5	8	11	12	78	101	8	8	24	35	
3143	7	7	13	12	69	97	9	8	36	34	83
3138	8	7	12	16	112	113	9	10	42	43	90
3142	6	6	12	12	85	85	5	4	16*	31	61
	6.5	**7.0**	**12.0**	**13.0**	**86.0**	**99.0**	**7.8**	**7.5**	**34.0**	**35.8**	**78.0**
	1.3	**0.8**	**0.8**	**2.0**	**18.5**	**11.5**	**1.9**	**2.5**	**9.2**	**5.1**	**15.1**
	4.0	**4.0**	**4.0**	**4.0**	**4.0**	**4.0**	**4.0**	**4.0**	**3.0**	**4.0**	**3.0**
	0.6	**0.4**	**0.4**	**1.0**	**9.3**	**5.8**	**0.9**	**1.3**	**5.3**	**2.6**	**8.7**

Mouse#	R.Sol	L.Sol	R. Plant	L. Plant	R. Gas	L. Gas	R. EDL	L. EDL	R. TA	L. TA	R. RF
108	6	5	13	16	na	94	6	8	30	35	47
3103	6	8	16	16	113	110	9	9	40	39	77
3104	10	7	12	13	101	107	8	9	37	38	72
3110	6	7	13	13	86	89	na	7	29	30	60
	7.0	**6.8**	**13.5**	**14.5**	**100.0**	**100.0**	**7.7**	**8.3**	**34.0**	**35.5**	**64.0**
	2.0	**1.3**	**1.7**	**1.7**	**13.5**	**10.1**	**1.5**	**1.0**	**5.4**	**4.0**	**13.4**
	4.0	**4.0**	**4.0**	**4.0**	**3.0**	**4.0**	**3.0**	**4.0**	**4.0**	**4.0**	**4.0**
	1.0	**0.6**	**0.9**	**0.9**	**7.8**	**5.0**	**0.9**	**0.5**	**2.7**	**2.0**	**6.7**

Mouse#	R.Sol	L.Sol	R. Plant	L. Plant	R. Gas	L. Gas	R. EDL	L. EDL	R. TA	L. TA	R. RF
105	8	9	16	17	115	114	13	10	41	43	86
109	5	6	11	14	95	120	8	9	29	37	67
3149	8	7	14	15	102	102	8	11	39	43	85
3148	9	9	20	20	129	129	11	11	48	49	107
	7.5	**7.8**	**15.3**	**16.5**	**110.3**	**116.3**	**10.0**	**10.3**	**39.3**	**43.0**	**86.3**
	1.7	**1.5**	**3.8**	**2.6**	**15.0**	**11.3**	**2.4**	**1.0**	**7.8**	**4.9**	**16.4**
	4.0	**4.0**	**4.0**	**4.0**	**4.0**	**4.0**	**4.0**	**4.0**	**4.0**	**4.0**	**4.0**
	0.9	**0.8**	**1.9**	**1.3**	**7.5**	**5.7**	**1.2**	**0.5**	**3.9**	**2.4**	**8.2**

Mouse#	R.Sol	L.Sol	R. Plant	L. Plant	R. Gas	L. Gas	R. EDL	L. EDL	R. TA	L. TA	R. RF
116fc	8	9	17	16	106	113	10	9	34	39	80
166fc	8	8	11	13	96	93	10	9	37	33	63
167fc	8	9	12	16	103	101	9	9	33	39	65
118fc	7	9	14	13	102	103	4*torn	11	39	42	68
120fc	8	8	16	16	114	118	9	10	42	44	70
	7.8	**8.6**	**14.0**	**14.8**	**104.2**	**105.6**	**9.5**	**9.6**	**37.0**	**39.4**	**69.2**
	0.4	**0.5**	**2.5**	**1.6**	**6.6**	**9.9**	**0.6**	**0.9**	**3.7**	**4.2**	**6.6**
	5.0	**5.0**	**5.0**	**5.0**	**5.0**	**5.0**	**4.0**	**5.0**	**5.0**	**5.0**	**5.0**
	0.2	**0.2**	**1.1**	**0.7**	**2.9**	**4.4**	**0.3**	**0.4**	**1.6**	**1.9**	**3.0**

Mouse#	R.Sol	L.Sol	R. Plant	L. Plant	R. Gas	L. Gas	R. EDL	L. EDL	R. TA	L. TA	R. RF
3175	8	10	13	13	100	100	8	9	33	36	50
3182	7	7	13	13	115	111	8	8	37	38	72
3185	7	8	12	13	101	104	9	10	24	37	65
3184	8	7	17	14	106	107	9	9	36	37	67
3183	7	8	12	14	99	94	7	8	33	36	65
3176	9	7	14	14	104	105	11	7	36	40	68
	7.7	**7.8**	**13.5**	**13.5**	**104.2**	**103.5**	**8.7**	**8.5**	**33.2**	**37.3**	**64.5**
	0.8	**1.2**	**1.9**	**0.5**	**5.9**	**5.9**	**1.4**	**1.0**	**4.8**	**1.5**	**7.6**
	6.0	**6.0**	**6.0**	**6.0**	**6.0**	**6.0**	**6.0**	**6.0**	**6.0**	**6.0**	**6.0**
	0.3	**0.5**	**0.8**	**0.2**	**2.4**	**2.4**	**0.6**	**0.4**	**2.0**	**0.6**	**3.1**

Mouse#	Liver	Spleen	Epi Fat	Testes	Heart	tumor (g)	Mes Fat	TL(mm)
110	1300	286	83	171	92	6.517	191	16.4
3143	1135	376	122	172	93	2.063	232	16.4
3138	1395	364	149	201	101	3.545	266	16.6
3142	902	564	88	171	103	0.96	190	16.2
	1183.0	**397.5**	**110.5**	**178.8**	**97.3**	**3.3**	**219.8**	**16.4**
	215.9	**118.0**	**31.0**	**14.8**	**5.6**	**2.4**	**36.5**	**0.2**
	4.0	**4.0**	**4.0**	**4.0**	**4.0**	**4.0**	**4.0**	**4.0**
	108.0	**59.0**	**15.5**	**7.4**	**2.8**	**1.2**	**18.3**	**0.1**

Mouse#	Liver	Spleen	Epi Fat	Testes	Heart	tumor	Mes Fat	TL(mm)
108	1667	255	141	160	98	5.15	254	16.5
3103	1436	183	302	175	97	1.341	331	16.4
3104	1301	577	127	185	144	0.82	315	16.6
3110	1259	403	91	155	102	1.743	216	16.3
	1415.8	**354.5**	**165.3**	**168.8**	**110.3**	**2.3**	**279.0**	**16.5**
	183.7	**174.3**	**93.6**	**13.8**	**22.6**	**2.0**	**53.5**	**0.1**
	4.0	**4.0**	**4.0**	**4.0**	**4.0**	**4.0**	**4.0**	**4.0**
	91.9	**87.2**	**46.8**	**6.9**	**11.3**	**1.0**	**26.8**	**0.1**

Mouse#	Liver	Spleen	Epi Fat	Testes	Heart	tumor	Mes Fat	TL(mm)
105	1371	243	217	181	116	3.085	331	16.5
109	1258	240	69	190	89	5.718	210	16.6
3149	1093	479	112	167	109	2.05	285	16.6
3148	1169	147	266	186	104	1.485	349	16.8
	1222.8	**277.3**	**166.0**	**181.0**	**104.5**	**3.1**	**293.8**	**16.6**
	119.6	**141.7**	**91.2**	**10.0**	**11.4**	**1.9**	**62.0**	**0.1**
	4.0	**4.0**	**4.0**	**4.0**	**4.0**	**4.0**	**4.0**	**4.0**
	59.8	**70.8**	**45.6**	**5.0**	**5.7**	**0.9**	**31.0**	**0.1**

Mouse#	Liver	Spleen	Epi Fat	Testes	Heart	tumor (g)	Mes Fat	TL(mm)
116fc	1068	296	190	185	97	1.145	278	16.3
166fc	1228	307	74	180	101	3.411	289	16.7
167fc	1266	434	116	177	109	2.97	290	16.4
118fc	1123	372	90	151	102	1.826	267	16.6
120fc	1267	268	274	92	91	3.626	291	16.7
	1190.4	**335.4**	**148.8**	**157.0**	**100.0**	**2.6**	**283.0**	**16.5**
	90.2	**67.0**	**82.9**	**38.6**	**6.6**	**1.1**	**10.4**	**0.2**
	5.0	**5.0**	**5.0**	**5.0**	**5.0**	**5.0**	**5.0**	**5.0**
	40.3	**30.0**	**37.1**	**17.3**	**3.0**	**0.5**	**4.6**	**0.1**

Mouse#	Liver	Spleen	Epi Fat	Testes	Heart	tumor	Mes Fat	TL(mm)
3175	1194	275	45	186	114	4.091	243	16.6
3182	1195	282	221	203	99	0.333	295	16.7
3185	1107	262	125	201	100	1.071	283	16.5
3184	1102	328	77	194	113	2.171	271	16.6
3183	1160	355	22	175	106	0.652	253	16.9
3176	1214	456	85	191	108	1.65	268	16.8
	1162.0	**326.3**	**95.8**	**191.7**	**106.7**	**1.7**	**268.8**	**16.7**
	47.8	**72.6**	**70.7**	**10.3**	**6.3**	**1.4**	**19.0**	**0.1**
	6.0	**6.0**	**6.0**	**6.0**	**6.0**	**6.0**	**6.0**	**6.0**
	19.5	**29.7**	**28.9**	**4.2**	**2.6**	**0.6**	**7.8**	**0.1**

Mouse	Genotype	treatment	Pre BW	BW at Sac	BW-tumor	% change BW	**% change from control**
988	BL/6	13wk control	20.9	23.6	23.6	13%	
989	BL/6	13wk control	24.6	26.3	26.3	7%	
990	BL/6	13wk control	23.4	25.3	25.3	8%	
991	BL/6	13wk control	23.1	25.1	25.1	9%	
992	BL/6	13wk control	24.4	25.7	25.7	5%	
		Average	**23.3**	**25.2**	**25.2**	**8.4%**	
		SE	**0.7**	**0.4**	**0.4**	**1.3%**	
2518	skm-gp130	13wk control	25.6	26.7	26.7	4%	
2524	skm-gp130	13wk control	26.2	28	28	7%	
2574	skm-gp130	13wk control	24.5	27.5	27.5	12%	
2575	skm-gp130	13wk control	23.9	26.1	26.1	9%	
2598	skm-gp130	13wk control	25.7	27.8	27.8	8%	
		Average	**25.2**	**27.2**	**27.2**	**8.2%**	
		SE	**0.4**	**0.4**	**0.4**	**1.3%**	
1794	BL/6	LLC	17.4	23.3	21.8	25%	-14%
1	BL/6	LLC	23.2	28.7	22.7	-2%	-10%
2792	BL/6	LLC	22.1	22.5	22.2	1%	-12%
2791	BL/6	LLC	23.8	26.5	24.7	4%	-2%
1793	BL/6	LLC	18.6	23.7	21.1	13%	-16%
1792	BL/6	LLC	19.1	21.8	21.6	13.0%	-14%
		Average	**20.7**	**24.4**	**22.4**	**9.0%**	**-11.3%**
		SE	**1.1**	**1.1**	**0.5**	**4.1%**	**2.1%**
2669	skm-gp130	LLC	22.1	26	23.5	6%	-14%
2634	skm-gp130	LLC	25.6	29.7	26.3	3%	-3%
2635	skm-gp130	LLC	24.5	25.4	24.2	-1%	-11%
2636	skm-gp130	LLC	26.2	27.6	25.3	-4%	-7%
9715	skm-gp130	LLC	23.3	26.5	23.7	2%	-13%
9716	skm-gp130	LLC	24.2	29.7	27.6	14%	1%
		Average	**24.3**	**27.5**	**25.1**	**3.3%**	**-7.8%**
		SE	**0.6**	**0.8**	**0.7**	**2.5%**	**2.4%**

Mouse	Genotype	R. Sol	L. Sol	R. Plant	L. Plant	R. Gas	L. Gas	R. EDL	L. EDL	R. TA	L. TA	R. RF	L. RF
988	BL/6	8	9	16	17	127	136	12	12	48	49	89	91
989	BL/6	10	10	17	18	139	129	12	12	55	57	96	97
990	BL/6	9	8	20	18	141	142	13	11	55	53	98	96
991	BL/6	9	10	18	17	132	135	8	10	51	50	88	85
992	BL/6	10	9	18	18	120	134	11	10	49	42	73	81
		9.2	**9.2**	**17.8**	**17.6**	**131.8**	**135.2**	**11.2**	**11.0**	**51.6**	**50.2**	**88.8**	**90.0**
		0.4	**0.4**	**0.7**	**0.2**	**3.9**	**2.1**	**0.9**	**0.4**	**1.5**	**2.5**	**4.4**	**3.1**
2518	skm-gp130	12	8	22	22	134	127	13	15	52	55	108	94
2524	skm-gp130	11	10	19	20	127	142	14	14	50	57	102	100
2574	skm-gp130	8	10	17	19	108	126	11	10	46	50	102	95
2575	skm-gp130	8	9	14	16	107	116	9	11	43	48	89	97
2598	skm-gp130	9	11	18	19	135	136	11	12	52	56	116	92
		9.6	**9.6**	**18.0**	**19.2**	**122.2**	**129.4**	**11.6**	**12.4**	**48.6**	**53.2**	**103.4**	**95.6**
		0.8	**0.5**	**1.3**	**1.0**	**6.2**	**4.5**	**0.9**	**0.9**	**1.8**	**1.8**	**4.4**	**1.4**
1794	BL/6	7	8	12	11	89	92	8	8	32		66	
1	BL/6	8	8	14	12	109	99	9	9	36	38	74	77
2792	BL/6	5	5	15	13	108	108	8	9	31	35	71	67
2791	BL/6	8	5	17	17	129	131	11	12	45	17	91	93
1793	BL/6	7	6	12	13	101	106	8	8	34	32	71	70
1792	BL/6	7	8	14	13	104	106	8	8	41	38	69	71
		7.0	**6.7**	**14.0**	**13.2**	**106.7**	**107.0**	**8.7**	**9.0**	**36.5**	**32.0**	**73.7**	**75.6**
		0.4	**0.6**	**0.8**	**0.8**	**5.3**	**5.4**	**0.5**	**0.6**	**2.2**	**3.6**	**3.6**	**4.2**
2669	skm-gp130	9	7	15	14	101	93	8	9	43	41	71	71
2634	skm-gp130	10	9	17	18	133	118	12	10	47	47	95	83
2635	skm-gp130	12	10	16	17	138	127	11	11	47		86	91
2636	skm-gp130	5	6	14	14	133	126	9	9	48	43	79	84
9715	skm-gp130	9	7	15	14	114	109	9	8	39	41	77	78
9716	skm-gp130	8	9	16	14	128	127	11	11	45	47	85	83
		8.8	**8.0**	**15.5**	**15.2**	**124.5**	**116.7**	**10.0**	**9.7**	**44.8**	**43.8**	**82.2**	**81.7**
		0.9	**0.6**	**0.4**	**0.7**	**5.8**	**5.5**	**0.6**	**0.5**	**1.4**	**1.2**	**3.4**	**2.7**

Mouse	Genotype	liver	slpeen	epi fat	testes	heart	tumor (g)	Tibia Length (mm)
988	BL/6	1.3	100	309	180	97	0	16.6
989	BL/6	1.195	91	408	182	100	0	16.9
990	BL/6	1.309	79	302	187	95	0	16.7
991	BL/6	1.135	85	388	191	96	0	16.6
992	BL/6	1.26	83	472	173	96	0	16.8
		1.240	**87.6**	**375.8**	**182.6**	**96.8**	**0.0**	**16.7**
		0.033	**3.7**	**31.9**	**3.1**	**0.9**	**0.0**	**0.1**
2518	skm-gp130	1.461	90	394	205	123	0	17
2524	skm-gp130	1.597	92	385	210	128	0	17.2
2574	skm-gp130	1.466	98	283	227	101	0	16.6
2575	skm-gp130	1.391	87	366	231	114	0	16.7
2598	skm-gp130	1.463	92	432	201	119	0	16.9
		1.476	**91.8**	**372.0**	**214.8**	**117.0**	**0.0**	**16.9**
		0.0	**1.8**	**24.7**	**6.0**	**4.6**	**0.0**	
1794	BL/6	0.967	307	320	166	106	1.545	16.5
1	BL/6	1.327	360	0	198	108	5.974	16.9
2792	BL/6	1.104	402	241	199	120	0.271	16.9
2791	BL/6	1.248	123	370	178	97	1.768	17.1
1793	BL/6	1.161	271	188	156	86	2.603	16.6
1792	BL/6	0.949	79	317	172	85	0.209	16.6
		1.1	**257.0**	**239.3**	**178.2**	**100.3**	**2.1**	**16.8**
		0.1	**52.9**	**54.6**	**7.1**	**5.6**	**0.9**	**0.1**
2669	skm-gp130	1.466	180	222	217	108	2.538	16.6
2634	skm-gp130	1.577	251	271	191	111	3.397	16.8
2635	skm-gp130	1.128	101	363	218	100	1.229	16.8
2636	skm-gp130	1.284	383	218	212	114	2.334	16.8
9715	skm-gp130	1.273	355	184	203	103	2.783	16.6
9716	skm-gp130	1.349	194	287	221	98	2.116	16.9
		1.3	**244.0**	**257.5**	**210.3**	**105.7**	**2.4**	**16.8**
		0.1	**44.2**	**26.1**	**4.6**	**2.6**	**0.3**	**0.0**

Sample	IGF-1	GAPDH	dct	ddct	2^ddct	normalized
988	22.04	23.01	-0.62	-0.28	0.83	0.80
989	22.78	22.57	0.21	0.56	1.47	1.43
990	21.56	22.15	-0.59	-0.24	0.84	0.82
991	22.00	22.15	-0.15	0.20	1.15	1.12
992	21.48	22.06	-0.58	-0.23	0.85	0.83
1794	21.90	22.91	-1.02	-0.67	0.63	0.61
2792	21.62	22.59	-0.97	-0.62	0.65	0.63
2791	21.86	22.62	-0.77	-0.42	0.75	0.73
1793	21.55	22.72	-1.18	-0.83	0.56	0.55
1792	21.23	21.85	-0.97	-0.63	0.65	0.63
2518	23.17	23.04	0.13	0.48	1.39	1.35
2524	23.26	22.94	0.32	0.67	1.59	1.55
2574	22.25	22.35	-0.10	0.25	1.19	1.15
2575	22.23	23.07	-0.84	-0.50	0.71	0.69
2598	22.75	22.43	0.31	0.66	1.58	1.54
2669	22.07	23.71	-1.64	-1.30	0.41	0.40
2634	22.48	22.74	-0.26	0.09	1.06	1.03
2635	22.51	23.38	-0.87	-0.52	0.70	0.68
2636	22.18	23.02	-0.84	-0.50	0.71	0.69
9715	22.24	22.75	-0.50	-0.16	0.90	0.87
9716	22.21	22.56	-0.34	0.00	1.00	0.97

IGF-1	Mean	sem
BL-6	1.00	0.12
LLC	0.63	0.03
skm-gp130	1.26	0.16
skm-gp130+LLC	0.77	0.10

Sample	IL-6	18S	dCT	dddct	2^ddct	Normalized
988	35.62	16.34	19.28	0.47	1.38	1.32
989	34.64	15.65	18.99	0.18	1.13	1.08
990	34.44	16.31	18.14	-0.67	0.63	0.60
991	34.64	16.22	18.43	-0.38	0.77	0.73
992	35.07	15.85	19.22	0.41	1.33	1.27
1974	34.54	15.71	18.83	0.02	1.02	0.97
2792	34.30	15.59	18.72	-0.09	0.94	0.90
2791	34.51	14.02	20.49	1.68	3.21	3.06
1793	33.26	14.45	18.82	0.01	1.00	0.96
1792	34.72	14.53	20.19	1.38	2.61	2.49
2518	34.93	14.93	20.00	1.19	2.28	2.18
2524	34.94	17.10	17.84	-0.97	0.51	0.49
2474	34.47	14.06	20.41	1.60	3.03	2.89
2575	34.52	14.68	19.84	1.03	2.04	1.95
2598	35.01	14.46	20.56	1.75	3.36	3.20
2669	33.39	15.73	17.67	-1.14	0.45	0.43
2634	33.45	15.39	18.06	-0.75	0.60	0.57
2635	34.43	15.59	18.85	0.04	1.03	0.98
2636	35.59	17.48	18.11	-0.70	0.61	0.59
9715	33.29	16.27	17.03	-1.78	0.29	0.28
9716	34.55	15.08	19.47	0.66	1.58	1.51

IL-6	mean	sem
bl-6	1.00	0.14
bl-6+llc	1.68	0.46
skmgp130	0.73	0.18
skmgp130+llc	2.14	0.47

Sample	REDD1	GAPDH	dct	ddct	2^ddct	Normalizezd
9716	15.46	19.12	-3.66	1.212	2.317	2.299
9715	15.26	18.68	-3.42	1.452	2.736	2.715
2636	14.405	18.775	-4.37	0.502	1.416	1.405
2635	14.53	19.09	-4.56	0.312	1.241	1.232
2634	13.215	18.42	-5.205	-0.333	0.794	0.788
2669	14.575	19.27	-4.695	0.177	1.131	1.122
1792	14.055	18.545	-4.49	0.382	1.303	1.293
1793	14.05	18.665	-4.615	0.257	1.195	1.186
2792	13.915	18.745	-4.83	0.042	1.030	1.022
2791	14.085	18.11	-4.025	0.847	1.799	1.785
1	15.92	18.97	-3.05	1.822	3.536	3.509
2598	9.345	17.945	-8.6	-3.728	0.075	0.075
2575	12.955	18.54	-5.585	-0.713	0.610	0.605
2574	12.665	18.42	-5.755	-0.883	0.542	0.538
2524	11.75	18.225	-6.475	-1.603	0.329	0.327
2518	10.5	18	-7.5	-2.628	0.162	0.161
991	12.945	17.845	-4.9	-0.028	0.981	0.973
992	12.725	17.595	-4.87	0.002	1.001	0.994
990	12.855	17.585	-4.73	0.142	1.103	1.095
989	12.865	18.055	-5.19	-0.318	0.802	0.796
988	14.025	18.695	-4.67	0.202	1.150	1.142

REDD1	Mean	SEM
BL-6	1.00	0.06
BL-6+LLC	1.76	0.46
skm-gp130	0.34	0.10
skm-gp130+LLC	1.59	0.31

Sample	gp130	GAPDH	dCT	ddct	2^ddct	normalized to gas
sol	30.76	17.87	12.89	-0.65	0.64	0.53
sol	30.8	17.99	12.81	-0.73	0.60	0.50
sol	30.42	17.88	12.54	-1.01	0.50	0.41
sol	29.96	17.14	12.82	-0.72	0.60	0.50
gas	29.96	15.85	14.11	0.57	1.48	1.23
gas	30.04	16.54	13.5	-0.04	0.97	0.80
gas	28.47	15.84	12.63	-0.91	0.53	0.88
gas	29.65	15.71	13.94	0.40	1.31	1.09
TA	31.15	16.5	14.65	0.86	1.81	1.66
TA	31.36	16.77	14.59	0.80	1.74	1.71
TA	31.09	16.62	14.47	0.68	1.60	1.57
TA	32.74	17.25	15.49	1.70	3.24	3.19
heart	28.72	17.06	11.66	-1.89	0.27	0.22
heart	28.59	17.57	11.02	-2.53	0.17	0.14
heart	31.41	18.47	12.94	-0.60	0.66	0.55
heart	28.45	17.33	11.12	-2.43	0.19	0.15
kid	28.22	18	10.22	-3.33	0.10	0.08
kid	26.66	16.99	9.67	-3.88	0.07	0.06
kid	26.56	16.97	9.59	-3.96	0.06	0.05
kid	27.16	17.39	9.77	-3.78	0.07	0.06
liver	29.23	19.29	9.94	-3.61	0.08	0.07
liver	28.74	18.53	10.21	-3.34	0.10	0.08
liver	30.26	19.01	11.25	-2.30	0.20	0.17

gp130	Mean	SD	SEM
sol	0.48	0.05	0.02
gas	1.00	0.19	0.10
TA	2.04	0.77	0.39
heart	0.27	0.19	0.09
kidney	0.06	0.01	0.01
liver	0.11	0.05	0.03

Plasma IL-6

Standard	Abs1	Abs2	average	stdev	CV	-bg
0	0.0992	0.1006	0.0999	0.00099	1%	0
7.8	0.112	0.116	0.114	0.002828	2%	0.0141
15.6	0.1404	0.1416	0.141	0.000849	1%	0.0411
31.2	0.1916	0.183	0.1873	0.006081	3%	0.0874
62.5	0.2888	0.2696	0.2792	0.013576	5%	0.1793
125	0.4614	0.4546	0.458	0.004808	1%	0.3581
250	0.8858	0.8652	0.8755	0.014566	2%	0.7756
500	1.4506	1.4864	1.4685	0.025314	2%	1.3686
Chromagen Blank	0.0898	0.0926	0.0912	0.00198	2%	-0.0087
LC	0.1544	0.1468	0.1506	0.005374	4%	0.0507
HC	0.8202	0.7472	0.7837	0.051619	7%	0.6838

Sample	Abs1	Abs2	average	stdev	CV	-bg		Concentration
positive con	0.246	0.243	0.244	0.00	0.01	0.14	48.32	96.64
988	0.121	0.115	0.118	0.00	0.03	0.02	3.11	6.21
989	0.112	0.099	0.106	0.01	0.09	0.01	-1.25	0
990	0.120	0.116	0.118	0.00	0.02	0.02	3.18	6.36
991	0.113	0.105	0.109	0.01	0.05	0.01	0.00	0.00
992	0.102	0.105	0.104	0.00	0.02	0.00	-2.00	0
2518	0.117	0.114	0.115	0.00	0.02	0.02	2.18	4.36
2524	0.107	0.103	0.105	0.00	0.03	0.01	-1.39	0
2574	0.110	0.103	0.107	0.01	0.05	0.01	-0.89	0
2575	0.106		0.106			0.01	-1.04	0
2598	0.102		0.102			0.00	-2.61	01
1794	0.147	0.146	0.146	0.00	0.01	0.05	13.32	26.64
1793	0.109	0.108	0.109	0.00	0.01	0.01	-0.18	0
1792	0.105	0.106	0.106	0.00	0.00	0.01	-1.29	0
2792	0.280	0.265	0.273	0.01	0.04	0.17	58.36	116.71
2791	0.115	0.120	0.118	0.00	0.03	0.02	3.00	6.00
2669	0.117	0.119	0.118	0.00	0.01	0.02	3.32	6.64
2634	0.204	0.202	0.203	0.00	0.01	0.10	33.64	67.29
2635	0.120	0.109	0.115	0.01	0.07	0.01	1.93	3.86
2636	0.116	0.113	0.115	0.00	0.02	0.01	1.96	3.93
9715	0.120	0.122	0.121	0.00	0.01	0.02	4.21	8.43
9716	0.124	0.123	0.124	0.00	0.01	0.02	5.18	10.36

STAT3	Phos	total	P:total	norm		Mean	SEM
B6	85.63	43.36	1.98	0.81	BL-6	1.00	0.10
B6	90.11	34.29	2.63	1.08	LLC	1.55	0.29
B6	111.23	41.04	2.71	1.11	LLC+LLL12	0.87	0.15
LLC	133.57	37.57	3.56	1.46			
LLC	226.58	55.51	4.08	1.67			
LLC	164.07	29.82	5.50	2.26			
LLC	95.29	47.18	2.02	0.83			
LLC+LLL12	74.67	51.21	1.46	0.60			
LLC+LLL12	84.31	51.87	1.63	0.67			
LLC+LLL12	88.56	25.11	3.53	1.45			
LLC+LLL12	100.60	52.41	1.92	0.79			
LLC+LLL12	80.55	37.75	2.13	0.88			

AMPK	Phos	total	P:total	norm		Mean	SEM
B6	22.67	36.88	0.61	1.33	BL-6	1.00	0.17
B6	13.47	38.81	0.35	0.75	LLC	1.30	0.15
B6	20.32	47.67	0.43	0.92	LLC+LLL12	0.23	0.09
LLC	34.94	43.55	0.80	1.73			
LLC	24.85	47.15	0.53	1.14			
LLC	35.12	60.24	0.58	1.26			
LLC	26.25	52.97	0.50	1.07			
LLC+LLL12	13.01	50.86	0.26	0.55			
LLC+LLL12	1.83	37.80	0.05	0.10			
LLC+LLL12	2.67	49.04	0.05	0.12			
LLC+LLL12	6.03	51.72	0.12	0.25			
LLC+LLL12	2.11	45.06	0.05	0.10			

S6	Phos	total	P:total	norm		Mean	SEM
B6	11.108	89.99	0.12	0.80	BL-6	1.00	0.12
B6	11.861	77.60	0.15	0.99	LLC	0.28	0.09
B6	16.785	89.44	0.19	1.21	LLC+LLL12	0.17	0.04
LLC	2.143	89.75	0.02	0.15			
LLC	6.308	88.23	0.07	0.46			
LLC	5.481	86.61	0.06	0.41			
LLC	1.062	88.56	0.01	0.08			
LLC+LLL12	4.4	84.84	0.05	0.34			
LLC+LLL12	2.407	83.45	0.03	0.19			
LLC+LLL12	1.142	83.00	0.01	0.09			
LLC+LLL12	1.304	86.00	0.02	0.10			

Atrogin	-bg	norm		Mean	SEM
B6	35.0	1.13	BL-6	1.00	0.16
B6	37.1	1.20	LLC	1.51	0.23
B6	21.0	0.68	LLC+LLL12	0.25	0.10
LLC	44.0	1.42			
LLC	29.6	0.95			
LLC	49.7	1.60			
LLC	63.6	2.05			
LLC+LLL12	18.4	0.59			
LLC+LLL12	10.2	0.33			
LLC+LLL12	2.8	0.09			
LLC+LLL12	7.2	0.23			
LLC+LLL13	0.5	0.02			

FOXO3			-bg	norm	total norm	P:tot	norm		avg	stdev	se
BL-6	9424	195.156	18.84	0.71	0.89	0.80	0.81	BL-6	1.00	0.16	0.09
BL-6	9424	206.988	30.67	1.16	1.05	1.10	1.12				
BL-6	9424	206.159	29.84	1.13	1.06	1.06	1.07				
BL-6 + LLC	9424	206.237	29.92	1.13	0.98	1.15	1.16	BL-6 + LLC	1.08	0.11	0.06
BL-6 + LLC	9424	204.327	28.01	1.06	0.96	1.10	1.11				
BL-6 + LLC	9424	202.545	26.22	0.99	1.05	0.94	0.95				
skm-gp130	9424	200.594	24.27	0.92	1.13	0.81	0.82	fl/fl cre	0.73	0.17	0.10
skm-gp130	9424	200.014	23.69	0.90	1.09	0.82	0.83				
skm-gp130	9424	191.158	14.84	0.56	1.06	0.53	0.54				
Skm-gp130+ LLC	9424	196.553	20.23	0.77	0.57	1.34	1.35	fl/fl cre + LLC	1.09	0.24	0.12
Skm-gp130+ LLC	9424	203.569	27.25	1.03	1.04	0.99	1.00				
Skm-gp130+ LLC	9424	201.924	25.60	0.97	0.82	1.18	1.19				
Skm-gp130+ LLC	9424	191.985	15.66	0.59	0.75	0.79	0.80				

p:total AMPK		p:total	p:total norm		avg	stdev	se
BL-6	41.833	2.42	0.89	BL-6	1.00	0.22	0.13
BL-6	38.089	3.39	1.25				
BL-6	35.117	2.32	0.86				
BL-6 + LLC	38.759	11.26	4.16	BL-6 + LLC	3.79	0.76	0.44
BL-6 + LLC	37.623	12.60	4.66				
BL-6 + LLC	29.526	8.96	3.31				
skm-gp130	29.105	8.18	3.02	skm-gp130	1.07	1.23	0.71
skm-gp130	21.275	2.88	1.06				
skm-gp130	19.097	2.00	0.74				
skm-gp130	19.504	3.80	1.41	skm-gp130+LLC	2.71	0.61	0.35
skm-gp130 + LLC	17.477	8.28	3.06				
skm-gp130 + LLC	13.645	5.45	2.01				
skm-gp130 + LLC	20.494	8.29	3.06				

ratio P:total	P-STAT3	P-P65	P-AMPK	P-P38	P-AKT	P-S6	Atrogin
LLC	1.042	0.856	1.102	0.966	0.900	1.06	0.99
LLC	0.932	0.834	1.020	0.994	0.996	1.00	1.00
LLC	1.060	0.945	0.945	0.965	1.063	1.03	0.99
LLC	0.966	1.364	0.933	1.074	1.041	0.91	1.02
LLC+PDTC	0.332	0.041	0.983	1.100	0.999	3.40	1.01
LLC+PDTC	0.496	0.163	0.969	1.079	1.130	1.90	1.12
LLC+PDTC	0.227	0.358	0.965	1.084	1.077	3.00	1.05
LLC+PDTC	0.500	0.250	0.988	0.991	1.114	2.40	1.20
LLC+IL-6rAb	0.515	1.387	0.971	0.926	0.986	0.82	1.11
LLC+IL-6rAb	1.029	1.179	0.884	0.989	1.183	0.12	1.08
LLC+IL-6rAb	1.079	1.011	0.898	0.935	1.048	0.15	1.07
LLC+IL-6rAb	0.986	1.181	0.952	0.974	1.130	0.56	1.11

Normalized	Puromycin
BL/6	1.019
BL/6	1.031
BL/6	0.951
LLC	0.504
LLC	0.353
LLC	0.088
LLC + PDTC	0.933
LLC + PDTC	1.364
LLC + PDTC	1.050
LLC + PDTC	0.508
LLC + IL-6r Ab	0.302
LLC + IL-6r Ab	0.210
LLC + IL-6r Ab	0.370
LLC + IL-6r Ab	0.072

S6		P:total	normalized
b6	125.448	36.019	1.029414
b6	128.922	39.493	1.1287
b6	132.232	42.803	1.223299
b6	125.328	35.899	1.025985
b6	110.164	20.735	0.592601
B6+ LLC	110.194	20.765	0.593459
B6+ LLC	120.3	30.871	0.882286
B6+ LLC	110.9	21.471	0.613636
B6+ LLC	106.796	17.367	0.496345
B6+ LLC	109.429	20	0.571595
skm-gp130	123.234	33.805	0.966139
skm-gp130	121.571	32.142	0.918611
skm-gp130	124.734	35.305	1.009008
skm-gp130	121.803	32.374	0.925241
skm+LLC	74.601	39.82633	0.54087
skm+LLC	60.268	25.49333	0.346217
skm+LLC	78.416	43.64133	0.59268
skm+LLC	92.473	57.69833	0.783584
skm+LLC	77.578	42.80333	0.581299

Atrogin	IOD	-bg	Normalized
b6	106.987	13.35267	0.44719
b6	119.49	25.85567	0.865923
b6	134.328	40.69367	1.362858
b6	129.61	35.97567	1.204849
b6	127.052	33.41767	1.11918
B6+ LLC	141.455	47.82067	1.601546
B6+ LLC	131.318	37.68367	1.262051
B6+ LLC	140.542	46.90767	1.570969
B6+ LLC	143.029	49.39467	1.65426
B6+ LLC	142.351	48.71667	1.631554
skm-gp130	95.438	23.69767	0.520539
skm-gp130	115.744	44.00367	0.966577
skm-gp130	123.487	51.74667	1.136658
skm-gp130	122.984	51.24367	1.125609
skm-gp130	128.675	56.93467	1.250617
skm+LLC	135.75	64.00967	1.406025
skm+LLC	119.497	47.75667	1.049015
skm+LLC	115.01	43.26967	0.950454
skm+LLC	118.175	46.43467	1.019976
skm+LLC	130.692	58.95167	1.294922

P-STAT		P:total	normalized
b6	145.053	41.09	0.95429
b6	154.367	50.404	1.170602
b6	157.145	53.182	1.235119
b6	149.513	45.55	1.057871
b6	129.028	25.065	0.582119
B6+ LLC	156.088	52.125	1.210571
B6+ LLC	176.25	72.287	1.678821
B6+ LLC	181.141	77.178	1.792411
B6+ LLC	174.771	70.808	1.644472
B6+ LLC	180.573	76.61	1.77922
skm-gp130	130.363	26.4	0.613124
skm-gp130	125.32	21.357	0.496003
skm-gp130	115.156	11.193	0.25995
skm-gp130	122.825	18.862	0.438058
skm-gp130	124	20.037	0.465347
skm+LLC	148.577	44.614	1.036132
skm+LLC	134.586	30.623	0.7112
skm+LLC	141.256	37.293	0.866107
skm+LLC	137.906	33.943	0.788305
skm+LLC	129.966	26.003	0.603904

P38	IOD Phos	-bg	norm	IOD tot	-bg	Norm	P:Total	norm	Mean	SEM
BL-6	88.26	1.59	0.23	136.50	49.83	0.92	0.26	0.26	1.00	0.46
BL-6	92.67	6.00	0.89	142.00	55.33	1.02	0.87	0.90		
BL-6	99.35	12.68	1.88	143.86	57.19	1.06	1.78	1.84		
LLC	100.01	13.34	1.97	144.39	57.72	1.07	1.85	1.91	2.58	0.36
LLC	106.27	19.60	2.90	147.46	60.79	1.12	2.58	2.67		
LLC	108.61	21.94	3.25	144.19	57.52	1.06	3.05	3.16		
skm-gp130	98.15	11.48	1.70	145.58	58.91	1.09	1.56	1.62	1.15	0.20
skm-gp130	98.06	11.39	1.69	144.84	58.17	1.07	1.57	1.62		
skm-gp130	93.52	6.85	1.01	147.59	60.92	1.13	0.90	0.93		
skm-gp130	89.51	2.84	0.42	140.46	53.79	0.99	0.42	0.44		
skm-gp130LLC	89.93	3.26	0.48	131.52	44.85	0.83	0.58	0.60	0.52	0.07
skm-gp130LLC	90.64	3.97	0.59	136.94	50.27	0.93	0.63	0.65		
skm-gp130LLC	91.48	4.80	0.71	133.43	46.76	0.86	0.82	0.85		
skm-gp130LLC	86.48	-0.19	-0.03	127.91	41.24	0.76	-0.04	-0.04		

Sacrifice DEXA Data

				Bone			TISSUE			
			WEIGHT	BMD	BMC	AREA	LEAN	FAT	TOTAL	%FAT
Geno	**LLC**	**Mouse**	(g)	(g/cm2)	(g)	(cm2)	(g)	(g)	(g)	%
BL/6	control	988	23.6	0.0481	0.313	6.51	18	3	21	14.4
BL/6	control	989	26.3	0.0532	0.375	7.05	19.9	3.2	23.1	14
BL/6	control	990	25.2	0.0536	0.365	6.81	18.8	3.2	22.1	14.7
BL/6	control	991	25.1	0.0501	0.335	6.69	18.1	3.6	21.7	16.7
BL/6	control	992	25.7	0.0518	0.342	6.61	19	4.1	23.1	17.6
		mean	25.18	0.05136	0.346	6.734	18.76	3.42	22.2	15.48
		se	0.45	0.00	0.01	0.09	0.34	0.20	0.41	0.71
		n	5	5	5	5	5	5	5	5
fl/fl cre/cre	control	2518	26.1	0.0494	0.381	7.71	19.2	4.1	23.3	17.8
fl/fl cre/cre	control	2524	28.4	0.0475	0.332	6.98	23.4	2.5	25.9	9.7
fl/fl cre/cre	control	2574	25	0.0464	0.329	7.08	18.3	3.4	21.7	15.6
fl/fl cre/cre	control	2575	25.6	0.0493	0.358	7.25	19.8	3.8	23.6	16.1
fl/fl cre/cre	control	2598	na							
		mean	26.275	0.04815	0.35	7.255	20.175	3.45	23.625	14.8
		se	0.74	0.00	0.01	0.16	1.12	0.35	0.87	1.76
		n	4	4	4	4	4	4	4	4
BL/6	LLC	1794	NA							
BL/6	LLC	1	28.7	0.0482	0.296	6.14	24.5	2.9	27.5	10.6
BL/6	LLC	2792	22.5	0.0447	0.318	7.12	17.2	2.2	19.3	11.6
BL/6	LLC	2791	26.5	0.051	0.352	6.91	19.7	3.3	22.9	14.2
BL/6	LLC	1793	23.7	0.0438	0.281	6.42	19.4	2.4	21.7	10.9
BL/6	LLC	1792	21.8	0.0458	0.29	6.34	16.6	2.9	19.5	14.9
		mean	24.64	0.0467	0.3074	6.586	19.48	2.74	22.18	12.44
		se	1.29	0.00	0.01	0.18	1.39	0.20	1.49	0.88
		n	5	5	5	5	5	5	5	5
fl/fl cre/cre	LLC	2669	NA							
fl/fl cre/cre	LLC	2634	NA							
fl/fl cre/cre	LLC	2635	25.4	0.0487	0.328	6.75	19.3	3.8	23.1	16.5
fl/fl cre/cre	LLC	2636	27.6	0.0511	0.334	6.54	21.9	2.8	24.7	11.4
fl/fl cre/cre	LLC	9715	26.5	0.0483	0.324	6.7	23.5	3.6	27	13.2
fl/fl cre/cre	LLC	9716	29.7	0.0491	0.326	6.64	21	2.6	23.6	11.1
		mean	27.3	0.0493	0.328	6.6575	21.425	3.2	24.6	13.05
		se	0.92	0.00	0.00	0.05	0.88	0.29	0.87	1.24
		n	4	4	4	4	4	4	4	4

Mouse	Geno	MAX BW	SAC BW	R. Sol	R. Plant	R. Gas	R. TA	R EDL	R. RF	L. Sol	L. Plant	L. Gas	L TA	L. EDL	L. RF
900	Min	27.8	21	8	10	83	26	6	43	6	10	74	18	6	49
216	Min	23	19.4	7	10	89	31	5	61	7	12	94	28	7	63
981	Min	25.8	23.2	7	12	102	29	6	68	7	12	101	31	8	74
196	Min	23.1	20.8	6	11	68	22	6	48	7	10	78	21	6	49
901	Min	25.9	24.3	10	13	95	35	7	64	8	13	99	30	8	64
	mean	**25.1**	**21.7**	**7.6**	**11.2**	**87.4**	**28.6**	**6.0**	**56.8**	**7.0**	**11.4**	**89.2**	**25.6**	**7.0**	**59.8**
	se	**0.9**	**0.9**	**0.7**	**0.6**	**5.8**	**2.2**	**0.3**	**4.8**	**0.3**	**0.6**	**5.5**	**2.6**	**0.4**	**4.8**
210	Min	24.3	22.9	8	12	81	25	7	61	7	14	95	17	4	53
1935	Min	25.8	24.6	8	13	107	35	8	72	8	17	110	36	9	78
984	Min	26.4	25.5	8	16	116	36	8	88	8	16	121	41	9	76
979	Min	26.6	26.3	10	13	111	42	10	86	8	17	119	39	9	88
	mean	**25.8**	**24.8**	**8.5**	**13.5**	**103.8**	**34.5**	**8.3**	**76.8**	**7.8**	**16.0**	**111.3**	**33.3**	**7.8**	**73.8**
	se	**0.5**	**0.7**	**0.5**	**0.9**	**7.8**	**3.5**	**0.6**	**6.3**	**0.3**	**0.7**	**5.9**	**5.5**	**1.3**	**7.4**
1910	BL-6	27.6	27.6	9	16	127	46	11	100	9	16	134	45	10	97
2735	BL-6	28.8	28.8	10	18	136	37	9	101	9	15	142	40	10	102
2737	BL-6	29.1	29.1	9	19	142	46	11	89	10	19	140	43	12	94
2738	BL-6	30.8	30.8	8	17	139	50	10	89	10	19	139	45	13	91
1909	BL-6	27.3	27.3	8	14	132	42	10	101	9	22	157	46	10	96
1911	BL-6	29	29	8	15	140	32	11	106	9	17	138	45		99
	mean	**28.8**	**28.8**	**8.7**	**16.5**	**136.0**	**42.2**	**10.3**	**97.7**	**9.3**	**18.0**	**141.7**	**44.0**	**11.0**	**96.5**
	se	**0.7**	**0.7**	**0.5**	**1.1**	**3.2**	**3.8**	**0.5**	**4.1**	**0.3**	**1.5**	**4.6**	**1.3**	**0.8**	**2.2**

Mouse #	Geno	Liver	Spleen	Testes	Heart	Epi Fat	Tibia
900	Min	0.897	444	180	108	0	16.7
216	Min	1.045	293	162	91	42	16.7
981	Min	1.555	531	132	107	53	17
196	Min	0.893	343	138	100	0	16.7
901	Min	1.533	578	197	125	53	17.3
	mean	**1.2**	**437.8**	**161.8**	**106.2**	**29.6**	**16.9**
	se	**0.1**	**54.0**	**12.3**	**5.6**	**12.2**	**0.1**
210	Min	1.369	579	171	104	0	16.9
1935	Min	1.546	455	182	104	41	17
984	Min	1.689	460	180	134	248	17.2
979	Min	1.8	469	181	126	266	17.1
	mean	**1.6**	**490.8**	**178.5**	**117.0**	**138.8**	**17.1**
	se	**0.1**	**29.6**	**2.5**	**7.7**	**68.9**	**0.1**
1910	BL-6	1.117	78		104	392	17
2735	BL-6	1.291	89	215	110	489	17
2737	BL-6	1.233	103	217	107	561	16.8
2738	BL-6	1.208	89	201	106	756	17.2
1909	BL-6	1.206	90	214	105	578	17
1911	BL-6	1.17	84	212	114	481	16.6
	mean	**1.2**	**88.8**	**211.8**	**107.7**	**542.8**	**16.9**
	se	**0.0**	**4.8**	**3.6**	**2.1**	**71.4**	**0.1**

Grip Strength

				Set 1					Set 2				
mouse	geno	sex	BW	Trial 1	Trial 2	Trial 3	Trial 4	Trial 5	Trial 1	Trial 2	Trial 3	Trial 4	Trial 5
979	Min	Male	26.3	1.47	1.71	2.04	1.95	2.00	1.80	1.94	1.67	2.00	1.62
900	Min	Male	21	1.11	2.02	1.42	0.84	0.92	0.31	0.64	0.72	0.67	0.70
901	Min	Male	24.3	1.52	1.74	1.67	1.77	1.75	1.52	1.52	1.74	1.99	1.90
981	Min	Male	23.2	1.96	2.23	1.61	1.85	2.40	1.74	1.81	1.83	2.00	1.80
984	Min	Male	25.9	1.88	1.84	2.35	1.94	1.97	1.68	1.88	1.54	1.92	2.17
1935	Min	Male	24.8	1.69	1.56	2.45	2.08	2.00	1.65	1.72	2.10	2.10	2.08
1936	Min	Male	22.2	1.74	1.34	1.48	1.58	1.53	1.46	1.55	1.65	1.37	1.41
1912	Min	Male	22.5	1.38	1.96	1.54	1.72	1.72	1.57	2.07	1.16	1.38	1.62
1909	BL6	Male	27.7	2.32	2.40	2.73	1.99	1.95	2.41	2.66	2.35	2.48	2.18
1910	BL6	Male	27.3	2.18	2.61	2.18	1.79	1.85	1.86	1.83	2.07	1.58	2.69
1911	BL6	Male	29.1	2.38	2.11	2.42	2.58	2.48	1.90	3.03	2.07	2.68	2.07
1913	BL6	Male	30.8	2.35	2.57	2.31	1.97	2.73	2.02	2.15	1.99	2.59	2.39

								Set 1	Set 2
mouse	geno	sex	BW	Average	Max Set 1	Max Set 2	avg/bw	max/bw	max/bw
979	Min	Male	26.3	1.82	2.04	2.00	0.07	0.08	0.08
900	Min	Male	21	0.935	2.02	0.72	0.04	0.10	0.03
901	Min	Male	24.3	1.712	1.77	1.99	0.07	0.07	0.08
981	Min	Male	23.2	1.923	2.4	2.00	0.08	0.10	0.09
984	Min	Male	25.9	1.917	2.35	2.17	0.07	0.09	0.08
1935	Min	Male	24.8	1.943	2.45	2.10	0.08	0.10	0.08
1936	Min	Male	22.2	1.511	1.74	1.65	0.07	0.08	0.07
1912	Min	Male	22.5	1.612	1.96	2.07	0.07	0.09	0.09
1909	BL6	Male	27.7	2.347	2.73	2.66	0.08	0.10	0.10
1910	BL6	Male	27.3	2.064	2.61	2.69	0.08	0.10	0.10
1911	BL6	Male	29.1	2.372	2.58	3.03	0.08	0.09	0.10
1913	BL6	Male	30.8	2.307	2.73	2.59	0.07	0.09	0.08

Low frequency Stimulation
Western Blots

Strain	Treat	p-P65	total P65	Phos:total	Mean	SEM
		norm.	norm.			
BL-6	con	1.362	1.144	1.19	1.00	0.11
BL-6	con	0.787	0.973	0.81		
BL-6	con	1.046	1.025	1.02		
Min	con	4.879	1.139	4.28	8.72	2.52
Min	con	8.320	0.937	8.88		
Min	con	11.371	0.874	13.01		
Min + PDTC	con	2.139	1.329	1.61	1.55	0.03
Min + PDTC	con	1.937	1.328	1.46		
Min + PDTC	con	1.792	1.147	1.56		
Min + PDTC	con	1.447	0.928	1.56		
BL-6	stim	15.050	0.944	15.95	15.59	0.6
BL-6	stim	20.402	1.244	16.40		
BL-6	stim	23.869	1.654	14.43		
Min	stim	2.536	0.937	2.71	8.18	2.77
Min	stim	8.409	0.832	10.11		
Min	stim	17.477	1.492	11.71		
Min + PDTC	stim	7.385	1.340	5.51	5.76	0.21
Min + PDTC	stim	5.933	1.043	5.69		
Min + PDTC	stim	6.785	1.239	5.48		
Min + PDTC	stim	5.302	0.832	6.37		

Strain	Treat	p-STAT3 norm.	total STAT3 norm.	phos:total	Mean	SEM
BL-6	con	-1.243	1.114	-1.12	1.00	0.11
BL-6	con	1.131	0.933	1.21		
BL-6	con	2.831	0.975	2.90		
Min	con	3.455	1.119	3.09	8.72	2.52
Min	con	8.523	1.007	8.46		
Min	con	6.581	0.744	8.85		
Min + PDTC	con	2.504	1.319	1.90	1.55	0.03
Min + PDTC	con	2.948	1.288	2.29		
Min + PDTC	con	1.824	1.127	1.62		
BL-6	stim	6.429	0.844	4.74	15.59	0.6
BL-6	stim	8.246	1.184	7.62		
BL-6	stim	18.259	1.62	6.96		
Min	stim	10.223	0.907	11.27	8.18	2.77
Min	stim	15.832	0.822	19.26		
Min	stim	16.156	1.372	11.77		
Min + PDTC	stim	9.448	1.300	7.27	5.76	0.21
Min + PDTC	stim	7.570	0.973	7.78		
Min + PDTC	stim	8.983	1.239	7.25		

Strain	Treat	p-Akt norm.	total Akt norm.	phos:total	Mean	SEM
BL-6	con	0.847	1.00	0.85	1.00	0.08
BL-6	con	1.152	0.95	1.22		
BL-6	con	0.944	1.01	0.94		
BL-6	con	1.046	1.04	1.00		
Min	con	3.605	0.99	3.65	4.12	0.17
Min	con	4.064	0.95	4.27		
Min	con	4.098	0.92	4.45		
Min	con	3.865	0.94	4.12		
BL-6	stim	1.468	0.92	1.59	1.63	0.66
BL-6	stim	1.738	1.03	1.69		
BL-6	stim	1.513	0.94	1.61		
Min	stim	3.902	0.99	3.93	3.76	0.05
Min	stim	3.868	1.04	3.70		
Min	stim	3.937	1.07	3.69		
Min	stim	3.644	0.98	3.73		

Strain	Treat	p-p38	total p38	phos:total	Mean	SEM
		norm.	norm.			
BL-6	con	0.643	0.960	0.67	1.00	0.17
BL-6	con	1.481	1.029	1.44		
BL-6	con	0.894	1.003	0.89		
Min	con	0.797	1.008	0.79	1.05	0.27
Min	con	0.902	1.015	0.89		
Min	con	0.668	1.000	0.67		
Min	con	1.849	0.995	1.86		
BL-6	stim	3.076	0.960	3.09	3.71	0.38
BL-6	stim	4.374	0.966	4.56		
BL-6	stim	3.369	0.913	3.49		
Min	stim	3.181	1.051	3.00	3.70	0.31
Min	stim	3.159	1.007	4.49		
Min	stim	3.159	1.010	3.75		
Min	stim	4.525	0.996	3.55		

Strain	Treat	p-AMPK	total AMPK	phos:total	Mean	SEM
		norm.	norm.			
BL-6	con	1.095	1.050	1.04	1.00	0.05
BL-6	con	1.109	0.994	1.12		
BL-6	con	0.948	1.029	0.92		
BL-6	con	0.853	0.928	0.92		
Min	con	1.571	1.032	1.52	2.35	0.32
Min	con	1.776	0.802	2.21		
Min	con	2.694	1.027	2.62		
Min	con	2.809	0.928	3.03		
BL-6	stim	1.734	0.898	1.93	1.79	0.05
BL-6	stim	1.747	1.022	1.71		
BL-6	stim	1.921	1.105	1.74		
BL-6	stim	1.759	0.998	1.76		
Min	stim	4.191	1.054	3.97	3.44	0.37
Min	stim	3.600	0.989	3.64		
Min	stim	2.568	1.098	2.34		
Min	stim	3.485	0.913	3.82		

Strain	Treat	p-S6	total S6	phos:total	Mean	SEM
		norm.	norm.			
Min	con	0.949	0.978	0.97	1.00	0.03
Min	con	0.930	0.993	0.94		
Min	con	1.104	1.028	1.07		
Min	con	1.033	1.001	1.03		
Min + PDTC	con	1.831	1.032	1.77	1.55	0.12
Min + PDTC	con	0.962	0.801	1.20		
Min + PDTC	con	1.707	1.026	1.66		
Min + PDTC	con	1.456	0.927	1.57		
Min	stim	1.658	0.898	1.85	1.99	0.10
Min	stim	2.330	1.021	2.28		
Min	stim	2.028	1.098	1.85		
Min	stim	2.184	1.103	1.98		

Strain	Treat	Cyto C	Mean	SEM
		norm.		
Min	con	1.00	1.00	0.03
Min	con	1.07		
Min	con	0.93		
Min	con	1.00		
Min + PDTC	con	1.30	1.28	0.01
Min + PDTC	con	1.28		
Min + PDTC	con	1.27		
Min + PDTC	con	1.28		
Min	stim	1.05	1.14	0.04
Min	stim	1.23		
Min	stim	1.11		
Min	stim	1.20		

Strain	Treat	TFAM	Mean	SEM
		norm.		
Min	con	0.88	1.00	0.05
Min	con	1.05		
Min	con	1.10		
Min	con	0.97		
Min + PDTC	con	2.23	2.21	0.01
Min + PDTC	con	2.17		
Min + PDTC	con	2.22		
Min + PDTC	con	2.21		
Min	stim	2.28	1.97	0.25
Min	stim	2.17		
Min	stim	2.20		
Min	stim	1.23		

Strain	Treat	PGC-1α	Mean	SEM
		norm.		
BL-6	con	0.93	1.00	0.08
BL-6	con	0.90		
BL-6	con	1.16		
Min	con	0.61	0.63	0.12
Min	con	0.77		
Min	con	0.85		
Min	con	0.30		
BL-6	stim	1.15	1.29	0.10
BL-6	stim	1.23		
BL-6	stim	1.48		
Min	stim	0.74	0.84	0.10
Min	stim	1.14		
Min	stim	0.80		
Min	stim	0.69		

Strain	Treat	Cyto C	Mean	SEM
		norm.		
BL-6	con	0.88	1.00	0.06
BL-6	con	1.05		
BL-6	con	1.06		
Min	con	0.84	0.86	0.09
Min	con	1.13		
Min	con	0.79		
Min	con	0.69		
BL-6	stim	1.43	1.42	0.10
BL-6	stim	1.58		
BL-6	stim	1.25		
Min	stim	0.80	0.80	0.02
Min	stim	0.82		
Min	stim	0.83		
Min	stim	0.76		

Strain	Treat	P-S6	total S6	phos:total	Mean	SEM
		norm.	norm.	norm.		
BL-6	con	0.750	0.850	0.88	1.00	0.06
BL-6	con	0.938	0.890	1.05		
BL-6	con	1.341	1.260	1.06		
Min	con	0.946	1.122	0.84	0.86	0.09
Min	con	1.498	1.323	1.13		
Min	con	0.911	1.152	0.79		
Min	con	1.032	1.497	0.69		
BL-6	stim	2.144	1.012	1.43	1.42	0.10
BL-6	stim	1.602	1.303	1.58		
BL-6	stim	1.632	1.046	1.25		
Min	stim	1.310	1.145	1.00	1.18	0.12
Min	stim	1.150	1.288	1.29		
Min	stim	2.171	1.474	1.47		
Min	stim	1.537	1.601	0.96		

Strain	Treat	TFAM	Mean	SEM
		norm.		
BL-6	con	0.89	1.00	0.06
BL-6	con	1.01		
BL-6	con	1.11		
Min	con	0.96	0.95	0.04
Min	con	1.01		
Min	con	0.83		
Min	con	0.99		
BL-6	stim	1.41	1.48	0.06
BL-6	stim	1.59		
BL-6	stim	1.43		
Min	stim	0.93	0.87	0.11
Min	stim	1.14		
Min	stim	0.73		
Min	stim	0.66		

Control	PGC-1B	GAPDH	dct	ddct	2^ddct	Normalized
210	25.67	24.305	1.365	-1.38	0.39	0.38
216	26.44	26.025	0.415	-2.33	0.20	0.19
979	26.06	23.84	2.22	-0.52	0.70	0.68
197	25.39	25.55	-0.16	-2.90	0.13	0.13
901	25.6	24.48	1.12	-1.62	0.33	0.32
900	25.205	24.68	0.525	-2.22	0.22	0.21
984	26.46	24.835	1.625	-1.12	0.46	0.45
981	25.29	23.725	1.565	-1.18	0.44	0.43
1910	25.425	22.545	2.88	0.14	1.10	1.07
1911	25.44	23.28	2.16	-0.58	0.67	0.65
1919	25.755	22.9	2.855	0.11	1.08	1.05
1913	25.87	22.8	3.07	0.33	1.26	1.22
Stim						
210	26.955	25.83	1.125	-1.62	0.33	0.32
216	25.86	25.47	0.39	-2.35	0.20	0.19
979	26.595	23.2	3.395	0.65	1.57	1.53
197	26.82	26.305	0.515	-2.23	0.21	0.21
901	25.265	25.205	0.06	-2.68	0.16	0.15
900	26.875	26.95	-0.075	-2.82	0.14	0.14
984	25.955	24.725	1.23	-1.51	0.35	0.34
981	26.83	26.12	0.71	-2.03	0.24	0.24
1910	26.07	24.06	2.01	-0.73	0.60	0.59
1911	26.885	25.115	1.77	-0.97	0.51	0.50
1919	26.195	24.31	1.885	-0.86	0.55	0.54

Control	average	sem
Severe	0.26	0.05
Mild	0.50	0.09
BL/6	1.00	0.12
Stim	**average**	**sem**
Severe	0.19	0.02
Mild	0.73	0.40
BL/6	0.54	0.03

	Sample	PGC-1	GAPDH	dct	ddct	2^ddct	Normalized
Control	197R	28.62	21.17	7.45	-1.00	0.50	0.49
	210R	26.655	19.045	7.61	-1.16	0.45	0.44
	216R	25.8	19.25	6.55	-0.10	0.94	0.91
	900R	26.8	19.29	7.51	-1.06	0.48	0.47
	901R	26.425	19.22	7.21	-0.75	0.59	0.58
	981R	26.64	19.5	7.14	-0.69	0.62	0.60
	986R	26.995	19.765	7.23	-0.78	0.58	0.57
	1909R	25.38	19.2	6.18	0.27	1.21	1.18
	1910R	26.33	19.39	6.94	-0.49	0.71	0.69
	1911R	25.86	19.62	6.24	0.21	1.16	1.13
Stim	197L	25.645	21.2	4.45	2.01	4.02	3.92
	210L	25.475	19.825	5.65	0.80	1.75	1.70
	216L	23.915	19.99	3.93	2.53	5.77	5.62
	900L	26	20.57	5.43	1.02	2.03	1.98
	901L	25.9	19.745	6.16	0.30	1.23	1.20
	979L	23.3	19.51	3.79	2.66	6.33	6.17
	981L	25.215	21.2	4.02	2.44	5.42	5.28
	986L	24.88	18.865	6.02	0.44	1.36	1.32
	1909L	26.76	20.57	6.19	0.26	1.20	1.17
	1910L	26.305	20.065	6.24	0.21	1.16	1.13
	1911L	26.24	20.72	5.52	0.93	1.91	1.86

	Control		Stim	
PGC-1a	**Mean**	**SEM**	**Mean**	**SEM**
BL/6	1.00	0.15	1.39	0.24
Mild	0.50	0.07	3.06	1.56
Severe	0.61	0.08	3.60	0.88

		NRF1	GAPDH	dct	ddct	2^ddct	Normalized
Control	**1909**	24.73	23.53	1.2	0.00	1.00	0.99
Stim	**1909**	25.14	22.82	2.32	1.12	2.17	2.15
Control	**1910**	24.61	23.63	0.98	-0.22	0.86	0.85
Stim	**1910**	24.75	22.25	2.5	1.30	2.46	2.44
Control	**1911**	24.24	22.76	1.48	0.28	1.21	1.20
Stim	**1911**	25.52	23.28	2.24	1.04	2.05	2.04
Control	**1936**	24.87	23.72	1.15	-0.05	0.96	0.96
Control	**900**	23.2	24.72	-1.52	-2.72	0.15	0.15
Stim	**900**	24.85	23.28	1.57	0.37	1.29	1.28
Control	**981**	24.54	23.39	1.15	-0.05	0.96	0.96
Stim	**981**	25.74	25.77	-0.03	-1.23	0.43	0.42
Control	**216**	24.12	25.64	-1.52	-2.72	0.15	0.15
Stim	**216**	24.74	25.9	-1.16	-2.36	0.19	0.19
Control	**197**	23.63	25.28	-1.65	-2.85	0.14	0.14
Stim	**197**	25.65	25.54	0.11	-1.09	0.47	0.47
Control	**901**	23.94	24.32	-0.38	-1.58	0.33	0.33
Stim	**901**	24.3	24.74	-0.44	-1.64	0.32	0.32

	control		stim	
	Mean	SEM	Mean	SEM
BL/6	1.00	0.07	2.21	0.12
Min	0.35	0.16	0.54	0.19

		TFAM	GAPDH	dct	ddct	2^ddct	Normalized
Control	**1909**	24.71	23.53	1.18	0.13	1.10	1.07
Stim	**1909**	24.75	22.82	1.93	0.88	1.84	1.80
Control	**1910**	24.1	23.63	0.47	-0.58	0.67	0.65
Stim	**1910**	24.51	22.25	2.26	1.21	2.32	2.26
Control	**1911**	24.05	22.76	1.29	0.24	1.18	1.15
Stim	**1911**	25.12	23.28	1.84	0.79	1.73	1.69
Control	**1936**	24.97	23.72	1.25	0.20	1.15	1.12
Control	**900**	24.47	24.72	-0.25	-1.30	0.41	0.40
Stim	**900**	23.59	23.28	0.31	-0.74	0.60	0.59
Control	**981**	24.37	23.39	0.98	-0.07	0.95	0.93
Stim	**981**	25.56	25.77	-0.21	-1.26	0.42	0.41
Control	**216**	24.58	25.64	-1.06	-2.11	0.23	0.23
Stim	**216**	25.41	25.9	-0.49	-1.54	0.34	0.34
Control	**197**	25.03	25.28	-0.25	-1.30	0.41	0.40
Stim	**197**	26.26	25.54	0.72	-0.33	0.80	0.78
Control	**901**	24.09	24.32	-0.23	-1.28	0.41	0.40
Stim	**901**	24.57	24.74	-0.17	-1.22	0.43	0.42

	control		stim	
	Mean	SEM	Mean	SEM
BL/6	1.00	0.12	1.92	0.18
Min	0.47	0.12	0.51	0.08

		Cyto B	GAPDH	dct	ddct	2^ddct	Normalized
Control	**1909**	11.16	23.53	-12.37	-0.31	0.81	0.79
Stim	**1909**	12.07	22.82	-10.75	1.32	2.49	2.44
Control	**1910**	11.32	23.63	-12.31	-0.24	0.84	0.83
Stim	**1910**	11.65	22.25	-10.6	1.47	2.76	2.71
Control	**1911**	10.87	22.76	-11.89	0.17	1.13	1.11
Stim	**1911**	12.27	23.28	-11.01	1.06	2.08	2.04
Control	**1936**	12.03	23.72	-11.69	0.38	1.30	1.27
Control	**900**	11.81	24.72	-12.91	-0.84	0.56	0.55
Stim	**900**	11.73	23.28	-11.55	0.51	1.43	1.40
Control	**981**	11.74	23.39	-11.65	0.41	1.33	1.31
Stim	**981**	12.15	25.77	-13.62	-1.56	0.34	0.33
Control	**216**	11.68	25.64	-13.96	-1.90	0.27	0.26
Stim	**216**	12.14	25.9	-13.76	-1.70	0.31	0.30
Control	**197**	12.45	25.28	-12.83	-0.77	0.59	0.58
Stim	**197**	12.99	25.54	-12.55	-0.48	0.71	0.70
Control	**901**	11.49	24.32	-12.83	-0.77	0.59	0.58
Stim	**901**	11.39	24.74	-13.35	-1.29	0.41	0.40

	control		stim	
	Mean	SEM	Mean	SEM
BL/6	1.00	0.11	2.39	0.19
Min	0.65	0.17	0.63	0.21

Control	PPAR-γ	GAPDH	dct	ddct	2^ddct	Normalized
1909	25.50	18.15	7.35	0.07	0.95	0.95
1910	25.26	18.30	6.97	-0.32	1.25	1.24
1911	25.40	18.04	7.36	0.07	0.95	0.94
1913	25.37	17.91	7.46	0.18	0.88	0.88
900	24.90	18.13	6.77	-0.52	1.43	1.42
981	25.43	18.30	7.13	-0.15	1.11	1.10
216	25.28	18.40	6.88	-0.41	1.33	1.31
197	25.24	18.37	6.88	-0.41	1.33	1.31
984	26.08	18.88	7.20	-0.08	1.06	1.05
Stim						
1909	24.89	20.01	4.88	-2.40	5.29	5.24
1910	25.25	18.95	6.30	-0.99	1.98	1.97
1911	26.42	19.97	6.46	-0.83	1.77	1.76
1913	25.43	18.16	6.37	-0.91	1.88	1.87
900	25.00	20.15	4.86	-2.43	5.38	5.33
981	25.41	20.62	4.79	-2.50	5.65	5.60
216	25.24	19.19	6.05	-1.23	2.35	2.33
197	25.43	21.74	3.69	-3.60	12.10	12.00
984	24.63	19.26	5.38	-1.91	3.75	3.72

	PPARγ	mean	sem
BL-6	Control	1.00	0.08
	Exercise	2.99	1.13
Min	Control	1.24	0.07
	Exercise	5.79	1.66

Control	NRF-1	GAPDH	dct	ddct	2^ddct	Normalized
321	25.71	22.65	3.06	3.53	11.56	3.99
341	24.62	22.86	1.76	2.24	4.71	1.63
3153	24.22	23.03	1.19	1.67	3.17	1.10
3216	25.05	22.90	2.15	2.62	6.15	2.12
901	24.69	24.76	-0.07	0.41	1.33	0.46
197	24.13	25.75	-1.62	-1.14	0.45	0.16
216	24.69	24.43	0.26	0.74	1.67	0.58
Stim						
321	25.58	24.36	1.22	1.70	3.24	1.12
341	24.61	23.23	1.38	1.86	3.62	1.25
3153	25.04	25.11	-0.07	0.40	1.32	0.46
3216	25.26	22.18	3.08	3.55	11.73	4.05
901	25.02	25.22	-0.20	0.28	1.21	0.42
197	25.84	23.28	2.56	1.10	2.14	0.32
216	25.00	24.99	0.01	0.20	1.15	1.58

	Mean	SEM
Min	0.35	0.16
Min+ PDTC	2.21	0.63
Min + PDTC+ Stim	1.72	0.80

Control	TFAM	GAPDH	dct	ddct	2^ddct	Normalized
321	26.01	22.65	3.36	3.24	9.46	4.45
341	25.39	22.86	2.53	2.41	5.32	2.50
3153	25.25	23.03	2.22	2.10	4.29	2.02
3216	24.85	22.90	1.95	1.84	3.57	1.68
901	24.87	24.76	0.11	0.00	1.00	0.47
1911	24.27	23.22	1.05	0.94	1.91	1.00
197	25.40	25.75	-0.35	-0.46	0.73	0.34
216	25.01	24.43	0.58	0.47	1.38	0.65
Stim						
321	25.38	24.36	1.02	0.90	1.87	0.88
341	25.20	23.23	1.97	1.85	3.61	1.70
3153	26.50	25.11	1.39	1.27	2.41	1.14
3216	25.41	22.18	3.23	3.12	8.67	4.08
901	25.48	25.22	0.26	0.15	1.11	0.52
197	26.63	23.28	3.35	3.24	9.43	4.44

	Mean	SEM
Min	0.47	0.12
Min+ PDTC	2.66	0.62
Min + PDTC+ Stim	1.95	0.73

Control	Cyto B	GAPDH	dct	ddct	2^ddct	Normalized
321	12.69	22.65	-9.97	2.91	7.49	4.90
341	11.93	22.86	-10.94	1.94	3.82	2.50
3153	12.48	23.03	-10.55	2.32	4.99	3.27
3216	11.28	22.90	-11.62	1.25	2.38	1.56
901	11.69	24.76	-13.07	-0.20	0.87	0.57
197	12.74	25.75	-13.01	-0.14	0.91	0.59
216	11.90	24.43	-12.53	0.34	1.27	0.83
Stim						
321	12.43	24.36	-11.94	0.94	1.91	1.25
341	12.24	23.23	-11.00	1.88	3.67	2.40
3153	12.95	25.11	-12.17	0.71	1.63	1.07
3216	12.38	22.18	-9.80	3.07	8.40	5.49

	Mean	sem
Min	0.65	0.17
Min+ PDTC	3.06	0.71
Min + PDTC+ Stim	2.55	1.02

Control	GLUT4	GAPDH	dCT	ddct	2^ddct	normalized
1909	19.28	16.35	2.93	0.537	1.45	1.40
1910	20.22	18.18	2.04	-0.353	0.78	0.75
1911	20.59	18.38	2.21	-0.183	0.88	0.85
197	21.91	20.26	1.65	-0.743	0.60	0.58
216	20.35	18.75	1.6	-0.793	0.58	0.56
900	20.63	18.68	1.95	-0.443	0.74	0.71
Stim						
1909	20.72	16.28	4.44	2.047	4.13	3.98
1910	20.33	16.75	3.58	1.187	2.28	2.19
1911	21.45	17.67	3.78	1.387	2.61	2.52
197	22.48	18.1	4.38	1.987	3.96	3.82
216	22.2	18.6	3.6	1.207	2.31	2.22
900	20.08	16.2	3.88	1.487	2.80	2.70

	Control		Stim	
GLUT4	**Mean**	**SEM**	**Mean**	**SEM**
BL/6	1.00	0.20	2.90	0.55
Min	0.61	0.05	2.91	0.47

APPENDIX E

PERMISSIONS TO REPRINT

The FASEB Journal

The Journal of the Federation of American Societies for Experimental Biology

www.fasebj.org

Copyright Permission Request

The FASEB Journal does not charge copyright permission fees for:

- Authors to replicate their own work, regardless of where they are publishing
- Authors to republish copyrighted material in publications owned by not-for-profit organizations
- Students wanting to republish their work
- Republications of the abstract only

If this describes your request, please fill out the following form and fax to 1-240-407-4430. If this does not describe your request, the publications office cannot grant you free permission; you must visit the Copyright Clearance Center online (www.copyright.com) to purchase permission.

The original material was published in:

- [x] *The FASEB Journal*
- [ ] *Federation Proceedings*
- [ ] Other: _____

Year, month, volume, issue, pages, and DOI: E-Pub ahead of print 2013 October

doi:10.1096/fj.13-240580

Names of all authors: Melissa J Puppa, Aditi A Narsale, Song Gao, James A Carson

Description of the desired material (use extra pages if necessary): Research Communication

Skeletal Muscle glycoprotein 130's role in Lewis lung carcinoma-induced cachexia

Journal/publication in which the material is to be republished (please use full title): (Dissertation). The regulation of Skeletal Muscle Mass & Mitochondrial Biogenesis by Gp130/STAT3 Signaling during cancer Cachexia

Company/organization that owns this journal: University of South Carolina Graduate School

Person making the request: Melissa Puppa

Fax number: 803-777-3504

Permissions can only be granted by fax. Staff will attempt to fax a reply within one week. You must provide an accurate fax number, and please be sure that the receiving fax machine is working properly.

Date received: 12/11/2013 Date processed: 12/11/2013

[x] Permission granted: [signature] Deputy Director

[ ] Permission denied